

PL-TR-91-2040  
Environmental Research Papers, No.1068

AD-A256 180

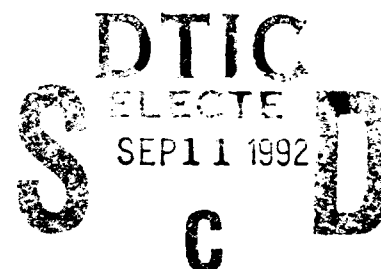


①

# EXPERIMENTAL DETERMINATION OF WAITING TIMES FOR METEOR TRAIL RETURNS OF SPECIFIED DURATIONS

J. C. Ostergaard  
A. D. Bailey  
P. M. Bench

9 January 1991



---

APPROVED FOR PUBLIC RELEASE; DISTRIBUTION UNLIMITED.

---

92-24971



92 5 10 019

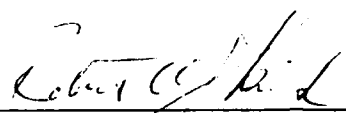


PHILLIPS LABORATORY  
DIRECTORATE OF GEOPHYSICS  
AIR FORCE SYSTEMS COMMAND  
HANSCOM AIR FORCE BASE, MA 01731-5000

"This technical report has been reviewed and is approved for publication"

  
\_\_\_\_\_  
JOHN E. RASMUSSEN  
Branch Chief

FOR THE COMMANDER

  
\_\_\_\_\_  
ROBERT A. SKRIVANEK  
Division Director

This report has been reviewed by the ESD Public Affairs Office (PA) and is releasable to the National Technical Information Service (NTIS).

Qualified requestors may obtain additional copies from the Defense Technical Information Center. All others should apply to the National Technical Information Service.

If your address has changed, or if you wish to be removed from the mailing list, or if the addressee is no longer employed by your organization, please notify GL/IMA, Hanscom AFB, MA 01731. This will assist us in maintaining a current mailing list.

Do not return copies of this report unless contractual obligations or notices on a specific document requires that it be returned.

REPORT DOCUMENTATION PAGE			Form Approved OMB No. 0704-0188	
Public reporting for this collection of information is estimated to average 1 hour per response, including the time for reviewing instructions, searching existing data sources, gathering and maintaining the data needed, and completing and reviewing the collection of information. Send comments regarding this burden estimate or any other aspect of this collection of information, including suggestions for reducing this burden, to Washington Headquarters Services, Directorate for Information Operations and Reports, 1215 Jefferson Davis Highway, Suite 1204, Arlington, VA 22202-4302, and to the Office of Management and Budget, Paperwork Reduction Project (0704-0188), Washington, DC 20503.				
1. AGENCY USE ONLY (Leave blank)		2. REPORT DATE 9 January 1991		3. REPORT TYPE AND DATES COVERED Scientific, Interim
4. TITLE AND SUBTITLE Experimental Determination of Waiting Times for Meteor Trail Returns of Specified Durations			5. FUNDING NUMBERS PE 62101F PR 4643 TA 10 WU 08	
6. AUTHOR(S) J.C. Ostergaard*, A.D. Bailey, P.M. Bench				
7. PERFORMING ORGANIZATION NAME(S) AND ADDRESS(ES) Phillips Laboratory (LID) Hanscom AFB, MA 01731-5000			8. PERFORMING ORGANIZATION REPORT NUMBER PL-TR-91-2040 ERP, No. 1068	
9. SPONSORING/MONITORING AGENCY NAME(S) AND ADDRESS(ES)			10. SPONSORING/MONITORING AGENCY REPORT NUMBER	
11. SUPPLEMENTARY NOTES * Center for Atmospheric Research University of Lowell, Lowell, MA 01854 Prepared in cooperation with BMO/MGEC, Norton AFB, CA				
12a. DISTRIBUTION/AVAILABILITY STATEMENT Approved for public release; distribution unlimited			12b. DISTRIBUTION CODE	
13. ABSTRACT (Maximum 200 words)  This report presents calculations by the Air Force's Geophysics Laboratory (GL) of waiting times for signals scattered from ionized meteor trails having durations between 50 and 400 msec. The calculations are based on a Signal-to-Noise Ratio (SNR) and bandwidth representative of a communication system using Binary Phase Shift Keying (BPSK) modulation with a Bit Error Rate (BER) of $10^{-3}$ and a signaling rate of 8000 bits/sec. The computations are based on data obtained on the Geophysics Laboratory's High Latitude Meteor Scatter Test Bed in Greenland. Statistics of arrival rates, duty cycles, and durations for meteor scatter returns exceeding selected SNRs have been included for interpretation of the waiting time statistics. Statistics for the months February, March, June, September, and December 1989 are included to evaluate the influence of seasonal variations on the waiting times.				
14. SUBJECT TERMS Meteor Scatter      Message Waiting Communication      Connectivity Propagation			15. NUMBER OF PAGES 194	
			16. PRICE CODE	
17. SECURITY CLASSIFICATION OF REPORT UNCLASSIFIED	18. SECURITY CLASSIFICATION OF THIS PAGE UNCLASSIFIED	19. SECURITY CLASSIFICATION OF ABSTRACT UNCLASSIFIED	20. LIMITATION OF ABSTRACT SAR	

Accession For	
NTIC 22441	<input checked="" type="checkbox"/>
Dist. File	<input type="checkbox"/>
Unpublished	<input type="checkbox"/>
Justification	
Distribution/	
Availability Codes	
Dist. and/or	
Dist	Special
A-1	

DTIC QUALITY INSPECTED 1

## Contents

1. FEATURES OF THE HIGH LATITUDE METEOR SCATTER TEST-BED	1
2. DESCRIPTION OF THE INVESTIGATION	7
3. ARRIVAL RATE STATISTICS	9
4. DUTY CYCLE STATISTICS	10
5. DURATION STATISTICS	11
6. WAITING TIME STATISTICS	12
6.1 Diurnal Variation of Waiting Times	13
6.2 Average Waiting Time Statistics	14
6.2.1 Waiting Time as a Function of Transmitter Power	14
6.2.2 Waiting Time as a Function of Duration	14
6.2.3 Waiting Time as a Function of Frequency	15
7. SUMMARY	15
REFERENCES	17
APPENDIX A: Receiver Noise Data	19
APPENDIX B: Meteor Arrival Rate Statistics	23
APPENDIX C: Duty Cycle Statistics	33

APPENDIX D: Average Duration Statistics	43
APPENDIX E: Waiting Time Data. Diurnal Variations	81
APPENDIX F: Average Waiting Time Statistics	157

## **Illustrations**

1. Geometry of the GL High Latitude Meteor Scatter Test Bed	3
2. Dynamic Range of the GL Test Bed Receiving System at Thule AB	5
3. Example of a Meteor Trail Signal	6

## **Tables**

1. Geographical Parameters for the Greenland Paths	2
2. Main Menu; Statistical Analysis Options	7

# **Experimental Determination of Waiting Times for Meteor Trail Returns of Specified Durations**

## **1. FEATURES OF THE HIGH LATITUDE METEOR SCATTER TEST BED**

The GL meteor scatter test bed in Greenland provides data to address a number of questions associated with the potential performance of meteor burst communication systems. The efforts under this measurements program are concentrated on characterizing the time and frequency variations of the meteor scatter channel and evaluating the effects of ionospheric disturbances on the channel. The channel description includes:

- The availability of useful meteor trails.
- The potential communication capacity associated with those trails.
- The occurrence, persistence, and effects of competing propagation media such as ionospheric scatter and sporadic E-layers.
- The variations in the instantaneous polarization.
- The signal-to-noise ratios of each meteor trail return.
- The fading characteristics of the channel.

The test-bed is comprised of two diagnostic meteor scatter links; one between Sondrestrom AB (SAB) and Thule AB (TAB), operating at 35, 45, 65, 85, 104, and 147 MHz; and one between Sondrestrom AB and Narsarsuaq (NSSQ), operating at 45, 65, 85, and 104 MHz. The 1200 km Sondrestrom - Thule link is within the Polar Cap, while the 700 km Sondrestrom - Narsarsuaq link passes through the auroral oval, as shown in Figure 1. This investigation used only the Sondrestrom - Thule link.

The frequency coverage has been selected to examine propagation effects such as absorption and depolarization from 35 MHz at the very low end of the VHF frequency band, where meteor scatter links have maximum yield during undisturbed ionospheric conditions, to 147 MHz where very little meteor scatter activity takes place, but where absorption and depolarization are much less severe than at lower frequencies.

Table 1 gives information on the geographical parameters of the sites, and path features that influence the properties of the test bed propagation paths.

Table 1. Geographical Parameters for the Greenland Paths

	TAB	SAB	NSSQ
LONGITUDE	67° 51'	50° 39'	45° 27'
LATITUDE	76° 33'	66° 59'	61° 10'
AZIMUTH			
SAB-TAB LINK	142°	339°	-
SAB-NSSQ LINK	-	159°	341°
TERMINAL ELEV.	240m	250m	10m
HORIZON ELEV.			
SAB-TAB LINK	1.1°-1.7°	1.8°-2.2°	-
SAB-NSSQ LINK	-	1°-3°	5°-9°
MIDPATH ELEV.			
FOR 100 km ALT.	6.5°	14.3°	
GREAT CIRCLE DIST.	1210 km	692 km	

The transmitters and receivers used in the links are not conventional communication system components; rather, they were developed to investigate both propagation and communication features of meteor scatter. The transmitters, located at Sondrestrom AB, sequentially transmit a 400 Hz frequency modulated carrier at the link's operating frequencies, repeating the sequence every 2 hours. The FM is added to distinguish the test bed transmitter signals from noise and interference. The transmitter power is 1000 W.



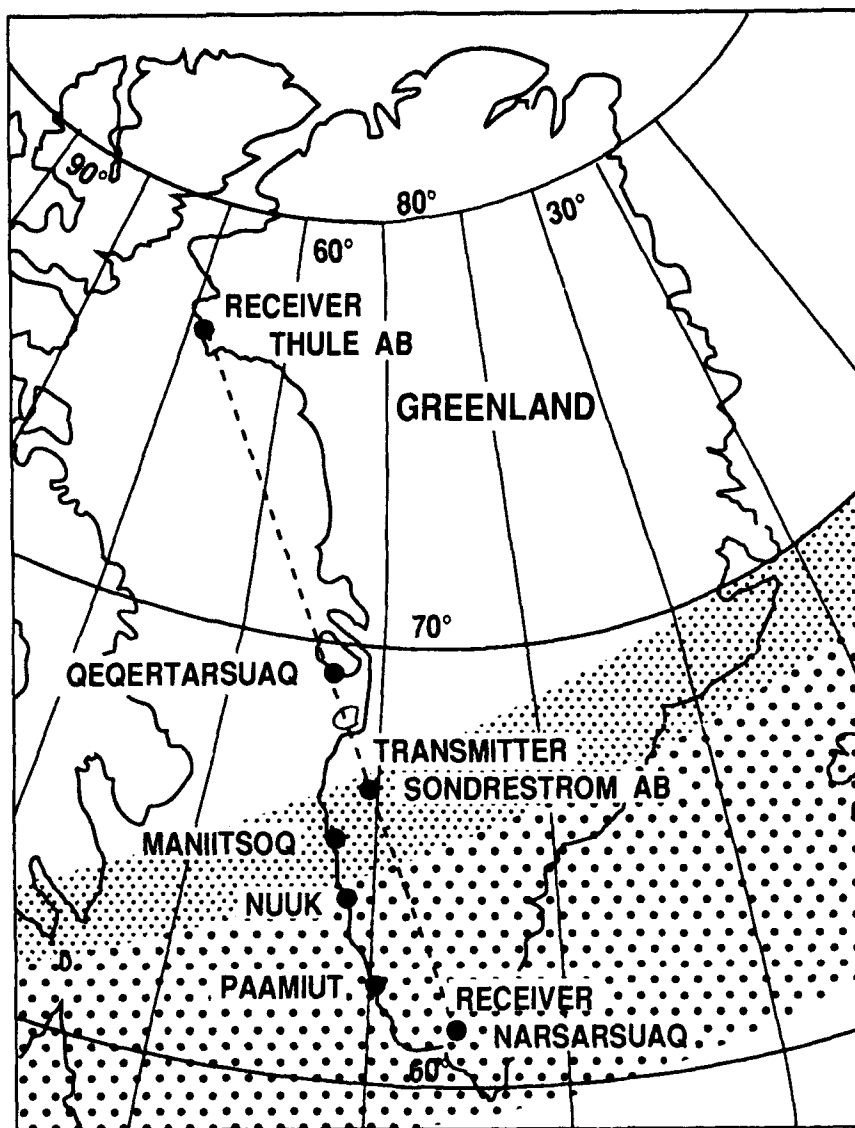


Figure 1. Geometry of the GL High Latitude Meteor Scatter Test-Bed

On the Sondrestrom - Thule link, the transmitting antenna polarization is horizontal for all frequencies. Five-element Yagi antennas, positioned approximately 1 1/2 wavelengths above the ground to equalize the gain and radiation patterns, are used, except at 147 MHz where a 14-element Yagi antenna is used. In addition, 65 and 104 MHz are transmitted with vertical polarization from vertical monopoles on the Sondrestrom AB - Narsarsuaq link to investigate the relative performance of horizontal and vertical polarization.

The receivers, at Thule AB and Narsarsuaq, measure the characteristics of the meteor scatter returns as well as signals carried by other modes of propagation that originate from the transmitters at Sondrestrom.

The receiving antennas are each composed of a pair of orthogonal, linearly polarized, Yagi antennas for horizontal and vertical polarization measurements. The two antennas are mounted on a common boom with separate lines feeding a phase locked-loop receiver with two identical RF-IF detector channels for each frequency. Thus, the amplitudes associated with each antenna and the phase difference between the two signals are acquired, permitting polarization measurement of the incident wave.

The dynamic range of the receivers covers the range from -90 dBm to -155 dBm referenced to the antenna connectors and the noise bandwidth is 100 Hz. The receiving system is galactic noise limited at all frequencies. The diurnal variation of the galactic noise for the receiving system at Thule AB for the months of February, March, June, September, and December (1989) is presented in Appendix A, Figures A1 to A5. The diurnal passage of the cluster of noise sources at the ecliptic plane is clearly seen. The diurnal variation of the galactic noise is not uniformly distributed around the mean due to the strength of this source compared to the galactic background temperature.

The noise varies from -140 to -144 dBm at 45 MHz, from -143 to -147 dBm at 65 MHz and from -147 to -150 dBm at 104 MHz. The average noise levels are -143 dBm at 45 MHz, -144 dBm at 65 MHz and -149 dBm at 104 MHz. The receivers require a 10 dB SNR for the phase locked loop to acquire the signal. Thus, the available dynamic range of the receiving system as a whole is 40-44 dB at 45 MHz, 43-47 dB at 65 MHz and 47-50 dB at 104 MHz. Figure 2 presents an overview of the dynamic range of the receiving system.

The signal amplitude data collected on the test bed is used to calculate the dynamic range for systems with transmitter powers and receiver bandwidths different from the 1000 W and 400 Hz inherent in the test bed. Lines marked with transmitter power levels in Figure 2 show the boundaries of combinations of transmitter power and system bandwidths available from analysis of the test bed data.

The received data consist of 5-second records of signal power from both the horizontally and vertically polarized channels, measurements of the phase difference between the vertical channel and the horizontal channel, and an indication of the presence of the 400 Hz FM signature. In operation, data are collected continuously in 5-second records. Those records in which the 400 Hz signature is detected are stored on tape. Data cartridges are sent to the Geophysics Laboratory for processing.

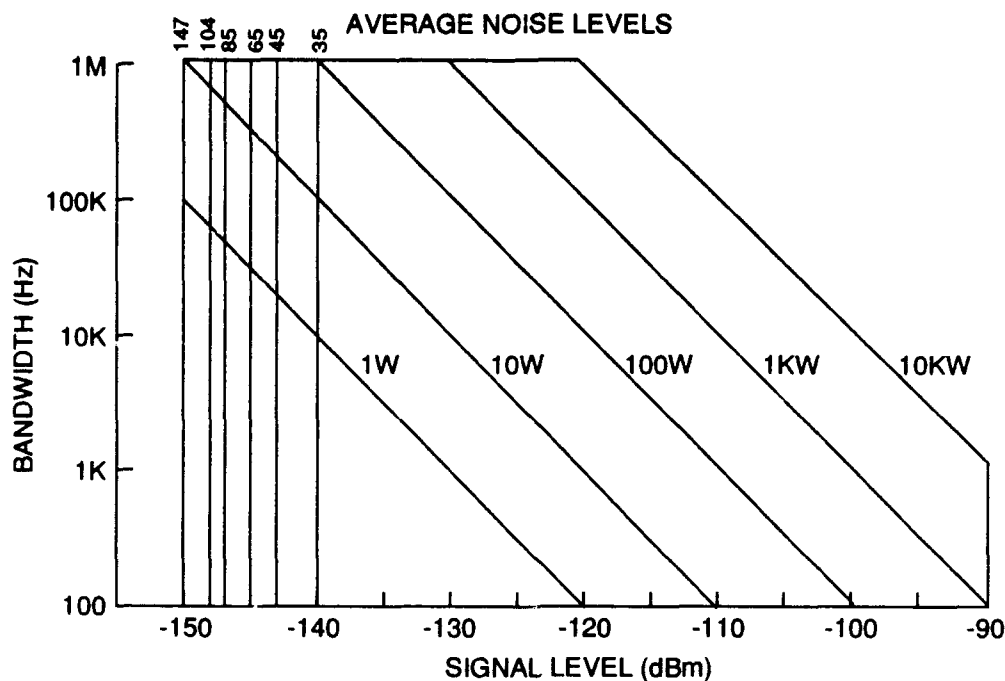


Figure 2. Dynamic Range of the GL Test Bed Receiving System at Thule AB

The data acquired on the test bed are transferred to the GL computer and the date, time, noise level, transmit power, frequency, and other information is attached to each data record. The next step is classification, in which the dominant propagation mechanism in each data record, or sequence of records, is identified.

Classification is an important element of the analysis procedure because several different propagation modes are routinely observed. Due to differences in propagation mechanisms these modes have different communication and propagation characteristics. In addition to underdense and overdense meteor trails, sporadic-E and low level ionospheric scatter propagation occur frequently. An example of a classified meteor trail record is shown in Figure 3.

If the dominant propagation mechanism in the record or sequence of records is meteor scatter, then the type of trail (underdense or overdense) is identified and entered, along with the time of the trail and its duration. The end product for this portion of the data analysis procedure is a set of data bases for each month of link operation.

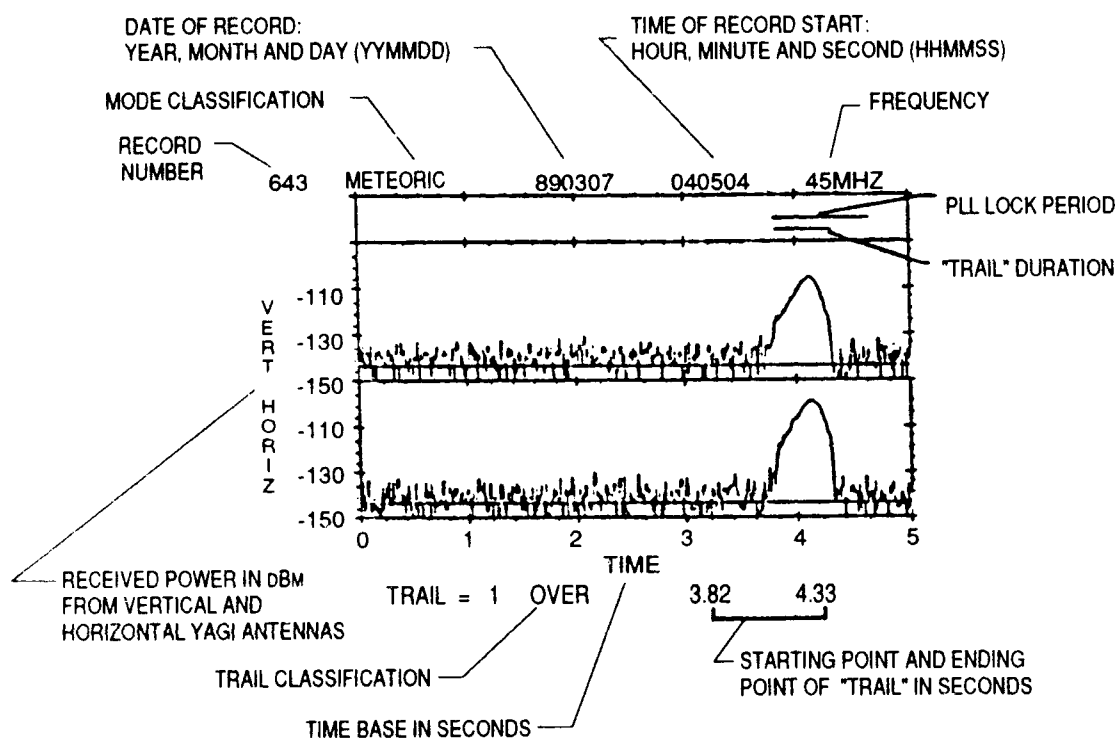


Figure 3. Example of a Meteor Trail Signal

The final step in the processing procedure is statistical analysis of the data bases. Information in the monthly data bases can be retrieved and processed using a menu-driven program that calls a subset of processing routines. The main menu is shown in Table 2. Each of the routines has approximately 10 options that allow the user to analyze the propagation and communication properties of the channel. Consequently, statistical analysis is divided into two general categories; propagation analysis and communication analysis.

The propagation statistics allow analysis of the arrival rate of trails, their duration and duty cycle as a function of trail type, signal level, time of day, day, and frequency. These statistics can be used for a variety of purposes including determination of the effect of ionospheric absorption and to calibrate meteor scatter prediction models.

The communication statistics allow a user to derive the performance of a specified link from the actual data. Parameters that can be defined by the user are the data rate, modulation, bit error rate, packet structure, and signaling protocol. Users can specify either a fixed data rate system or an adaptive data rate system. Available statistics include time to deliver a message, and throughput as a function of time of day, event type (underdense, overdense, sporadic-E, or low level scatter), frequency, modulation, data rate, error rate, packet length, and packet overhead.

The output of the analysis program is presented in either table form or as plots of the content of the tables.

Table 2. Main Menu; Statistical Analysis Options

1. Number of arrivals exceeding a RSL threshold
2. Number of arrivals exceeding a SNR threshold
3. Distribution of time above a RSL threshold
4. Distribution of time above a SNR threshold
5. Noise level and link-up time history
6. Distribution of durations above RSL threshold
7. Distribution of durations above SNR threshold
10. Throughput for idealized adaptive system (for all events)
11. Throughput for idealized adaptive system (for all frequencies)
12. Throughput for realistic fixed rate system (for all frequencies)
13. Throughput for realistic fixed rate system (for all events)
14. Time required to transmit a message (for realistic fixed rate system)
15. Time constants
16. Fade statistics
17. Throughput for realistic adaptive rate system (all frequencies)
18. Throughput for realistic adaptive rate system (all events)

## 2. DESCRIPTION OF THE INVESTIGATION

The aim of the investigation is to determine the power levels for which the waiting times for short duration trails shift from being primarily determined by underdense trails to primarily being determined by overdense trails. This shift occurs because the arrival rate of underdense trails is much larger than the arrival rate for overdense trails at low SNRs and much less than the arrival rate for overdense trails at high SNRs.

The decay time of a meteor trail return is not well correlated with the peak amplitude of the signal, so it is not a simple matter to derive it once the peak amplitude is known. For this reason the arrival rate of signals exceeding a given SNR cannot be translated into the waiting time for meteor scatter signals of a given duration. Most meteor scatter signals fade, so the duration of a signal exceeding a certain SNR is usually not determined by the decay time of the meteor scatter signal but rather by the fading frequency. Also, the signals that do not fade exhibit a wide variety of decay times.

The statistics program does not directly determine waiting time vs signal duration, but the waiting time for the transfer of messages of a given length based on a postulated communication system can be computed. This feature has been used to compute the waiting time statistics presented in this report by creating messages with lengths corresponding to signal durations of interest for the investigation.

In the following sections of this report, the basic meteor scatter signal statistics of arrival rate, duty cycle, and duration as a function of SNR are discussed. Then the waiting time

statistics for meteor scatter signals with durations exceeding 50, 75, 100, 150, 200, and 400 msec are presented and discussed.

To adapt the analysis program to compute waiting time as a function of signal duration rather than as a function of message length, a meteor scatter communication system with a signaling speed of 8000 bits/sec, binary PSK modulation, and a BER of  $10^{-3}$  is postulated. The system occupies a bandwidth of 8000 Hz, which is 19 dB above the 100 Hz bandwidth of the test bed. A SNR of 7 dB in the occupied bandwidth is required to obtain this BER performance. Thus, the SNR required for this system is 26 dB higher than the SNR measured by the test bed receivers.

The choice of signaling speed, and hence system bandwidth, is arbitrary for the computations as long as the resulting range of SNRs for different transmitter powers cover both values for which the arrival rate is dominated by underdense trails and values for which the arrival rate is dominated by overdense trails.

The statistics program allows the user to simulate a change in the transmitter power (nominally 1000 W) by moving the level of the noise floor with a user defined SNR power factor. Thus, a SNR power factor of -10 dB will simulate a system with 10 dB more power than the test bed transmitter, a SNR power factor of 20 dB will simulate a system with 20 dB less power than the test bed transmitter.

For a transmitter power of 10,000 W the required SNR for the postulated system is 16 dB relative to the SNR of the test bed receivers. Similarly, transmitter powers of 100, 10, 5, and 2.5 W require SNRs of 36, 46, 49, and 52 dB relative to the SNR of the test bed.

Message lengths of 400, 600, 800, 1200, 1600, and 3200 bits have been used to obtain the required durations of 50, 75, 100, 150, 200, and 400 msec. To convert from data rate to duration, it is necessary that the system does not use message piecing, and no overhead is added for synchronization. Such a system is an abstraction with no physical implementation, but it is a valid approach for computations.

The statistics program computes the waiting time presented in the tables and graphs from the average waiting time and the required confidence as:<sup>1</sup>

$$\text{confidence} = 1 - e^{-(\text{waiting time}/\text{average waiting time})} \quad (1)$$

For this analysis, a confidence of 0.5 has been chosen and the average waiting time is found by multiplying the waiting time presented on the graphs by  $-1/\ln(0.5) = 1.44$ .

The analysis software classifies the meteor scatter signals as underdense or overdense, and separate arrival rate and duration statistics are produced for the two types of trails, as well as the combination of both types. It is not, however, possible to separate the waiting time statistics according to trail type, because they occur interspersed in time. Thus, for a given transmitter power, the arrival rate statistics for the required SNR will show if the waiting

<sup>1</sup> Weltzen, J.A. (1989) USAF/GL meteor scatter data analysis program. A user's guide, *Geophysics Laboratory Tech Report GL-TR-89-0154*, ADA214988.

time is determined predominantly by underdense trails, overdense trails, or both. The waiting time statistics are presented as a function of frequency, transmitter power, and duration.

This report presents analyses of data collected at 45, 65, and 104 MHz in February, March, June, September, and December 1989, representative of the seasonal variation of meteor scatter activity. The month of February represents the yearly minimum meteor activity and the months of June and September represent the yearly maximum activity.

### 3. ARRIVAL RATE STATISTICS

The arrival rate is defined as the number of signals received each minute exceeding a selected SNR threshold. The arrival rate can be referenced either to a Received Signal Level (RSL) in dBm, or to a Signal-to-Noise Ratio in dB.

The average arrival rates of underdense and overdense meteor trails as a function of SNR, for the months of February, March, June, September, and December 1989 at 45, 65, and 104 MHz, are presented in Appendix B. The SNR's representing transmitter powers of 10 kW, 1000 W, 100 W, and 10 W for the postulated communication system used to compute the waiting times are marked on the figures.

As expected, the arrival rates for underdense trail signals exceed those for overdense trails at low SNRs while the arrival rates of overdense trail signals exceed those for underdense trails at high SNRs. Also, the arrival rates for February and March are almost equal and lower than the arrival rates for the other months.

The largest arrival rates occur in June at 65 and 104 MHz and in September at 45 MHz. It is seen that the arrival rate of overdense trails on all frequencies in June is a larger fraction of the overall arrival rate than for the other months. The effect of this is that the SNR of equal arrival rate for underdense and overdense trails is lower in June than in the other months. The crossover point is at 32-33 dB SNR for 45 MHz, at 39-40 dB SNR for 65 MHz, and at 41-45 dB for 104 MHz, 34 dB at 65 MHz, and 39 dB at 104 MHz. The reason for the difference between the June statistics and the statistics for the other months are not fully understood at this time. However, it is known that propagation during noon hours in June was dominated by sporadic E-layers, which obscured the meteor trails at 45 MHz, and also to a certain extent at 65 MHz, whereas little influence of sporadic E-layer propagation was seen at 104 MHz where the shift of the crossover point is smallest. Thus, the June statistics for 45 MHz must be used with caution. More thorough analysis of the seasonal variation of meteor trail availability is currently being undertaken to address this problem.

According to Forsyth et al<sup>2</sup> the asymptotic slopes of the total arrival rate in log-log coordinates should theoretically be -1 for the part dominated by underdense trails and -4 for the part dominated by overdense trails. Although slopes close to these numbers can be found

<sup>2</sup> Forsyth, P.A. et al (1959) The principles of Janet, a meteor burst communication system, *Proc. IRE*, p. 1650.

in the data, the figures show smoothly varying curves without any obvious knee or abrupt change in slope. This happens because there is no abrupt change from underdense to overdense trails as we increase the SNR, but instead a very gradual shift with a mixture of trail types at all values of SNR. The figures show that with 10,000 W or 1,000 W of transmitter power the arrival rate is dominated by underdense trails. At transmitter powers of 100 W or 10 W, the arrival rate becomes more and more dominated by overdense trails except at 104 MHz where the arrival rate of underdense trails is never much less than the arrival rate of overdense trails.

#### 4. DUTY CYCLE STATISTICS

The duty cycle statistics describe the percentage of time the meteor scatter channel is open, and the signal level or signal-to-noise ratio in the channel exceeds a selected value. The average communication capacity of a meteor scatter link is determined by the average duty cycle at the SNR required for the specified bit error rate. Thus, the average long term capacity for an idealized meteor scatter link can be evaluated from a presentation of the monthly average duty cycle as a function of SNR. It should be noted that the duty cycle does not describe the duration of the individual signals. However, the duty cycle can be used to determine the idealized average channel capacity for a target communication system when no overhead for signal acquisition and handshake is included.

The average duty cycles for the months of February, March, June, September, and December 1989 are presented as a function of SNR for frequencies 45, 65, and 104 MHz in Appendix C. The SNRs representing transmitter powers of 10,000, 1000, 100, and 10 W for the postulated communication system used for the waiting time computations are marked on the figures.

Although the number of underdense trails by far exceeds the number of overdense trails, the duty cycle from overdense trail signals exceeds the duty cycle of underdense trail signals for all SNR levels at 45 MHz, and dominates the duty cycle at high SNR levels for all frequencies. The larger part of the channel capacity is therefore due to the duty cycle of the overdense trails.

It is seen that an increase of 10 dB in SNR is not accompanied by a decrease of a factor 10 in the duty cycle. This means that an increase of signaling speed for a given modulation and bit error rate performance results in a net increase in the average channel capacity. Indefinite bandwidth expansion in order to gain channel capacity is not possible because the arrival rate becomes so low at very high SNRs that virtually no meteor trails exist. Also, the channel capacity will eventually be limited by dispersion. Measurements<sup>3</sup> of the dispersion of the meteor scatter channel have shown the coherence bandwidth to exceed several hundred kHz.

<sup>3</sup> Weltzen, J.A. (1986) The multipath and fading profile of the high latitude meteor burst communication channel, *Rome Air Development Center Tech. Rep.*, RADC-TR-86-166, ADA174718.



The waiting time for short messages will also increase with an increase of the signaling speed, as an increase in SNR is accompanied by a decrease in the arrival rate. The signaling speed that combines short waiting times and high channel capacity has been determined from the test bed data to be approximately 10 kBits/sec.<sup>4</sup> A more thorough discussion of the properties of meteor scatter systems using different signaling speeds as well as adaptive signaling based on analysis of test bed data can be found in Reference 4 and this brief discussion is intended only as an overview.

Thus, the general trend that the capacity of a meteor scatter link increases with signaling speed, that the overdense trails carry by far the largest part of the throughput, and that the waiting time for short messages increases, with signaling speed follow from the arrival rate and duty cycle statistics.

The lowest duty cycles are found in March, but the duty cycles for February are only slightly larger. The largest duty cycles are found in June on all three frequencies.

## 5. DURATION STATISTICS

Duration is defined as a continuous time interval in which the SNR exceeds a specified value. As a meteor signal theoretically has an exponential decay, the duration could be expected to decrease with an increase in SNR. This is true for individual trails without fades. The arrival rate of meteor trails increases with a lower SNR and the overall duration also gets shorter. This in turn will decrease the average duration expected at low SNRs from that of the individual trails. The analysis by Sugar<sup>5</sup> and Jacobsmeyer<sup>6</sup> of duration of meteor trails show the duration account for fading, which breaks a meteor trail signal into segments of shorter duration, and thereby influences the duration statistics.

The average duration of meteor signals as a function of SNR for February, March, June, September, and December 1989 for 45, 65, and 104 MHz are presented in Appendix D. The average duration is seen to be almost independent of SNR with a variation of less than a factor of 2 throughout a SNR range of 30 dB. The duration decreases with an increase of the SNR for low values of the SNR, but may increase again for larger values of the SNR. Thus, the expectation that the average duration should be independent of SNR is supported. The reason for this is presumed to be a combination of short underdense trail signals dominating at low SNRs, the fading associated with the longer lasting trails dominating at mid-range, and the decreasing duration expected from few but very strong signals at high SNRs. The classical

<sup>4</sup> Sowa, M.J., Quinn, J.M., Rasmussen, J.E., Kossey, P.A., Ostergaard, J.C. (1987) A statistical analysis of polar meteor scatter propagation in the 45-104 MHz band, *AGARD Conf. Proc.*, AGARD-CP-419, paper 44.

<sup>5</sup> Sugar, G.R. (1964) Radio propagation by reflection from meteor trails, *Proceedings of the IEEE*.

<sup>6</sup> Jacobsmeyer, J.M. (1987) Digital signal design for meteor scatter communications, Cornell University Thesis.

theory of meteor scatter predicts that the duration should show a strong frequency dependence due to shorter decay time constants at higher frequencies. However, the data presented here show that the duration has little dependence on frequency. Also, very little seasonal variation is seen at all frequencies.

The normalized distributions of signal durations exceeding a specified SNR for the frequencies 45, 64, and 104 MHz are presented in Appendix D. Three different levels of SNR (19, 29, and 39 dB) have been chosen. The normalized distributions show two main features. For each of the frequencies analyzed, the distributions of signal durations are almost independent of the SNR chosen throughout the 20 dB range presented. Also, although the average durations show little frequency dependence, the normalized distributions vary significantly. In particular, the number of long duration signals decreases rapidly as the frequency increases. The overall distributions of duration show little seasonal variation. However, the distributions of duration of underdense trails show a much lower percentage of long lasting trails in September on all frequencies than in any of the other months. The distributions of duration for June show the highest percentage of long enduring signals.

A thorough investigation of the dependence of duration on signal amplitude and fading is currently being undertaken as part of the ongoing research using the Greenland test bed.

## 6. WAITING TIME STATISTICS

The waiting times for trails with durations of 50, 75, 100, 150, 200, and 400 msec, with a confidence of 0.5, are presented as functions of time in 2-hour blocks in Appendix E. Statistics covering the five months (February, March, June, September, and December) are presented.

The waiting times have been computed as a function of transmitter power using the postulated meteor scatter communication system described in Section 2 (Binary PSK modulation  $10^{-3}$  BER, 8000 bits/sec signaling speed, no initialization time, and no message piecing). Messages of 400, 600, 800, 1200, 1600, and 3200 bits have been used to model durations of 50, 75, 100, 150, 200, and 400 msec respectively. SNR power factors of -10, 0, 10, 20, and 33 dB have been used to model communication systems with 10 kW, 1 kW, 100 W, 10 W, and 5 W of transmitter power. Due to the higher galactic noise background at 45 MHz, the dynamic range of the receiving system does not allow the performance as a function of power to be evaluated below 10 W. Because the galactic noise is lower at the higher frequencies, the data is valid for power levels as low as 5 W at 65 MHz and 104 MHz.

The waiting times for each 2-hour time block throughout the day have been calculated at three frequencies (45, 65, and 104 MHz) for each of the six specified durations (50, 75, 100, 150, 200, and 400 msec) and for each of the five power levels (10 W, 1 W, 100 W, 10 W, and 5 W) where applicable. This process resulted in the 150 curves presented in Appendix E. From these the average waiting times have been computed as the average value of the diurnal

variation multiplied by 1.44 as discussed in Section 2 of this report. The average values are presented in Appendix F and discussed below in Section 6.2.

### 6.1 Diurnal Variations of Waiting Times

The waiting time is, as expected, frequency dependent. The waiting times are much lower at 45 MHz than at 65 MHz and the waiting time at 104 MHz is the longest in all cases. The waiting time also increases with a decrease in transmitter power. In some cases, the waiting time is undetermined or exceeds 10,000 seconds, which is the realistic limit for the statistics to be valid. Thus, some time blocks, especially with transmitter powers less than 100 W, do not have a waiting time associated with them, as not enough trails were available to support the propagation.

At 45 MHz, however, another reason for missing data points exists. In June, between 10 UT and 20 UT, data points are missing even at transmitter powers of 1 kW and 10 kW, while at the same time the waiting time is low, on the order of a few seconds, on the edges of this time interval. This is caused by sporadic E-layer propagation supplying a nearly continuous propagation path between 10 UT and 20 UT. This means that there was no waiting time, but also that the meteor signals were obscured and the waiting time due to meteor trail signals could not be derived from the test bed data. At 65 and 104 MHz the meteor trail signals provided enough connectivity to enable the waiting time to be derived.

The diurnal variation is a function of season. In February a variation of approximately a factor of 3 is seen. A shallow minimum in the waiting time occurs at about 0600 UT and the maximum around 1200 UT, coinciding with the diurnal galactic noise maximum for the month of February. A secondary minimum is found around 1600 UT, which is most likely caused by the presence of the diurnal galactic noise minimum at this time during the month of February, combined with meteor trails arriving over the north pole. This contribution of meteor trails from the morning side of the earth is presumed to account for the partial absence of a late afternoon arrival rate minimum at high latitudes. For calculating local time, the midpoint of the link is geographically four hours west of Greenwich.

The diurnal variation is less pronounced in March where the diurnal noise maximum occurs at 10 UT, coinciding with the early morning maximum of meteor influx. The effects of higher noise and larger arrival rate of meteor trails counteract each other and the diurnal variation of the waiting time is smoothed out as a result. The overall waiting times are shortest in June compared to the other months, but a larger diurnal variation is seen, since the increase in waiting time caused by low arrival rates around midnight UT is enhanced by the presence of the diurnal noise maximum at the same time.

The magnitude of the diurnal variation seems to increase with frequency for transmitter powers less than 100 W. This is most likely an artifact of the statistics, as only few meteor trail signals have been available for computation of waiting times in excess of 30 minutes. Longer waiting times, presumably of limited interest, must be used with caution.

## 6.2 Average Waiting Times

The monthly average waiting times at Thule were obtained by taking the mean of the 12 daily time block values for each of the 90 curves. These average values provided the basis for the waiting time statistics shown in Appendix F. Lines separating statistics dominated by underdense trails from statistics dominated by overdense trails are shown on the figures. The lines of separation correspond to the points of equal arrival rates of underdense and overdense meteor trail signals in Appendix B. The lines do not mark a sharp boundary, as the contribution from either type of trail shows a smooth transition from predominantly underdense trails to predominantly overdense trails, as described in Section 3.

### 6.2.1 WAITING TIME AS A FUNCTION OF TRANSMITTER POWER

The waiting time for trails of a given length as a function of transmitter power are shown for 45, 65, and 104 MHz in Appendix F. As with the arrival rate statistics, we would expect the waiting time vs transmitter power statistics to show a change of slope as the waiting time moves from being dominated by overdense trail signals at low power to being dominated by underdense trails at high power. For the power levels modeled by the data base there appears to be no abrupt knee or change in slope, but a slow change indicating a very gradual shift in the contribution from overdense to underdense trails.

The waiting time at 45 MHz approximately doubles each time the duration is doubled over the range from 50 to 400 msec. At 65 and 104 MHz the waiting time increases by factors of about 2.3 and 2.6 respectively each time the required duration is doubled.

The seasonal variation shows minimum waiting times in June, very little difference between the waiting times in February and March, and surprisingly little difference between waiting times in September and December. The December waiting times could have been expected to be longer than the September waiting times because the meteor trail arrival rate is larger in September than in December. The explanation is found in the normalized distributions of duration presented in Appendix D. In September, the percentage of long durations, especially at high values of SNR, was much less than during the other months. Thus, shorter durations, not lower arrival rates, must be the cause for the longer than expected waiting times in September.

### 6.2.2 WAITING TIME AS A FUNCTION OF DURATION

Waiting times have also been computed as a function of duration for the selected transmitter power levels. As expected, the waiting time significantly increases with frequency. It takes 6 times longer to deliver a message requiring a 200 msec signal at 65 MHz than at 45 MHz and about 20 times longer at 104 MHz. Also, 100 W transmitter power is seen to be the practical lower limit for 45 and 65 MHz, whereas 1 kW is needed at 104 MHz to obtain waiting times less than several thousand seconds. Again, the seasonal variation shows little

difference between February and March and the shortest waiting times are found in June. The waiting times in September differ very little from the waiting times in December.

### 6.2.3 WAITING TIME AS A FUNCTION OF FREQUENCY

Finally, the average waiting time statistics are presented as a function of frequency and duration for four selected power levels (10 W, 100 W, 1 kW, 10 kW). From these curves it can be seen that for meteor signal durations from 50 to 400 msec, and regardless of frequency (45, 65, or 104 MHz), the waiting time can be reduced by a factor of about 3 1/2 by increasing the power from 100 W to 1 kW. For meteor signal durations of 200 msec at 65 MHz, the waiting time can be reduced by about a factor of 6 if the power is increased from 100 W to 10 kW.

The waiting times are dominated by underdense trails as expected, except at transmitter power levels of 10 W and 100 W where they are dominated by overdense trails. At a first glance it may seem paradoxical that the waiting times can be dominated by overdense trails, but inspection of the arrival rates presented in Appendix B shows that at low power the low frequency, short waiting times are indeed dominated by overdense trails.

## 7. SUMMARY

A special investigation of the average waiting times for meteor scatter signals exceeding selected durations has been performed by the Geophysics Laboratory using data from the GL meteor scatter test bed in Greenland. The investigation is based on data from the 1200 km link between Sondrestrom AB and Thule AB for the frequencies 45, 65, and 104 MHz. The location and properties of the test bed and the procedures used to analyze the data acquired with the test bed are described.

Meteor scatter statistics of arrival rates, duty cycles and durations as a function of the signal-to-noise ratio in the meteor scatter channel are provided as an aid to interpret the waiting time statistics.

The waiting times associated with specific signal durations (50, 75, 100, 150, 200, and 400 msec), are presented as a function of transmitter power for each frequency for the months of February, March, June, September and December 1989.

One aim of the analysis is to determine the transmitter power level for which the waiting time for a meteor trail signal of a specified duration changes from being dominated by underdense trails to being dominated by overdense trails. The transition is smooth and is found to be around 200 W at 45 MHz, 50 W at 65 MHz and approximately 10 W at 104 MHz.

The seasonal variation of the waiting times is to a certain degree unexpected. The waiting times for February and March differ very little and, as expected, are longer than the waiting times in June where the arrival rate of meteor trails is higher. However, the waiting times in September are longer than would have been expected for a summer month and they do not differ from the waiting times in December. It is found that the distribution of signal durations

in September has a larger percentage of short duration signals than do the other months. Thus, the unexpectedly long waiting times in September are caused by a lack of signals of sufficient endurance, rather than a low arrival rate.

## References

1. Weitzen, J.A. (1989) USAF/GL meteor scatter data analysis program. A user's guide, *Geophysics Laboratory Tech Report GL-TR-89-0154*, ADA214988.
2. Forsyth, P.A. et al (1959) The principles of Janet, a meteor burst communication system, *Proc. IRE*, p. 1650.
3. Weitzen, J.A. (1986) The multipath and fading profile of the high latitude meteor burst communication channel, *Rome Atr Development Center Tech. Rep.*, RADC-TR-86-166, ADA174718.
4. Sowa, M.J., Quinn, J.M., Rasmussen, J.E., Kossey, P.A., Ostergaard, J.C. (1987) A statistical analysis of polar meteor scatter propagation in the 45-104 MHz band, *AGARD Conf. Proc.*, AGARD-CP-419, paper 44.
5. Sugar, G.R. (1964) Radio propagation by reflection from meteor trails, *Proceedings of the IEEE*.
6. Jacobsmeier, J.M. (1987) Digital signal design for meteor scatter communications, Cornell University Thesis.

## **Appendix A**

### **Receiver Noise Data**



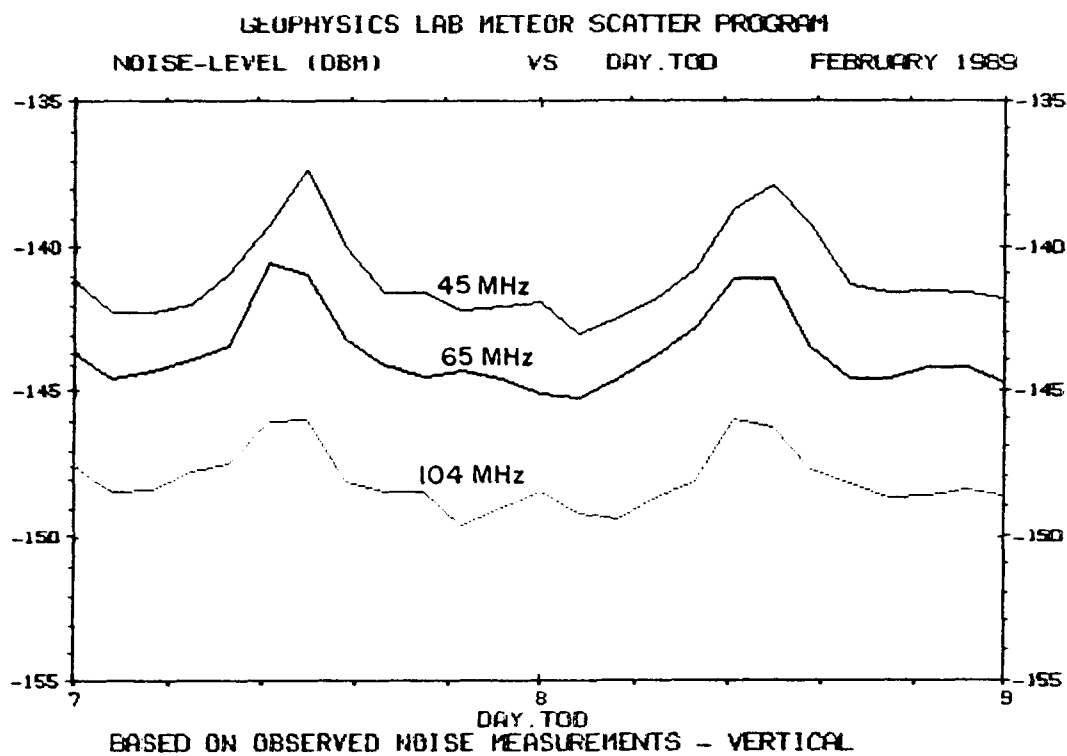


Figure A1. Diurnal Variation of the Receiver Noise at Thule AB.  
February 1989

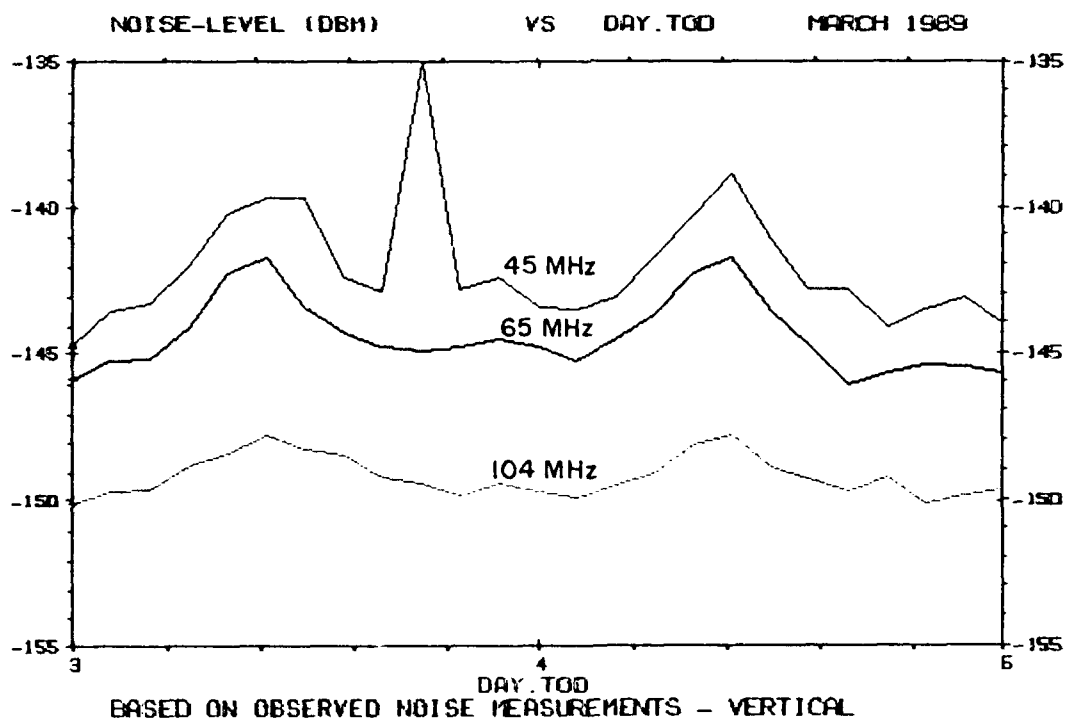


Figure A2. Diurnal Variation of the Receiver Noise at Thule AB.  
March 1989

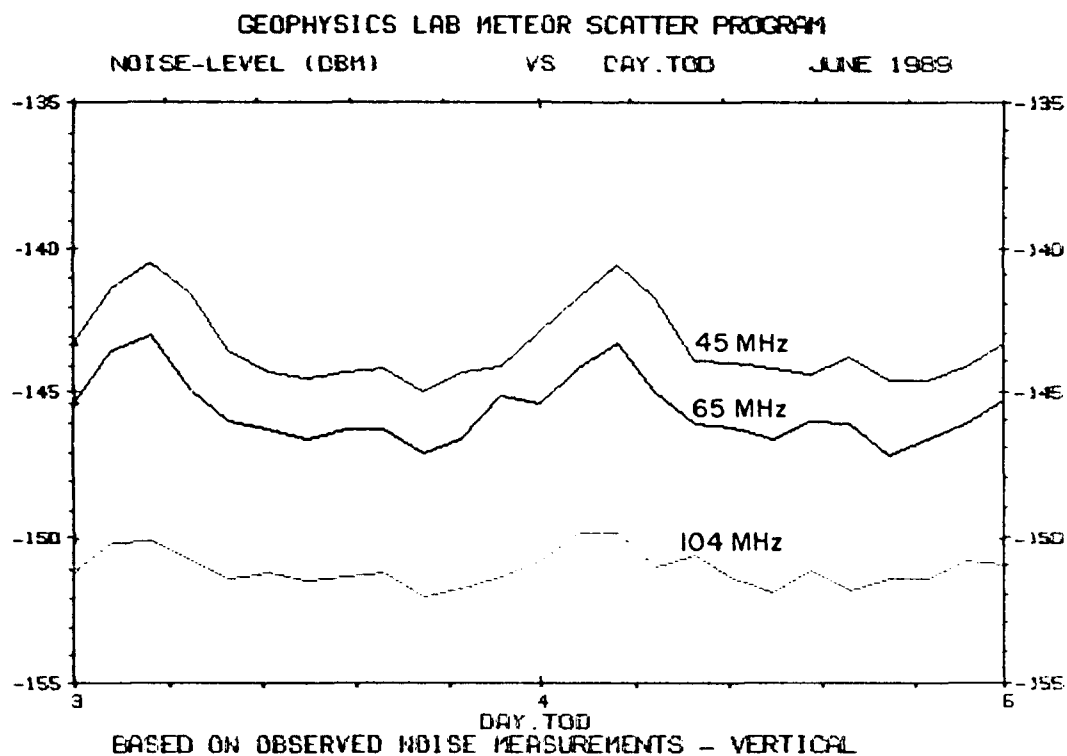


Figure A3. Diurnal Variation of the Receiver Noise at Thule AB.  
June 1989

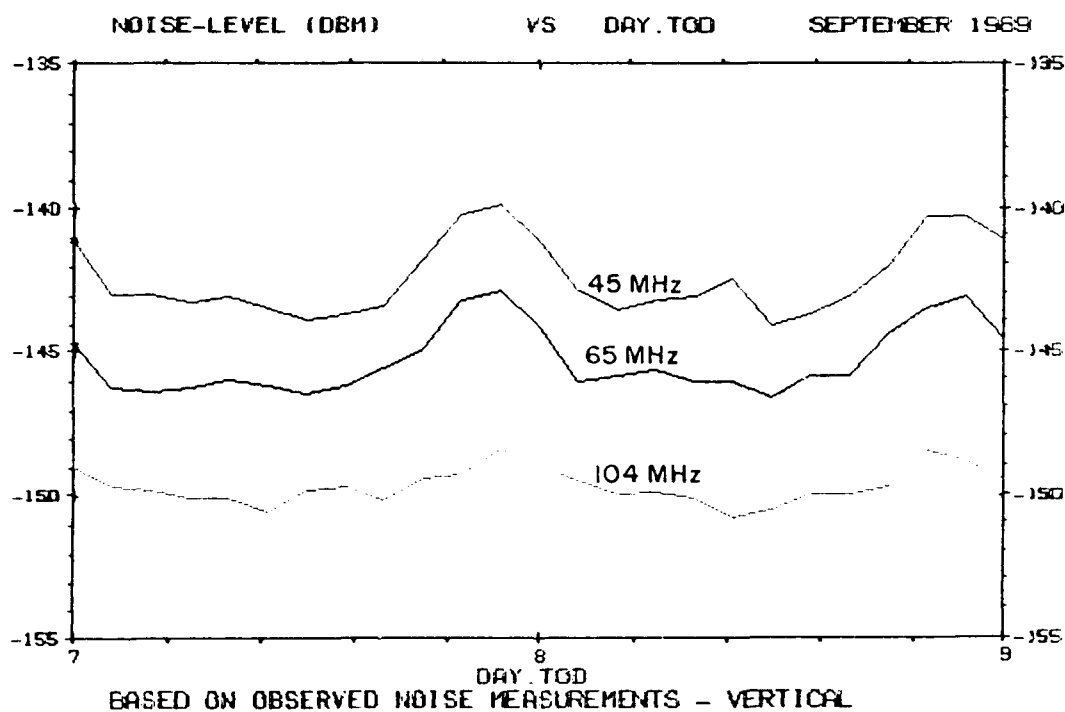


Figure A4. Diurnal Variation of the Receiver Noise at Thule AB.  
September 1989

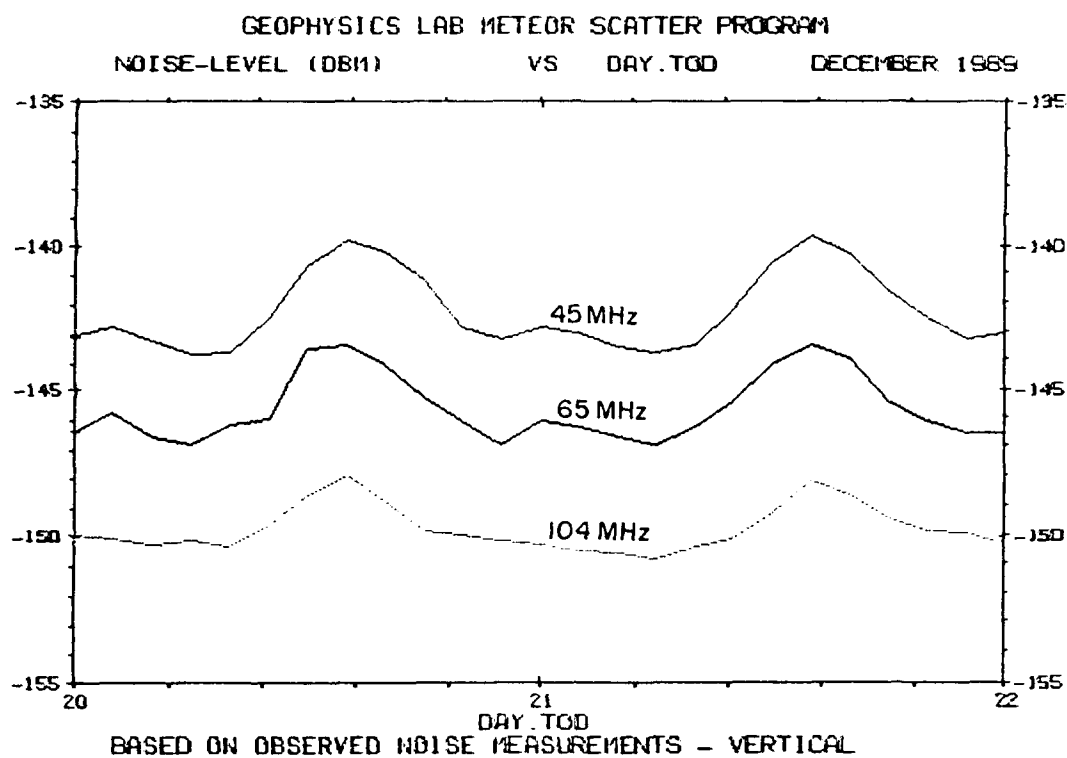
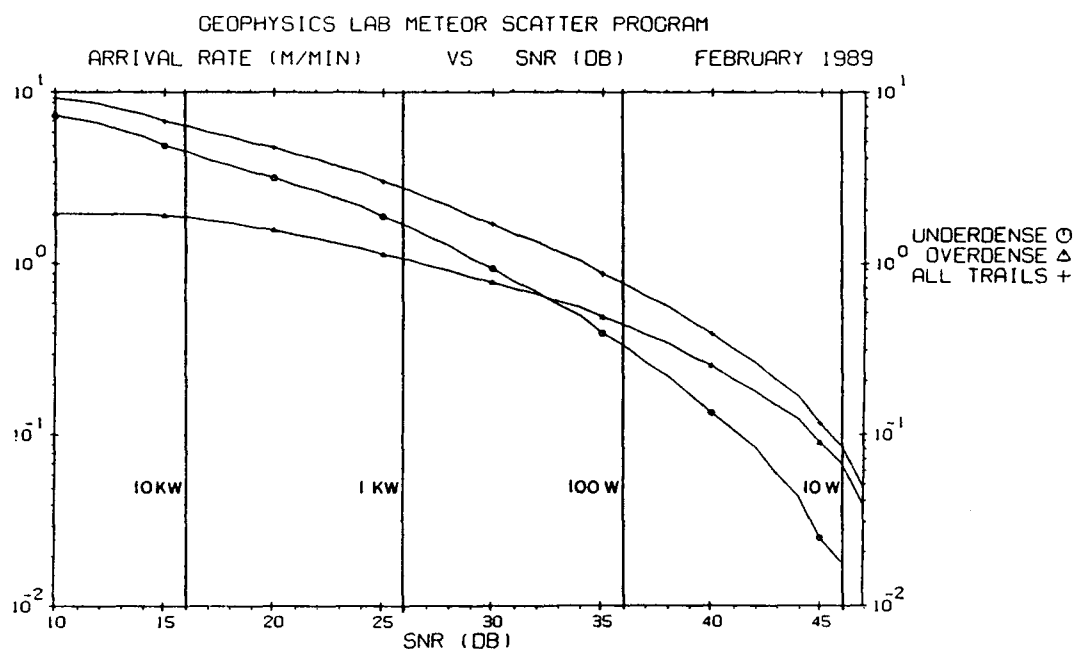


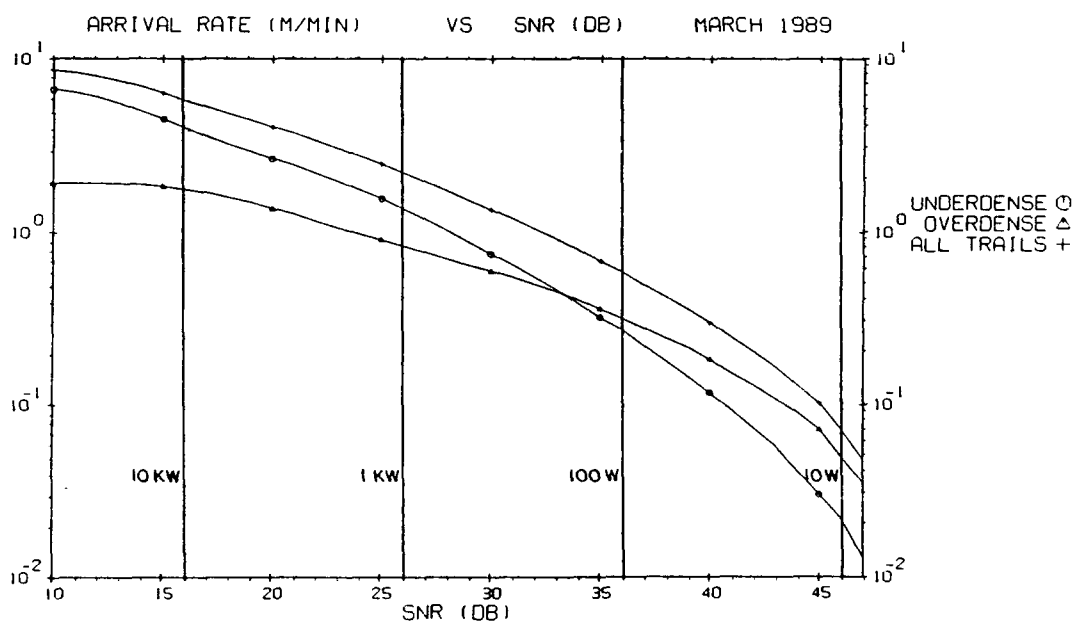
Figure A5. Diurnal Variation of the Receiver Noise at Thule AB.  
December 1989

## **Appendix B**

### **Meteor Arrival Rate Statistics**



**Figure B1. Meteor Arrival Rate for February 1989 at Thule. The Frequency is 45 MHz**



THE TIME OF DAY IS 0 - 24 HOURS U.T.  
FREQUENCY = 45 MHZ  
EFFECTIVE SYSTEM BANDWIDTH = 100.HZ  
POLARIZATION = HORIZONTAL  
MAXIMUM DOWN TIME DUE TO SPORADIC-E = 240 SECONDS  
BASED ON AVERAGED NOISE MEASUREMENTS - HORIZONTAL

**Figure B2. Meteor Arrival Rate for March 1989 at Thule. The Frequency is 45 MHz**

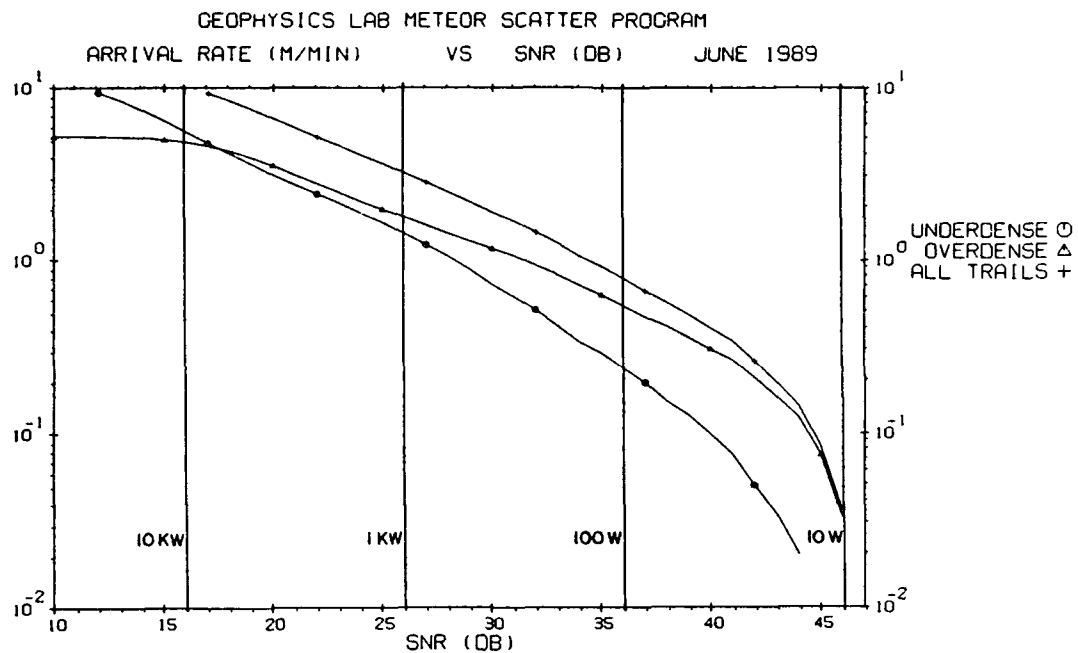


**Figure B3. Meteor Arrival Rate for June 1989 at Thule. The Frequency is 45 MHz**

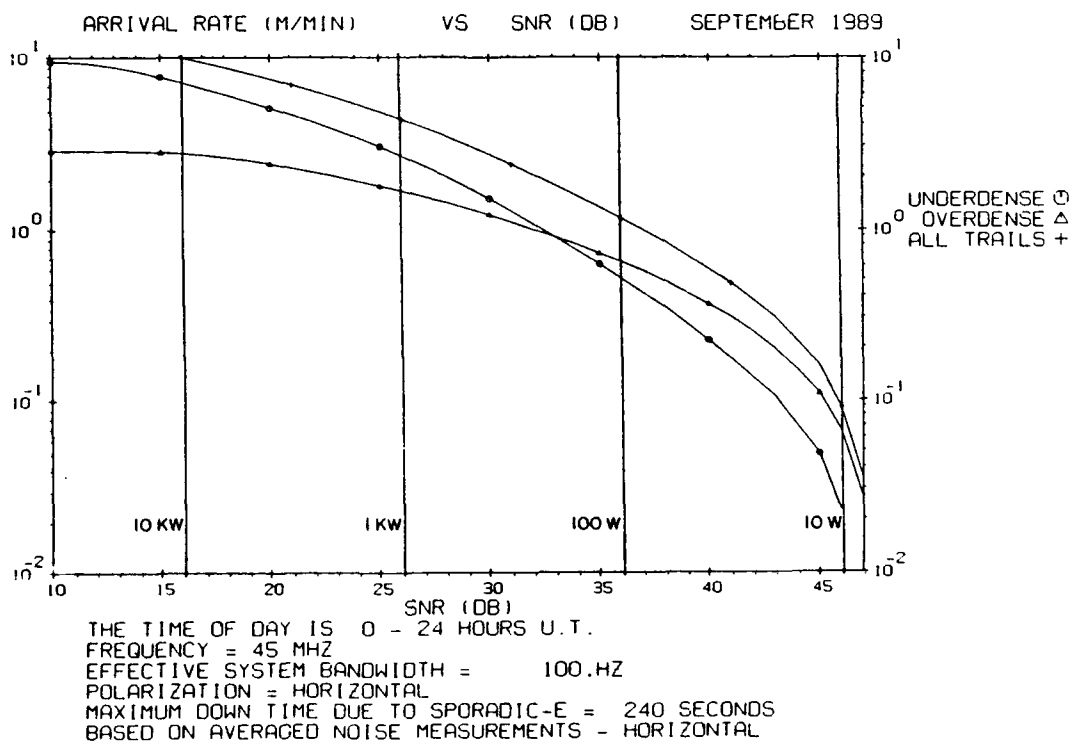


**Figure B4. Meteor Arrival Rate for September 1989 at Thule. The Frequency is 45 MHz**

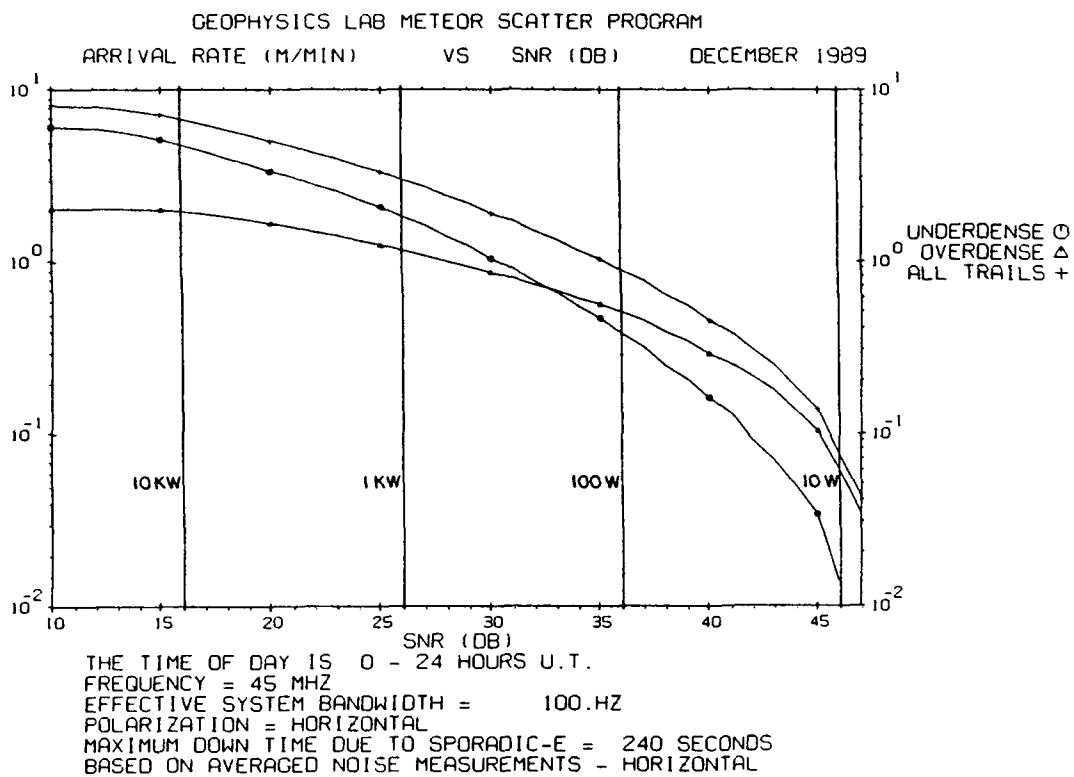


**Figure B5. Meteor Arrival Rate for December 1989 at Thule. The Frequency is 45 MHz**

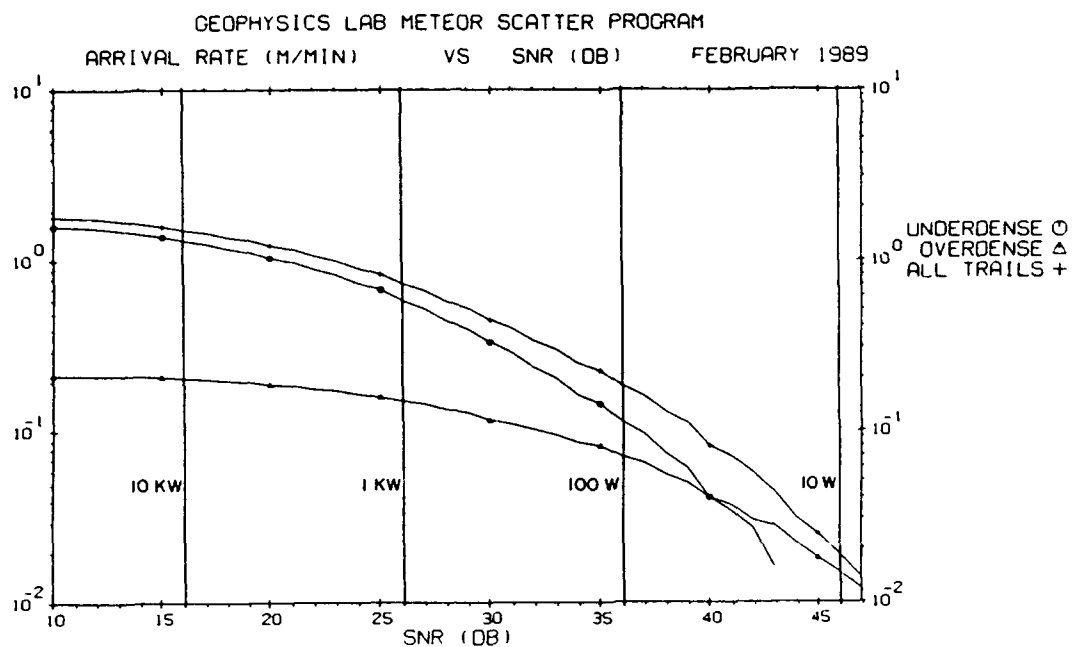


Figure B6. Meteor Arrival Rate for February 1989 at Thule. The Frequency is 65 MHz

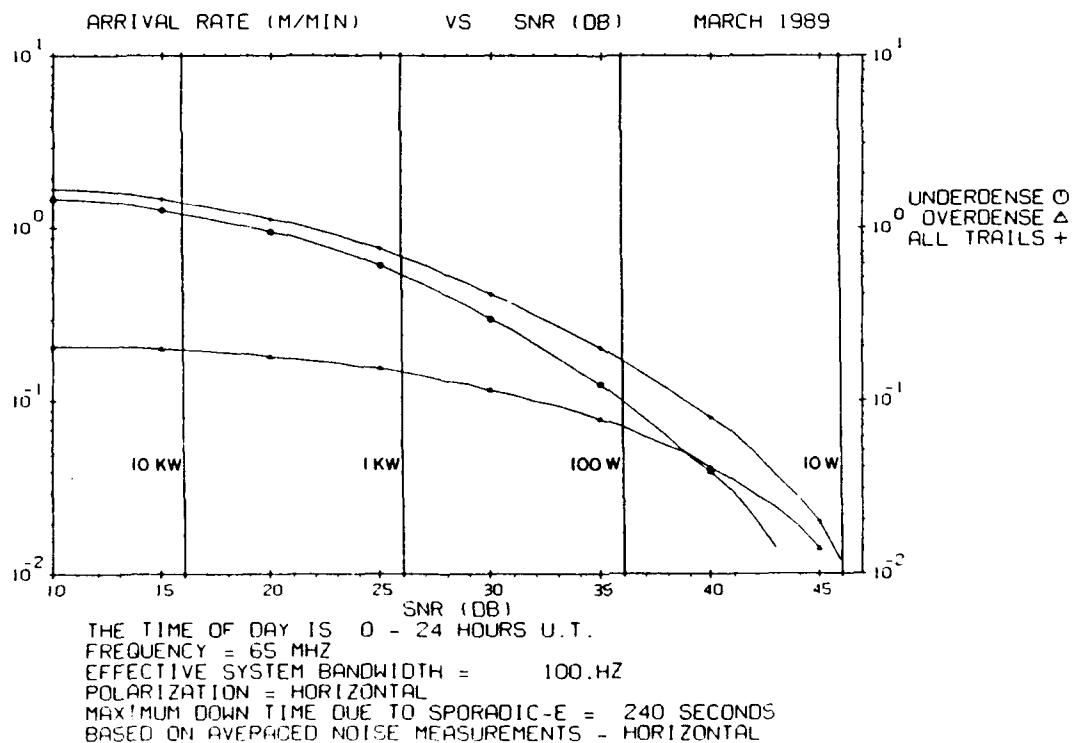
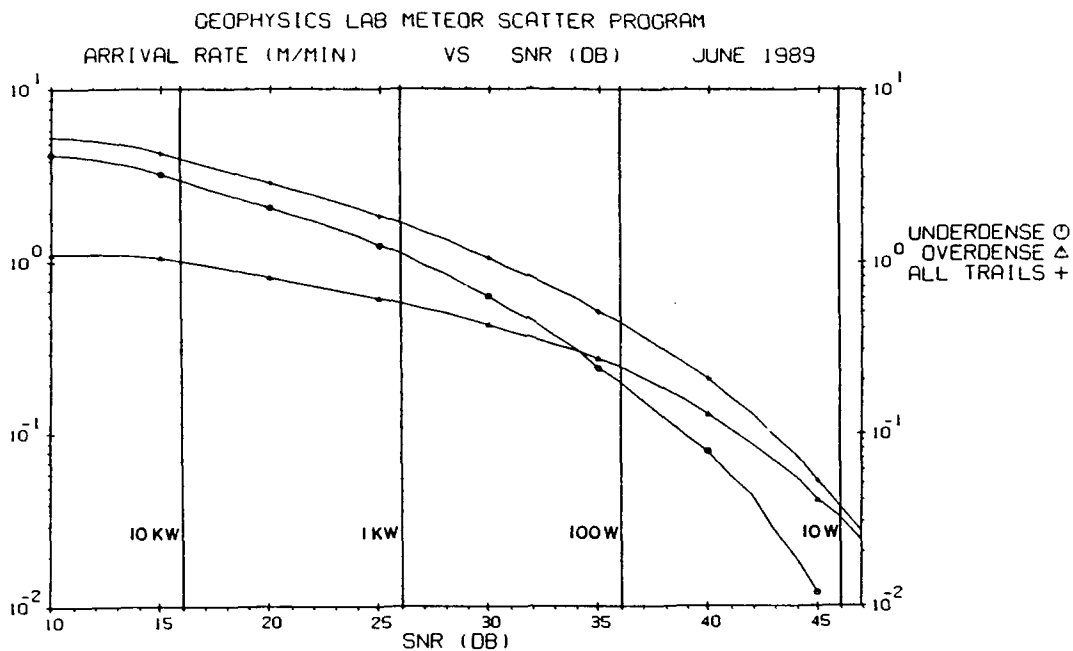
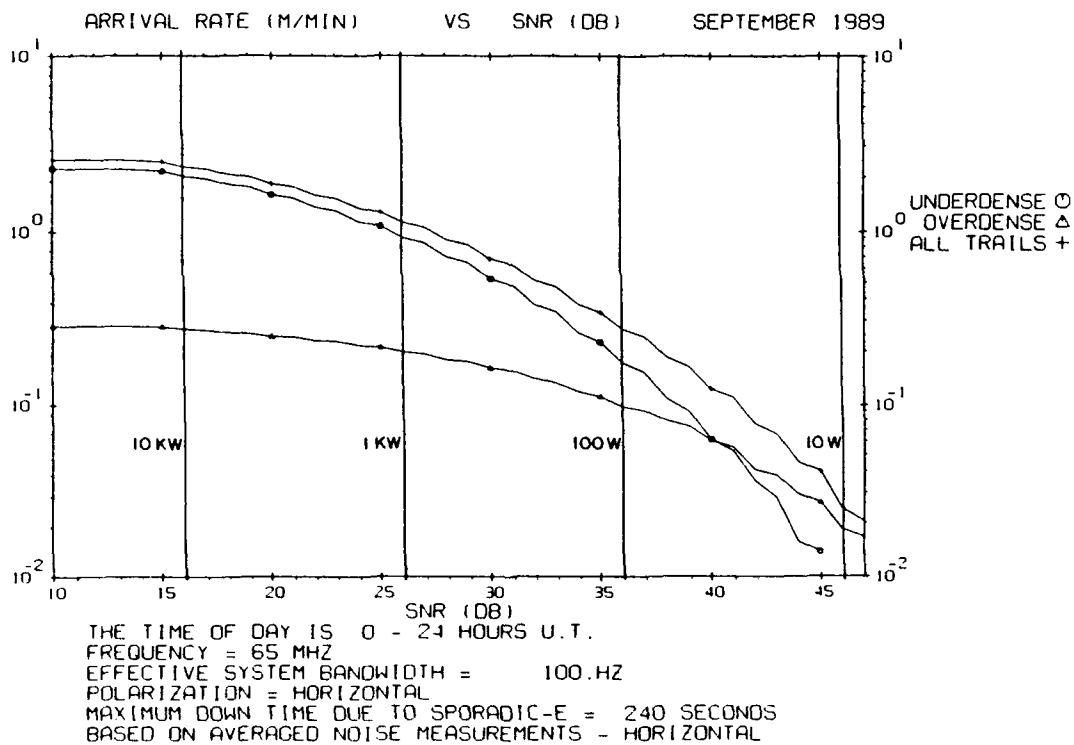


Figure B7. Meteor Arrival Rate for March 1989 at Thule. The Frequency is 65 MHz





**Figure B8. Meteor Arrival Rate for June 1989 at Thule. The Frequency is 65 MHz**



**Figure B9. Meteor Arrival Rate for September 1989 at Thule. The Frequency is 65 MHz**

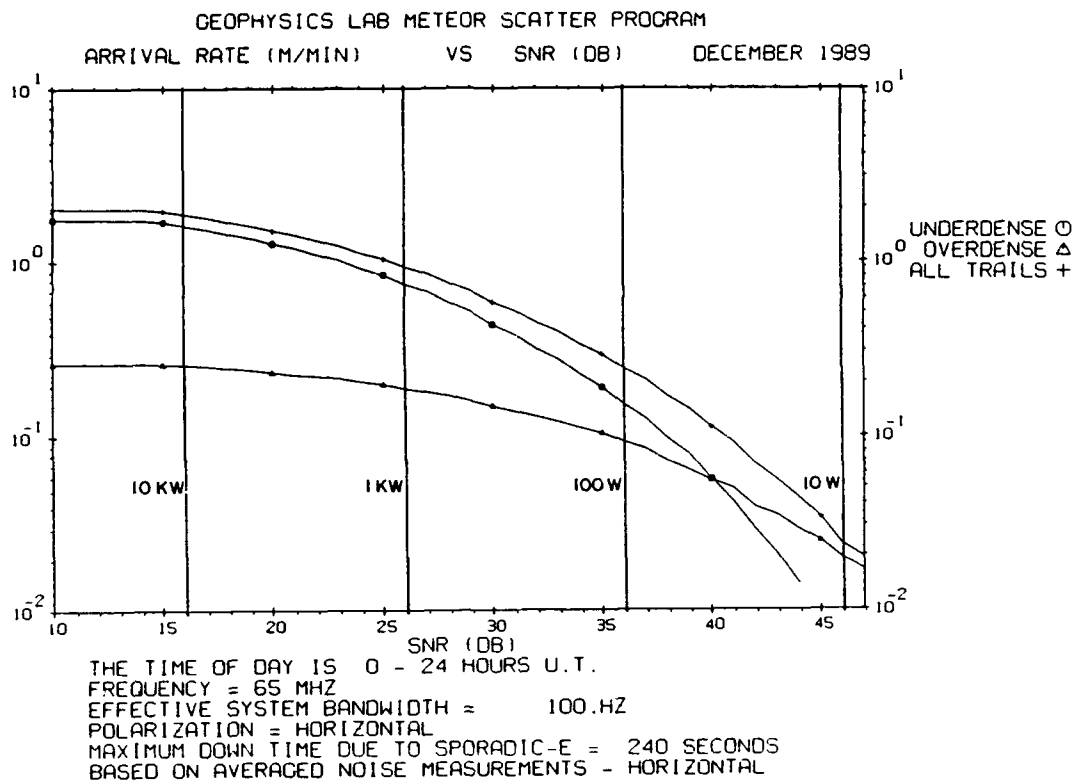


**Figure B10. Meteor Arrival Rate for December 1989 at Thule. The Frequency is 65 MHz**

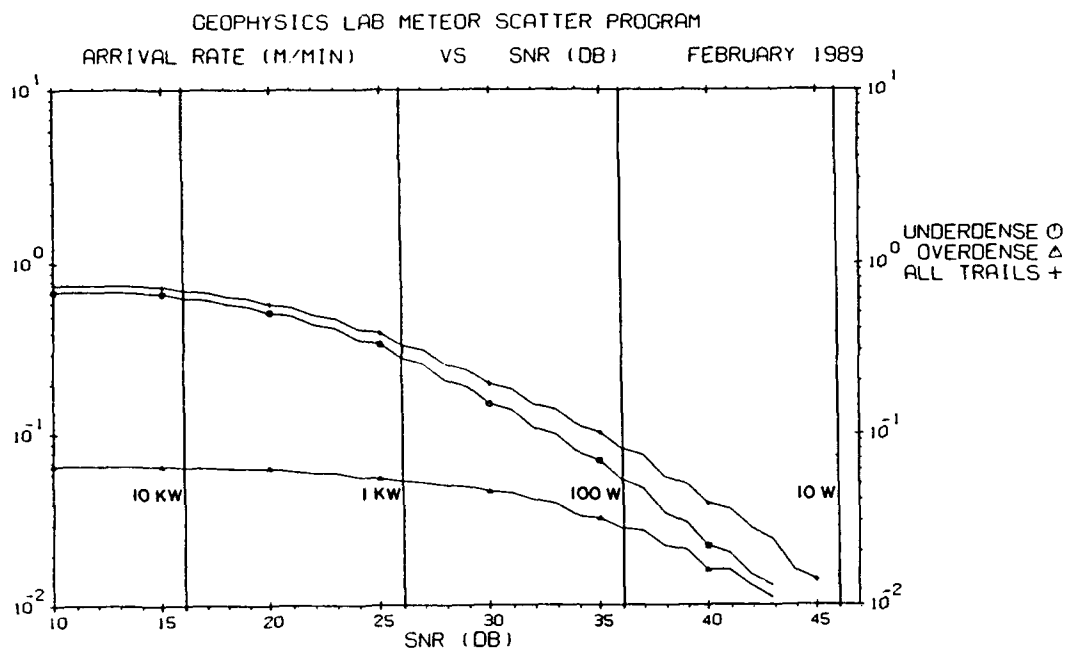


**Figure B11. Meteor Arrival Rate for February 1989 at Thule. The Frequency is 104 MHz**

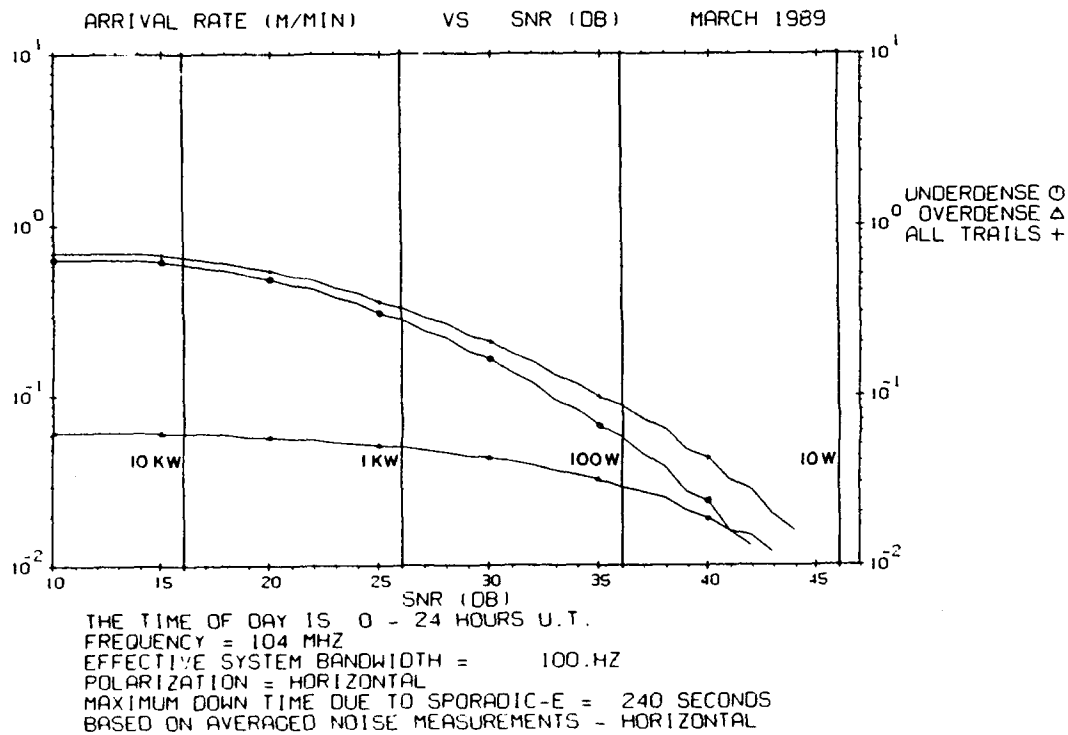


**Figure B12. Meteor Arrival Rate for March 1989 at Thule. The Frequency is 104 MHz**

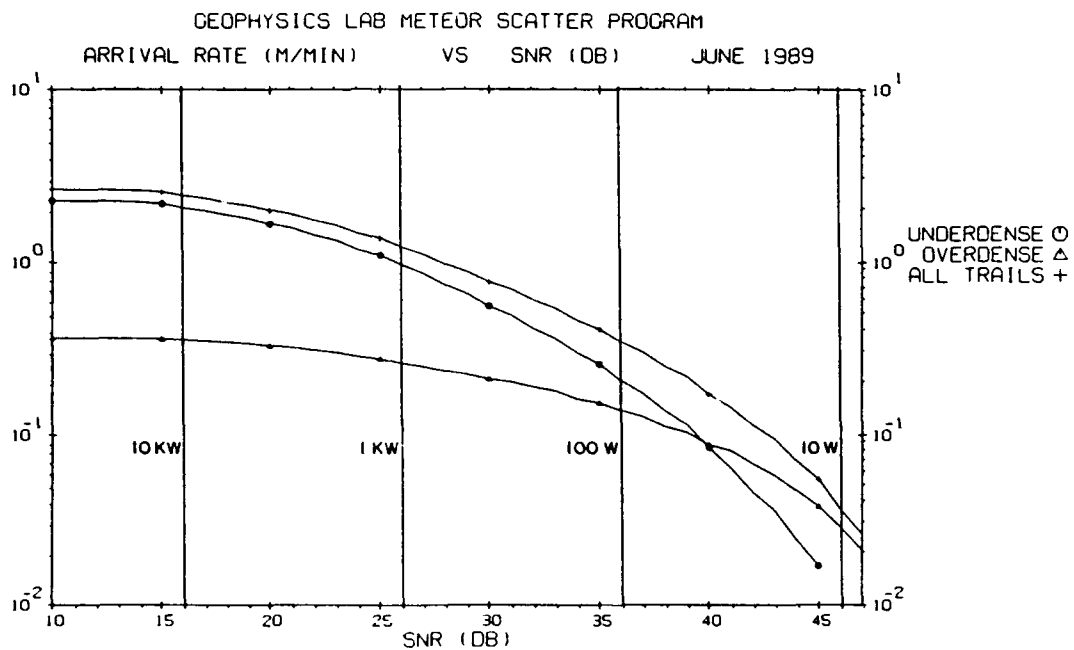


Figure B13. Meteor Arrival Rate for June 1989 at Thule. The Frequency is 104 MHz

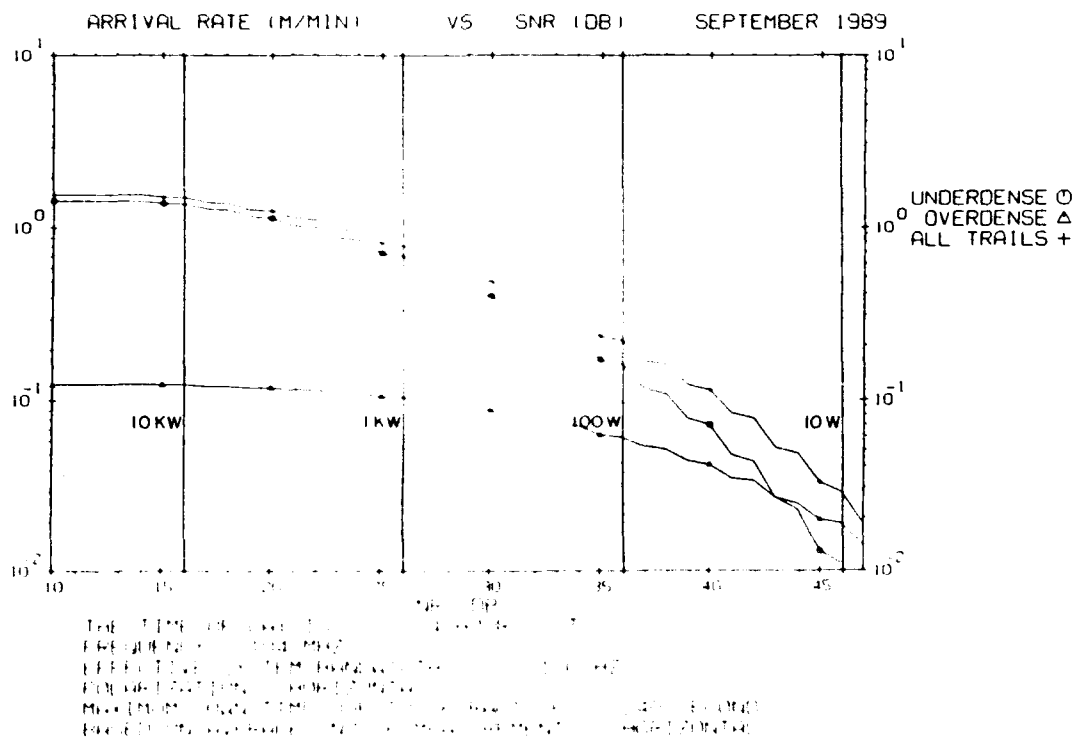
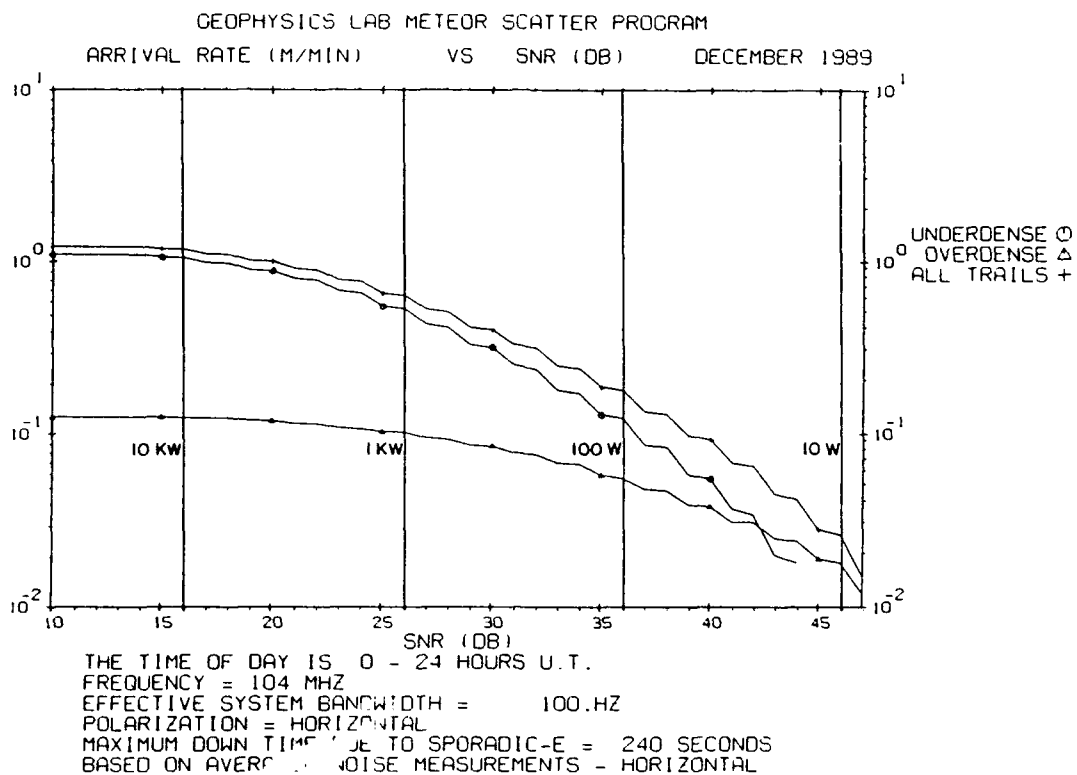


Figure B14. Meteor Arrival Rate for September 1989 at Thule. The Frequency is 104 MHz



**Figure B15. Meteor Arrival Rate for December 1989 at Thule. The Frequency is 104 MHz**

## **Appendix C**

### **Duty Cycle Statistics**

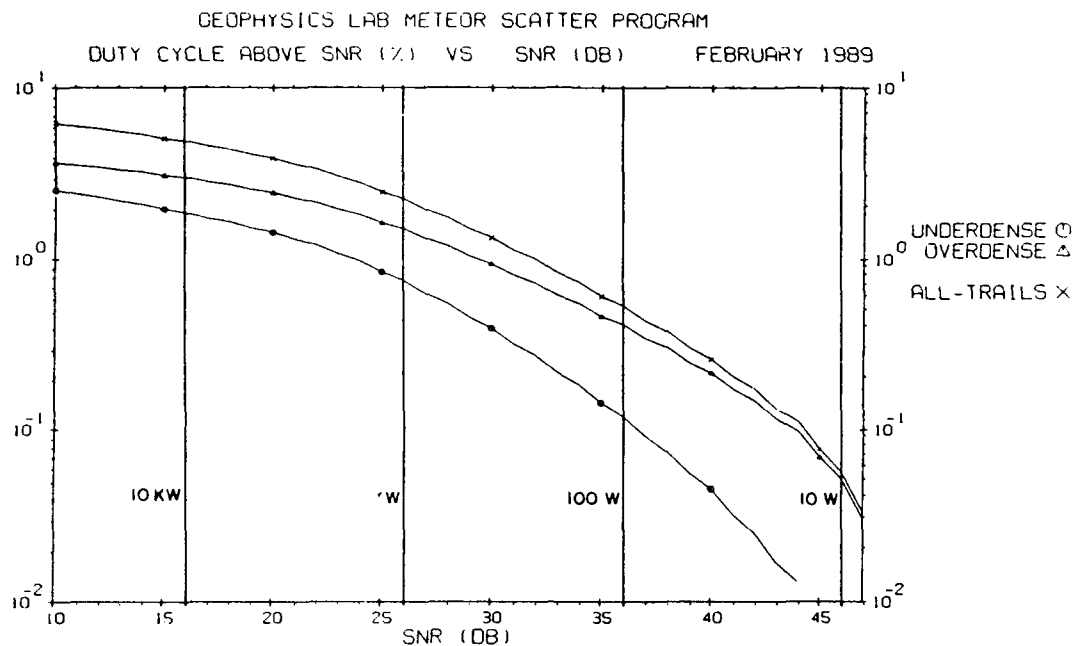


**Figure C1. Duty Cycle Exceeding a SNR Threshold for February 1989 at Thule. The frequency is 45 MHz**

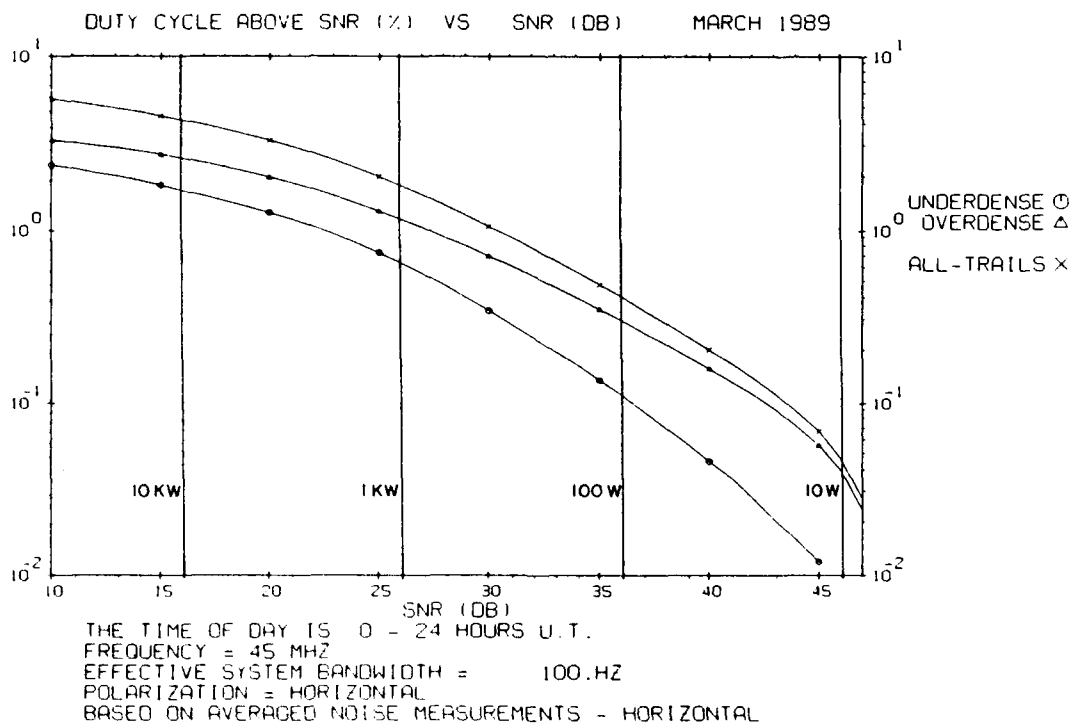


**Figure C2. Duty Cycle Exceeding a SNR Threshold for March 1989 at Thule. The frequency is 45 MHz**

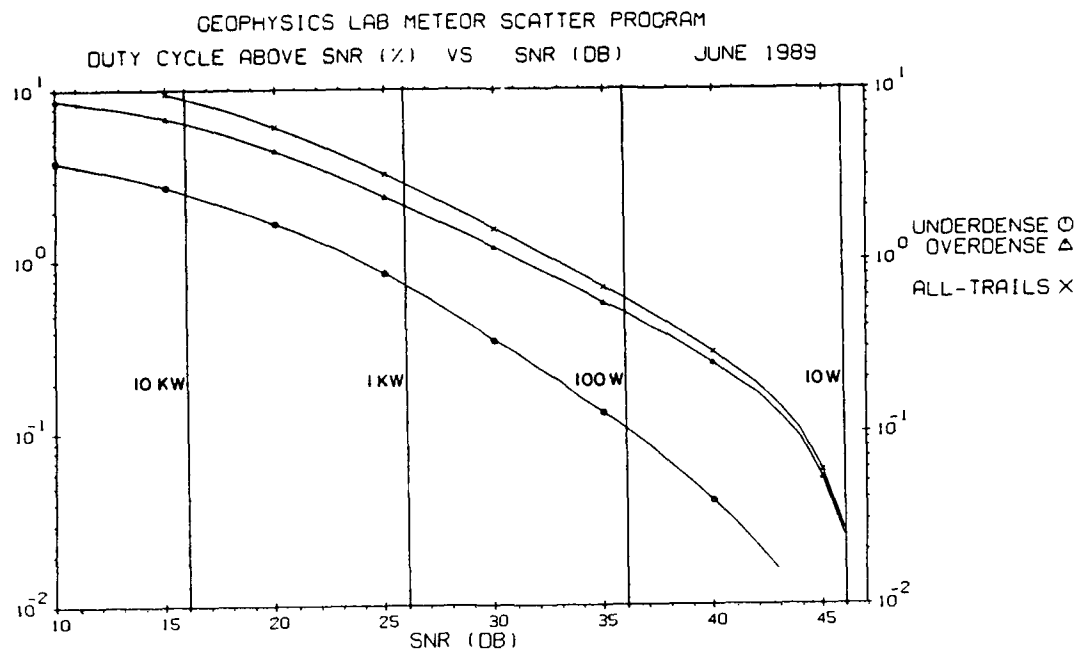


**Figure C3. Duty Cycle Exceeding a SNR Threshold for June 1989 at Thule. The frequency is 45 MHz.**

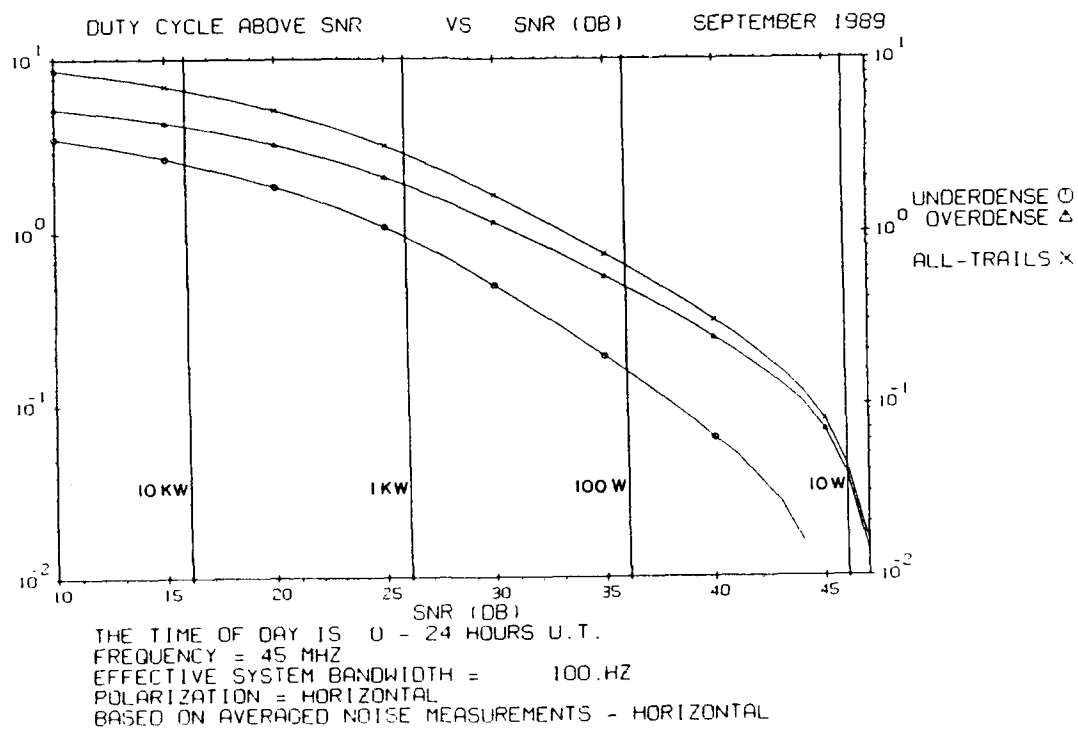


**Figure C4. Duty Cycle Exceeding a SNR Threshold for September 1989 at Thule. The frequency is 45 MHz**



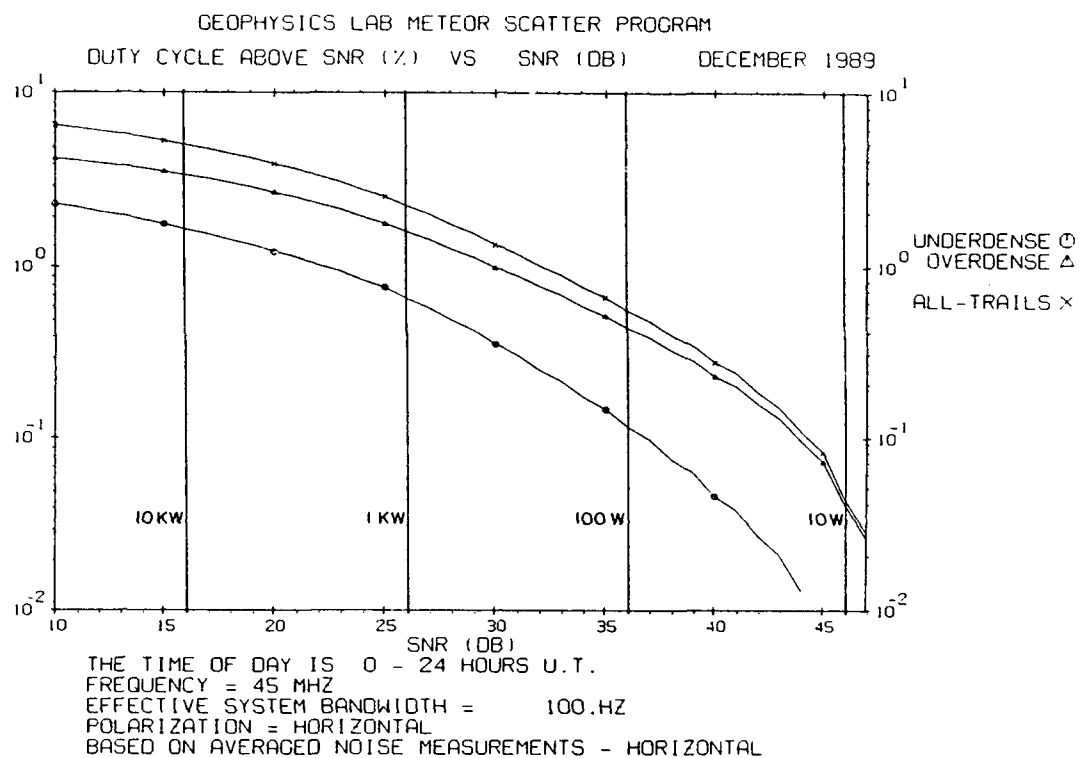


**Figure C5. Duty Cycle Exceeding a SNR Threshold for December 1989 at Thule. The frequency is 45 MHz**

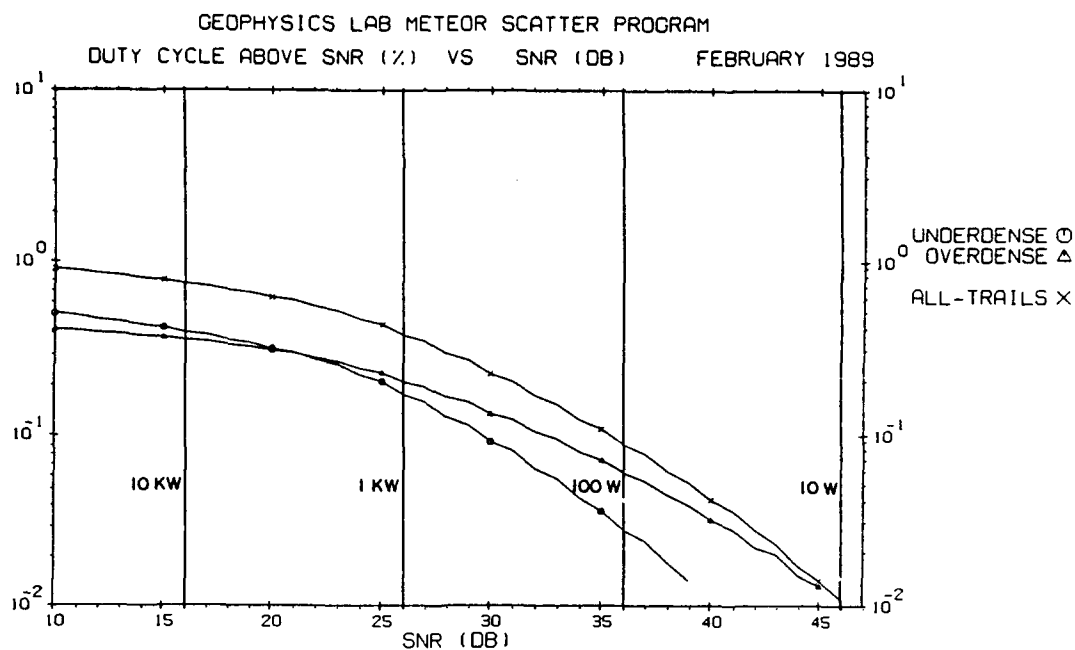


**Figure C6. Duty Cycle Exceeding a SNR Threshold for February 1989 at Thule. The frequency is 65 MHz**

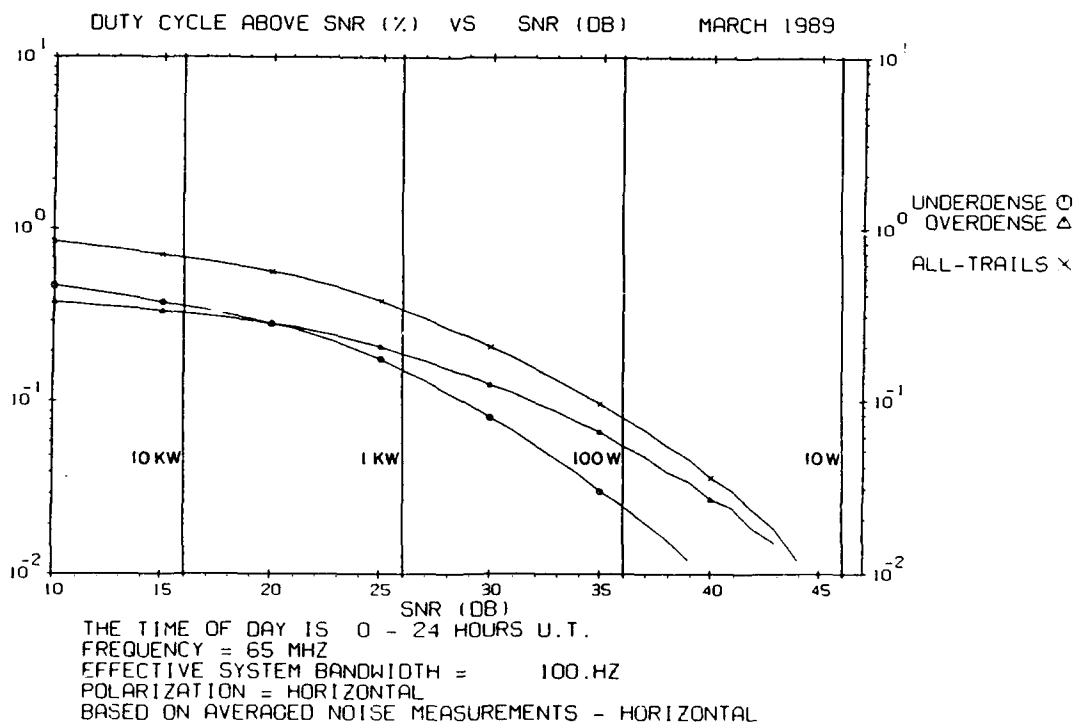


**Figure C7. Duty Cycle Exceeding a SNR Threshold for March 1989 at Thule. The frequency is 65 MHz**

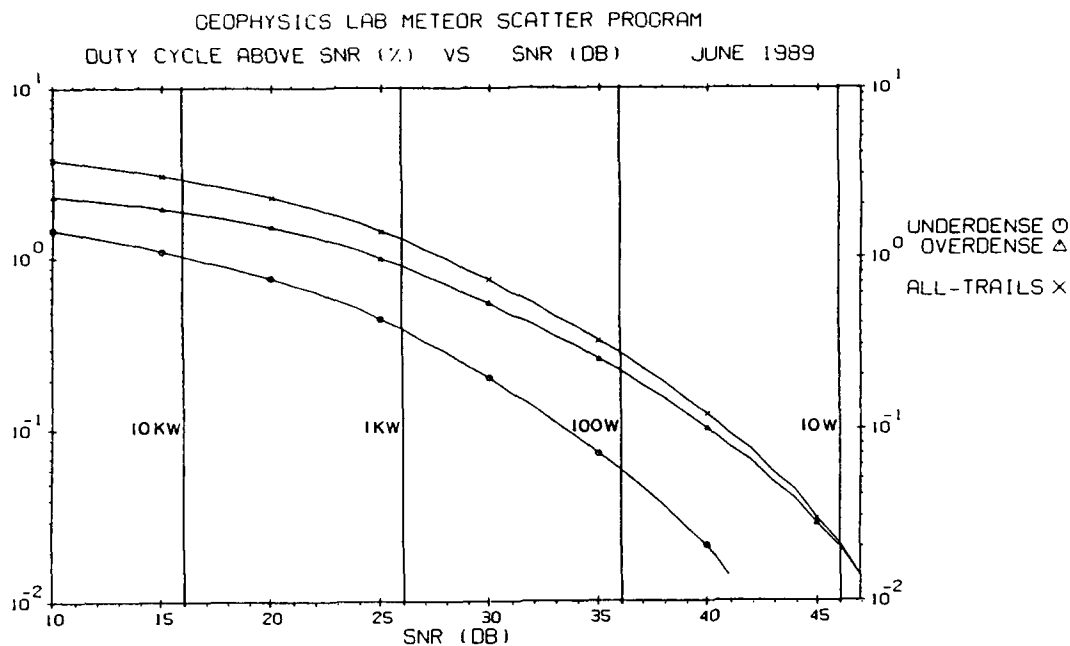


Figure C8. Duty Cycle Exceeding a SNR Threshold for June 1989 at Thule. The frequency is 65 MHz

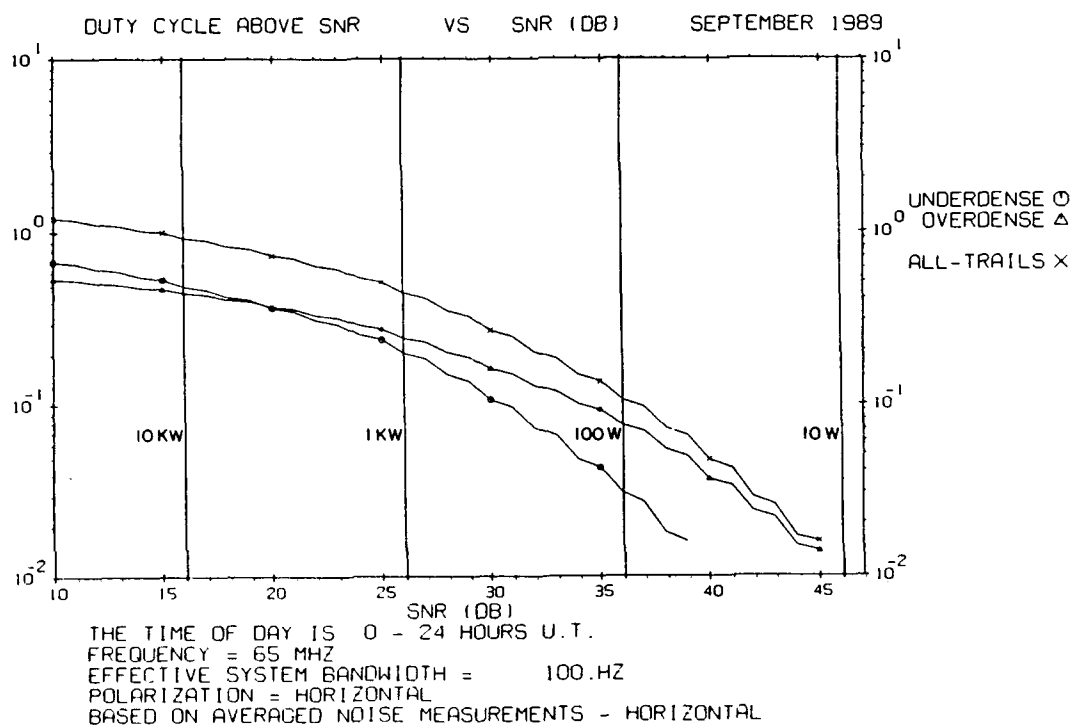
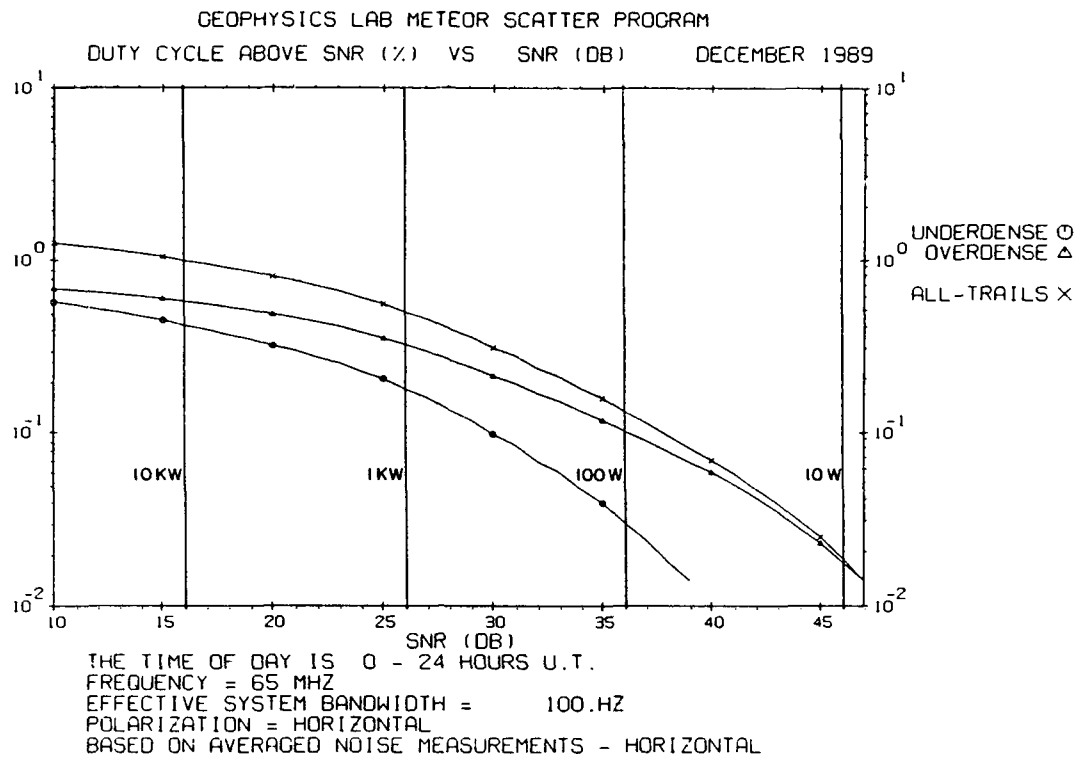
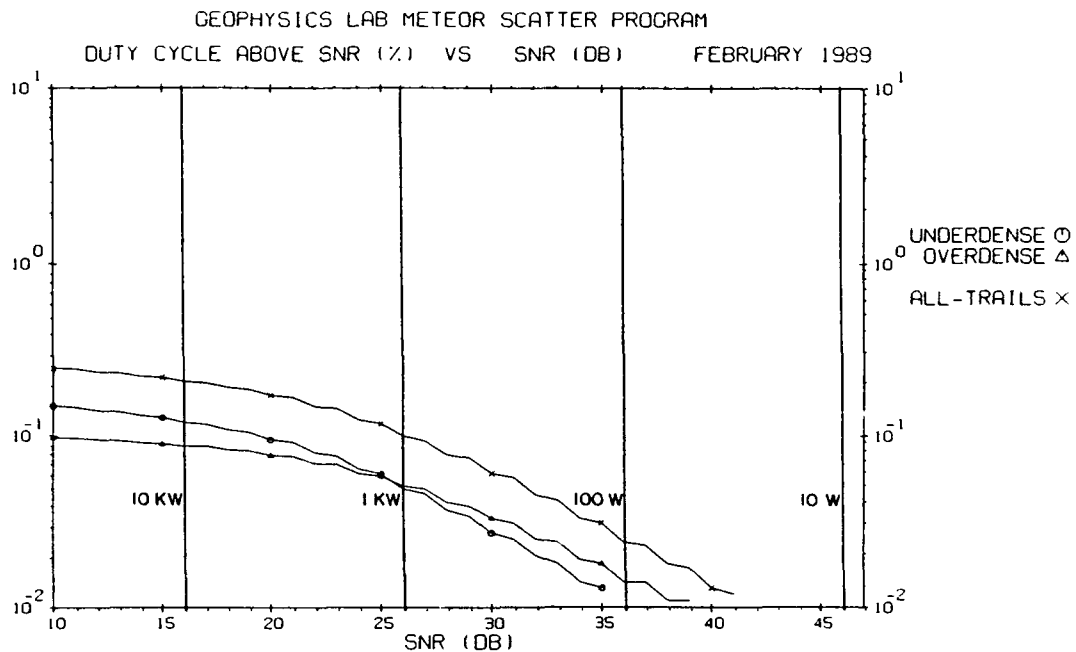


Figure C9. Duty Cycle Exceeding a SNR Threshold for September 1989 at Thule. The frequency is 65 MHz



**Figure C10. Duty Cycle Exceeding a SNR Threshold for December 1989 at Thule. The frequency is 65 MHz**



**Figure C11. Duty Cycle Exceeding a SNR Threshold for February 1989 at Thule. The frequency is 104 MHz**

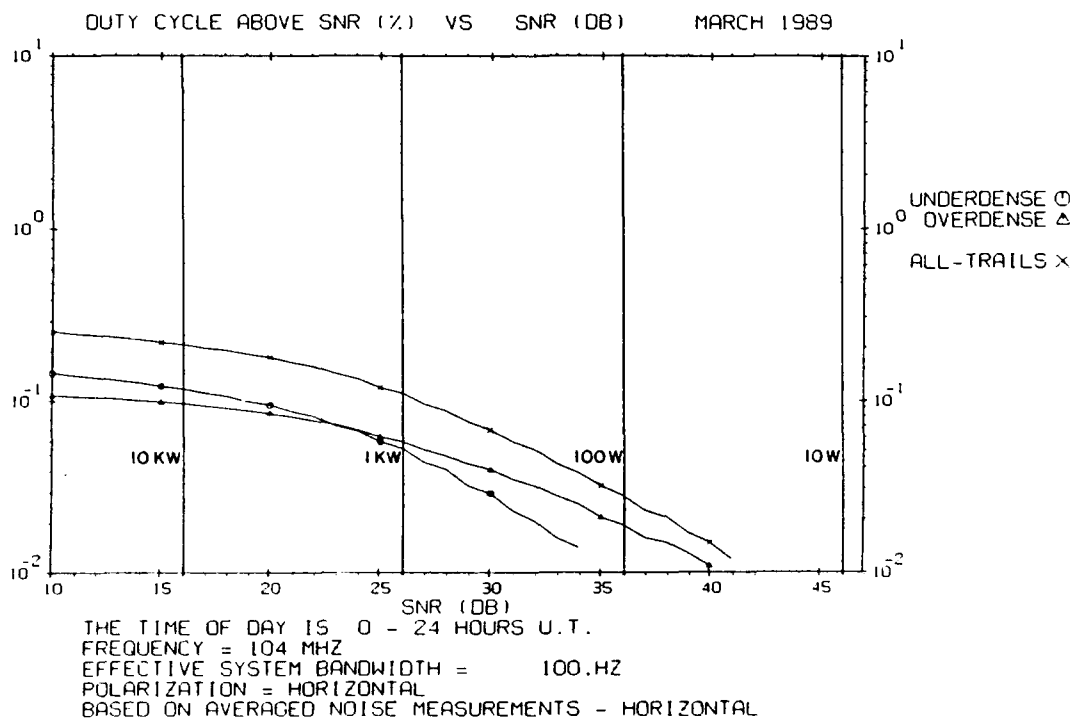


**Figure C12. Duty Cycle Exceeding a SNR Threshold for March 1989 at Thule. The frequency is 104 MHz**

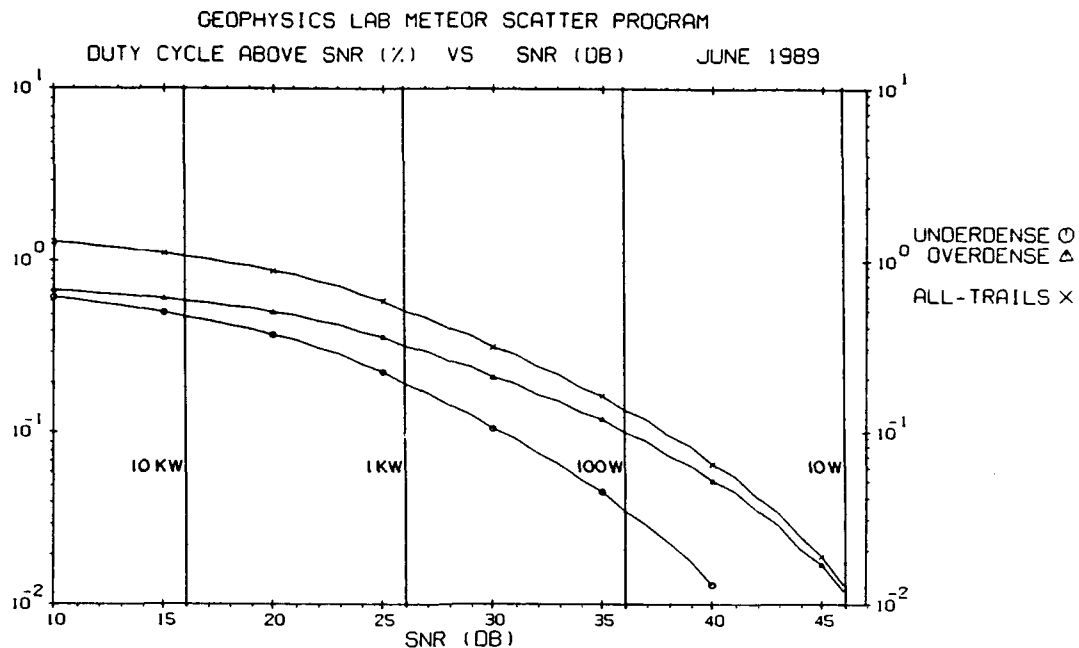


Figure C13. Duty Cycle Exceeding a SNR Threshold for June 1989 at Thule. The frequency is 104 MHz

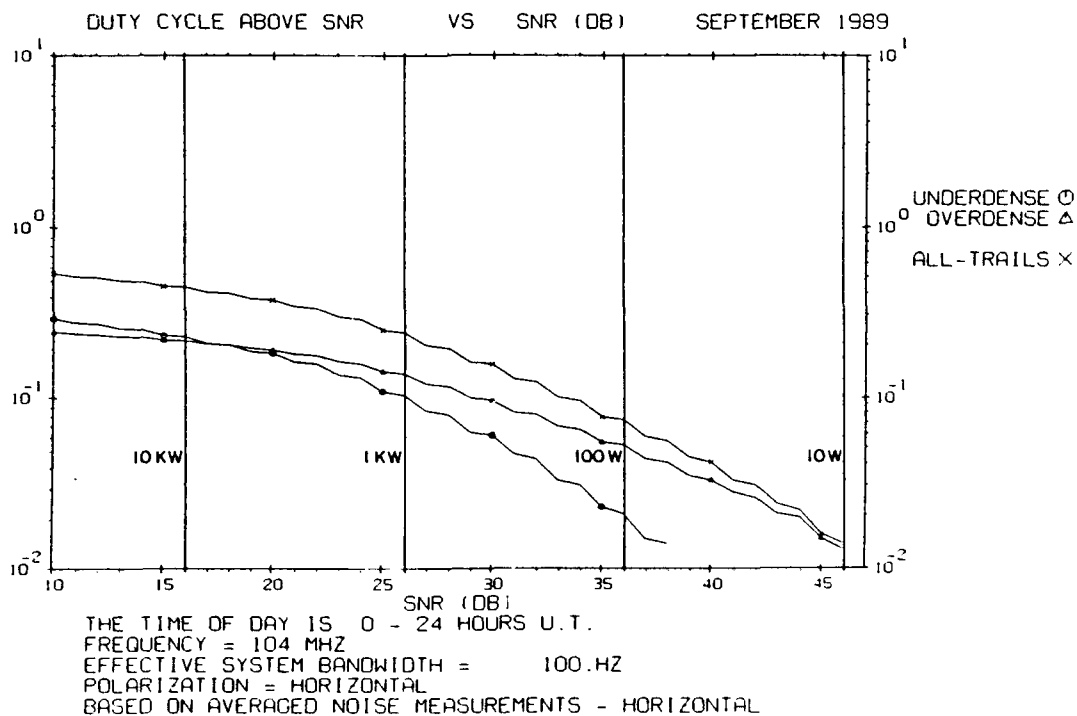
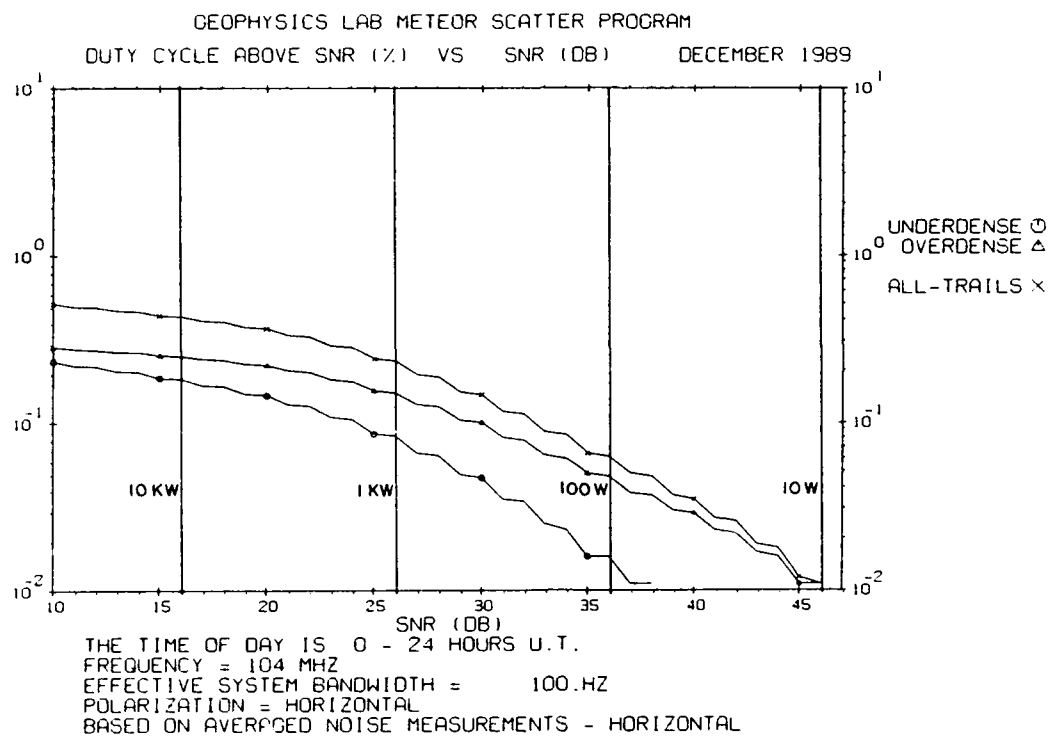


Figure C14. Duty Cycle Exceeding a SNR Threshold for September at Thule. The frequency is 104 MHz



**Figure C15. Duty Cycle Exceeding a SNR threshold for December 1989 at Thule. The frequency is 104 MHz**

## **Appendix D**

### **Average Duration Statistics**



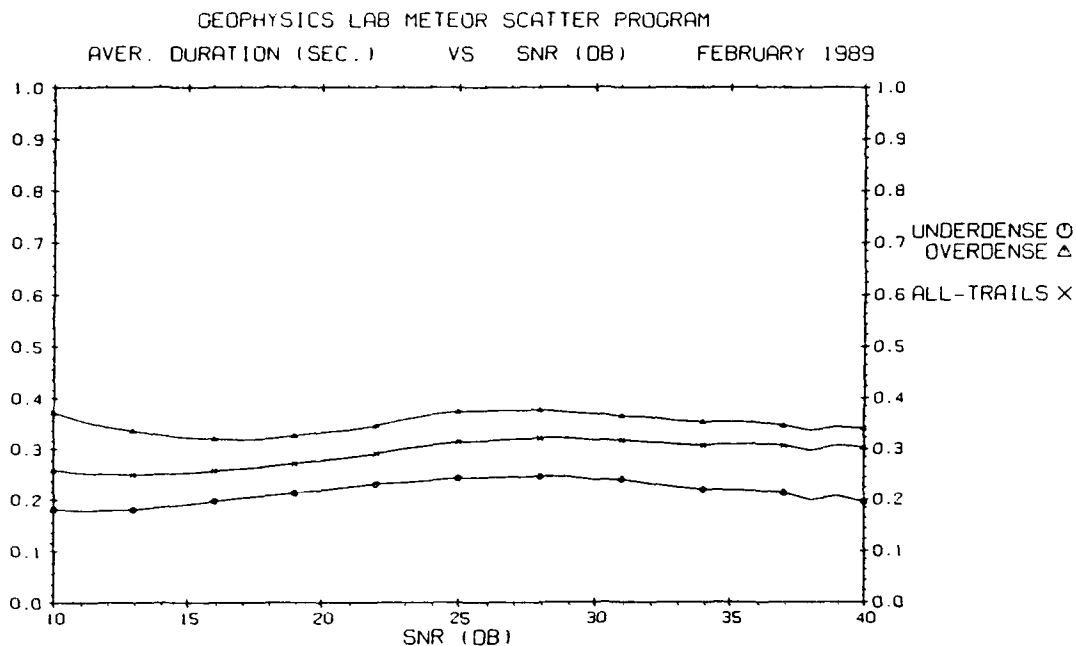


**Figure D1. Average Duration of Meteor Signals as a Function of SNR for February 1989. The frequency is 45 MHz**

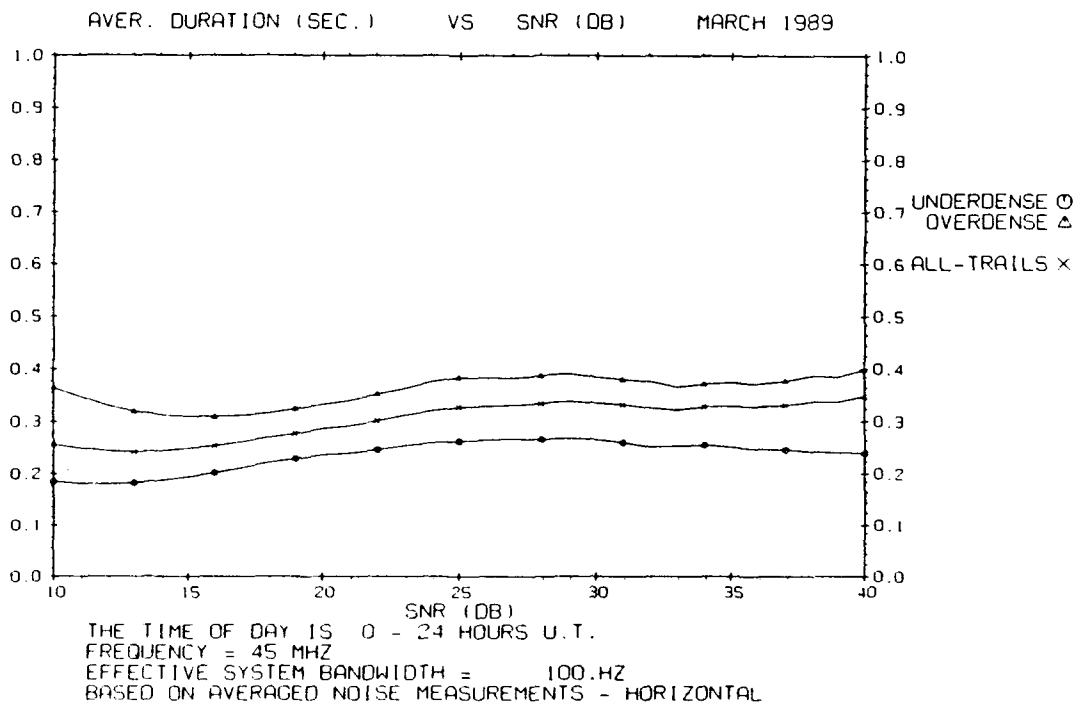


**Figure D2. Average Duration of Meteor Signals as a Function of SNR for March 1989. The frequency is 45 MHz**

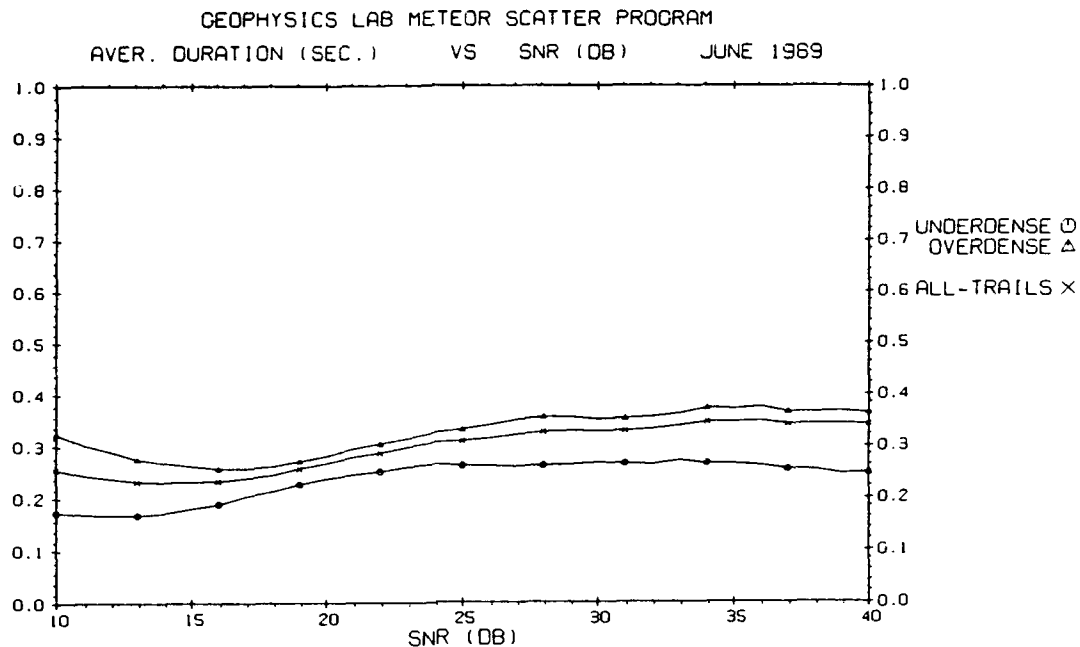


**Figure D3. Average Duration of Meteor Signals as a Function of SNR for June 1989. The frequency is 45 MHz**

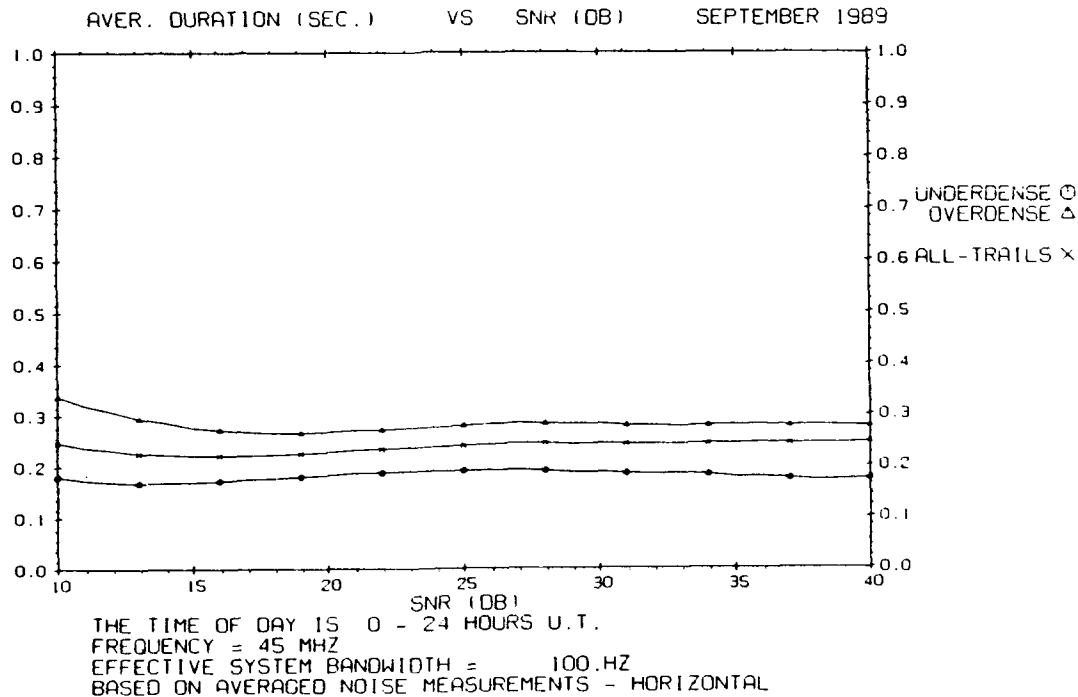


**Figure D4. Average Duration of Meteor Signals as a Function of SNR for September 1989. The frequency is 45 MHz**

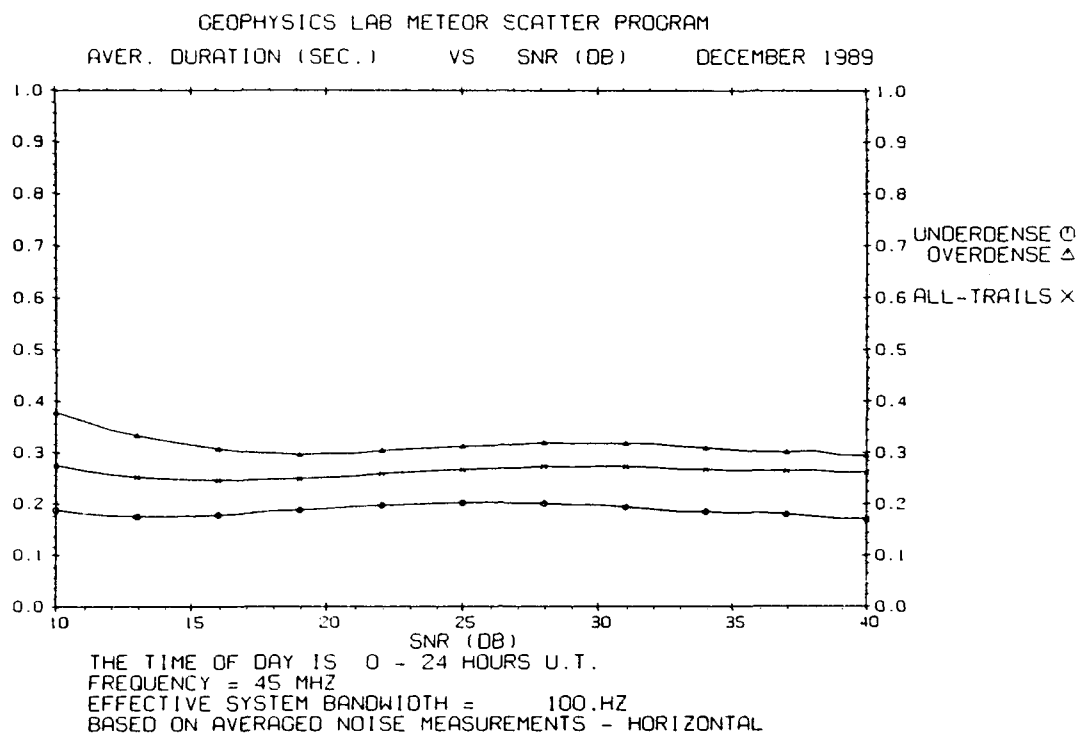


**Figure D5. Average Duration of Meteor Signals as a Function of SNR for December 1989.. The frequency is 45 MHz**

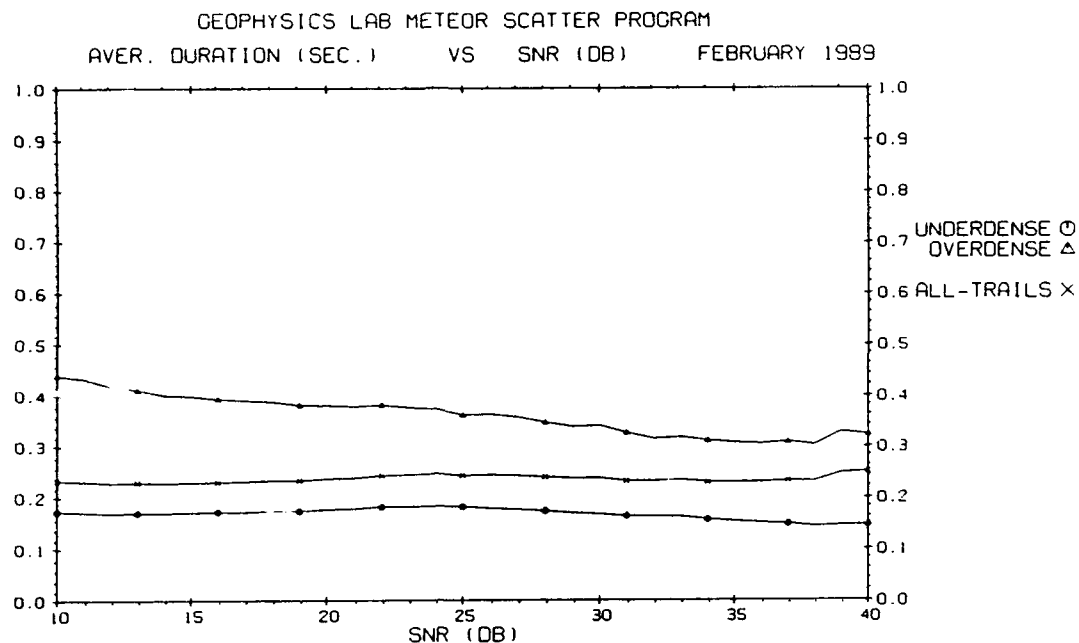


**Figure D6. Average Duration of Meteor Signals as a Function of SNR for February 1989. The frequency is 65 MHz**

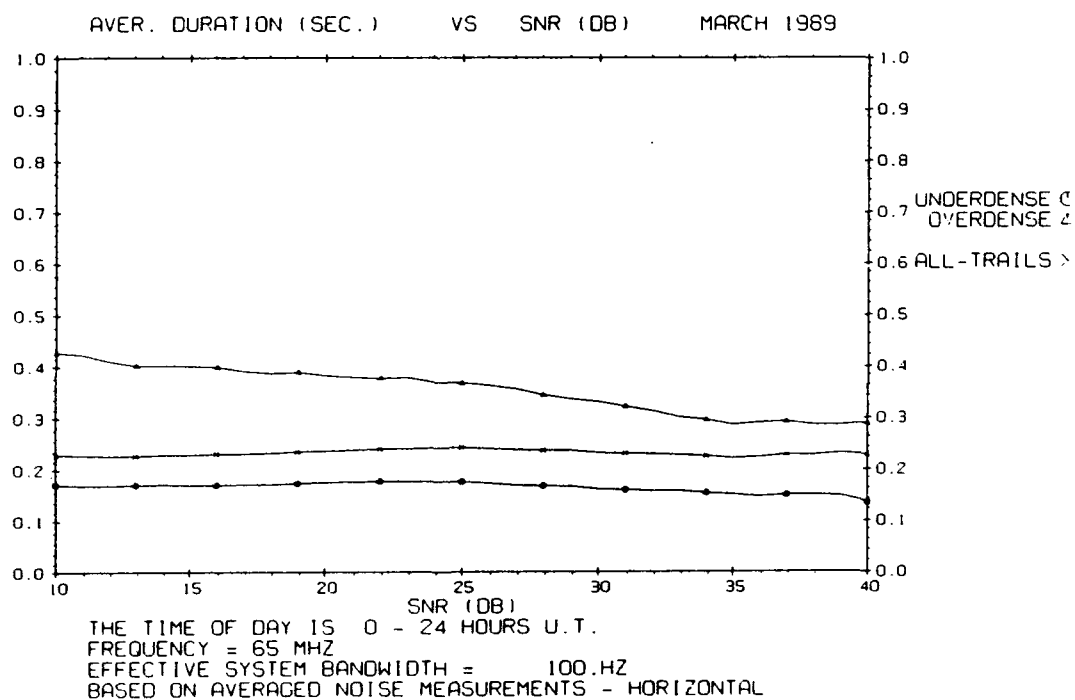


**Figure D7. Average Duration of Meteor Signals as a Function of SNR for March 1989. The frequency is 65 MHz**

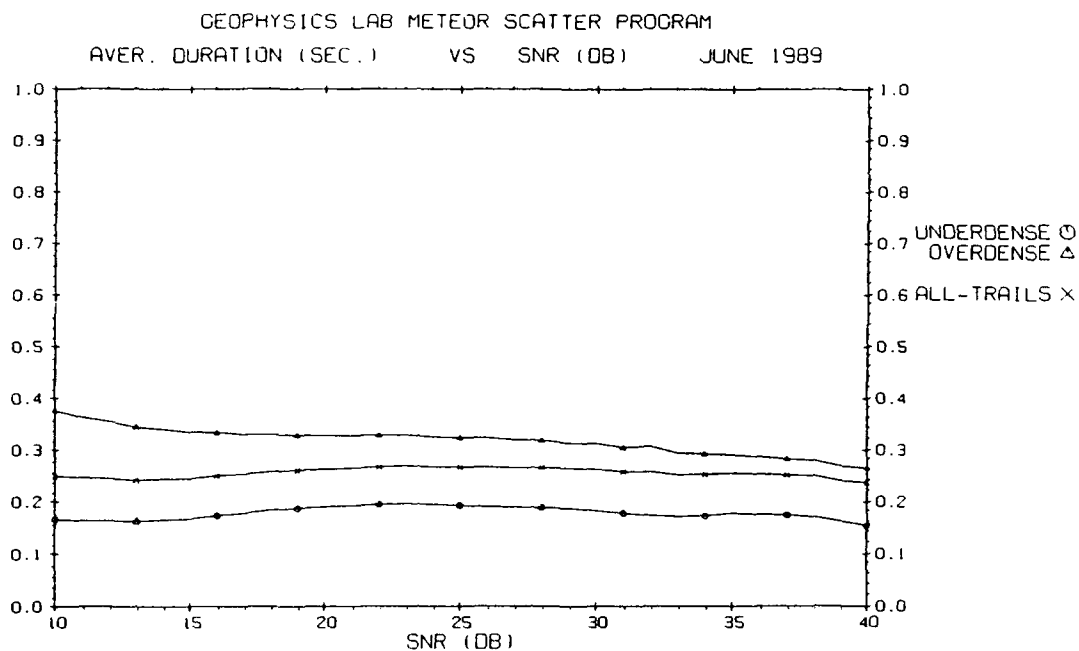


**Figure D8. Average Duration of Meteor Signals as a Function of SNR for June 1989. The frequency is 65 MHz**

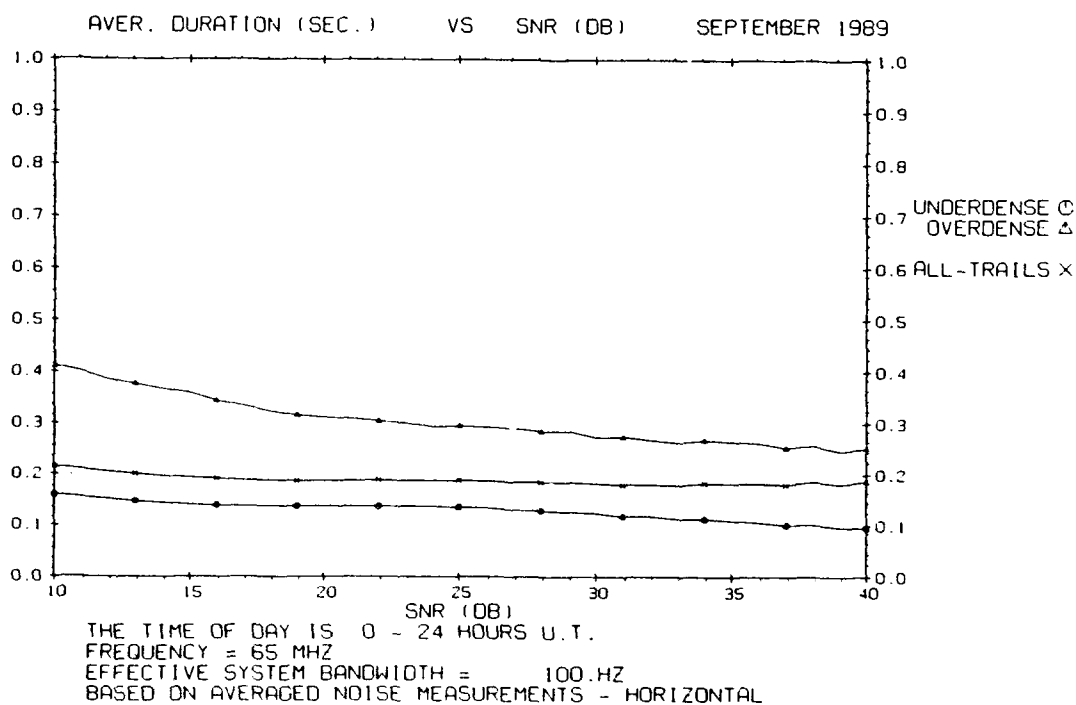


**Figure D9. Average Duration of Meteor Signals as a Function of SNR for September 1989. The frequency is 65 MHz**

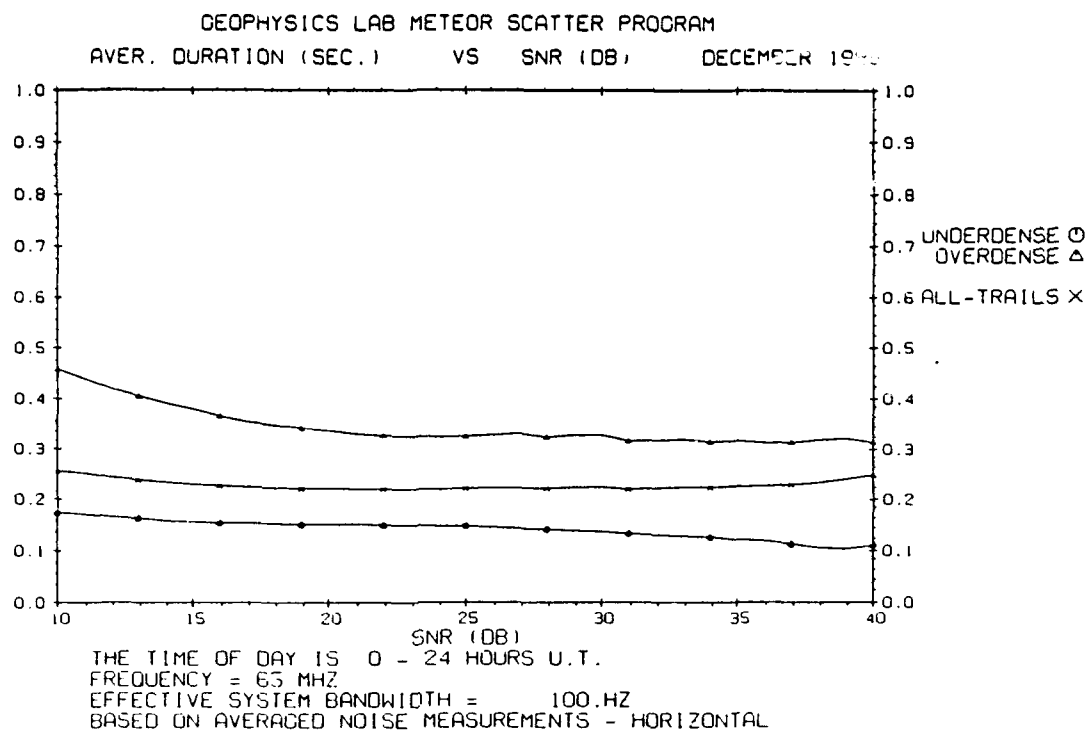


**Figure D10. Average Duration of Meteor Signals as a Function of SNR for December 1989. The frequency is 65 MHz**

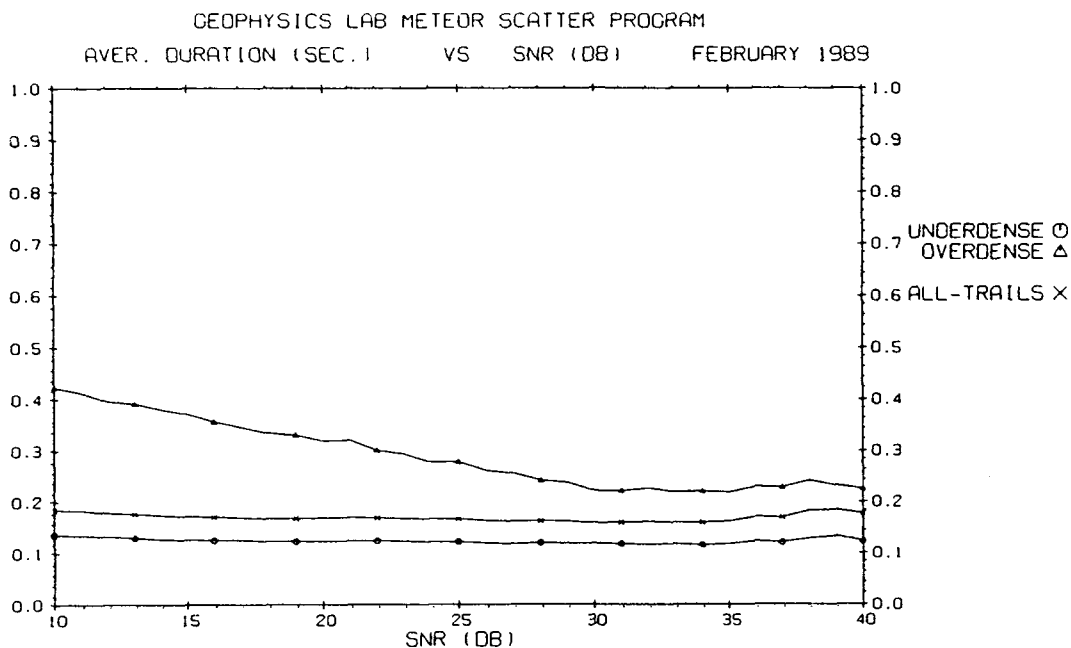


**Figure D11. Average Duration of Meteor Signals as a Function of SNR for February 1989. The frequency is 104 MHz**

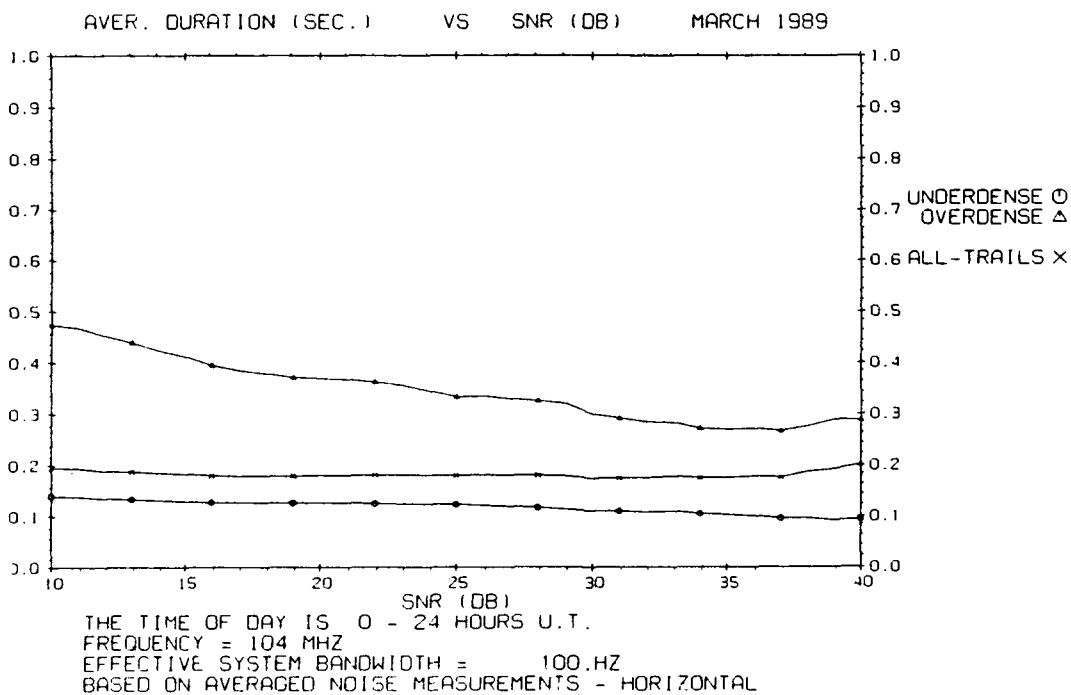


**Figure D12. Average Duration of Meteor Signals as a Function of SNR for March 1989. The frequency is 104 MHz**

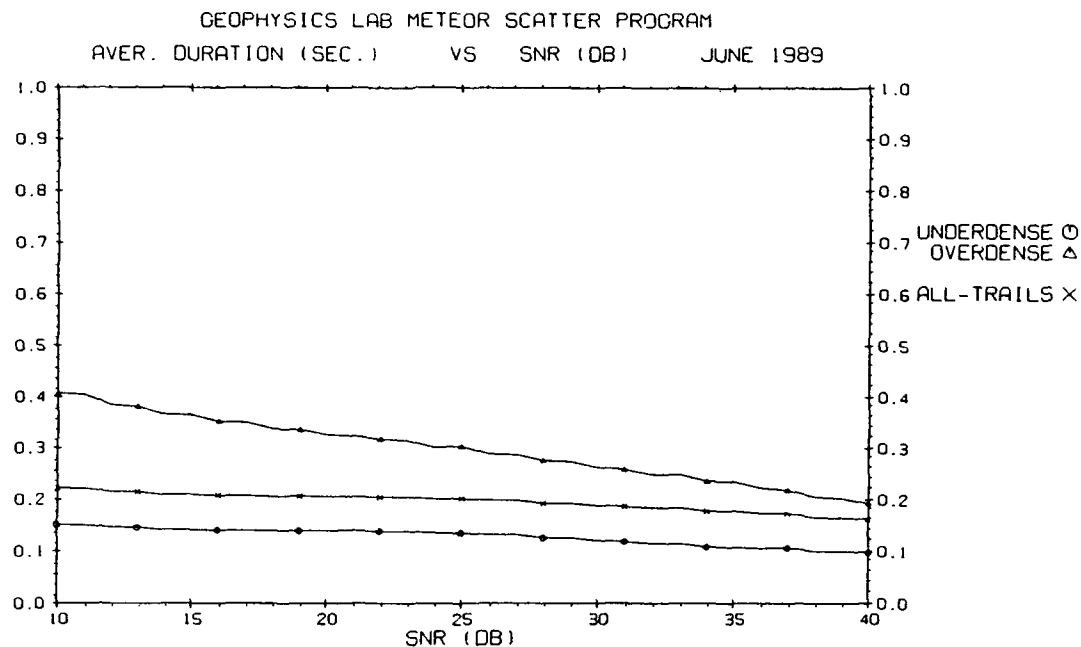


Figure D13. Average Duration of Meteor Signals as a Function of SNR for June 1989. The frequency is 104 MHz

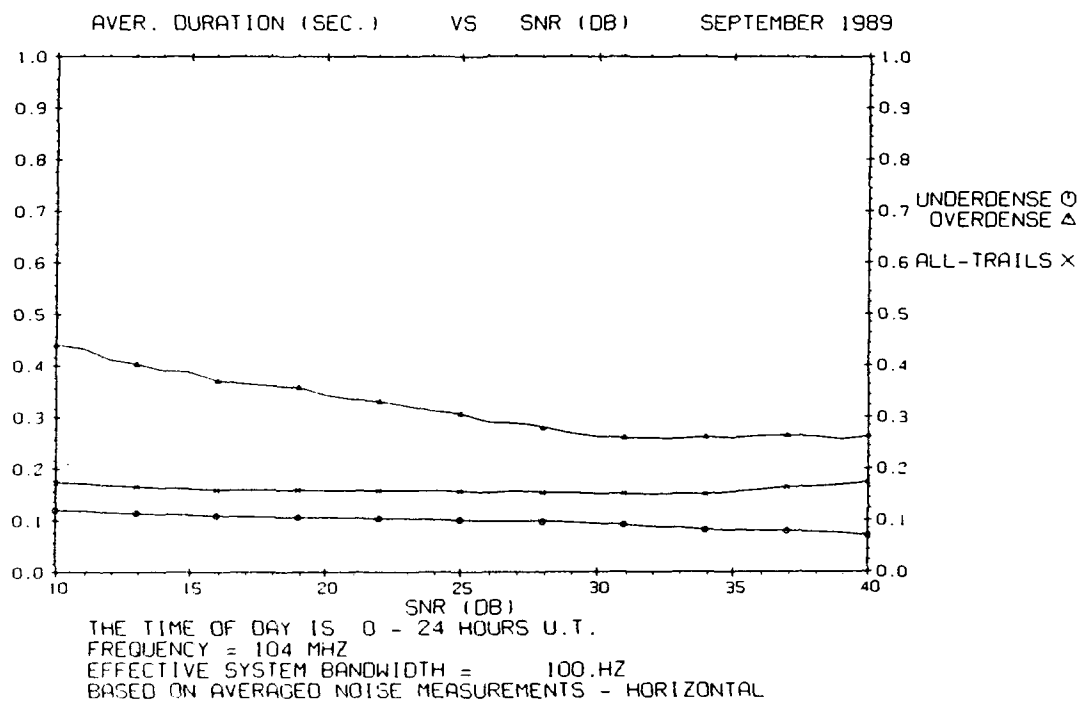
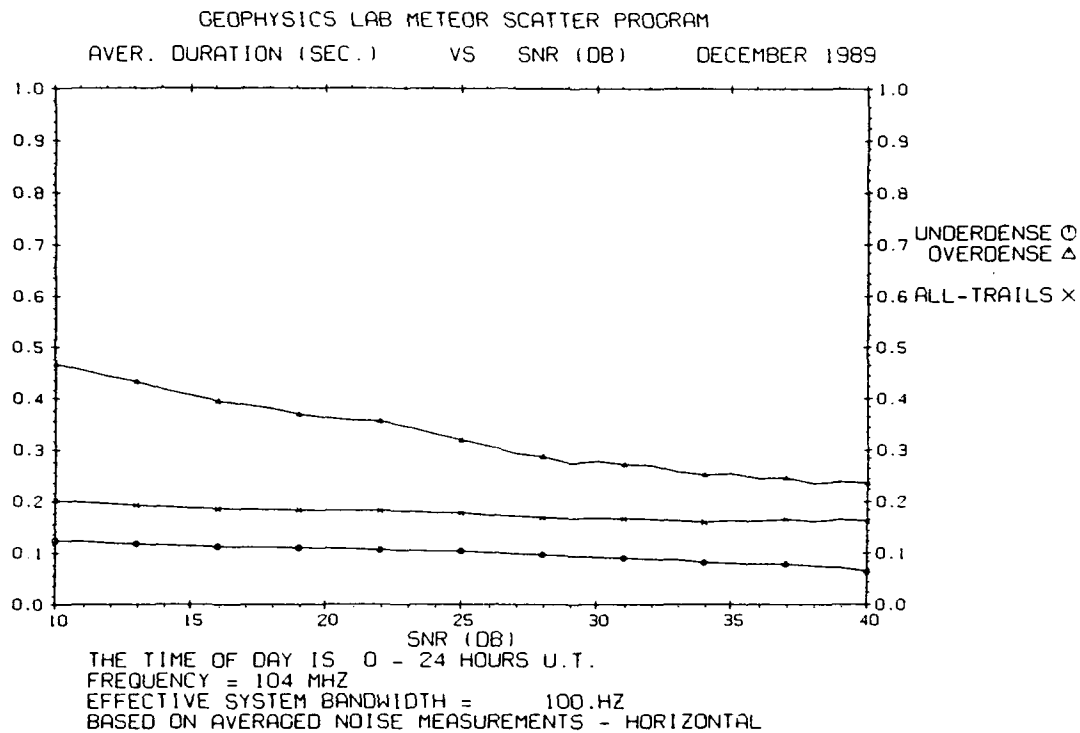
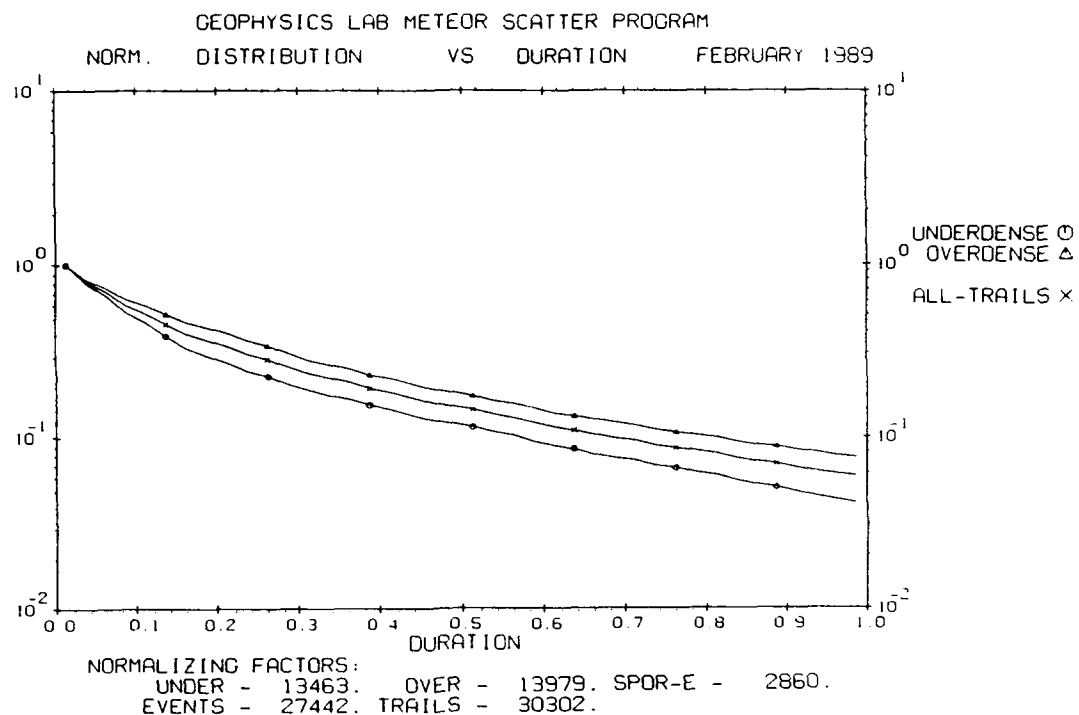


Figure D14. Average Duration of Meteor Signals as a Function of SNR for September 1989. The frequency is 104 MHz





**Figure D15. Average Duration of Meteor Signals as a Function of SNR for December 1989. The frequency is 104 MHz**



**Figure D16. Normalized Distribution of Signal Durations Exceeding 19 dB for February 1989. The frequency is 45 MHz**

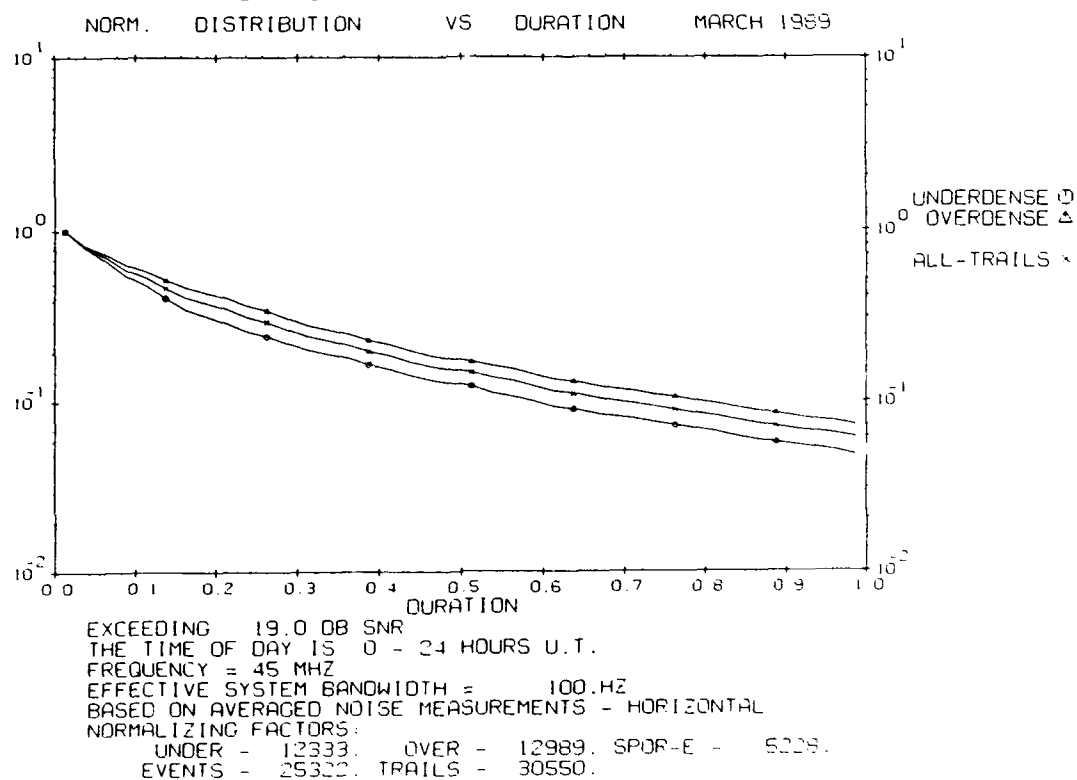


**Figure D17. Normalized Distribution of Signal Durations Exceeding 19 dB for March 1989. The frequency is 45 MHz**

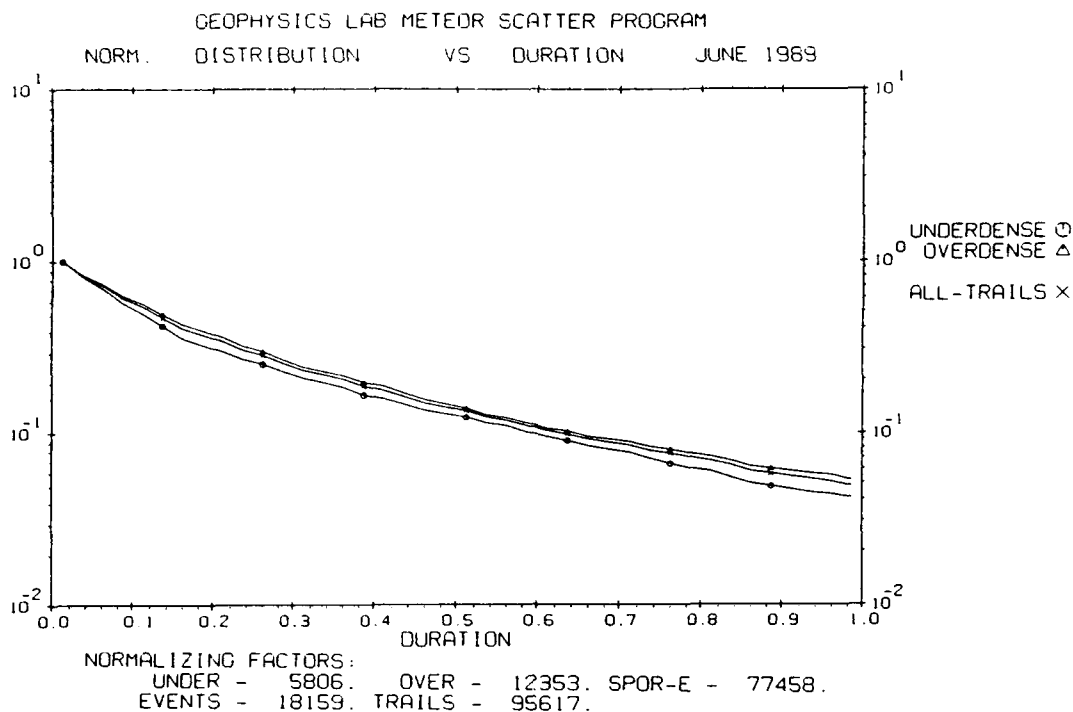


**Figure D18. Normalized Distribution of Signal Durations Exceeding 19 dB for June 1989. The frequency is 45 MHz**

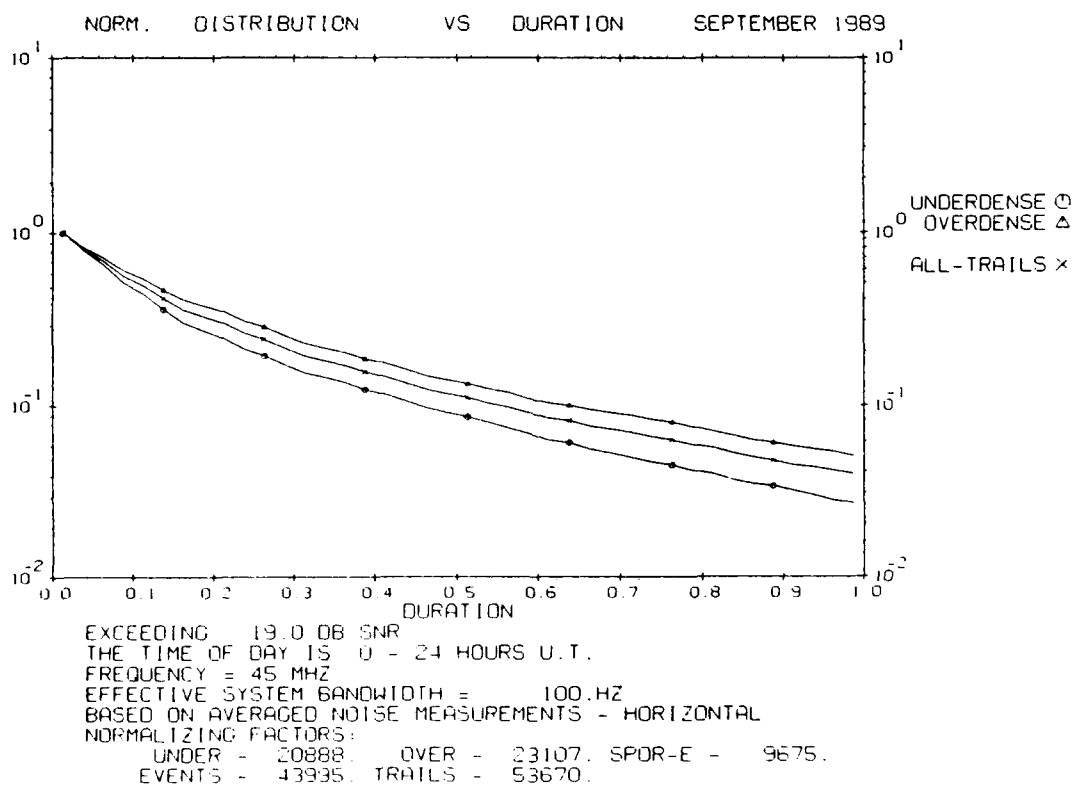


**Figure D19. Normalized Distribution of Signal Durations Exceeding 19 dB for September 1989. The frequency is 45 MHz**

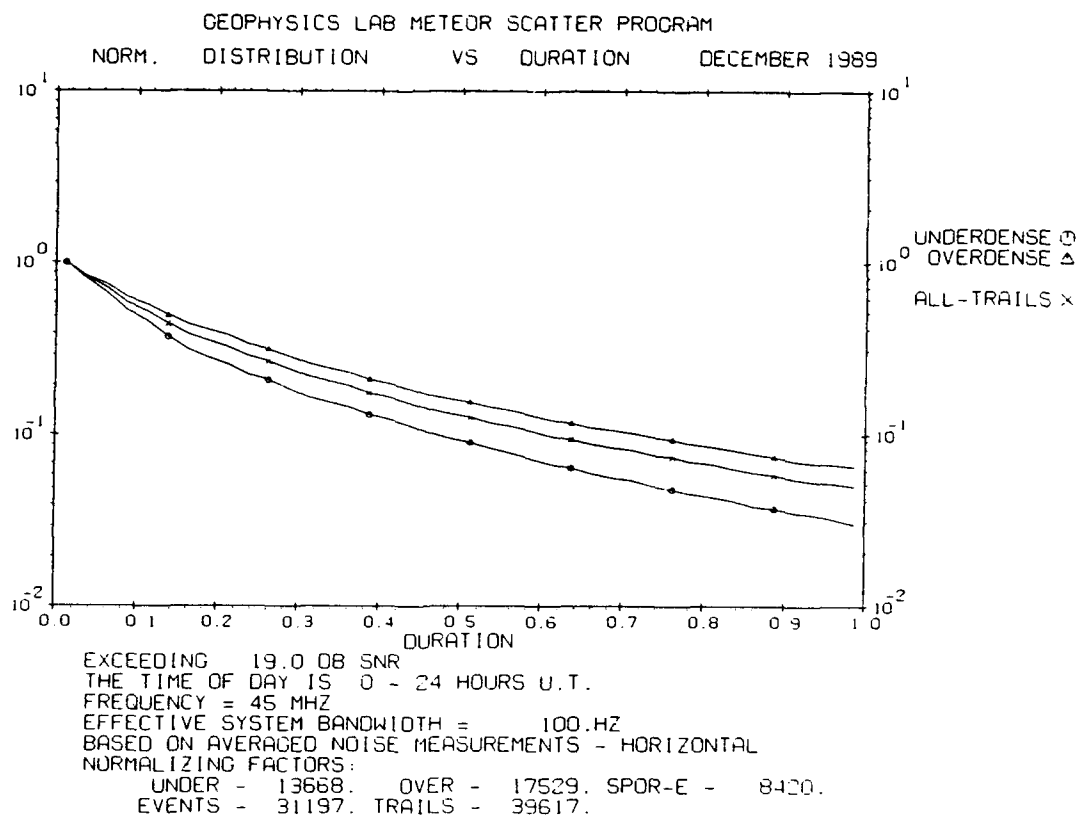


**Figure D20. Normalized Distribution of Signal Durations Exceeding 19 dB for December 1989. The frequency is 45 MHz**

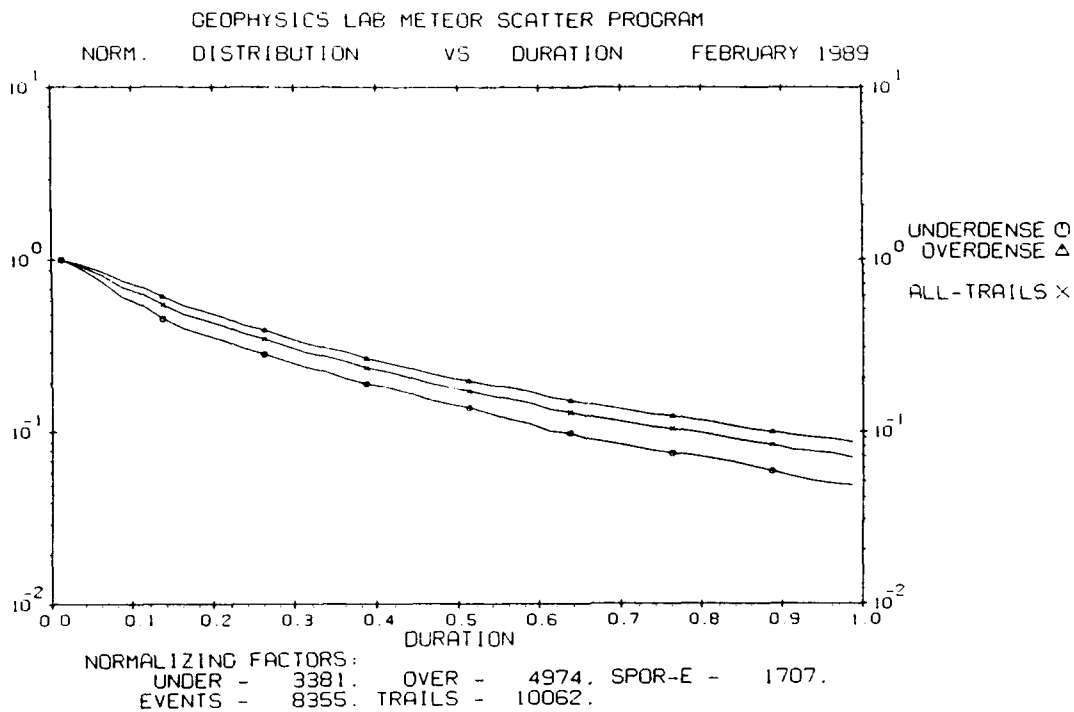


**Figure D21. Normalized Distribution of Signal Durations Exceeding 29 dB for February 1989. The frequency is 65 MHz**

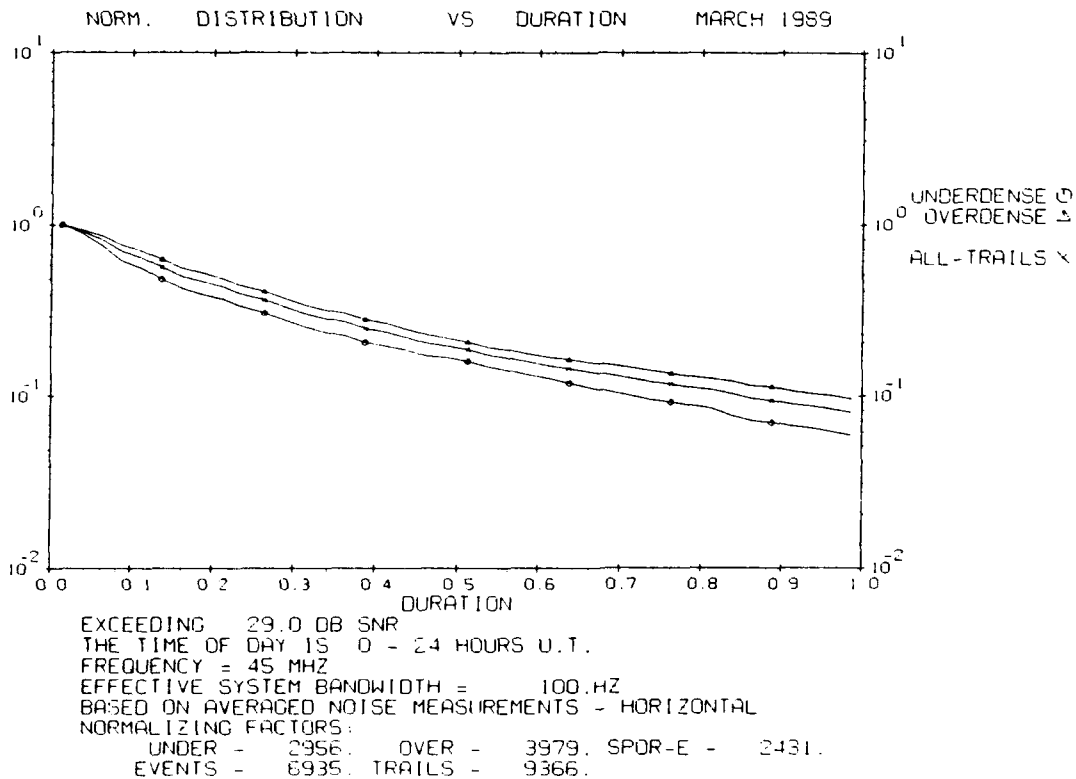


**Figure D22. Normalized Distribution of Signal Durations Exceeding 29 dB for March 1989. The frequency is 65 MHz**

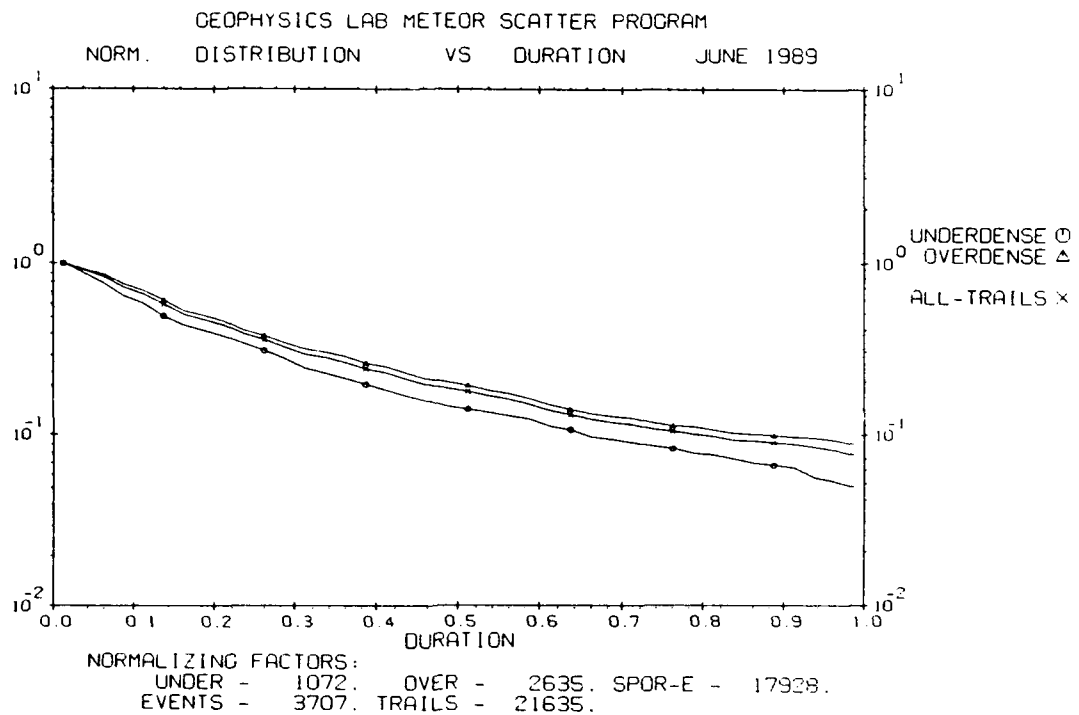


**Figure D23. Normalized Distribution of Signal Durations Exceeding 29 dB for June 1989. The frequency is 65 MHz**

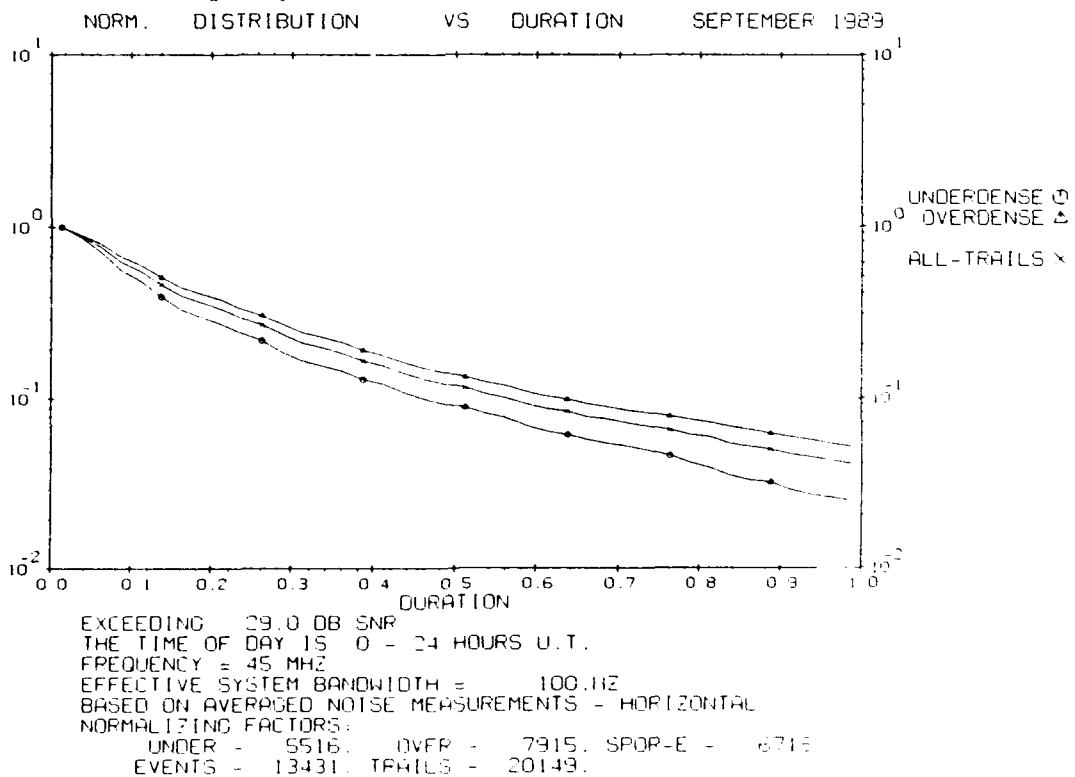


**Figure D24. Normalized Distribution of Signal Durations Exceeding 29 dB for September 1989. The frequency is 65 MHz**

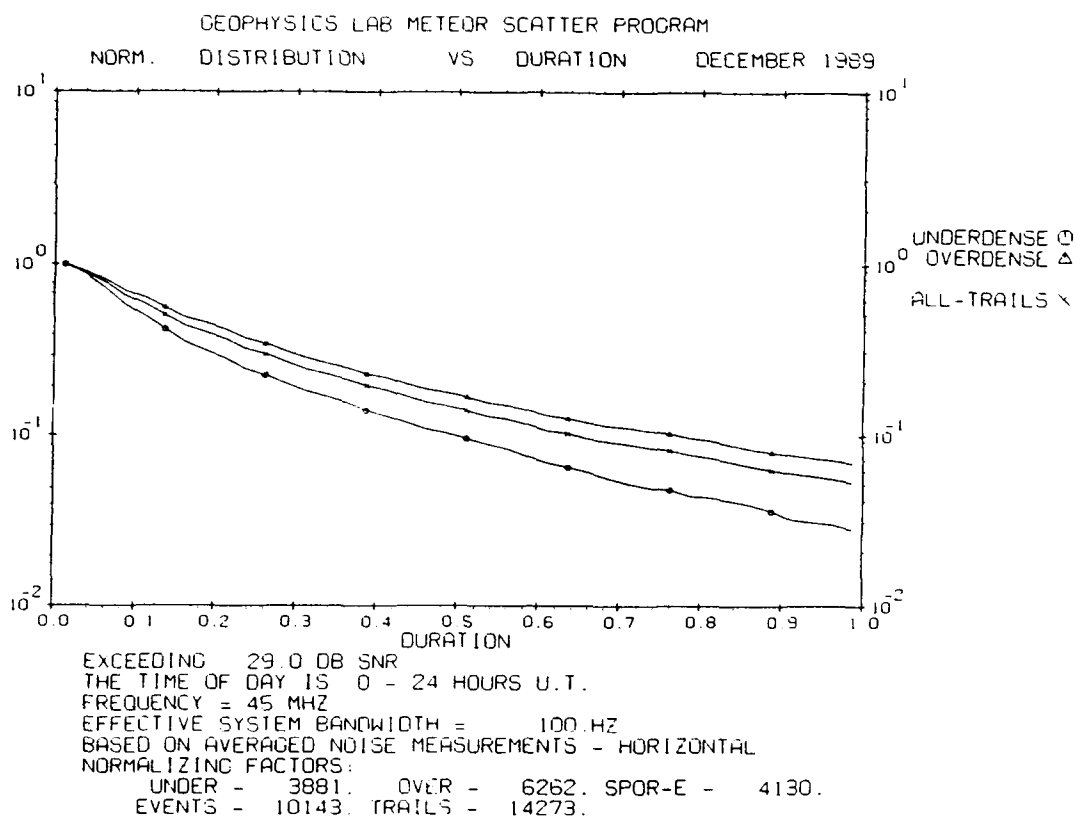


**Figure D25. Normalized Distribution of Signal Durations Exceeding 29 dB for December 1989. The frequency is 65 MHz**

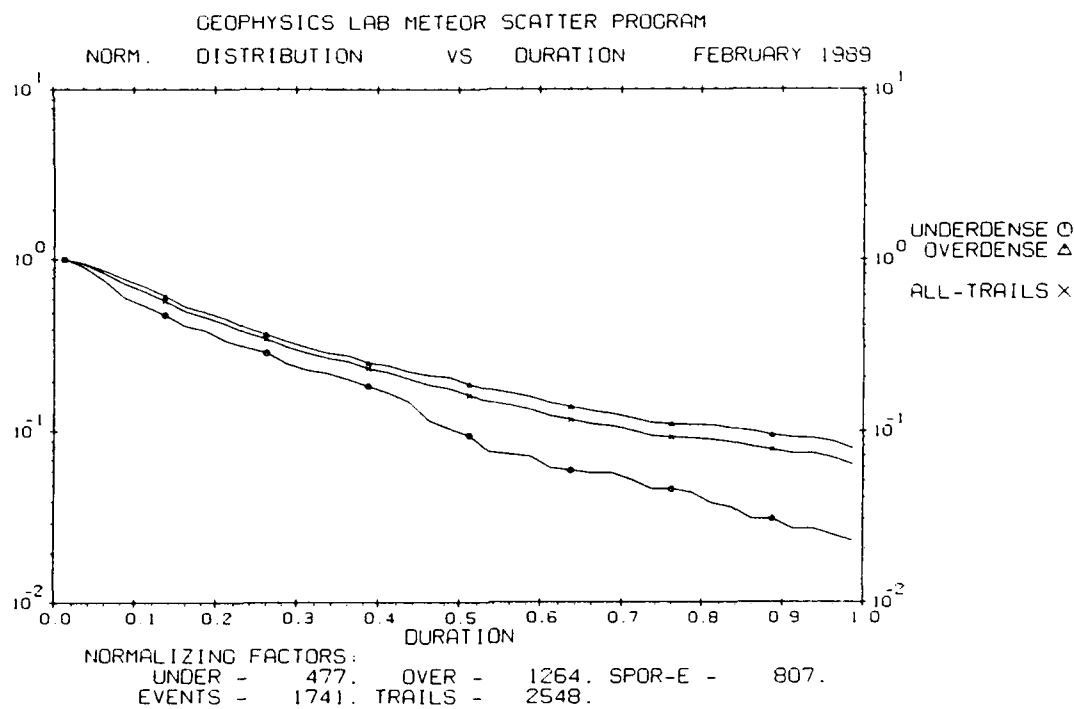


**Figure D26. Normalized Distribution of Signal Durations Exceeding 39 dB for February 1989. The frequency is 45 MHz**

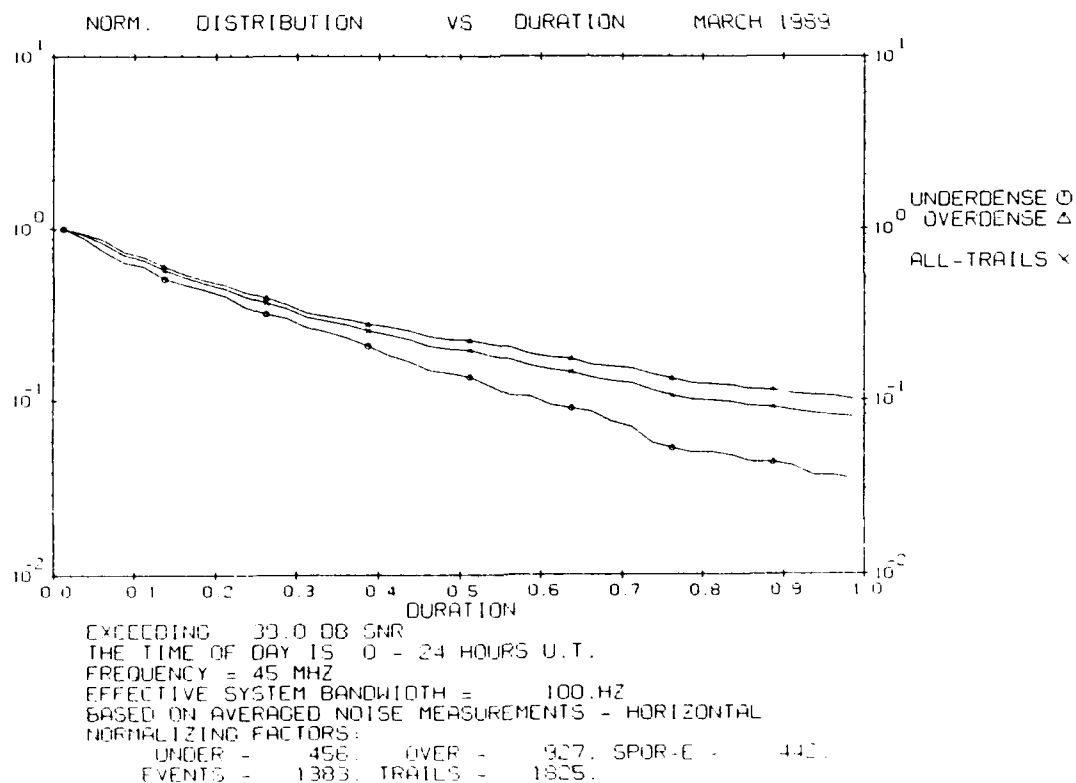


**Figure D27. Normalized Distribution of Signal Durations Exceeding 39 dB for March 1989. The frequency is 45 MHz**



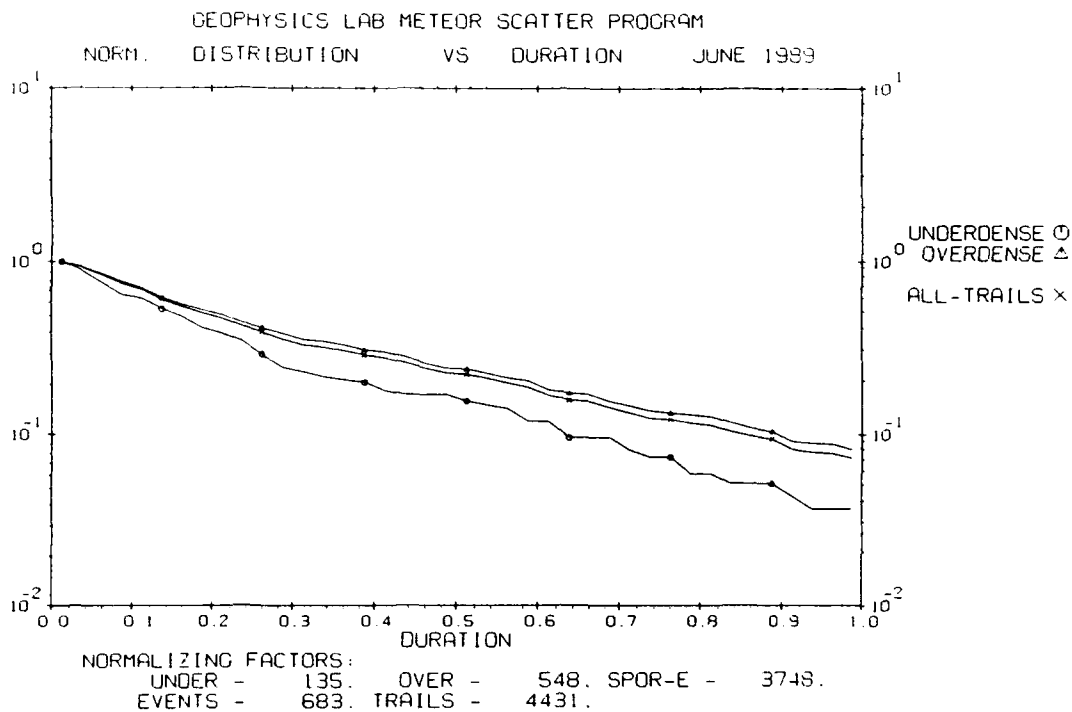


**Figure D28. Normalized Distribution of Signal Durations Exceeding 39 dB for June 1989. The frequency is 45 MHz**

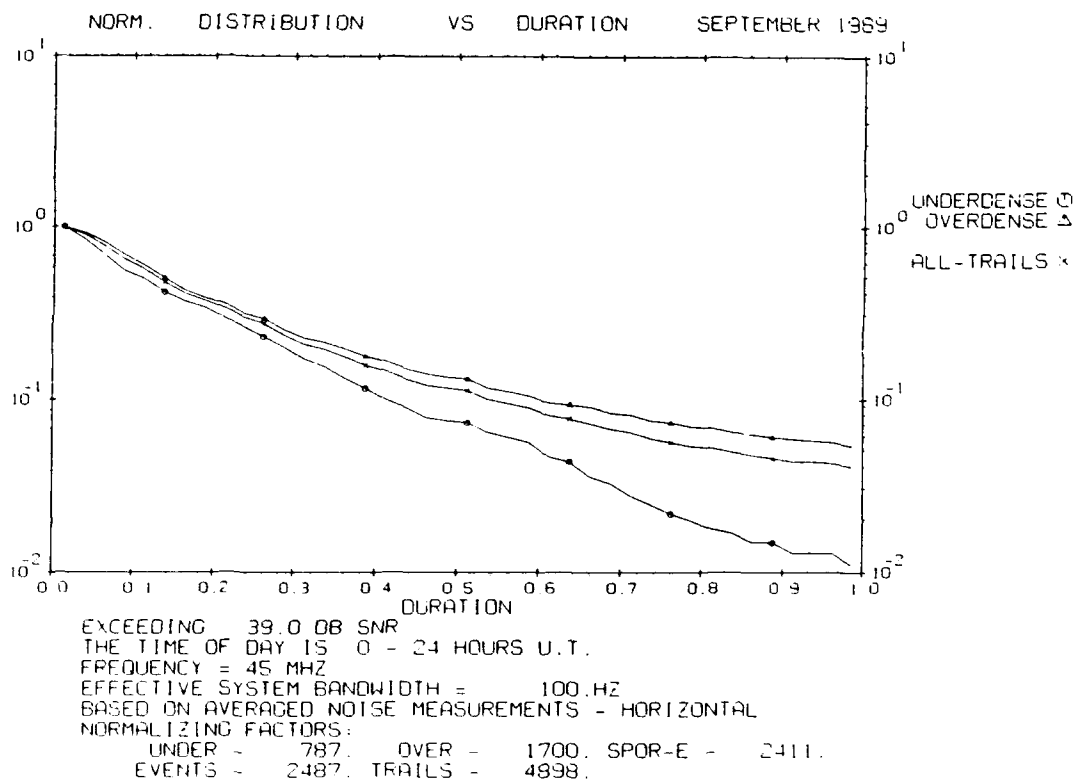


**Figure D29. Normalized Distribution of Signal Durations Exceeding 39 dB for September 1989. The frequency is 45 MHz**

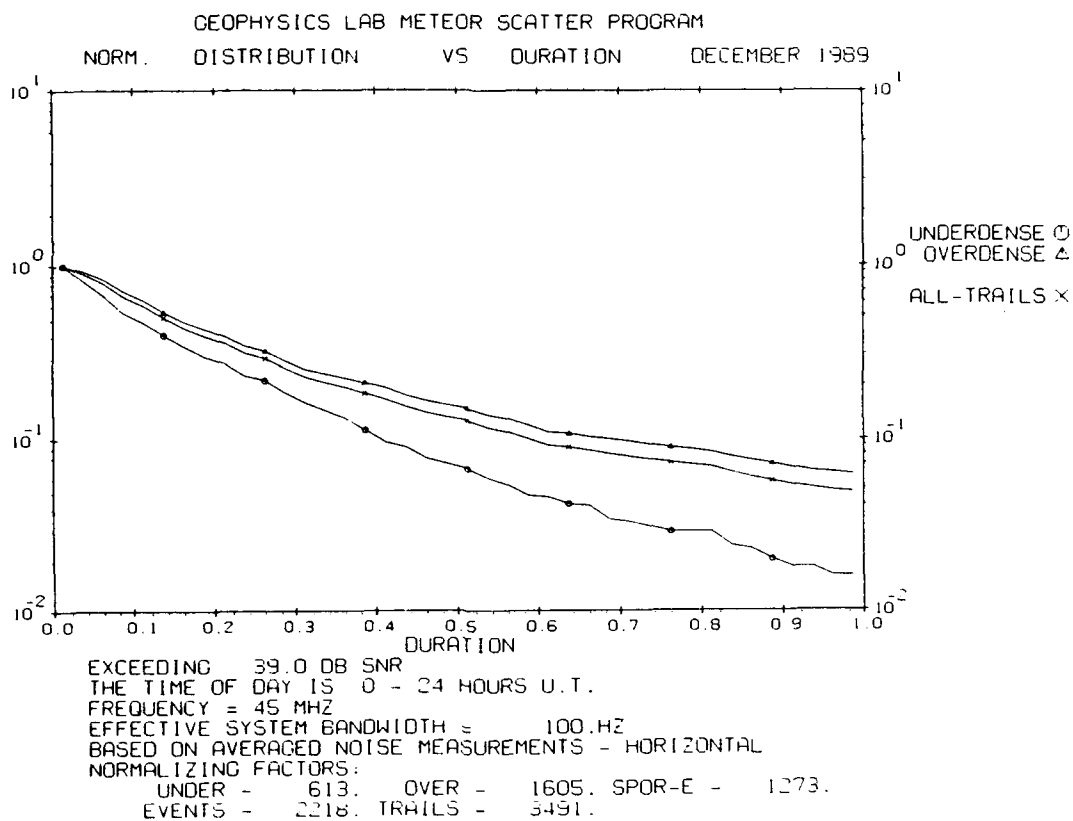


**Figure D30. Normalized Distribution of Signal Durations Exceeding 39 dB for December 1989. The frequency is 45 MHz**

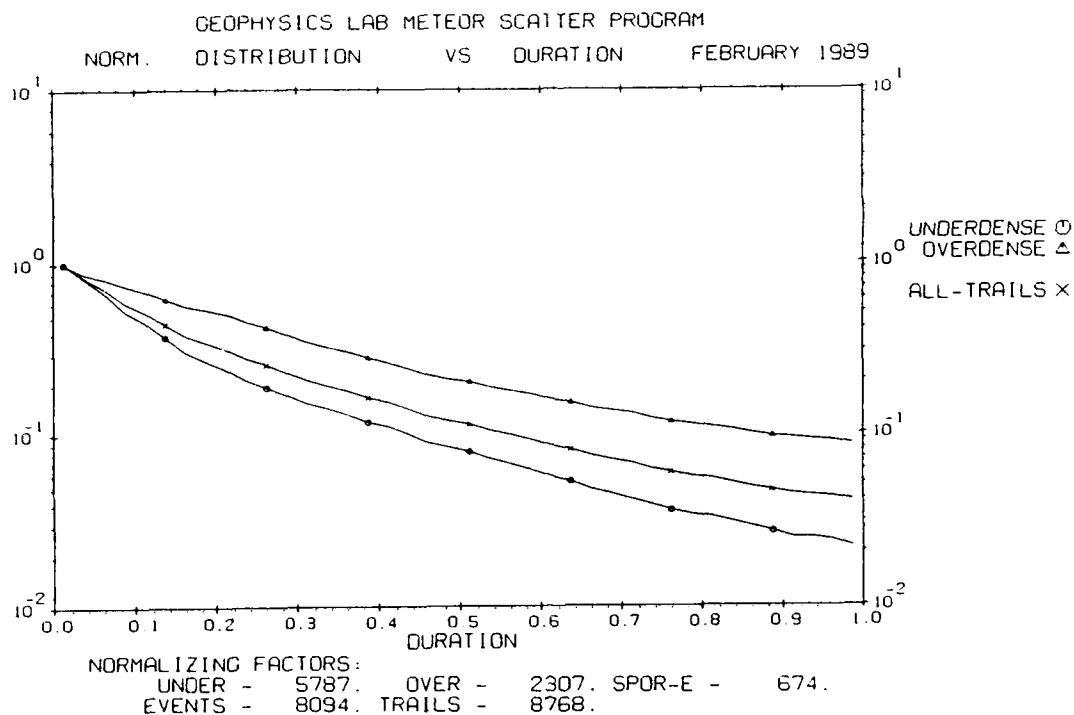


**Figure D31. Normalized Distribution of Signal Durations Exceeding 19 dB for February 1989. The frequency is 65 MHz.**

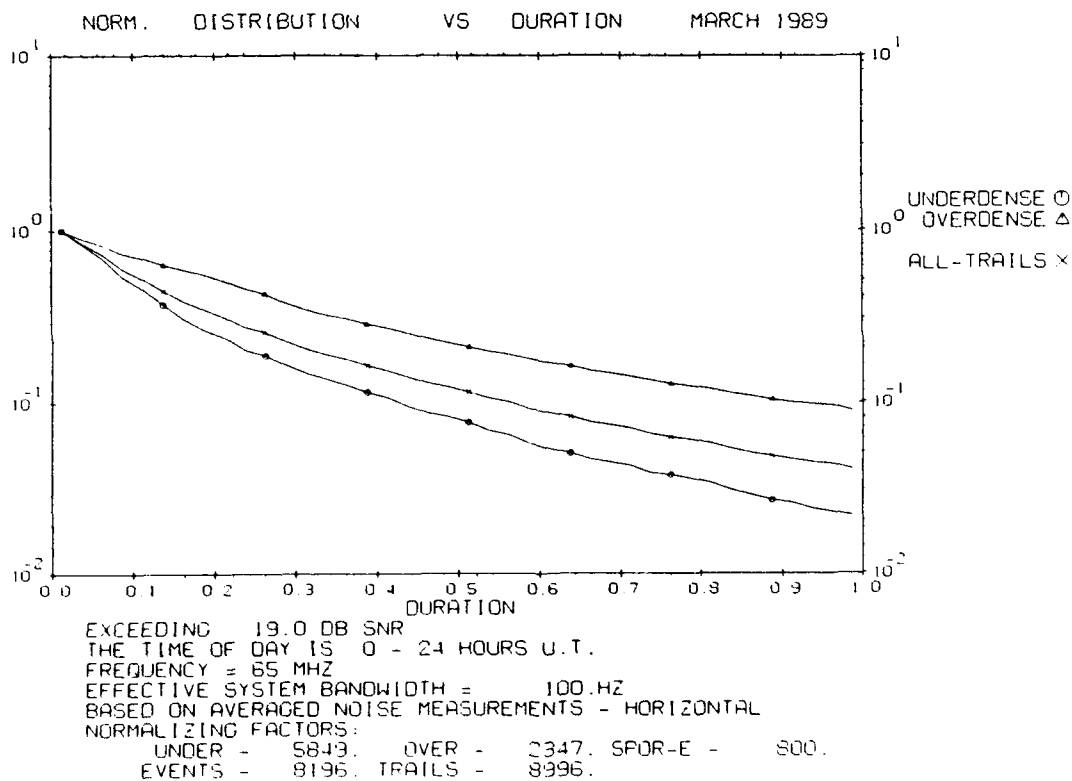


**Figure D32. Normalized Distribution of Signal Durations Exceeding 19 dB for March 1989. The frequency is 65 MHz.**

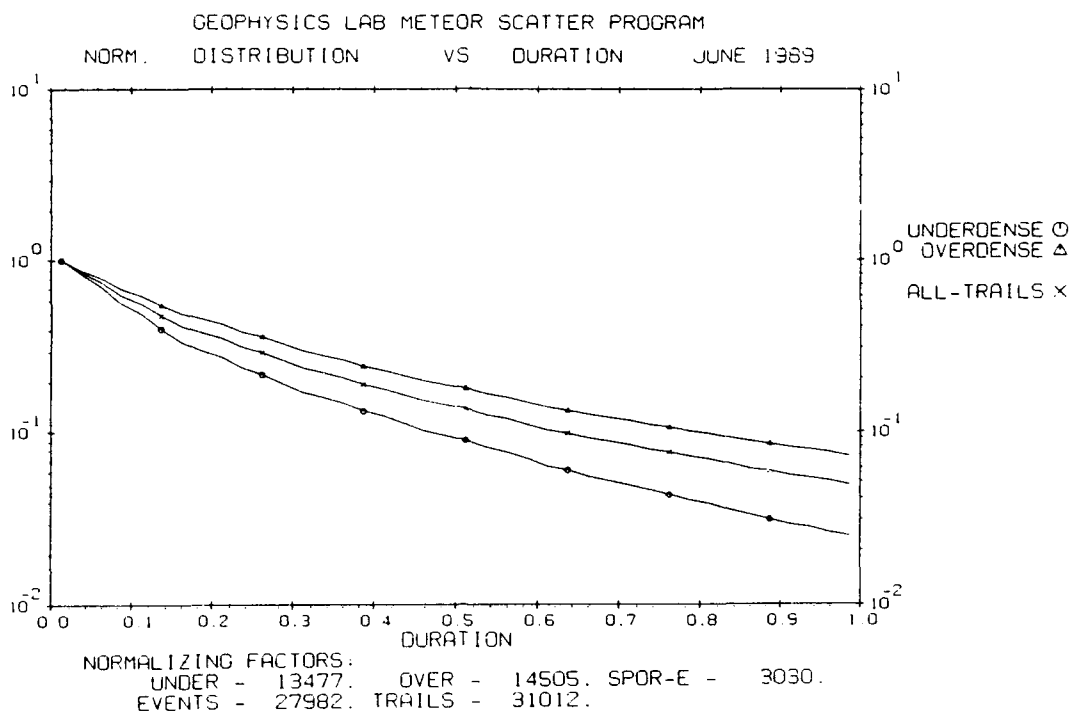


**Figure D33. Normalized Distribution of Signal Durations Exceeding 19 dB for June 1989. The frequency is 65 MHz.**

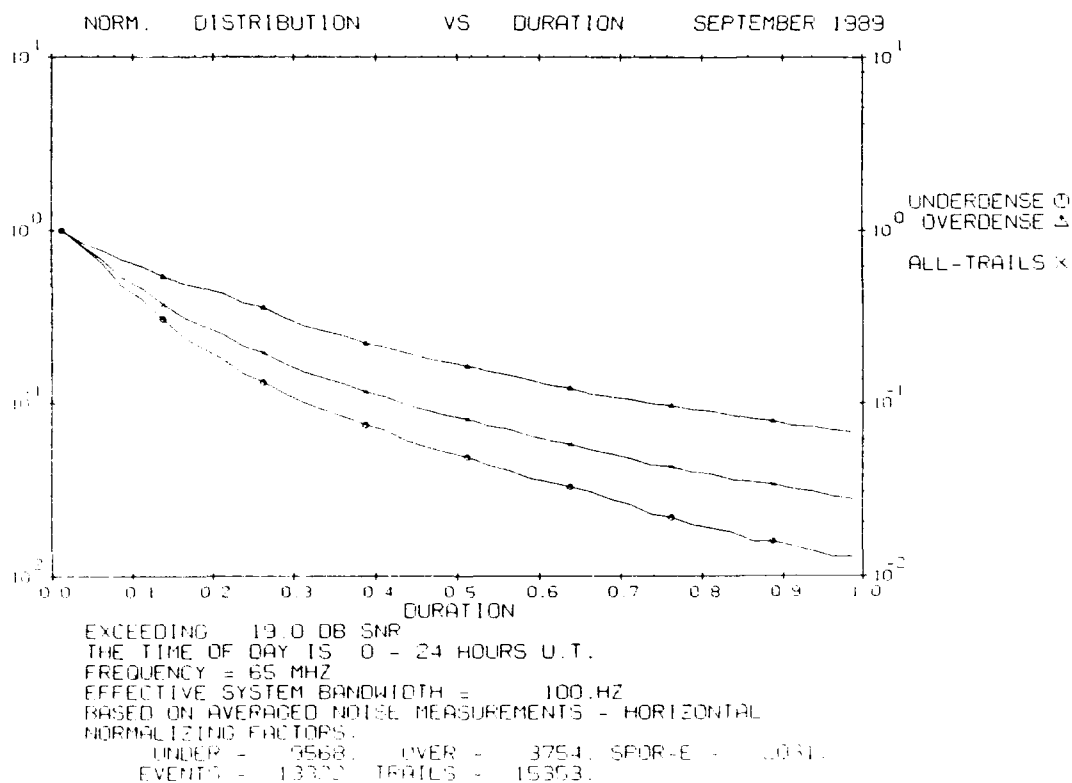


**Figure D34. Normalized Distribution of Signal Durations Exceeding 19 dB for September 1989. The frequency is 65 MHz.**

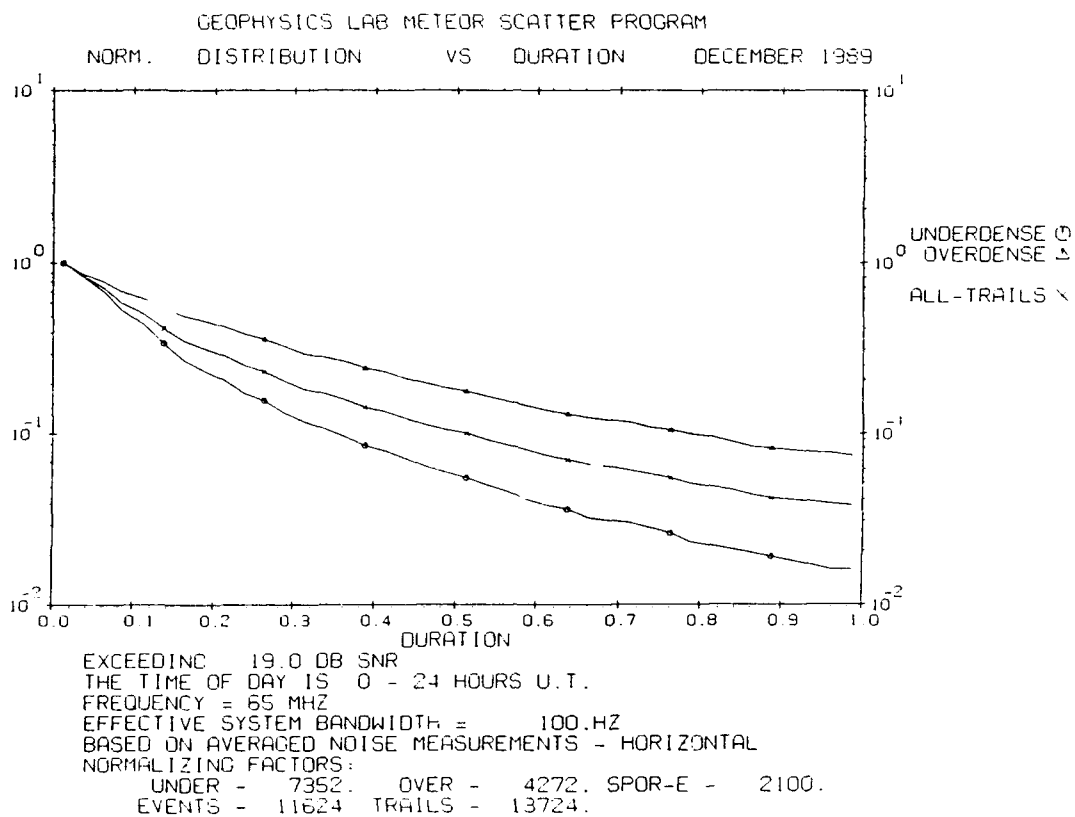


**Figure D35. Normalized Distribution of Signal Durations Exceeding 19 dB for December 1989. The frequency is 65 MHz.**

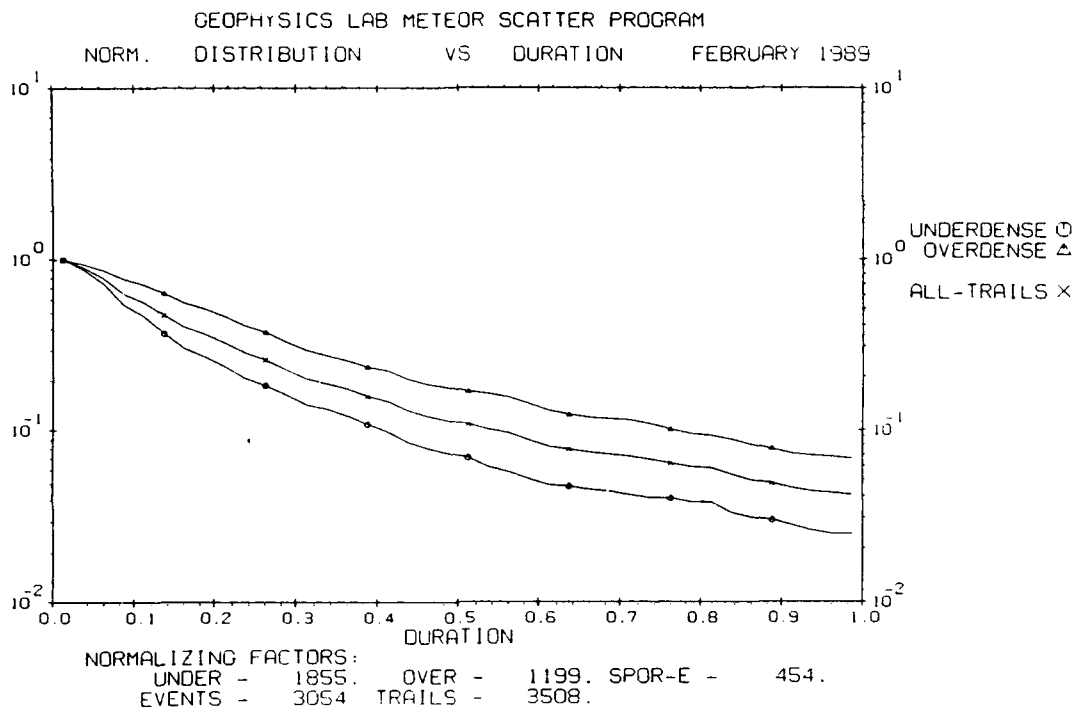


**Figure D36. Normalized Distribution of Signal Durations Exceeding 29 dB for February 1989. The frequency is 65 MHz.**

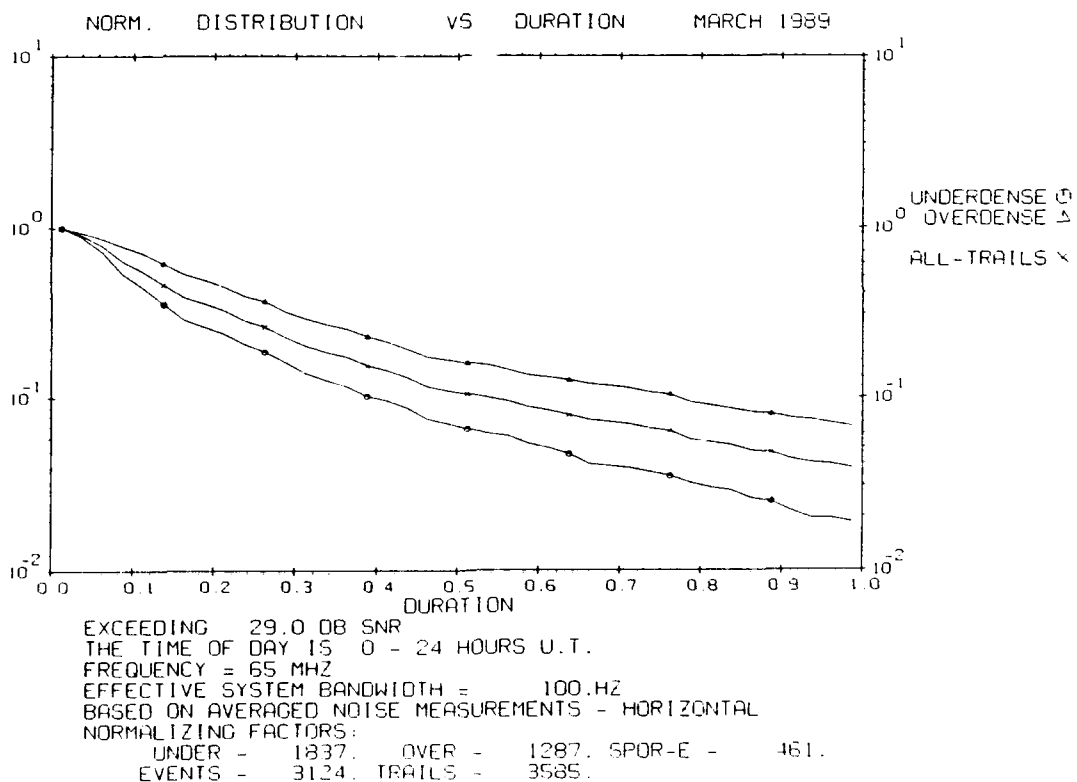


**Figure D37. Normalized Distribution of Signal Durations Exceeding 29 dB for March 1989. The frequency is 65 MHz.**

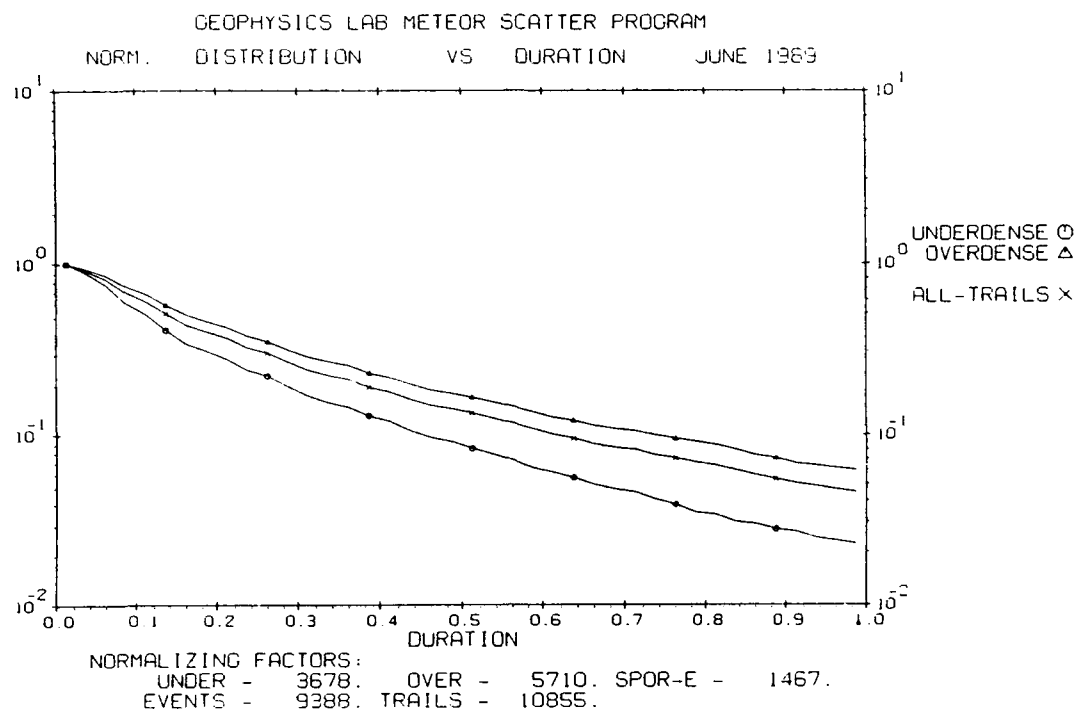


**Figure D38. Normalized Distribution of Signal Durations Exceeding 29 dB for June 1989. The frequency is 65 MHz.**

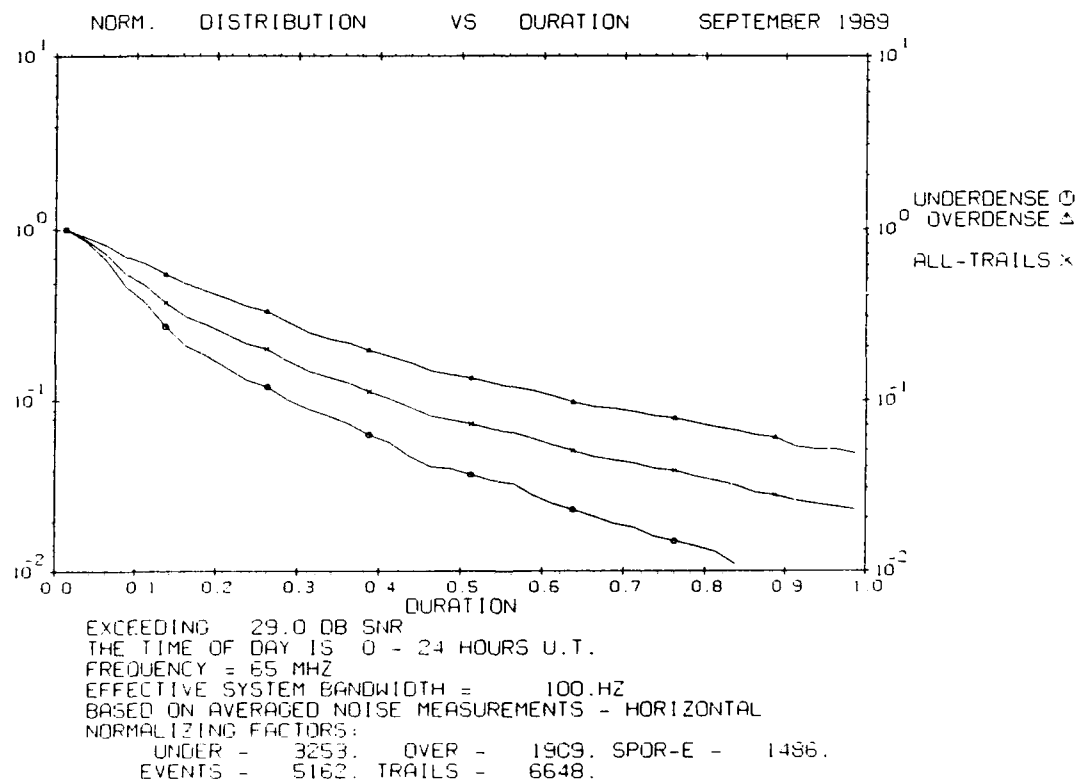


**Figure D39. Normalized Distribution of Signal Durations Exceeding 29 dB for September 1989. The frequency is 65 MHz.**

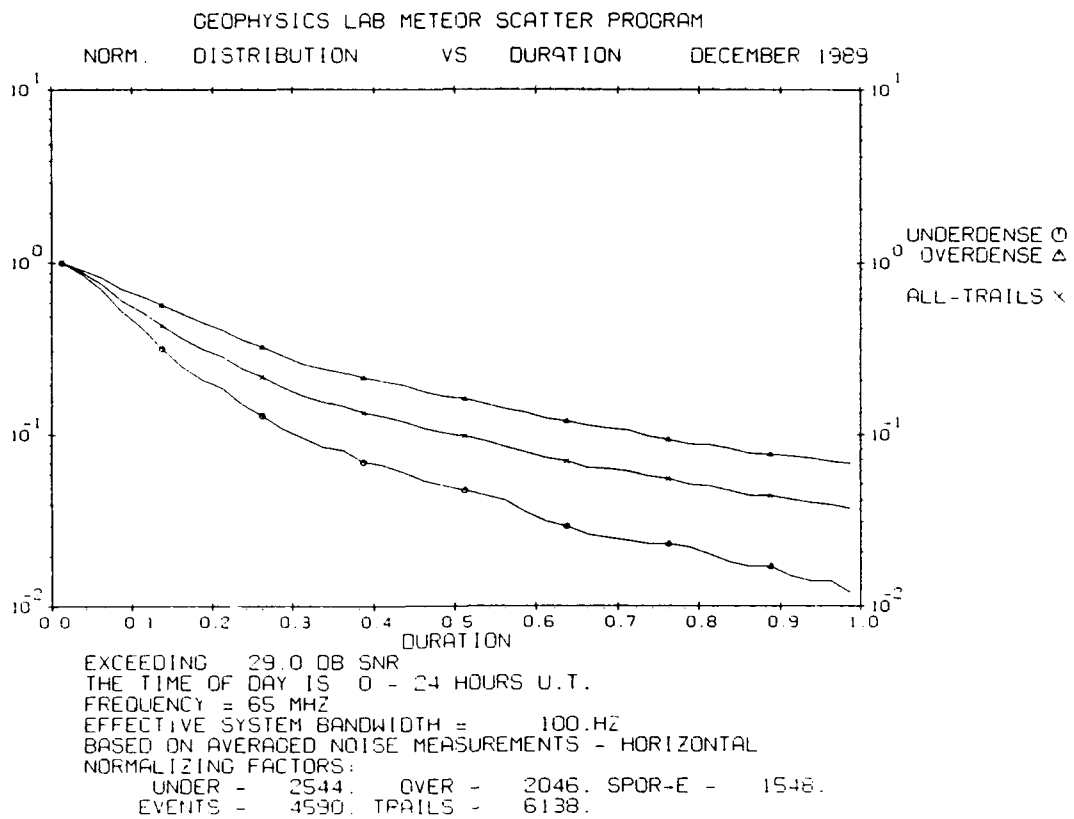


**Figure D40. Normalized Distribution of Signal Durations Exceeding 29 dB for December 1989. The frequency is 65 MHz.**



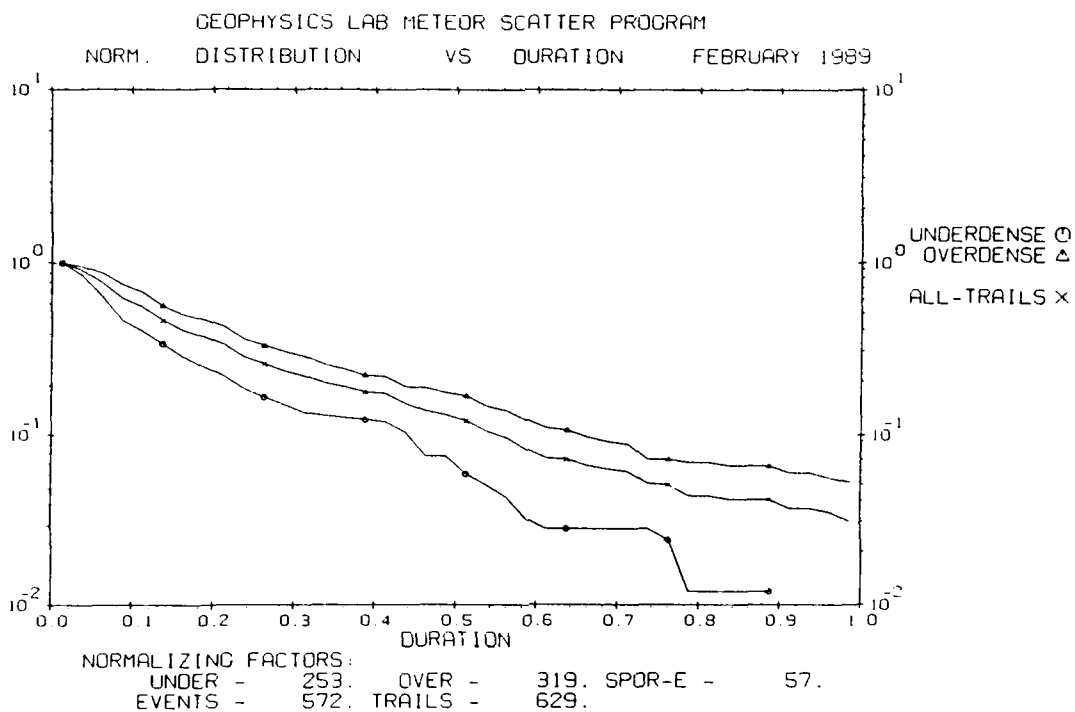


**Figure D41. Normalized Distribution of Signal Durations Exceeding 39 dB for February 1989. The Frequency is 65 MHz**

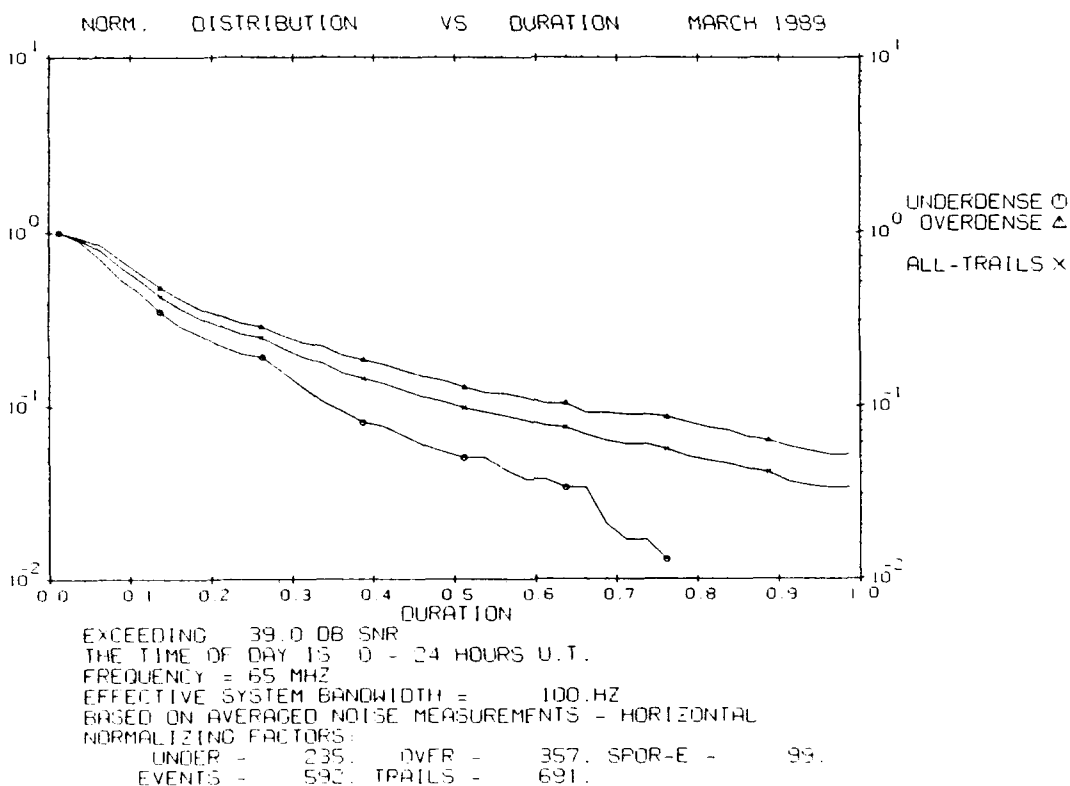


**Figure D42. Normalized Distribution of Signal Durations Exceeding 39 dB for March 1989. The Frequency is 65 MHz**

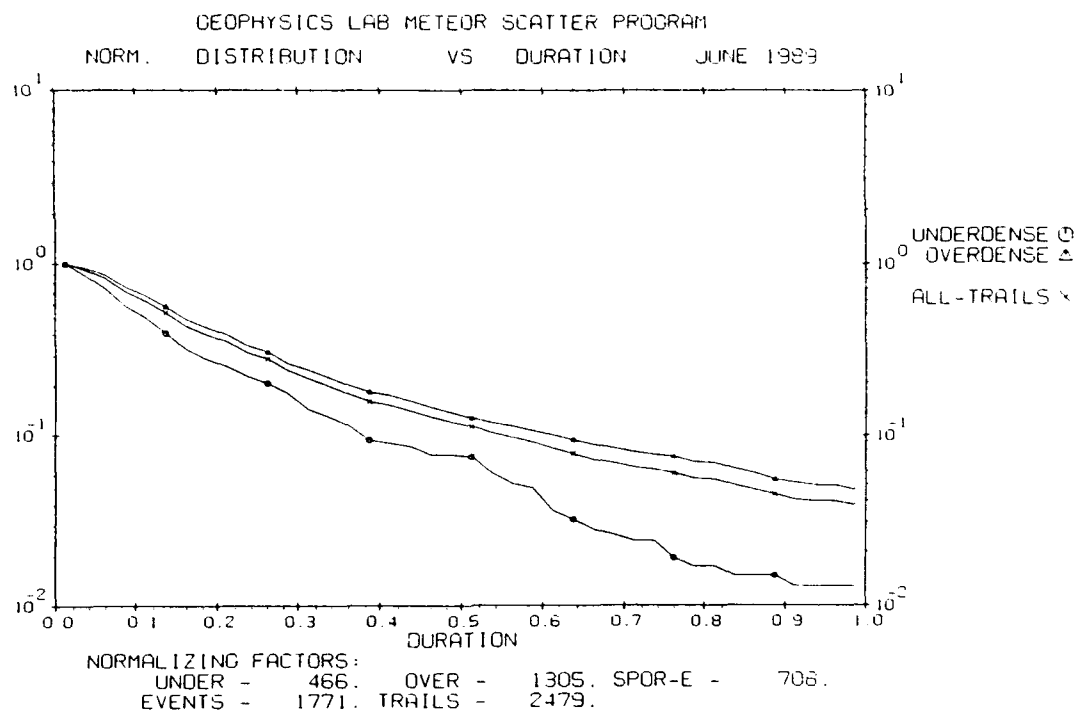


**Figure D43. Normalized Distribution of Signal Durations Exceeding 39 dB for June 1989. The Frequency is 65 MHz**

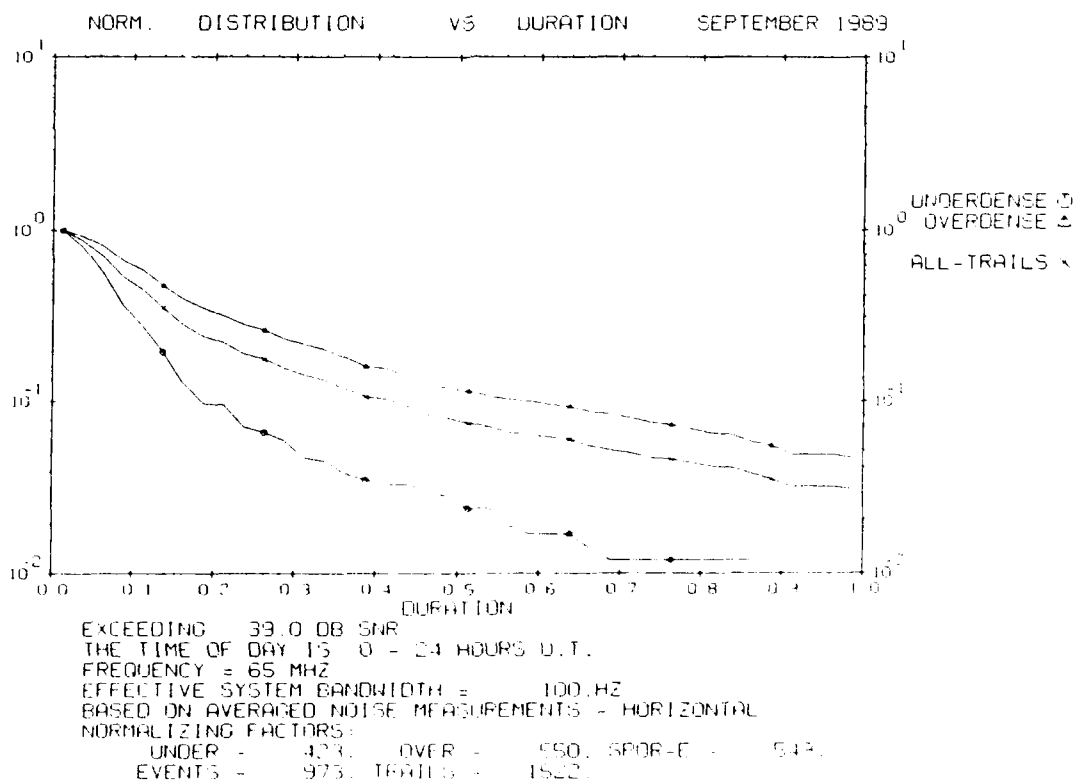


**Figure D44. Normalized Distribution of Signal Durations Exceeding 39 dB for September 1989. The Frequency is 65 MHz**

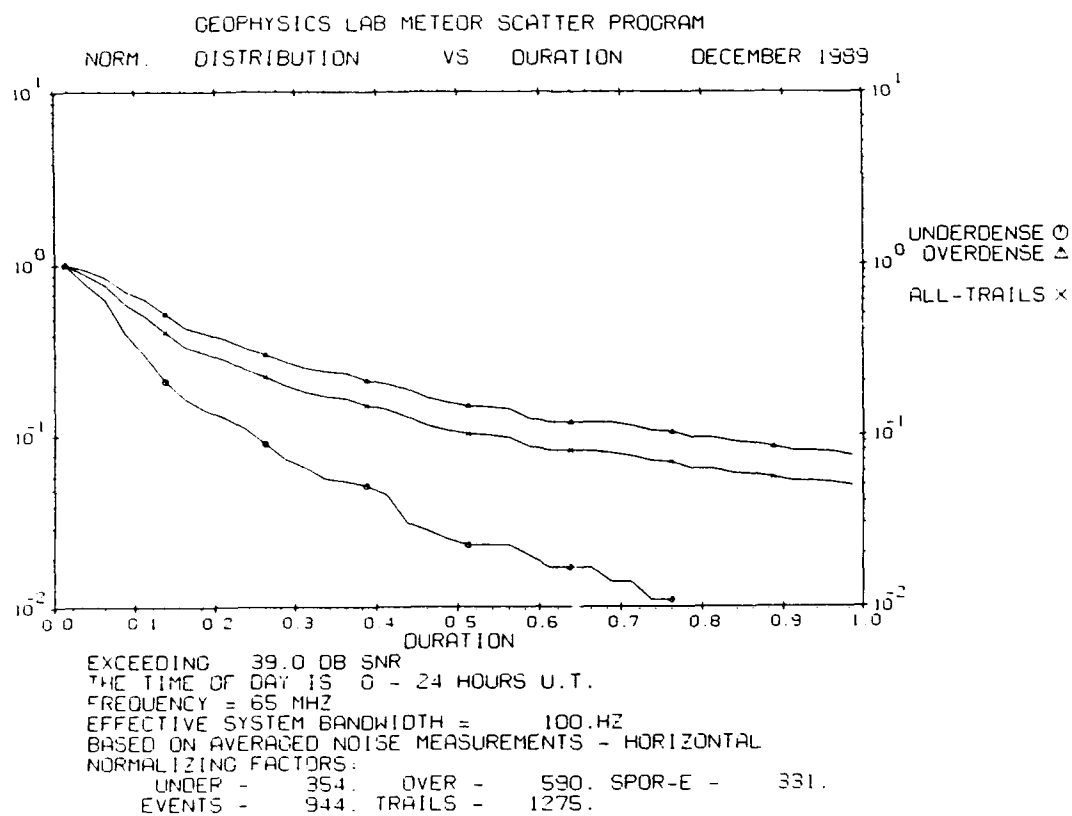


**Figure D' 5. Normalized Distribution of Signal Durations Exceeding 39 dB for December 1989. The Frequency is 65 MHz**

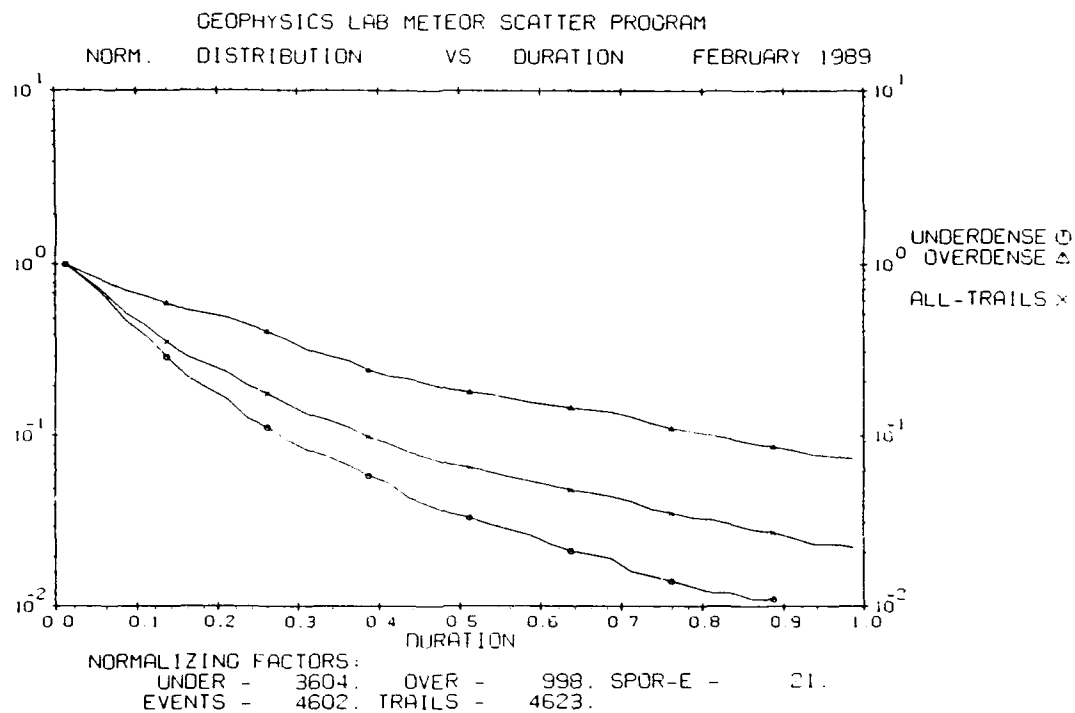


**Figure D46. Normalized Distribution of Signal Durations Exceeding 19 dB for February 1989. The frequency is 104 MHz**

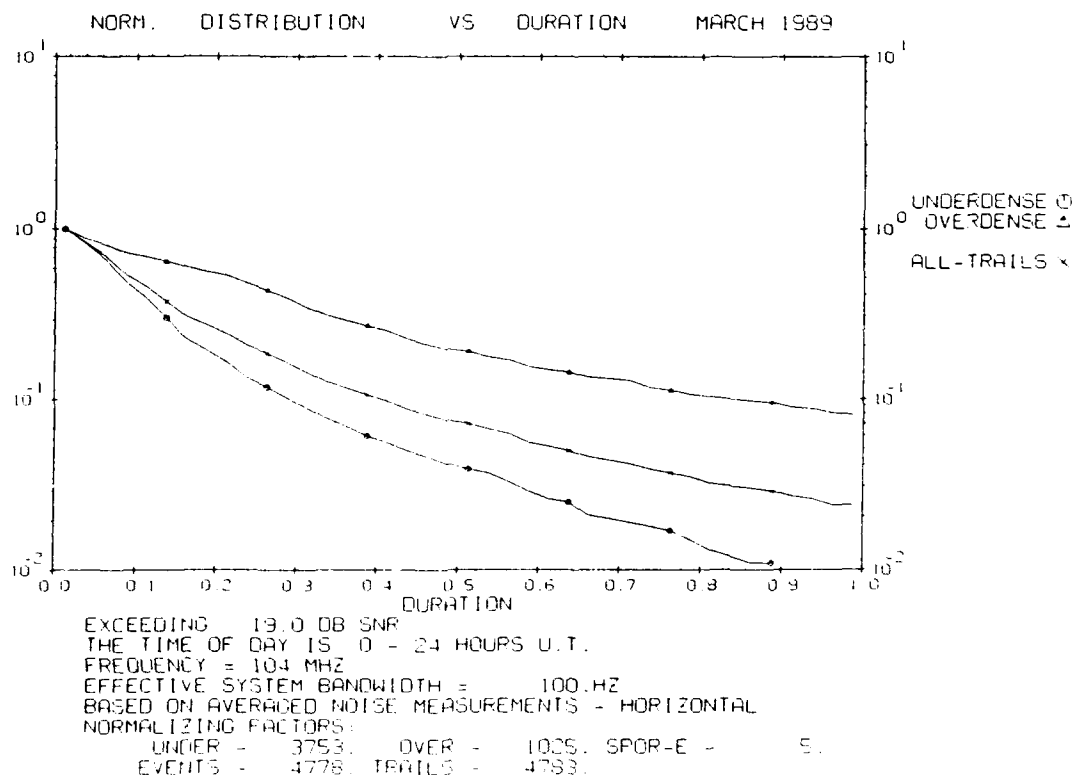


**Figure D47. Normalized Distribution of Signal Durations Exceeding 19 dB for March 1989. The frequency is 104 MHz**

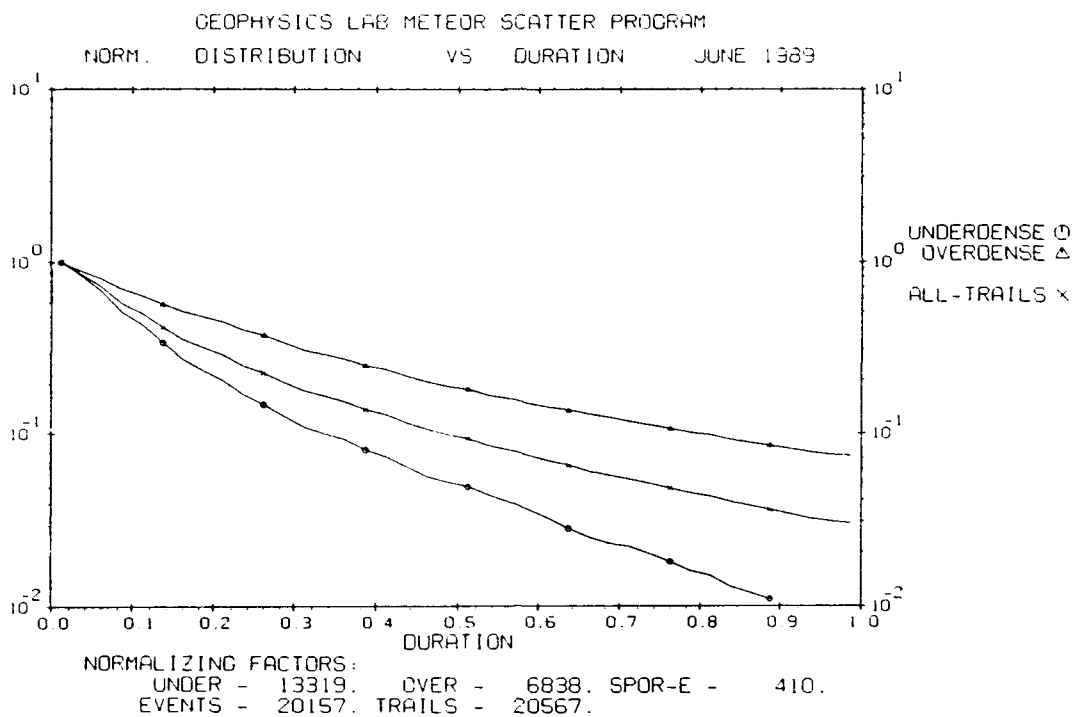


**Figure D48. Normalized Distribution of Signal Durations Exceeding 19 dB for June 1989. The frequency is 104 MHz**

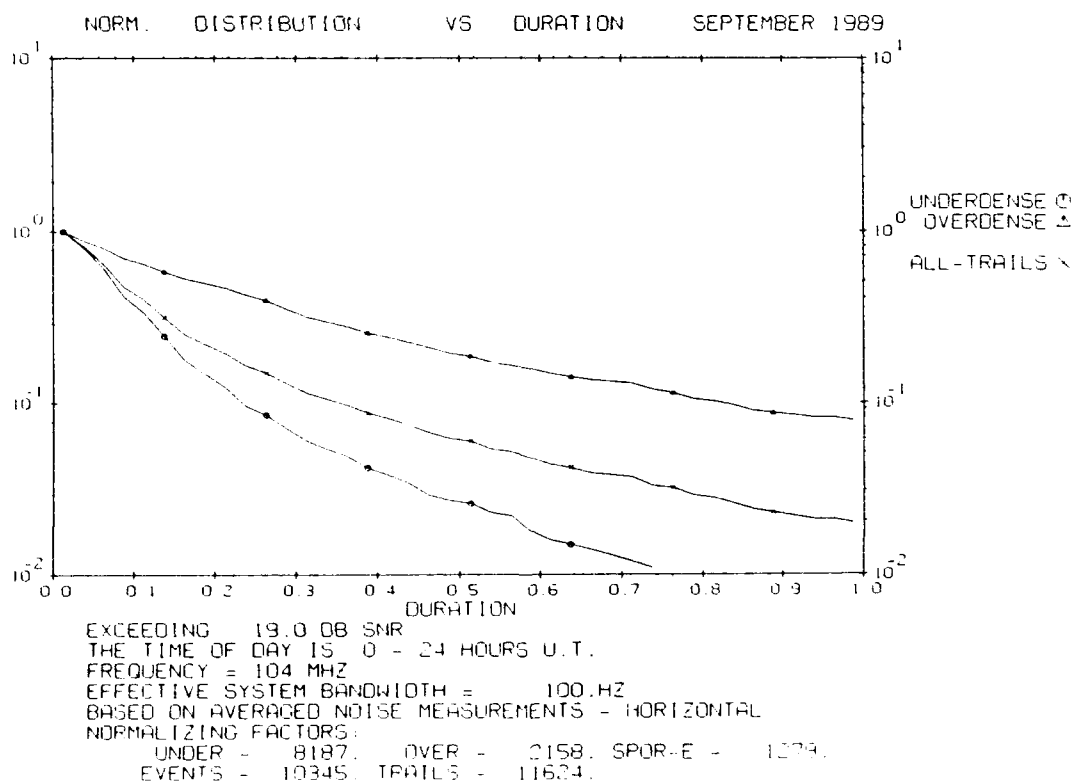


**Figure D49. Normalized Distribution of Signal Durations Exceeding 19 dB for September 1989. The frequency is 104 MHz**

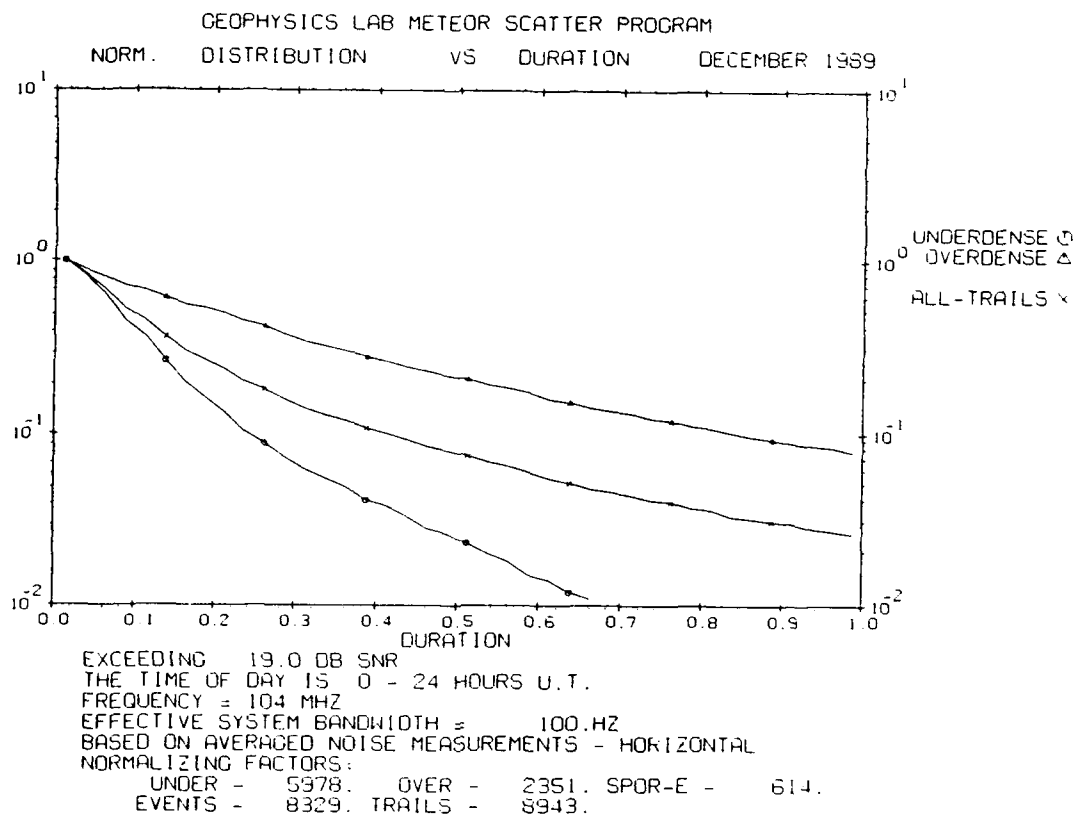


**Figure D50. Normalized Distribution of Signal Durations Exceeding 19 dB for December 1989. The frequency is 104 MHz**

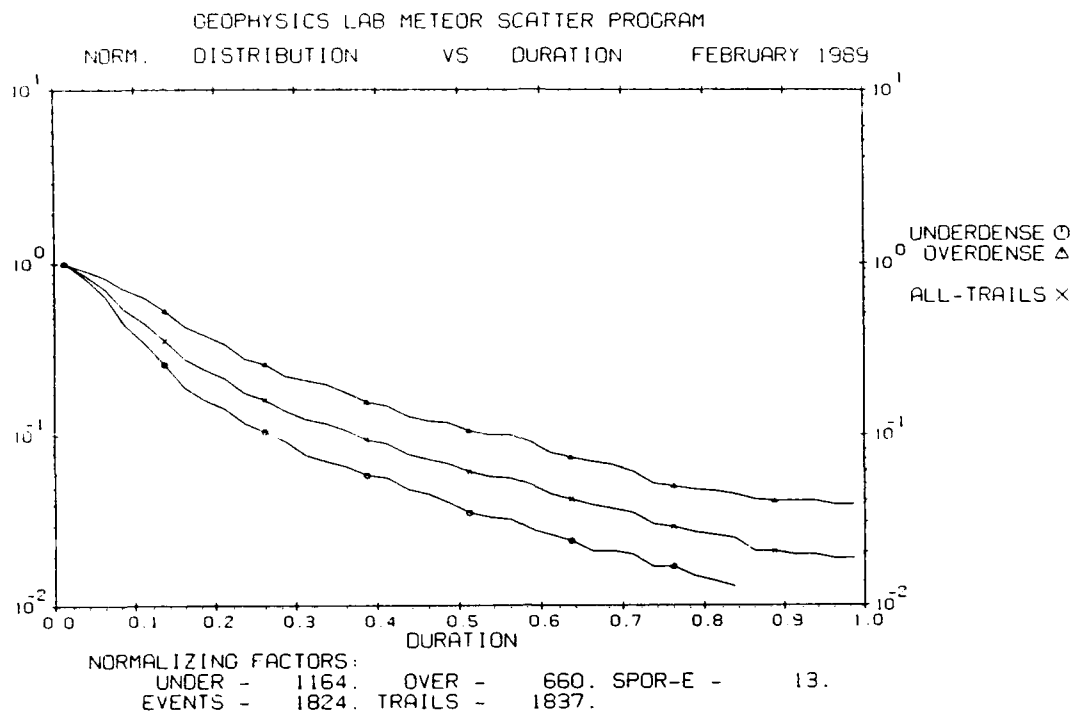


**Figure D51. Normalized Distribution of Signal Durations Exceeding 29 dB for February 1989. The frequency is 104 MHz**

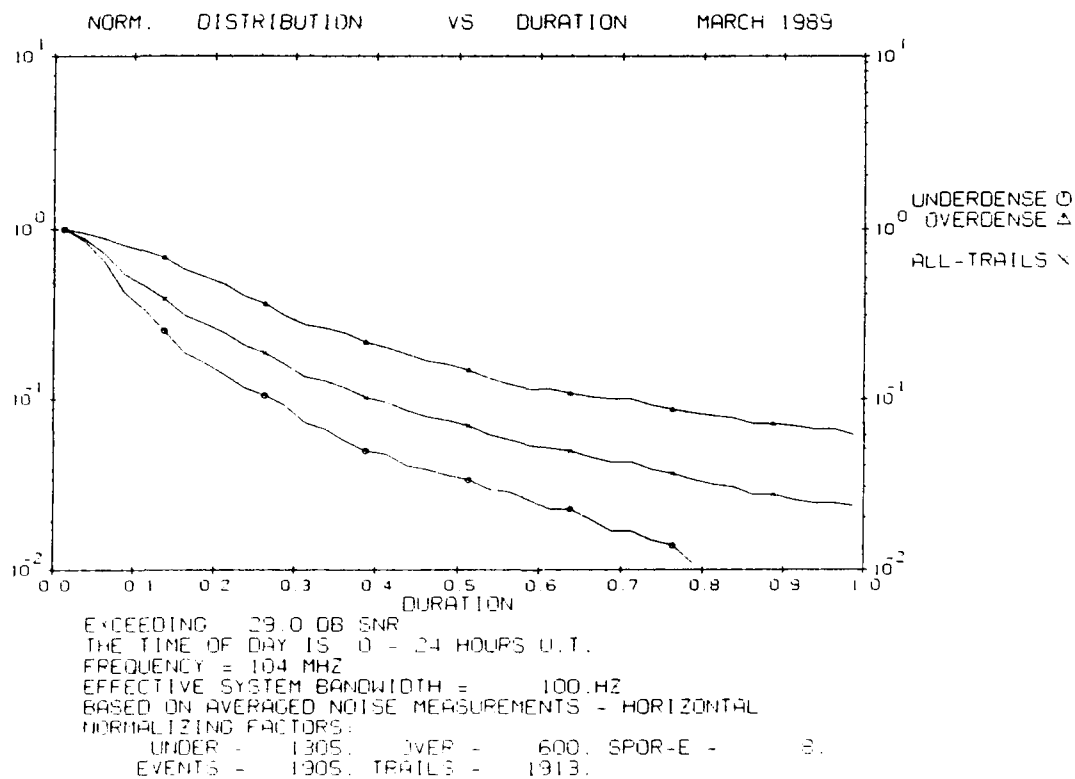


**Figure D52. Normalized Distribution of Signal Durations Exceeding 29 dB for March 1989. The frequency is 104 MHz**

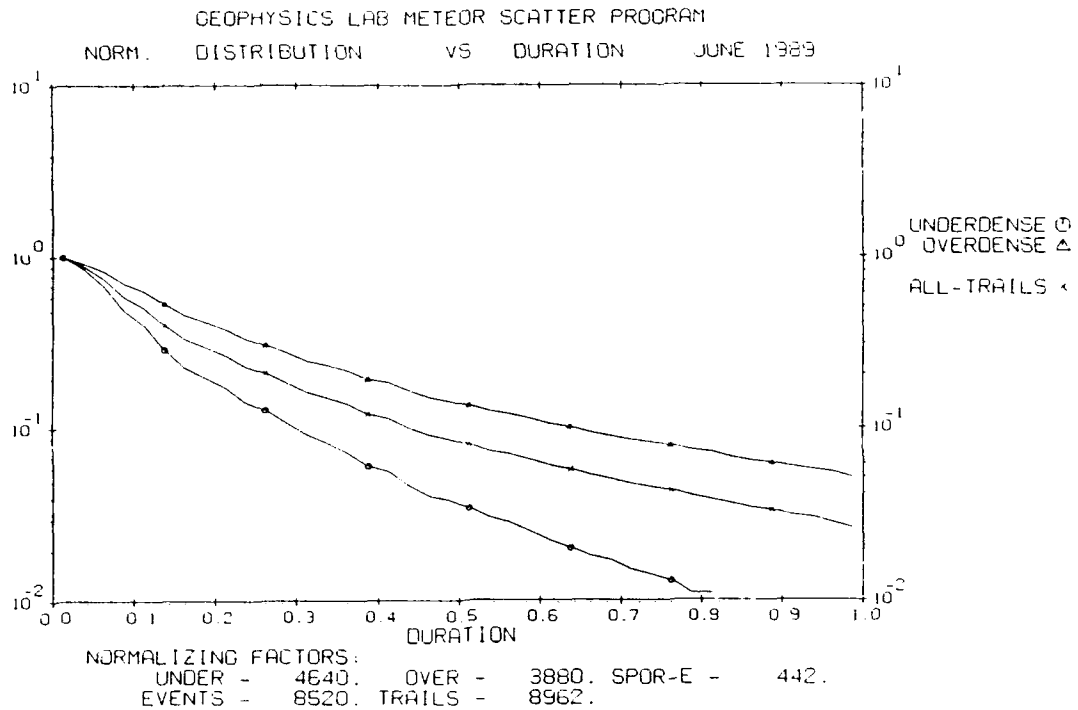


**Figure D53. Normalized Distribution of Signal Durations Exceeding 29 dB for June 1989. The frequency is 104 MHz**

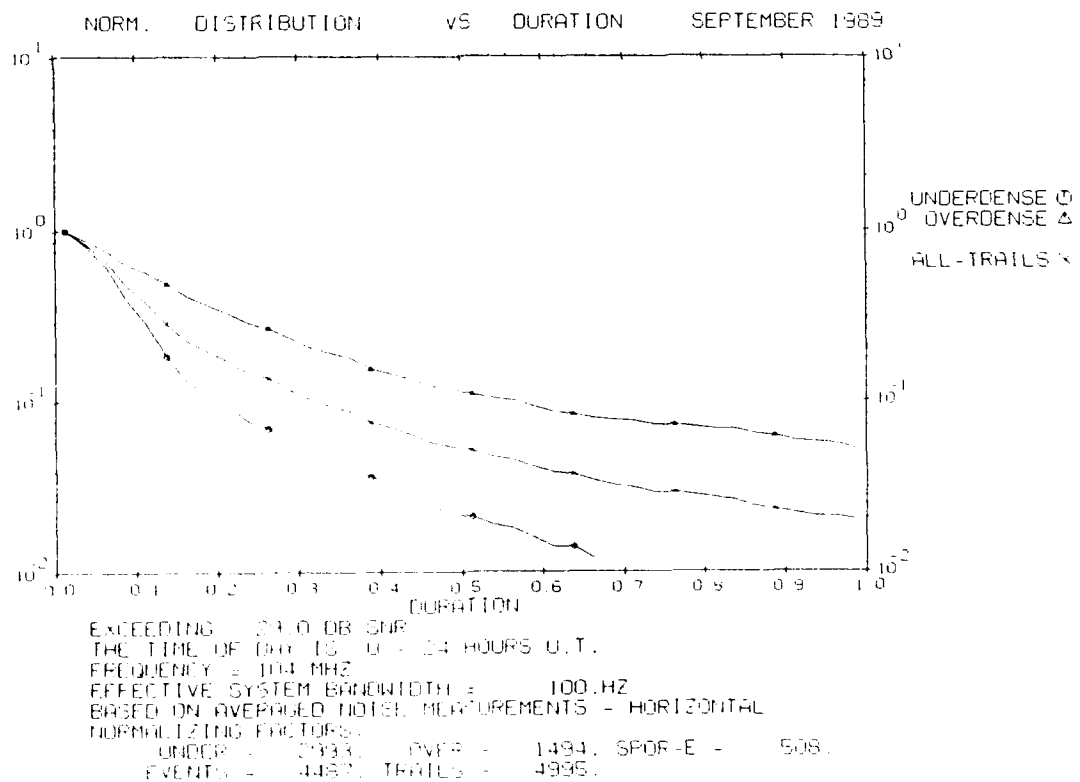


**Figure D54. Normalized Distribution of Signal Durations Exceeding 29 dB for September 1989. The frequency is 104 MHz**



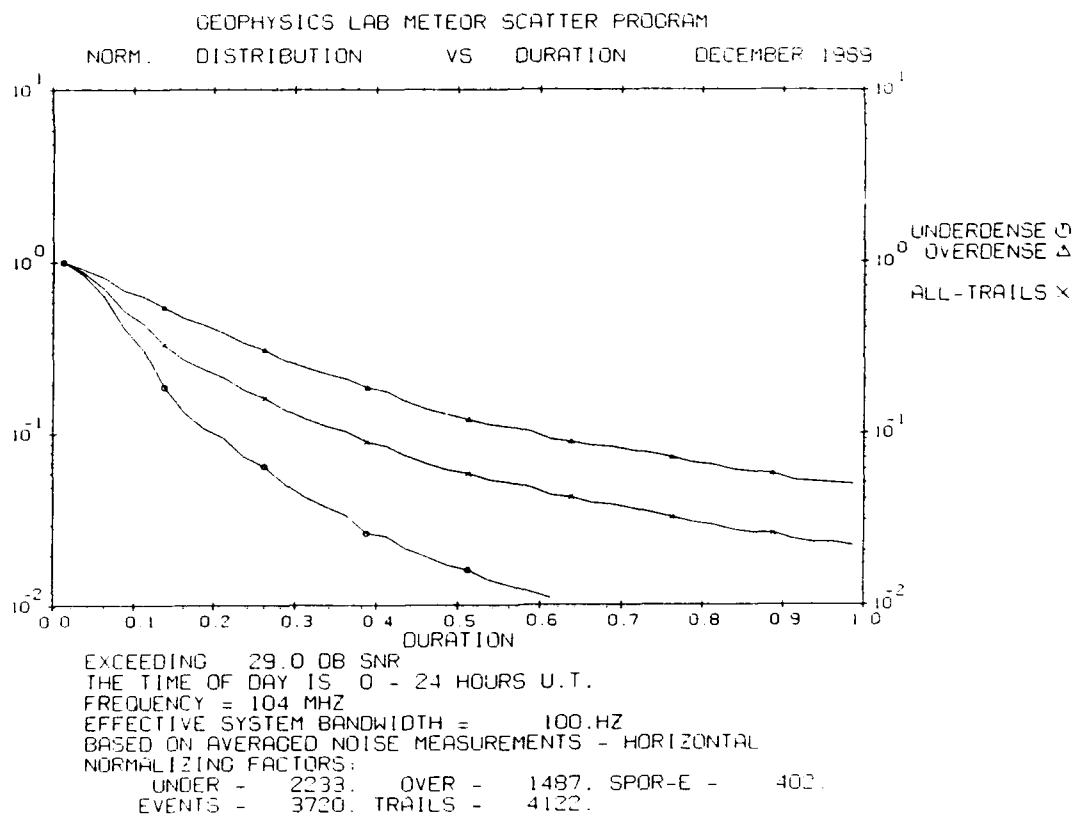


**Figure D55. Normalized Distribution of Signal Durations Exceeding 29 dB for December 1989. The frequency is 104 MHz**

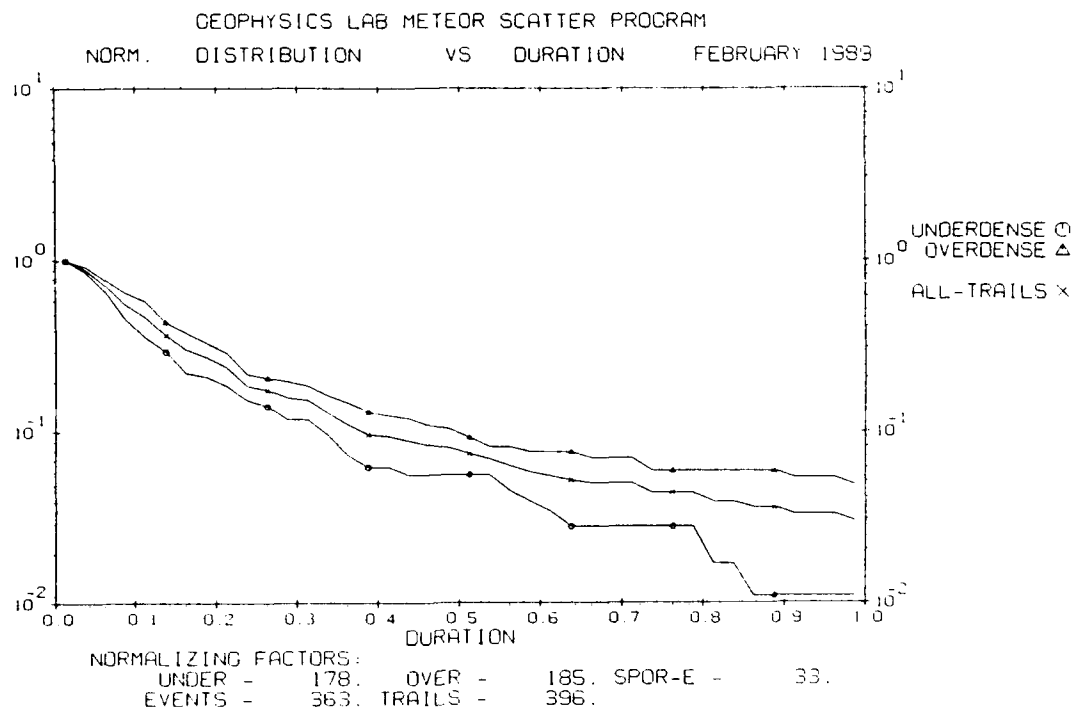


**Figure D56. Normalized Distribution of Signal Durations Exceeding 39 dB for February 1989. The frequency is 104 MHz**

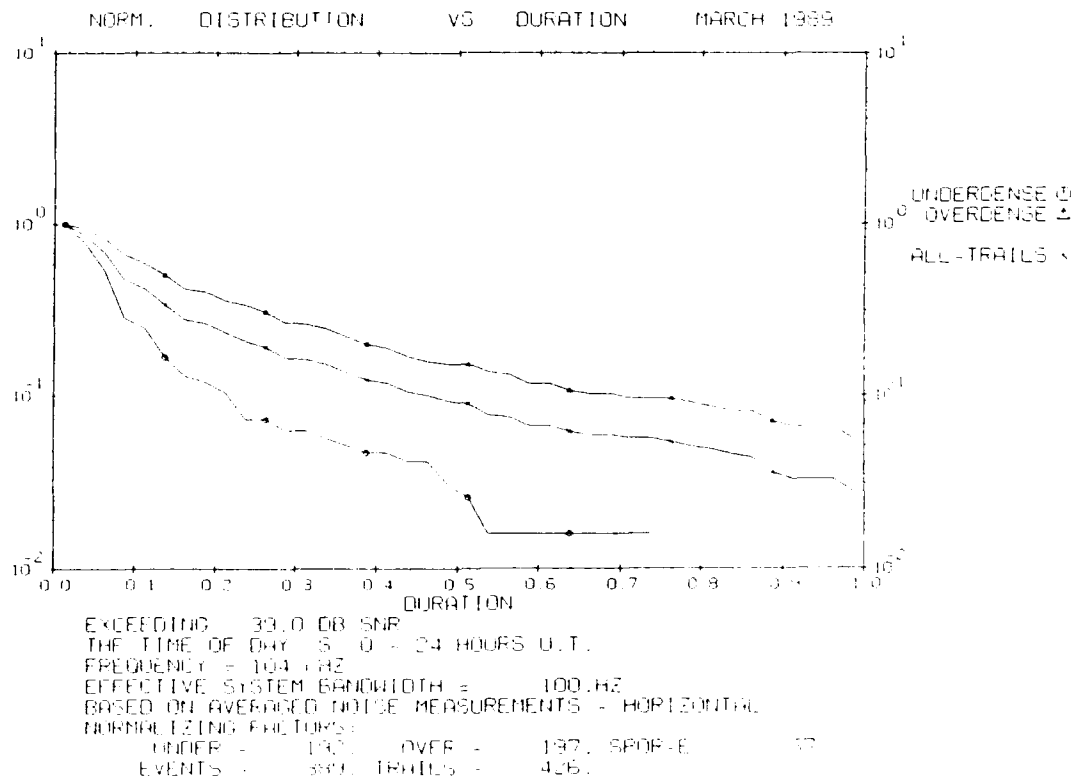


**Figure D57. Normalized Distribution of Signal Durations Exceeding 39 dB for March 1989. The frequency is 104 MHz**

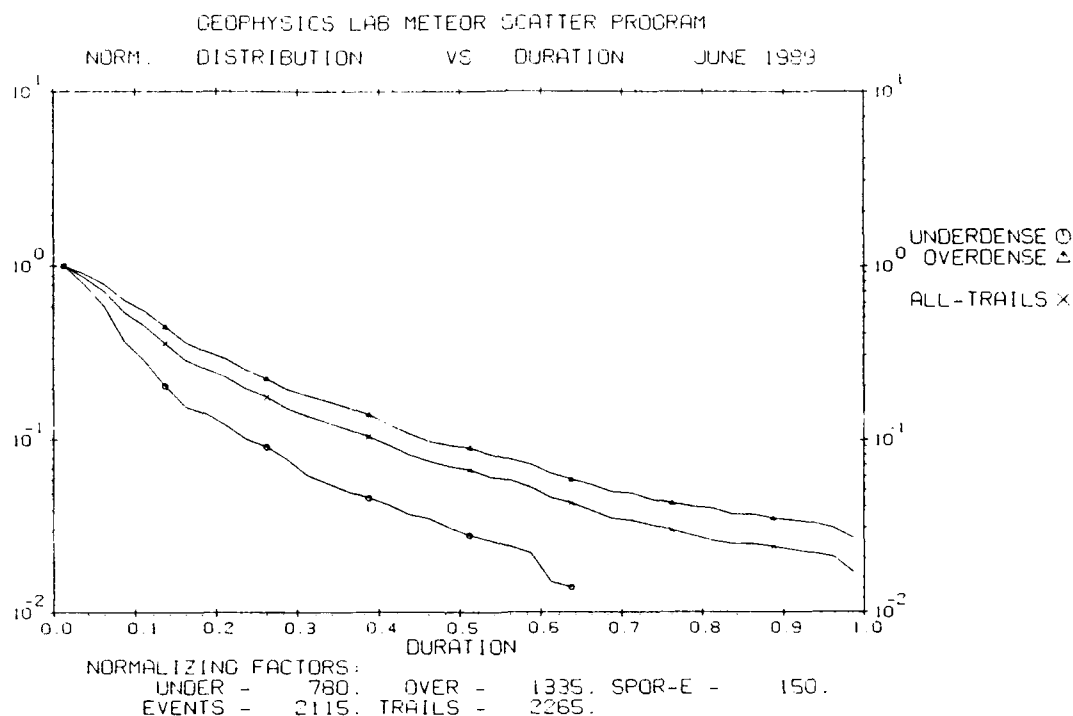


Figure D58. Normalized Distribution of Signal Durations Exceeding 39 dB for June 1989. The frequency is 104 MHz

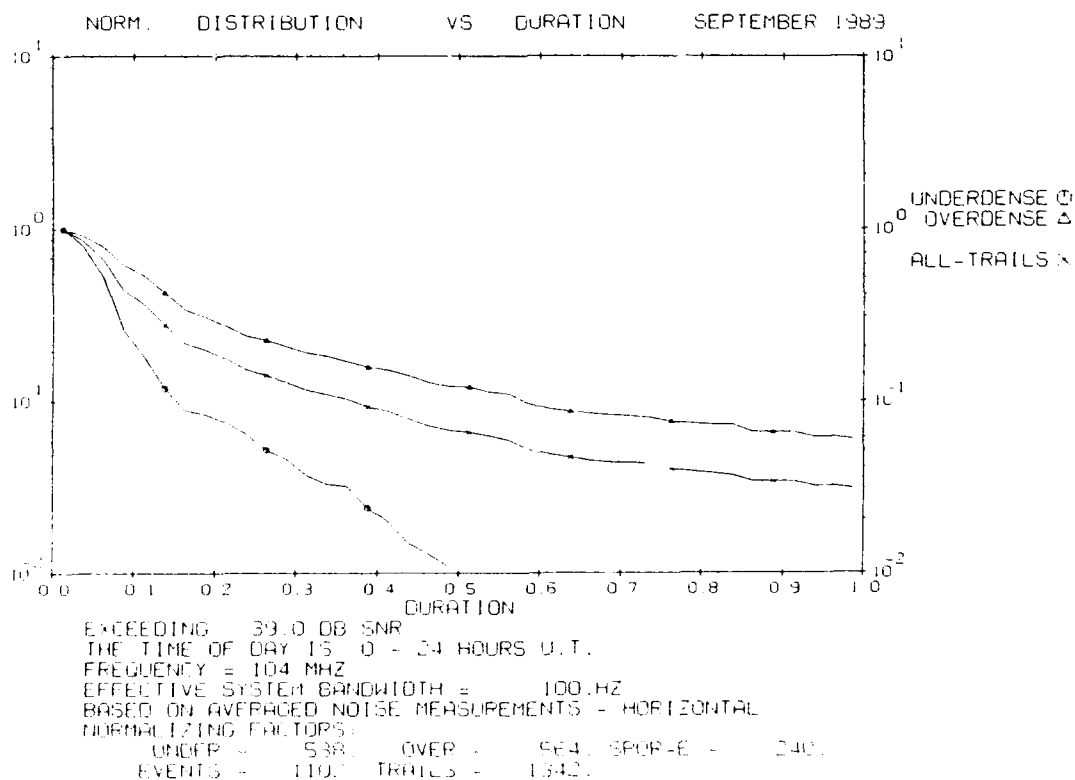
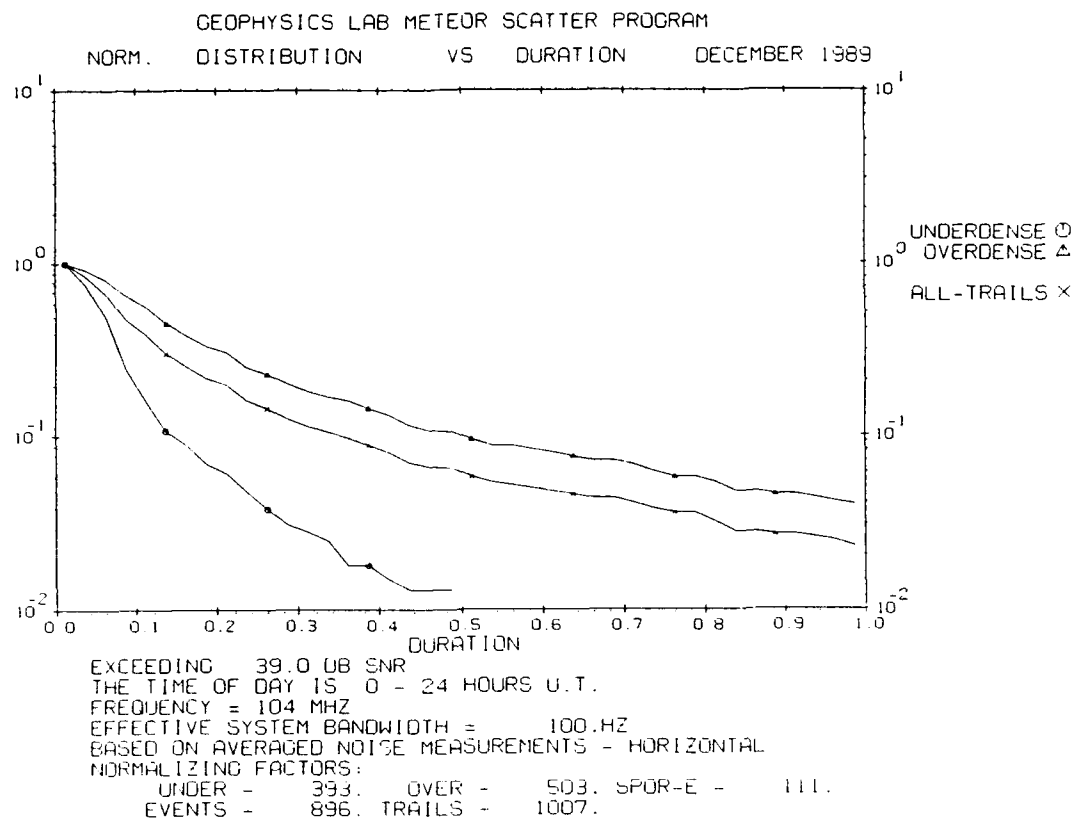


Figure D59. Normalized Distribution of Signal Durations Exceeding 39 dB for September 1989. The frequency is 104 MHz



**Figure D60. Normalized Distribution of Signal Durations Exceeding 39 dB for December 1989. The frequency is 104 MHz**

## **Appendix E**

Waiting Time Statistics. Diurnal Variations

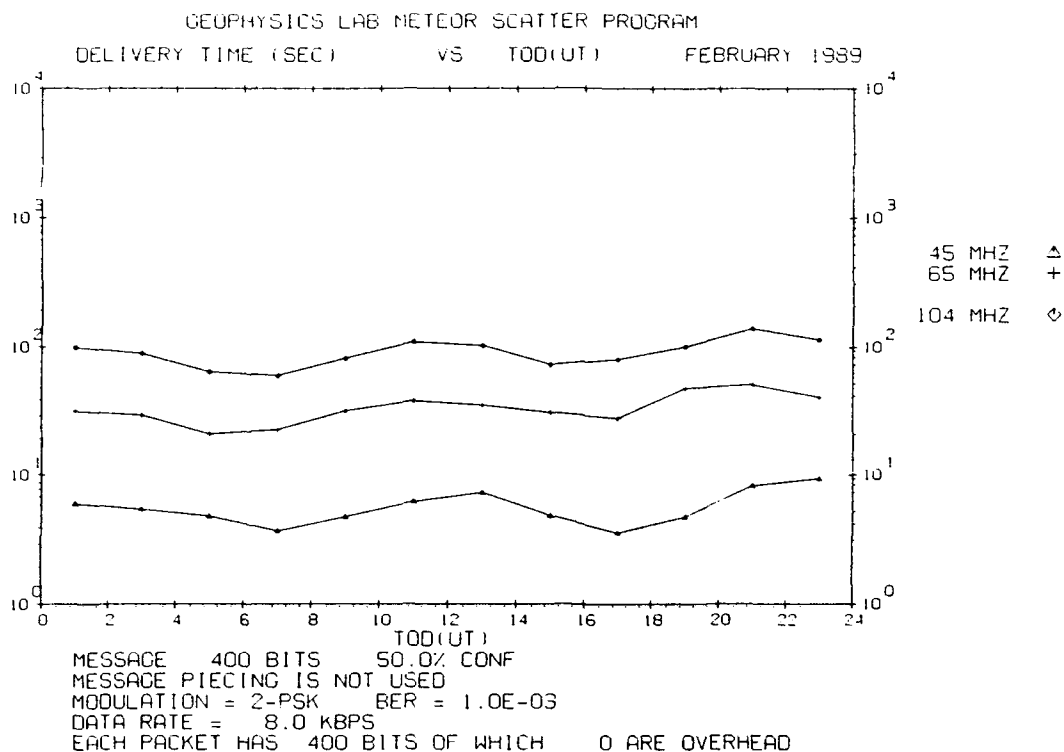


**Figure E1. Waiting Time vs Time of Day for Trails of 50 msec Duration for February 1989. The transmitter power is 10,000 W**

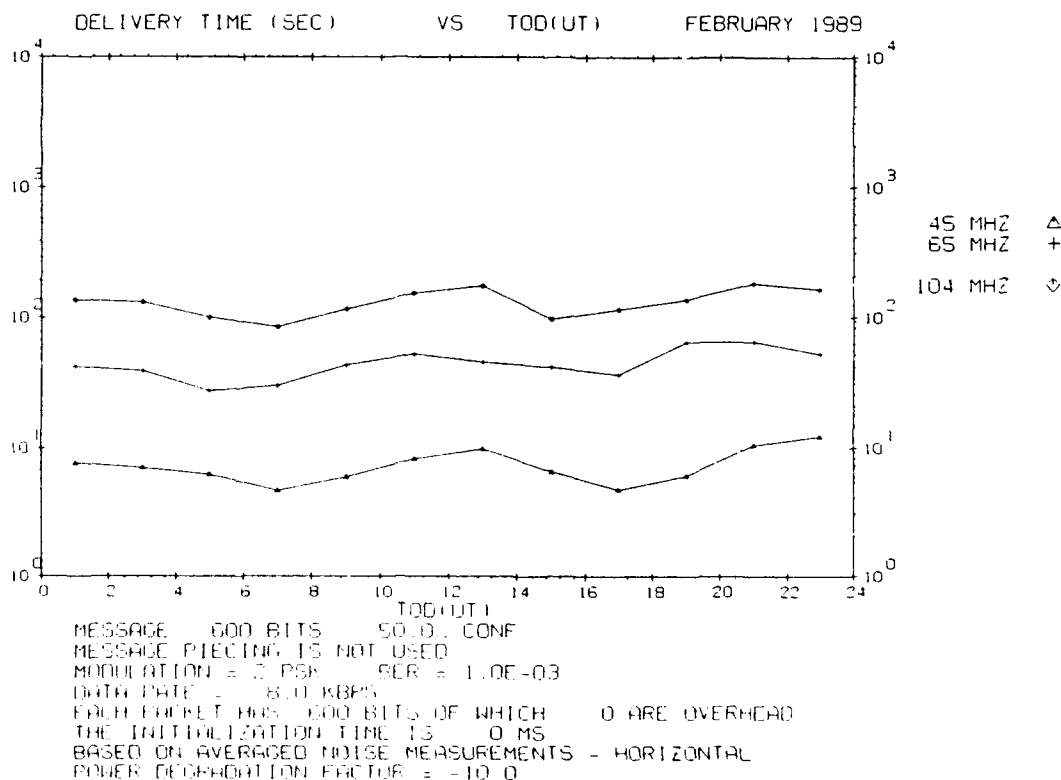


**Figure E2. Same as Figure E1 but for Trails of 75 msec**

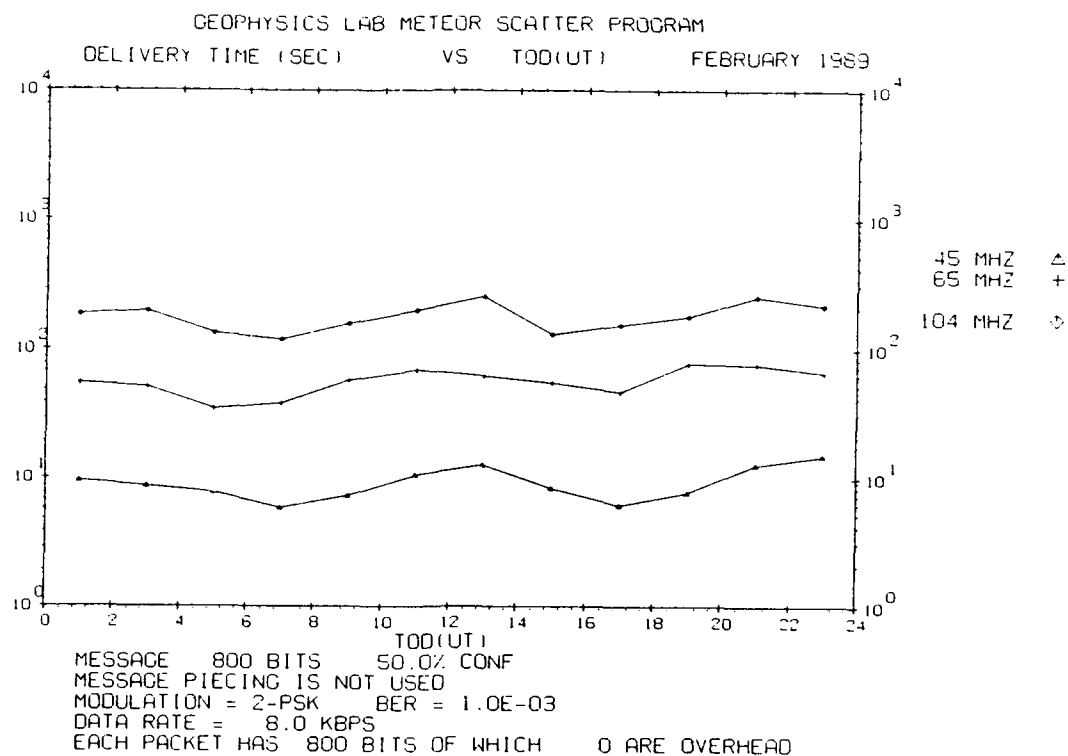


Figure E3. Same as Figure E1 but for Trails of 100 msec

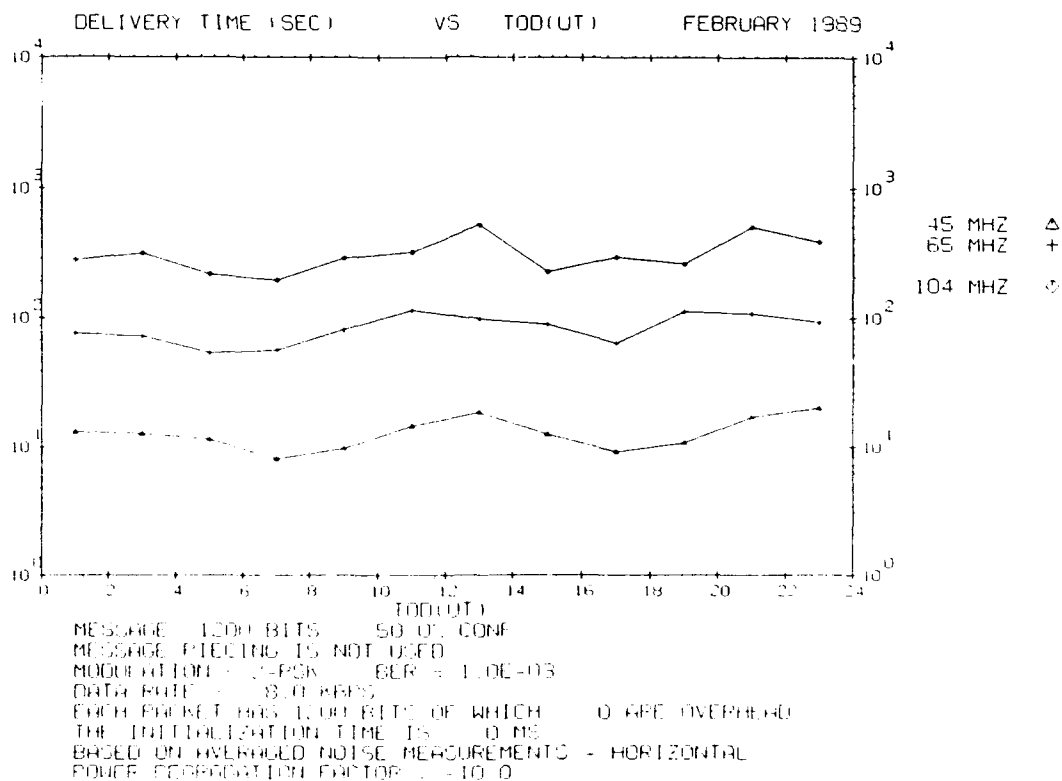


Figure E4. Same as Figure E1 but for Trails of 150 msec

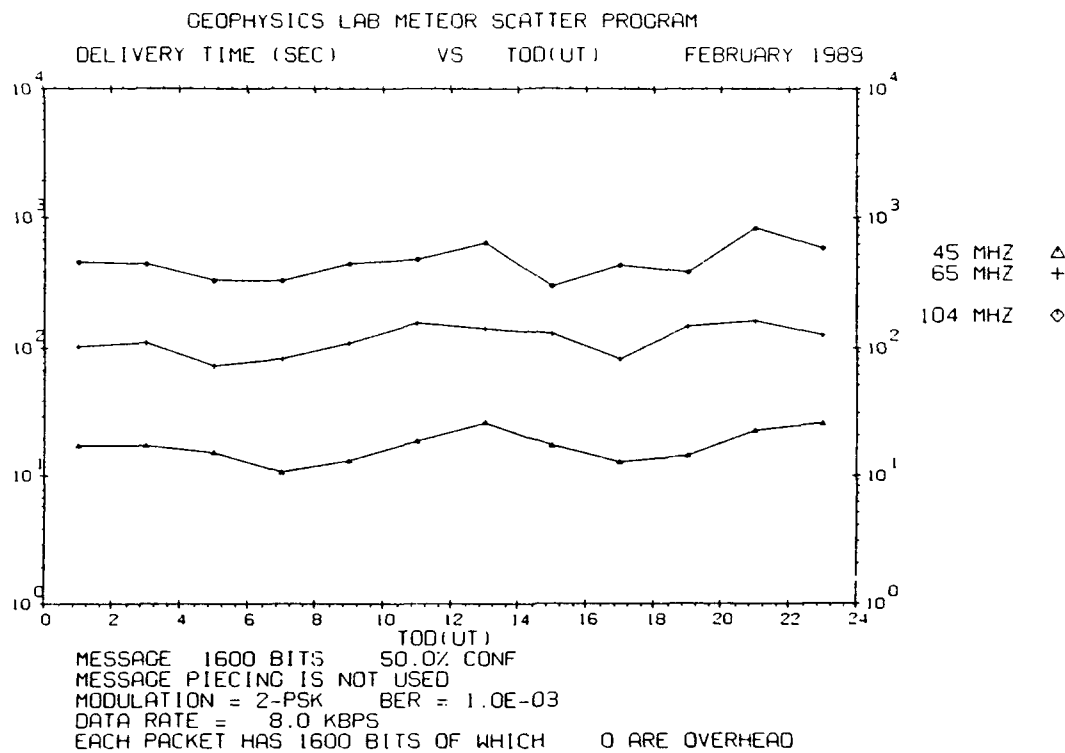


Figure E5. Same as Figure E1 but for Trails of 200 msec

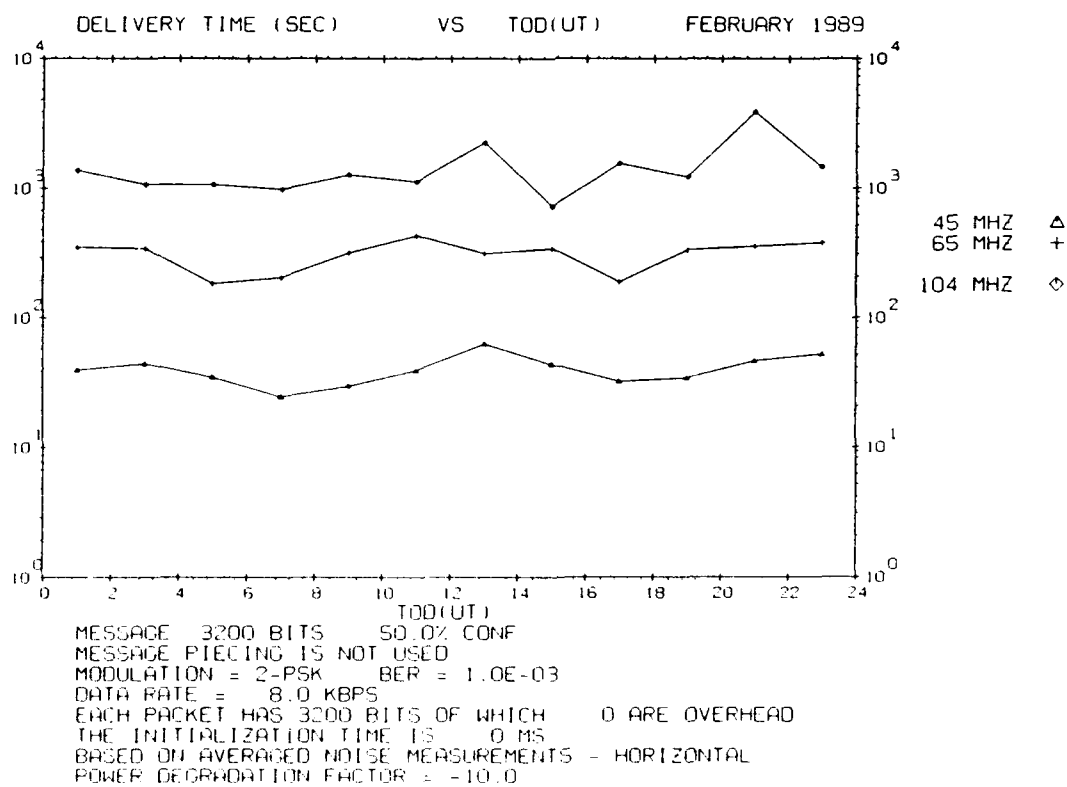
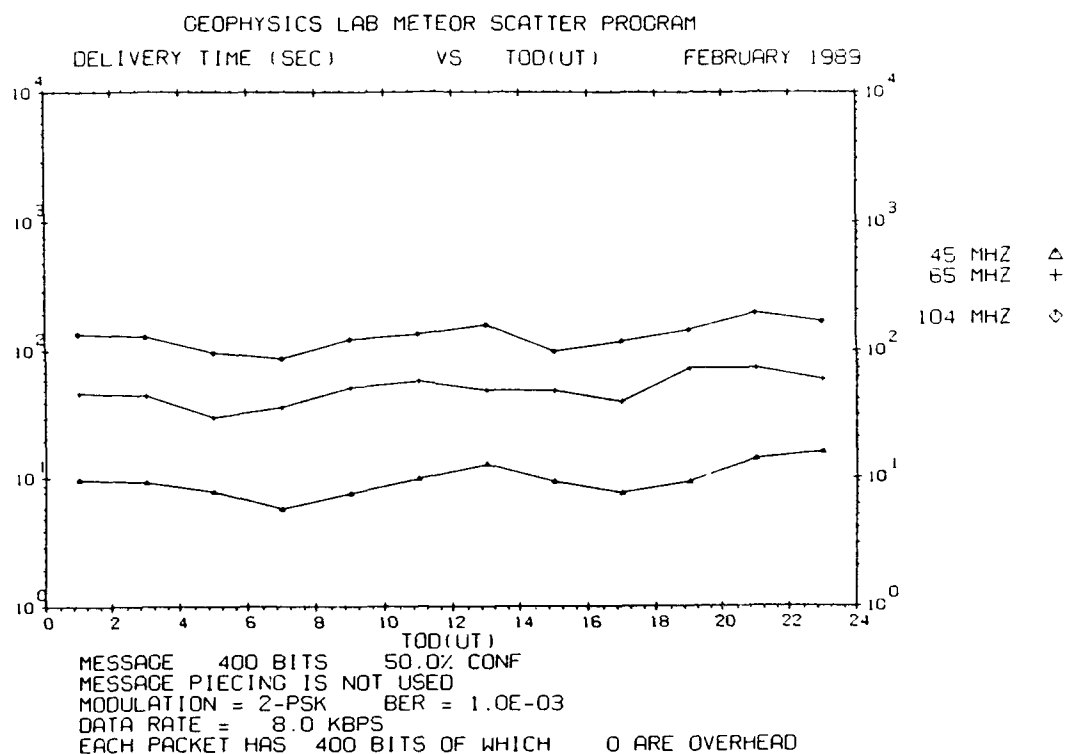
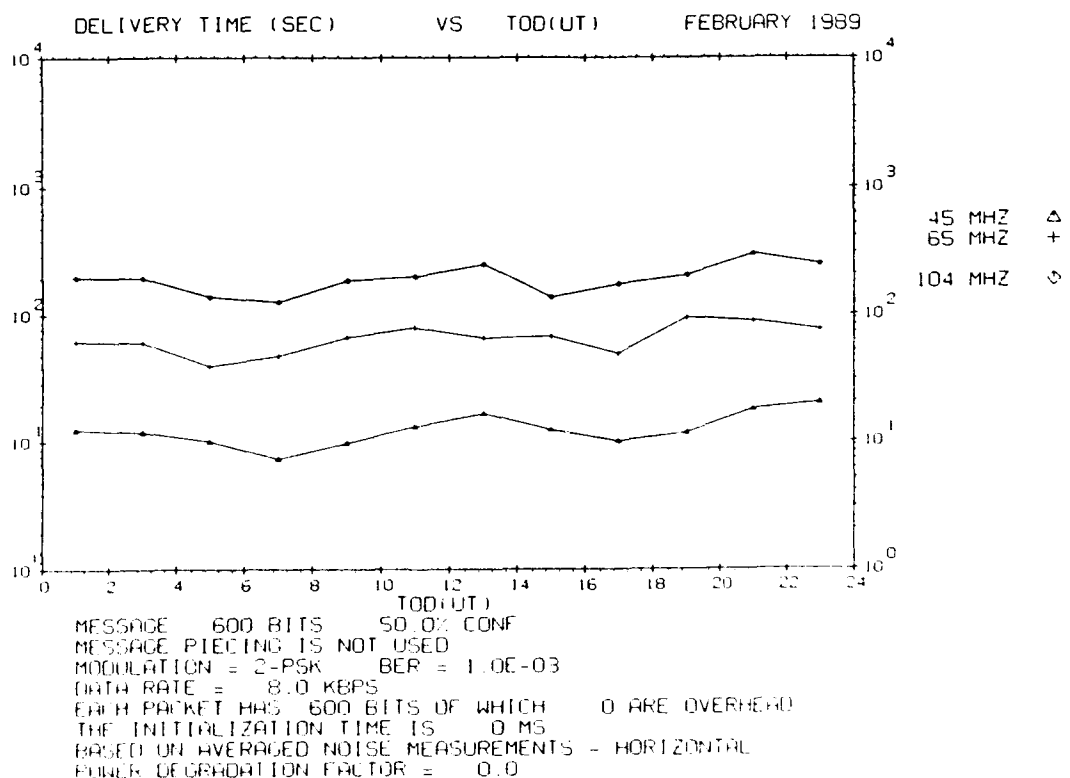


Figure E6. Same as Figure E1 but for Trails of 400 msec





**Figure E7. Waiting Time vs Time of Day for Trails of 50 msec Duration for February 1989. The Transmitter power is 1,000 W**



**Figure E8. Same as Figure E7 but for Trails of 75 msec**

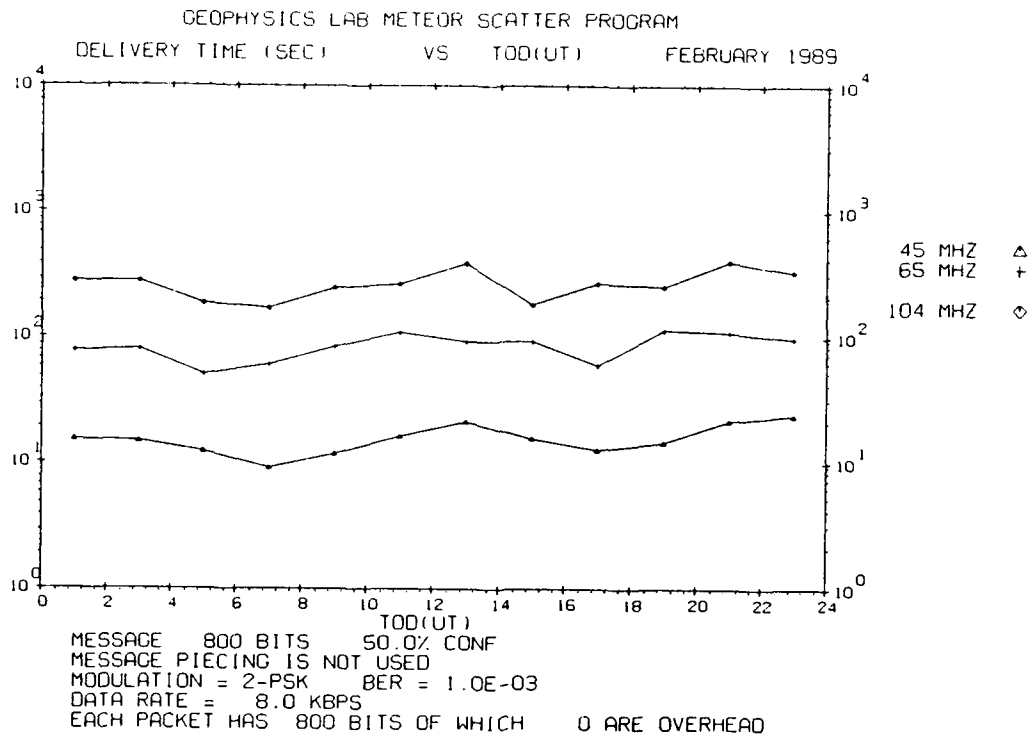


Figure E9. Same as Figure E7 but for Trails of 100 msec

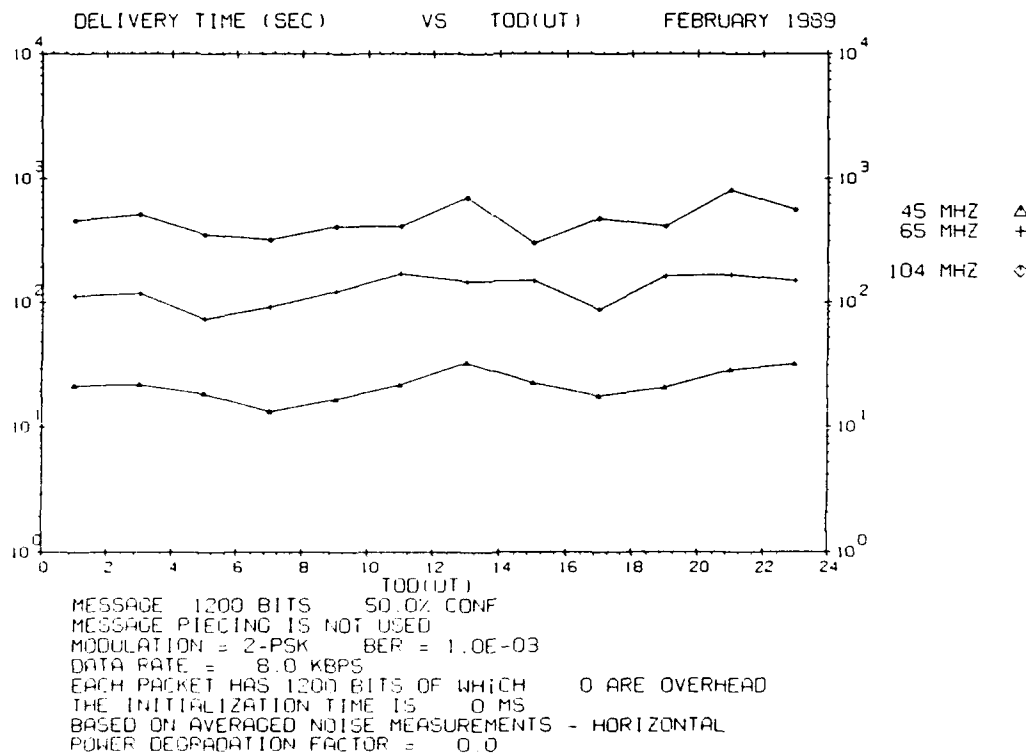


Figure E10. Same as Figure E7 but for Trails of 150 msec

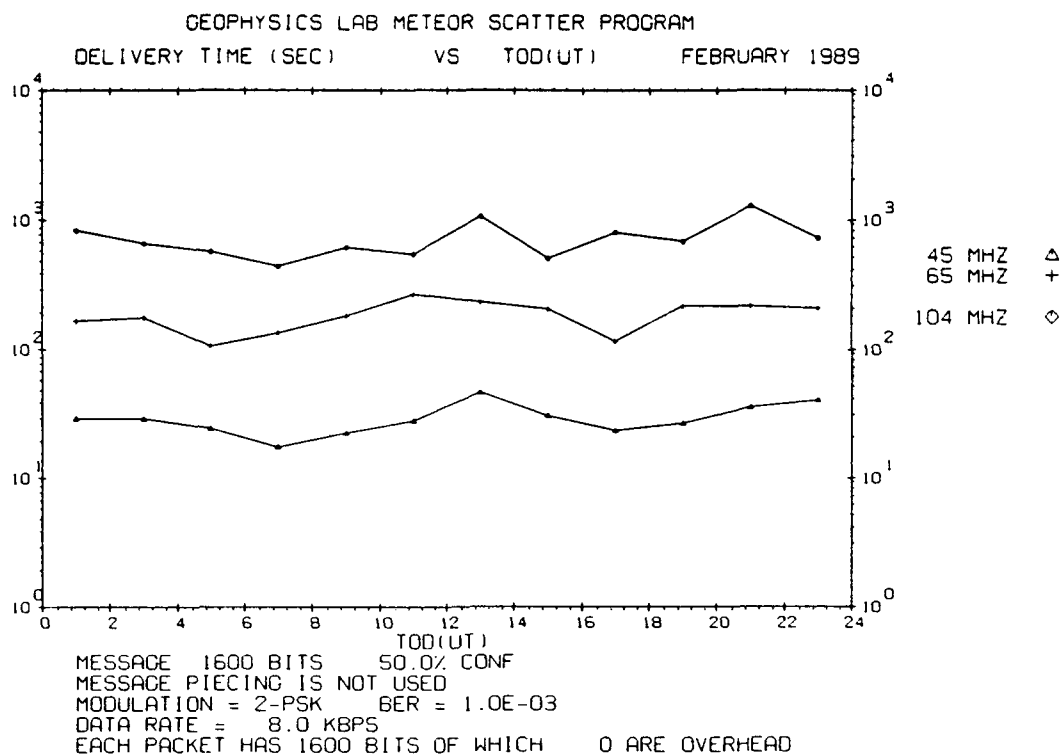


Figure E11. Same as Figure E7 but for Trails of 200 msec

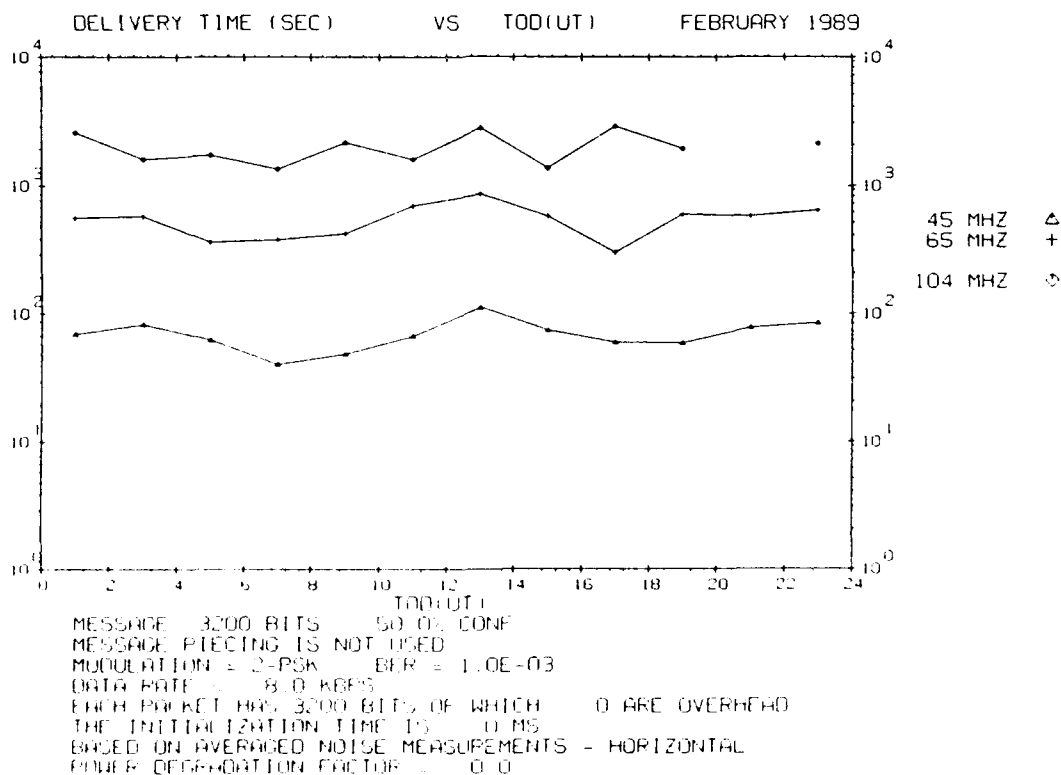
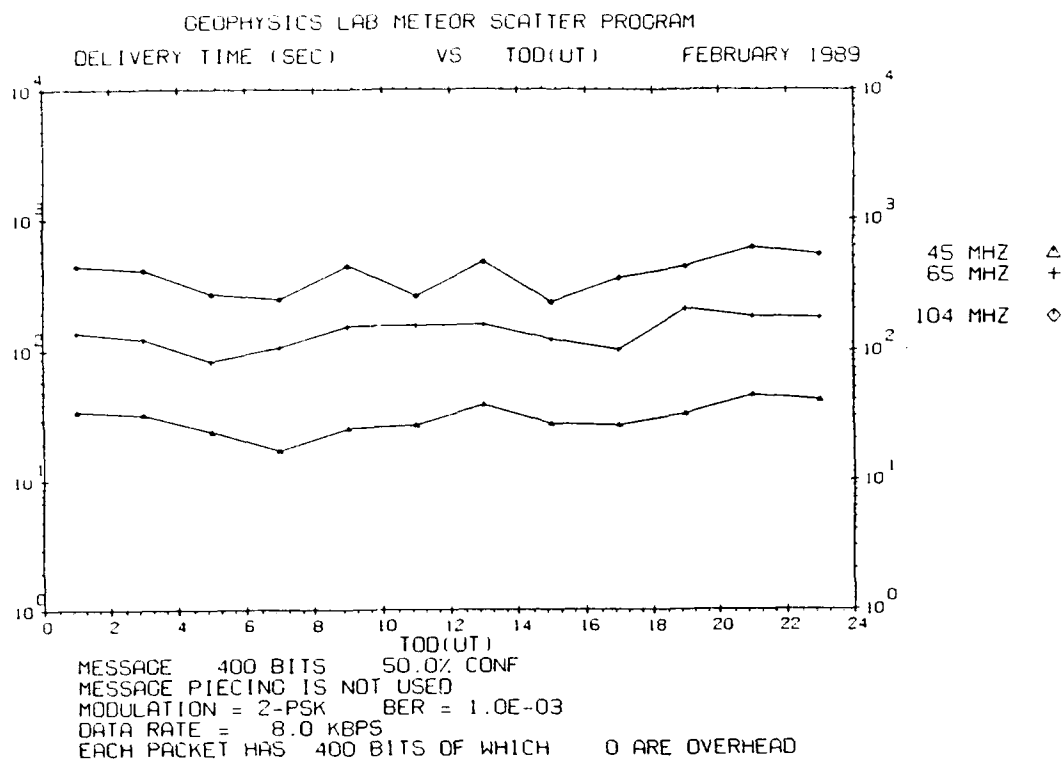
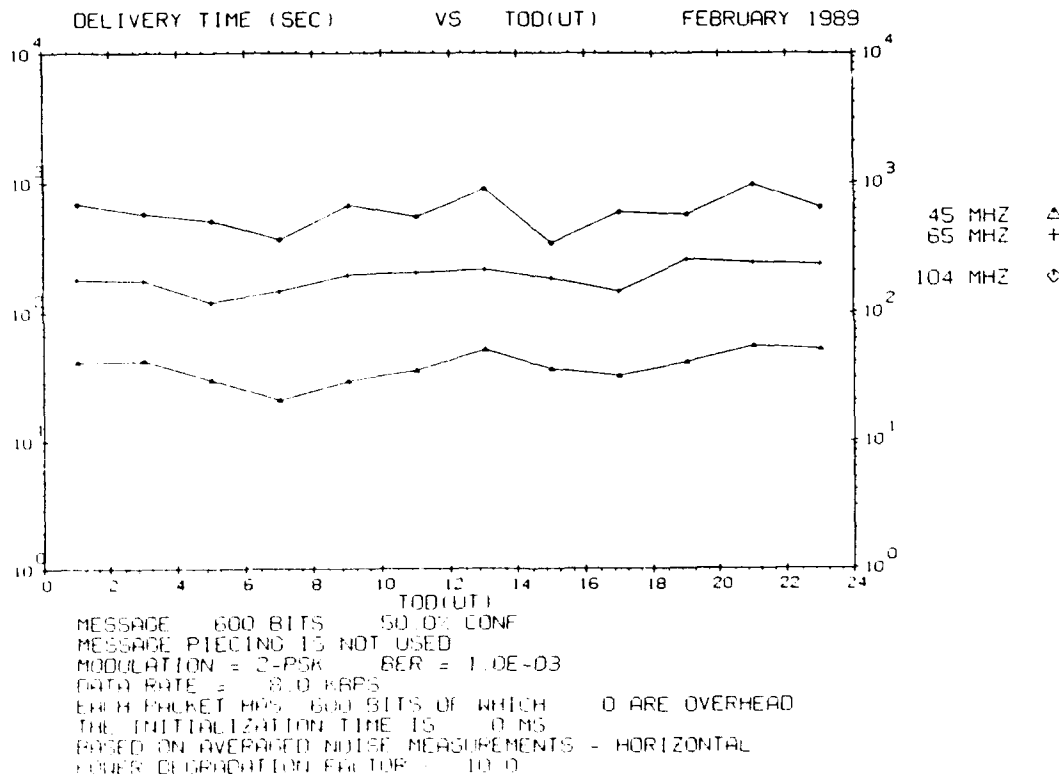


Figure E12. Same as Figure E7 but for Trails of 400 msec



**Figure E13. Waiting Time vs Time of Day for Trails of 50 msec Duration for February 1989. The transmitter power is 100 W**



**Figure E14. Same as Figure E13 but for Trails of 75 msec**

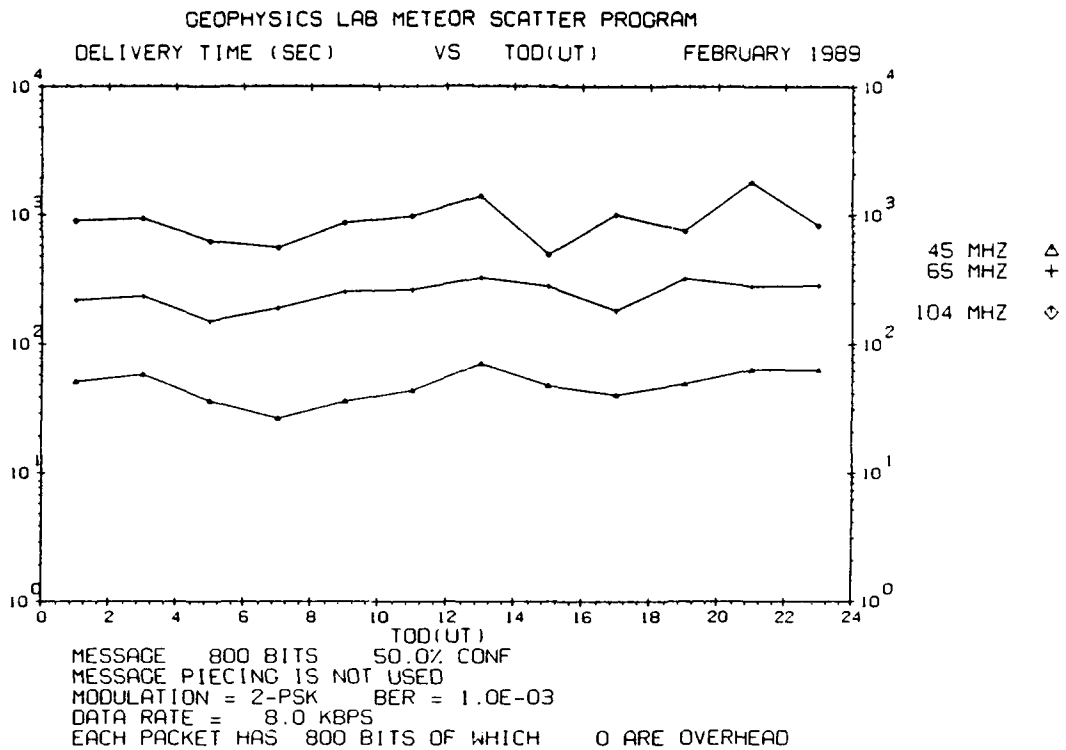


Figure E15. Same as Figure E13 but for Trails of 100 msec

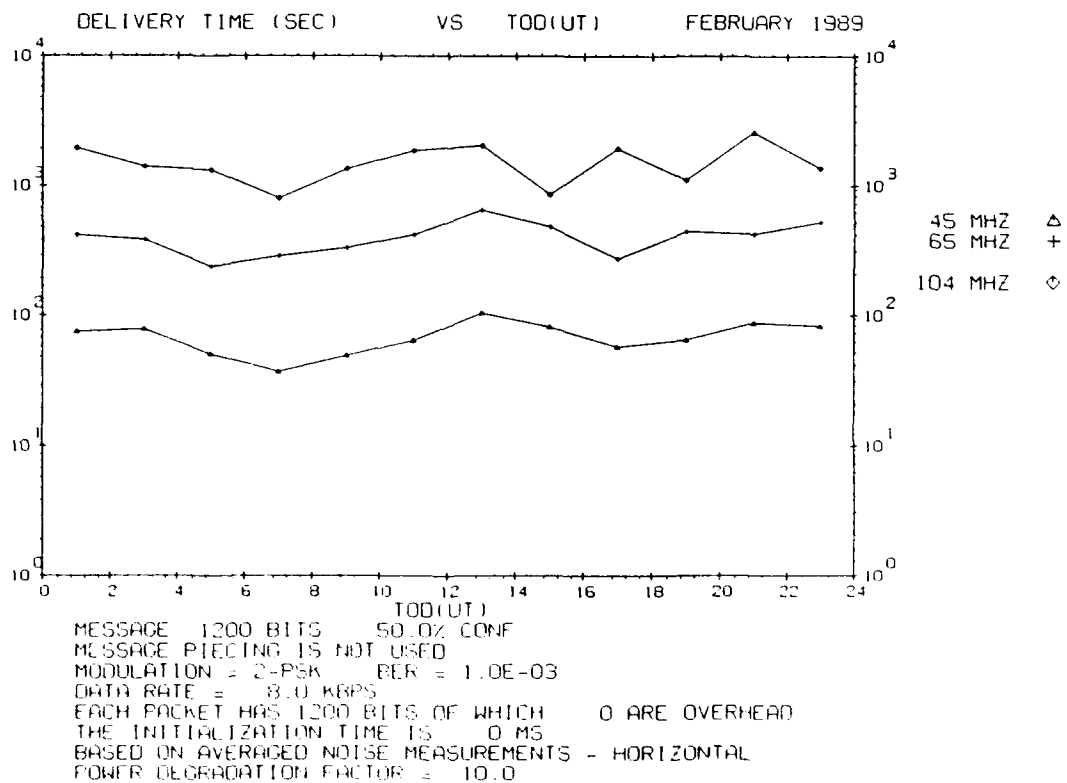


Figure E16. Same as Figure E13 but for Trails of 150 msec

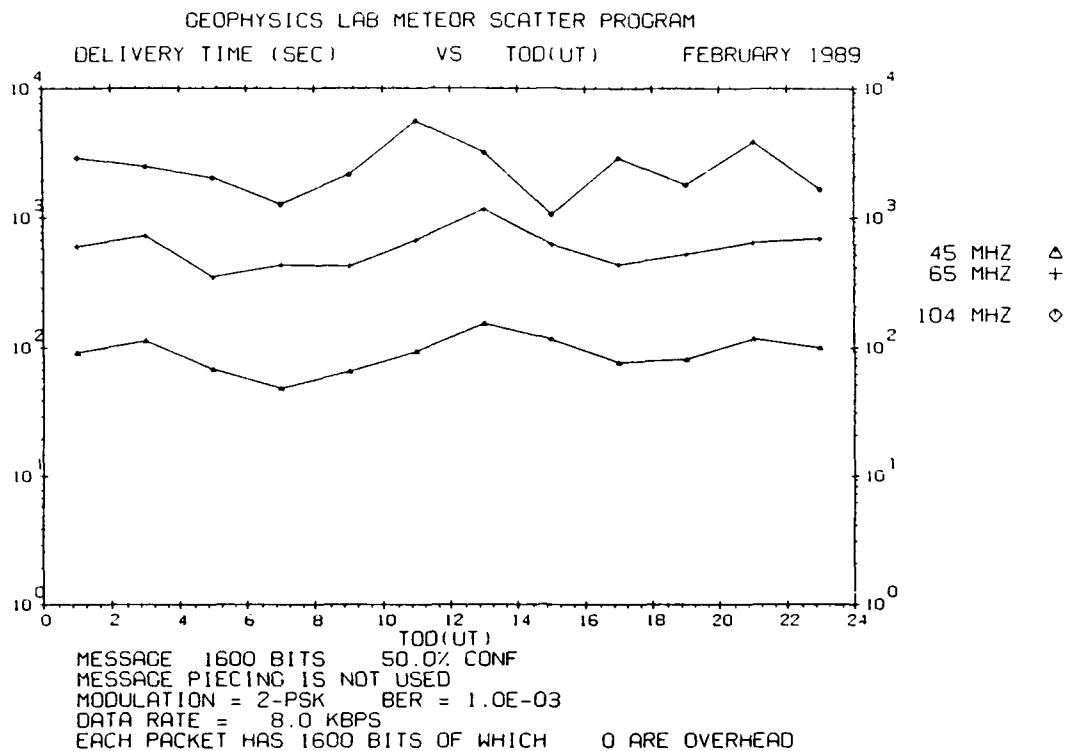


Figure E17. Same as Figure E13 but for Trails of 200 msec

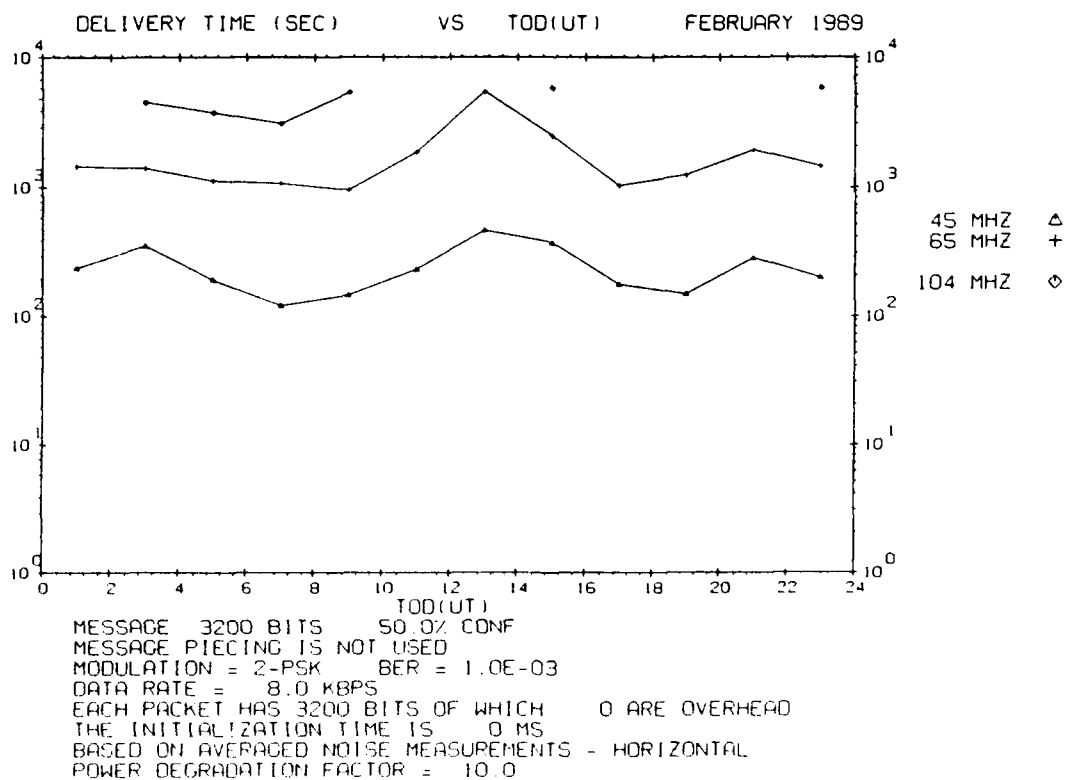
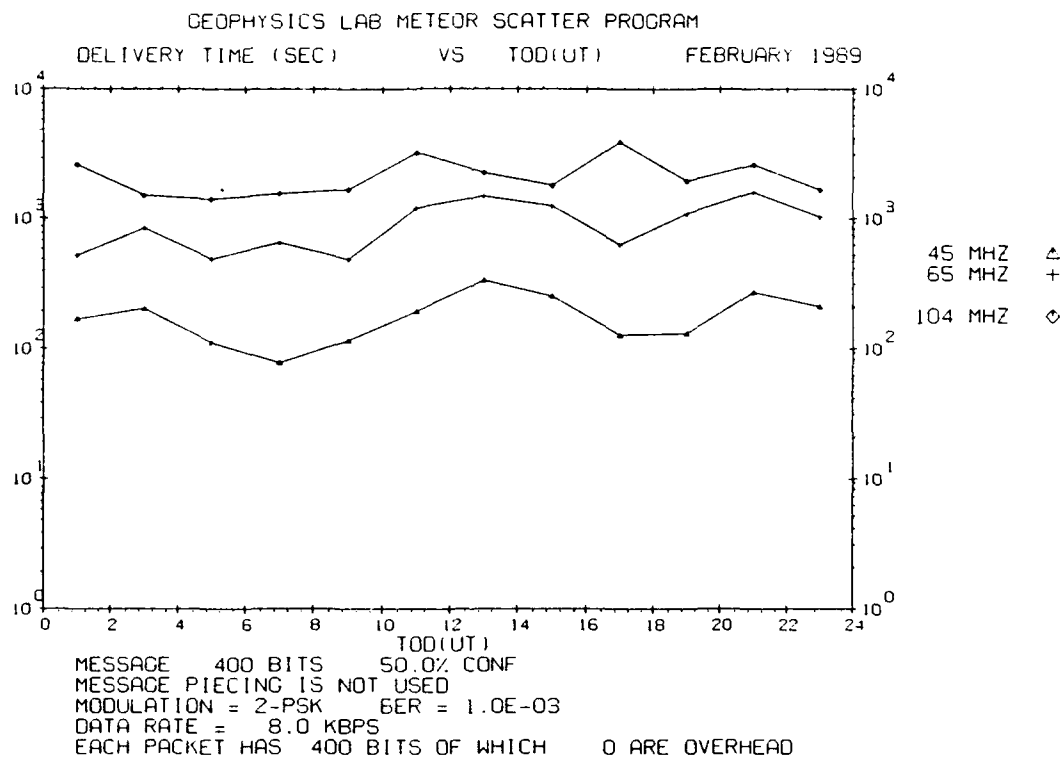
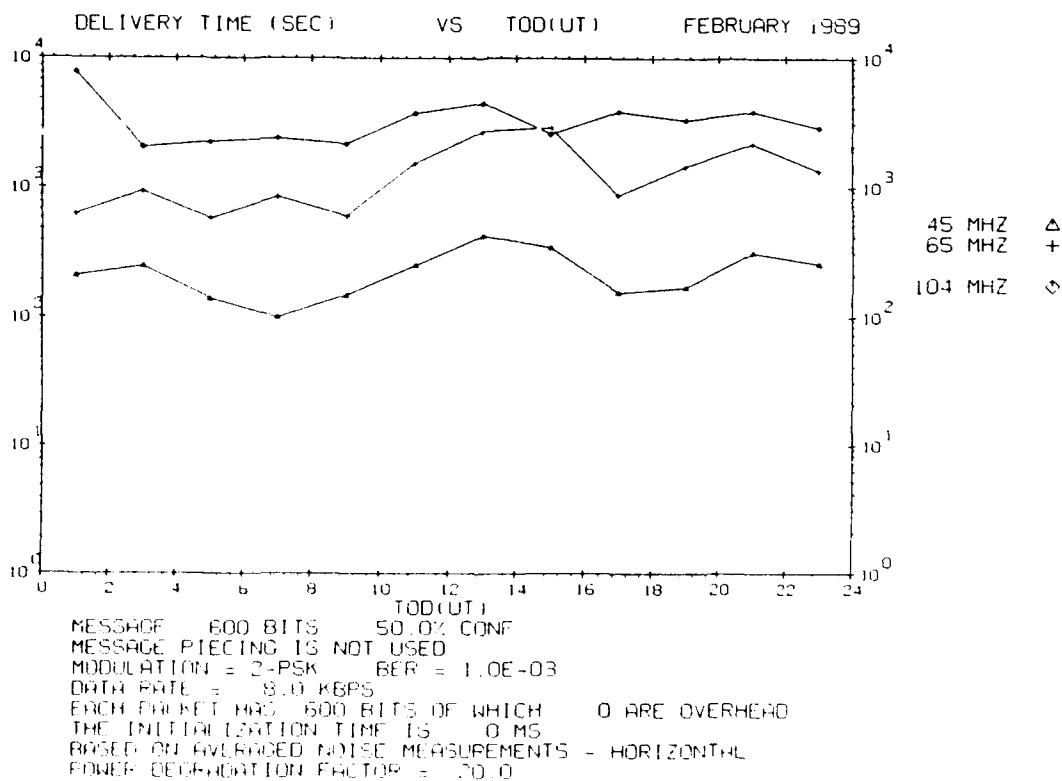


Figure E18. Same as Figure E13 but for Trails of 400 msec



**Figure E19. Waiting Time vs Time of Day for Trails of 50 msec Duration for February 1989. The transmitter power is 10 W**



**Figure E20. Same as Figure E19 but for Trails of 75 msec**

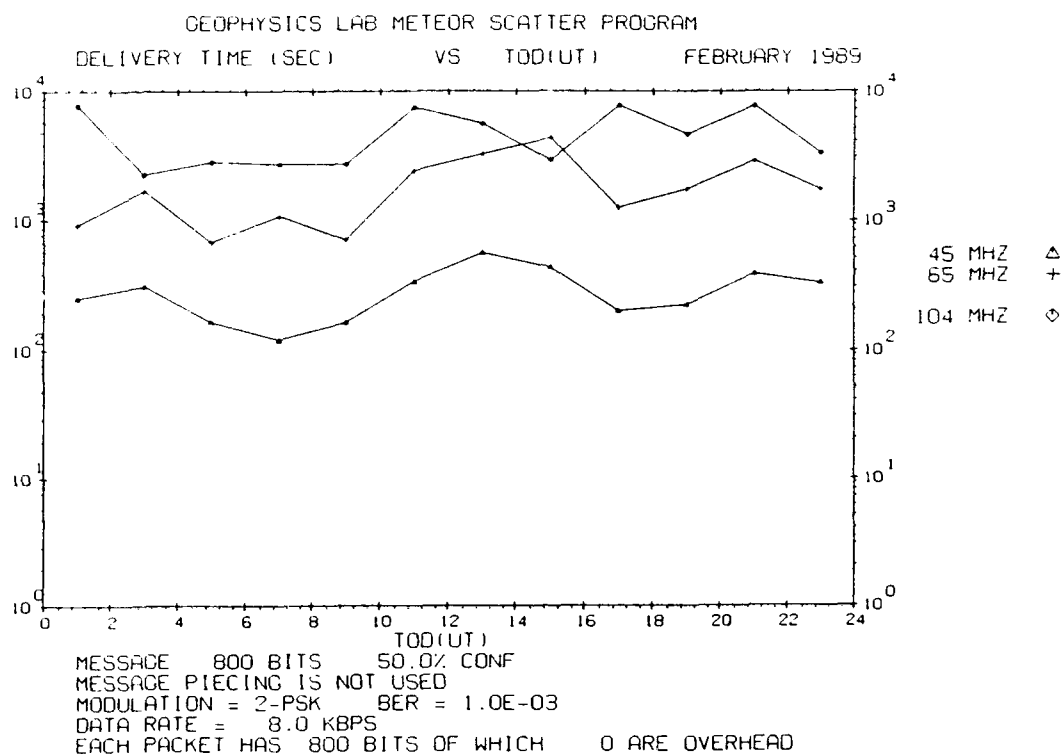


Figure E21. Same as Figure E19 but for Trails of 100 msec

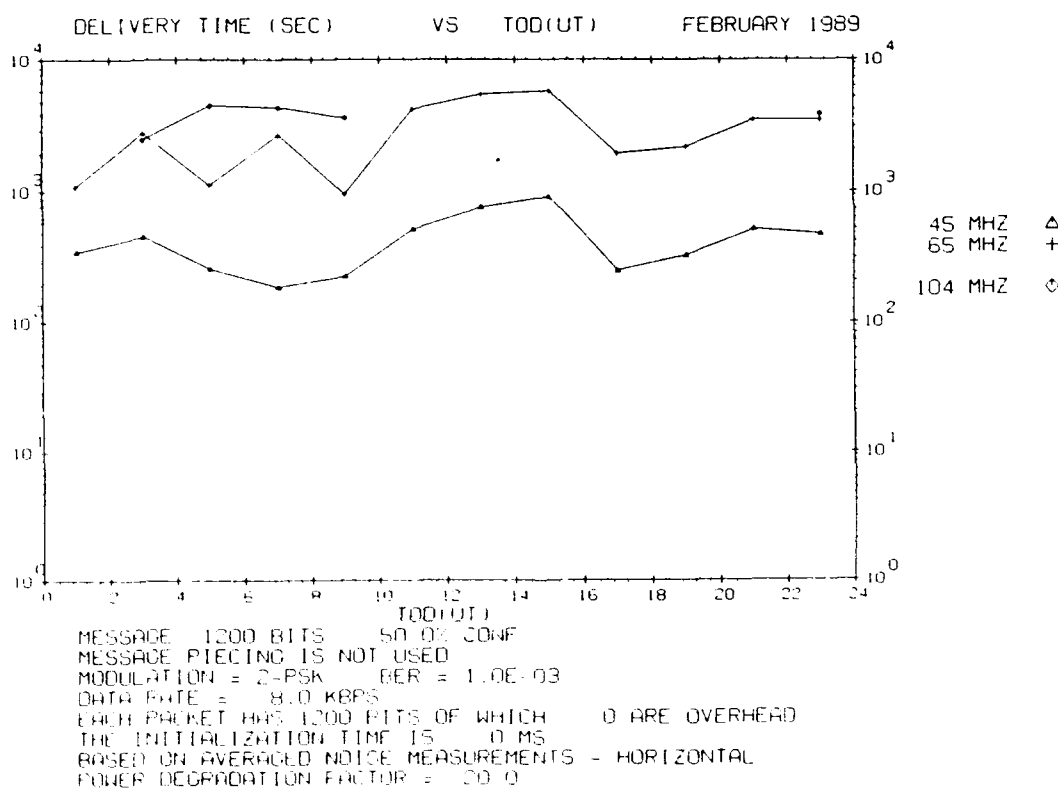


Figure E22. Same as Figure E19 but for Trails of 150 msec



AFB-NESS 100

EXPERIMENTAL DETERMINATION OF WRITING TIMES FOR METEOR

TRAIL RETURNS OF SPECIFIED DURATIONS(U) PHILLIPS LAB

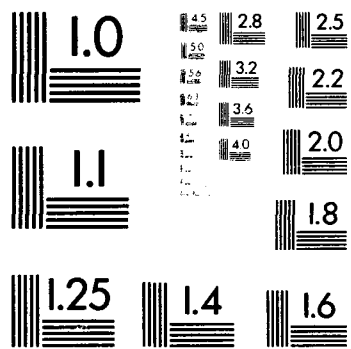
HANSCOM AFB MA J C OSTERGAARD ET AL. 9 JAN 91

PL-TR-91-2040 SBI-AD-E201 195

UNCLASSIFIED

NL

END  
FILMED  
DTIC



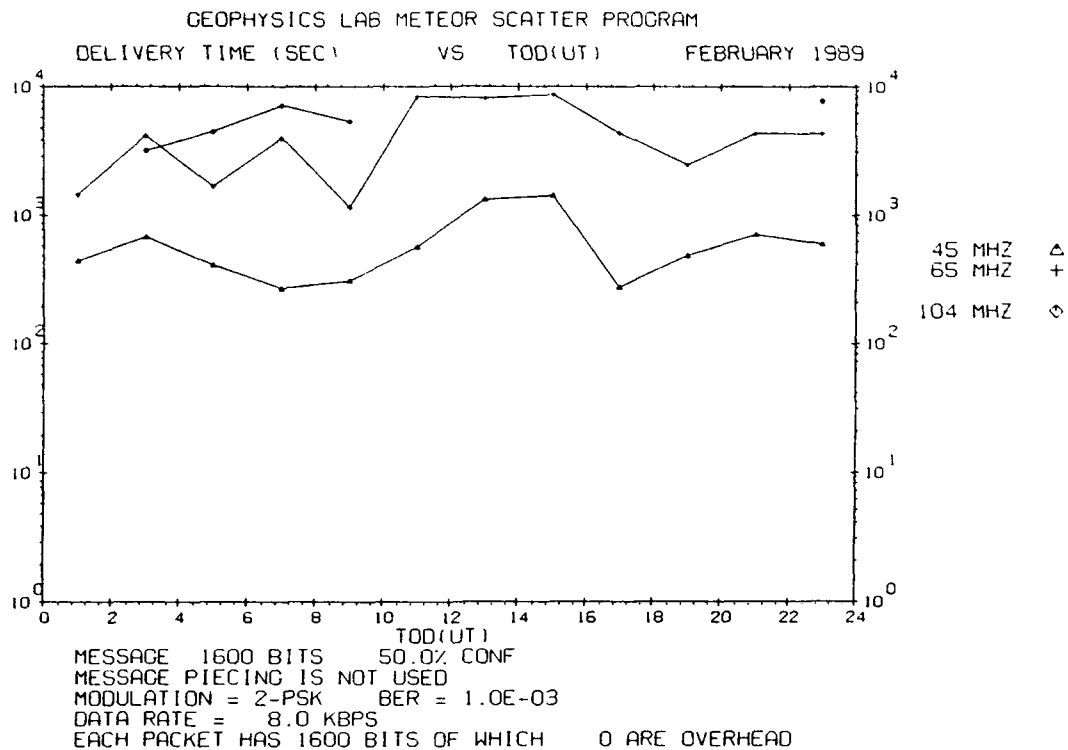


Figure E23. Same as Figure E19 but for Trails of 200 msec

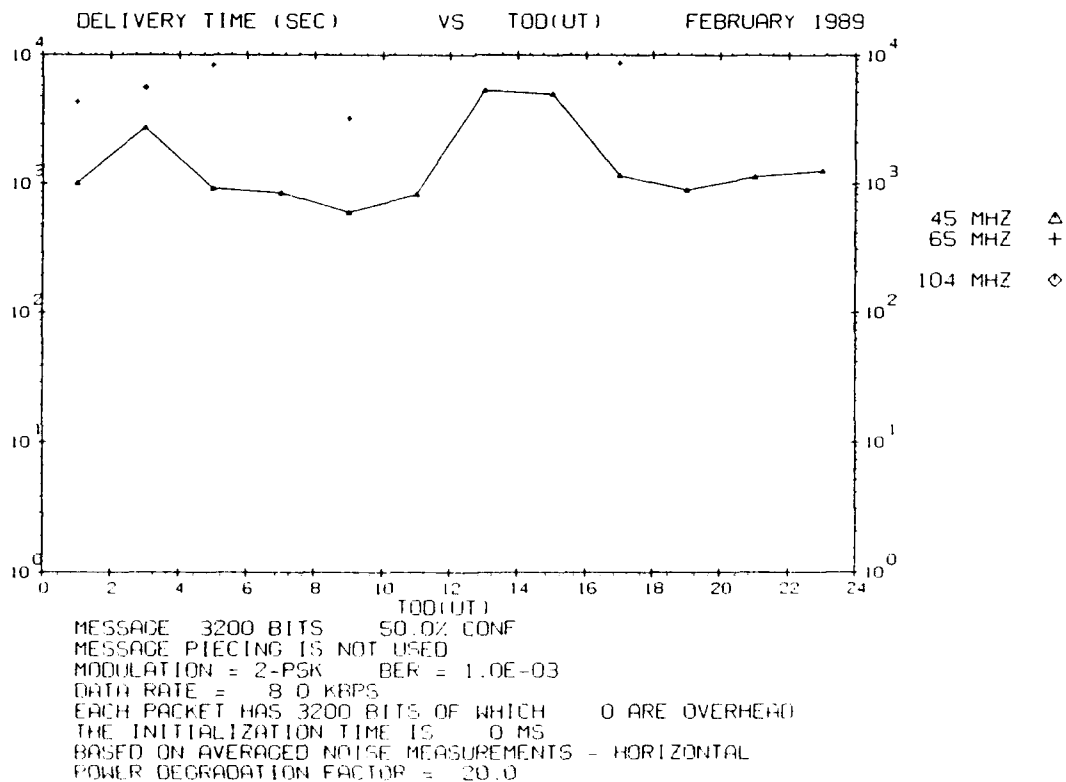
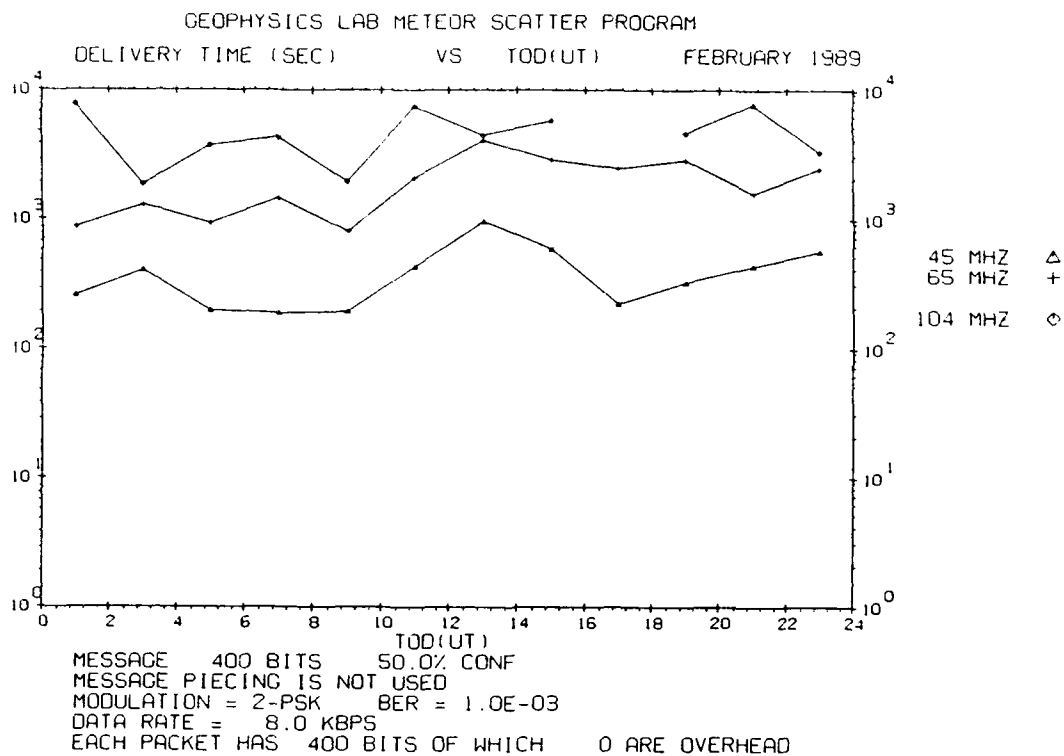
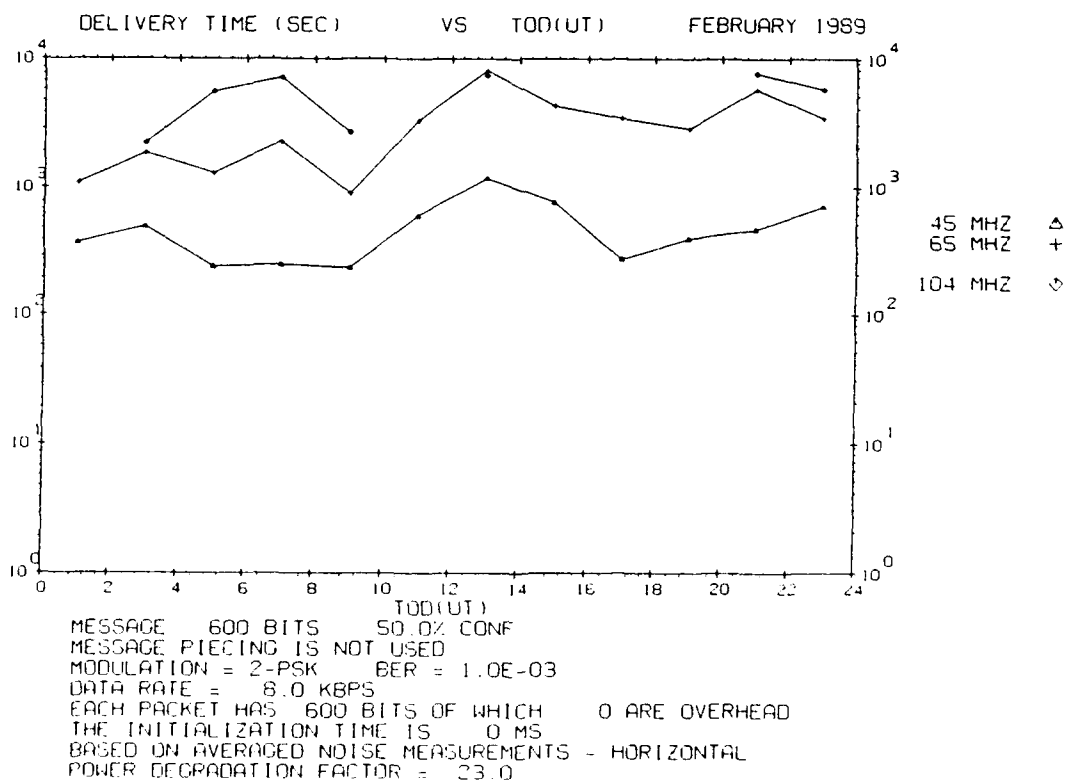


Figure E24. Same as Figure E19 but for Trails of 400 msec



**Figure E25. Waiting Time vs Time of Day for Trails of 50 msec Duration for February 1989. The transmitter power is 5 W**



**Figure E26. Same as Figure E25 but for Trails of 75 msec**

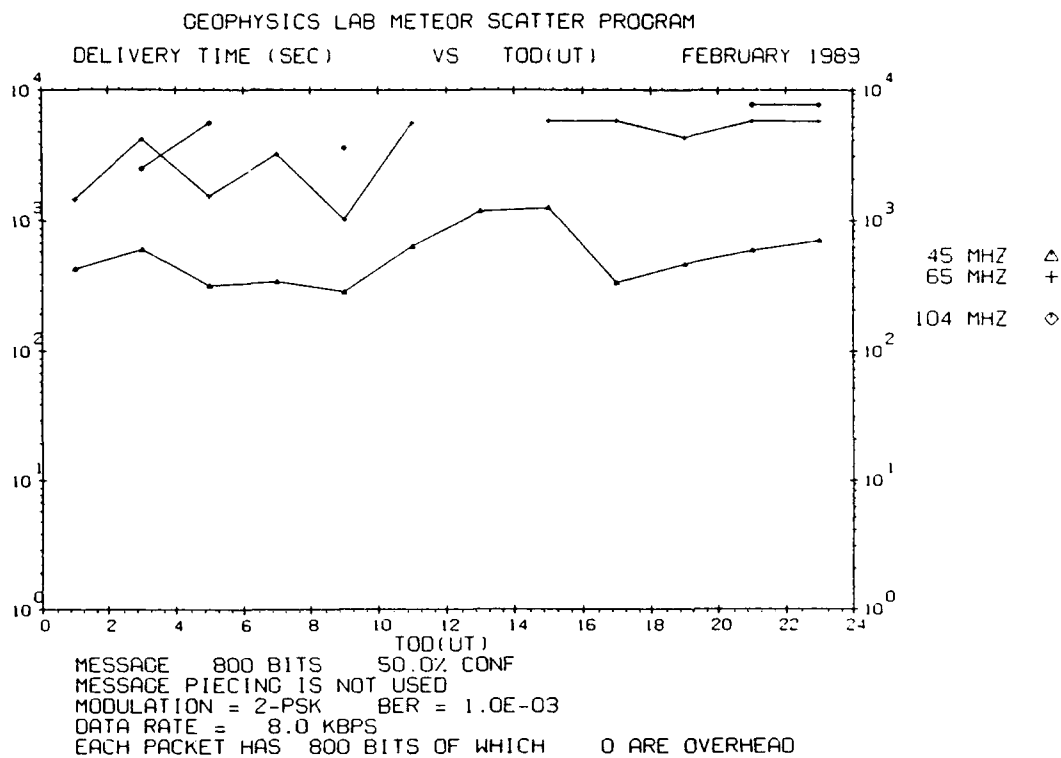


Figure E27. Same as Figure E25 but for Trails of 100 msec

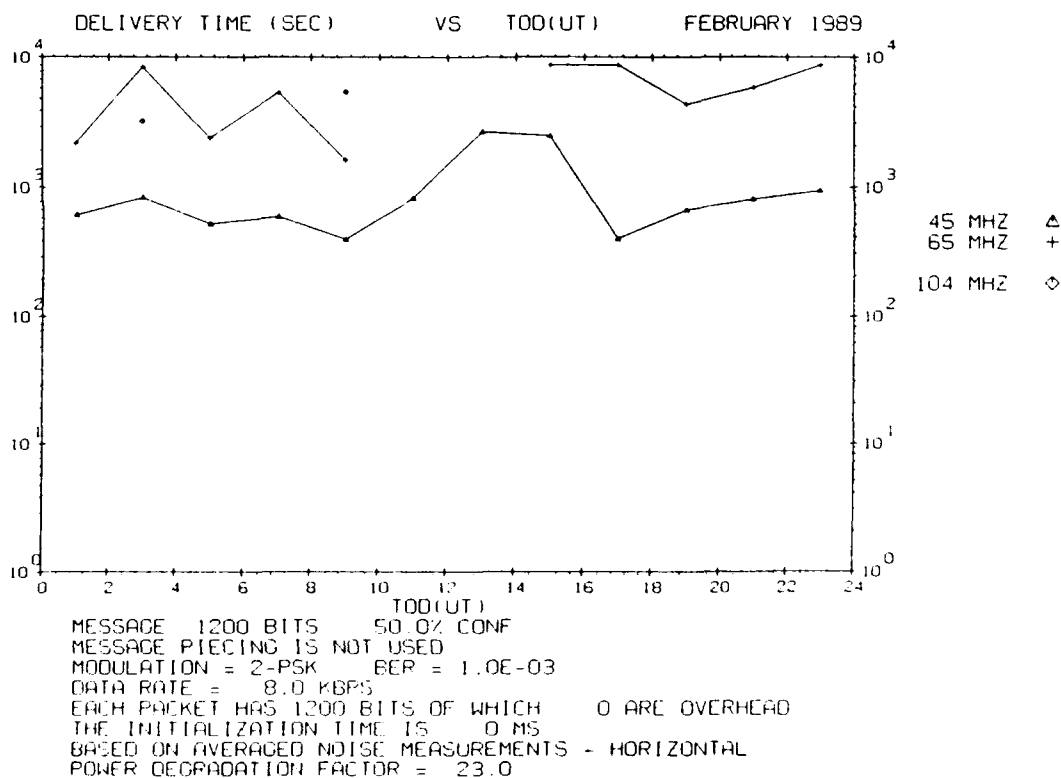


Figure E28. Same as Figure E25 but for Trails of 150 msec

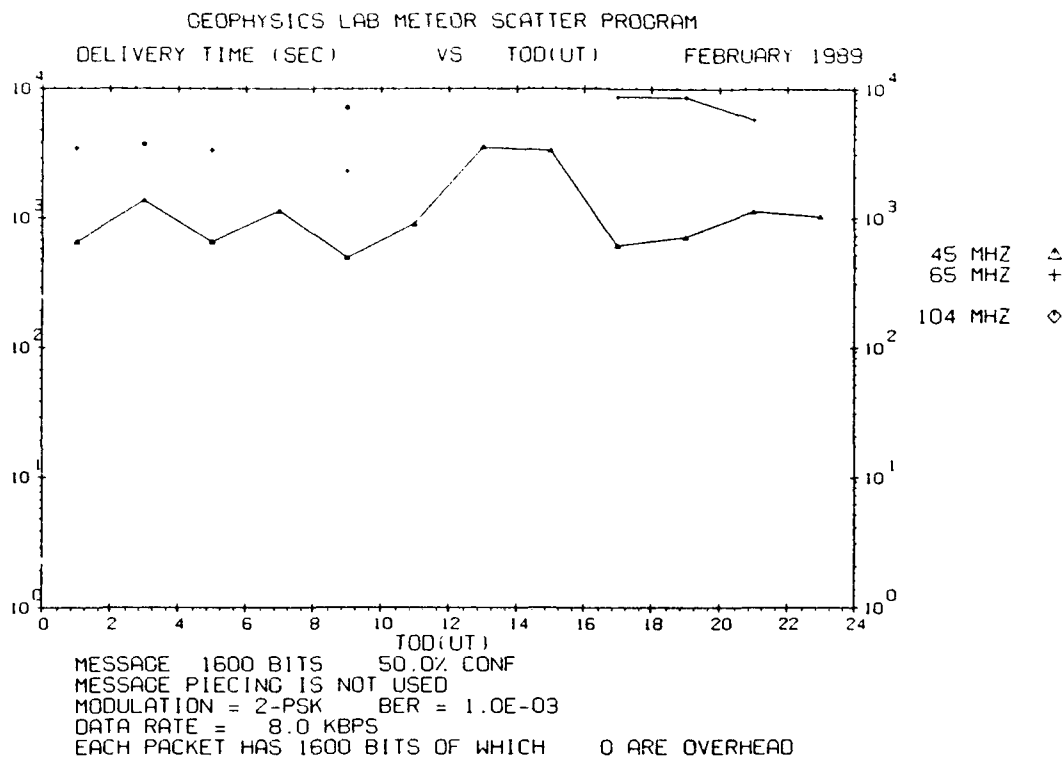


Figure E29. Same as Figure E25 but for Trails of 200 msec

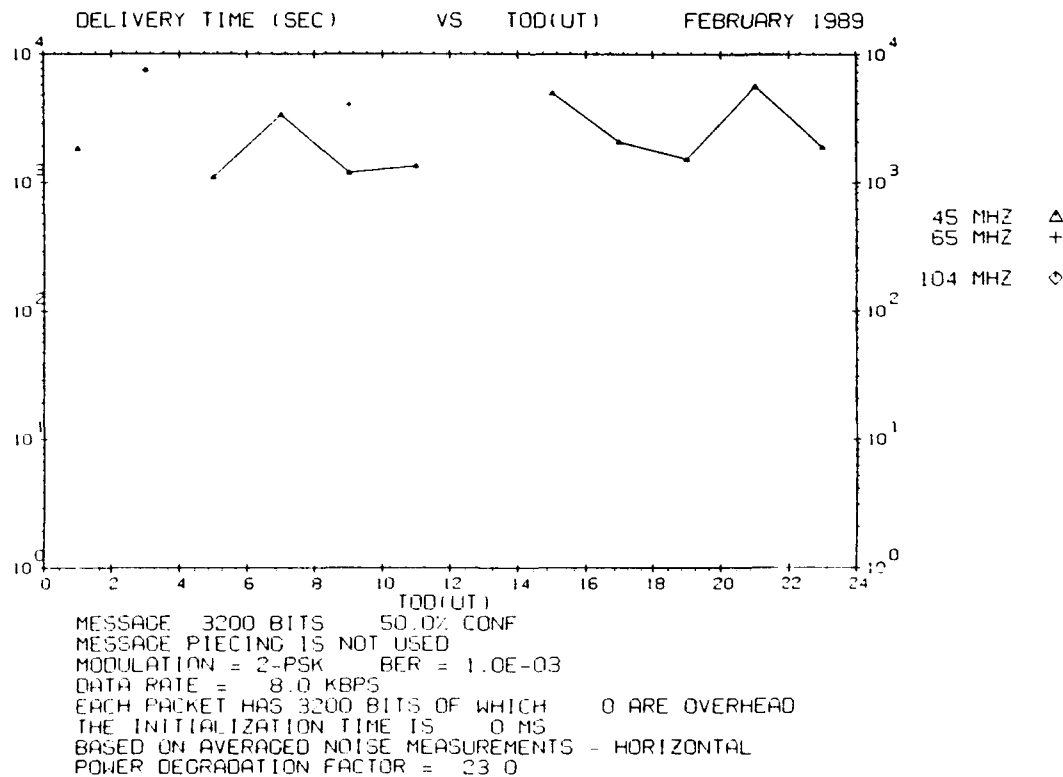
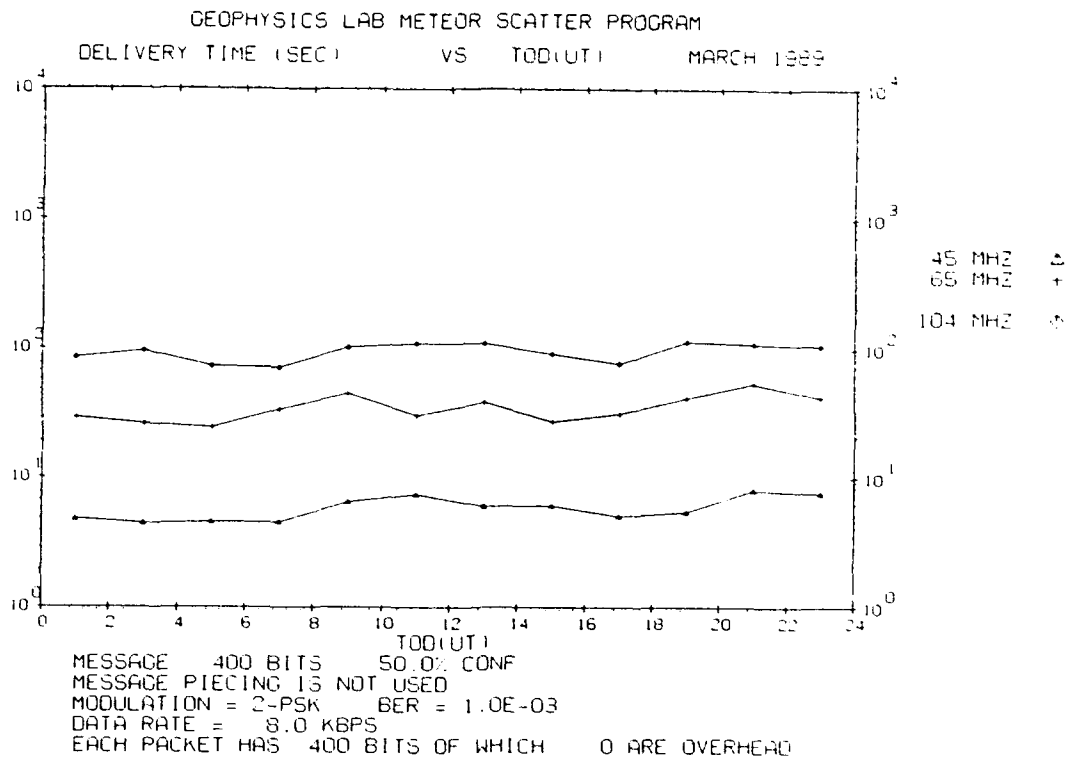
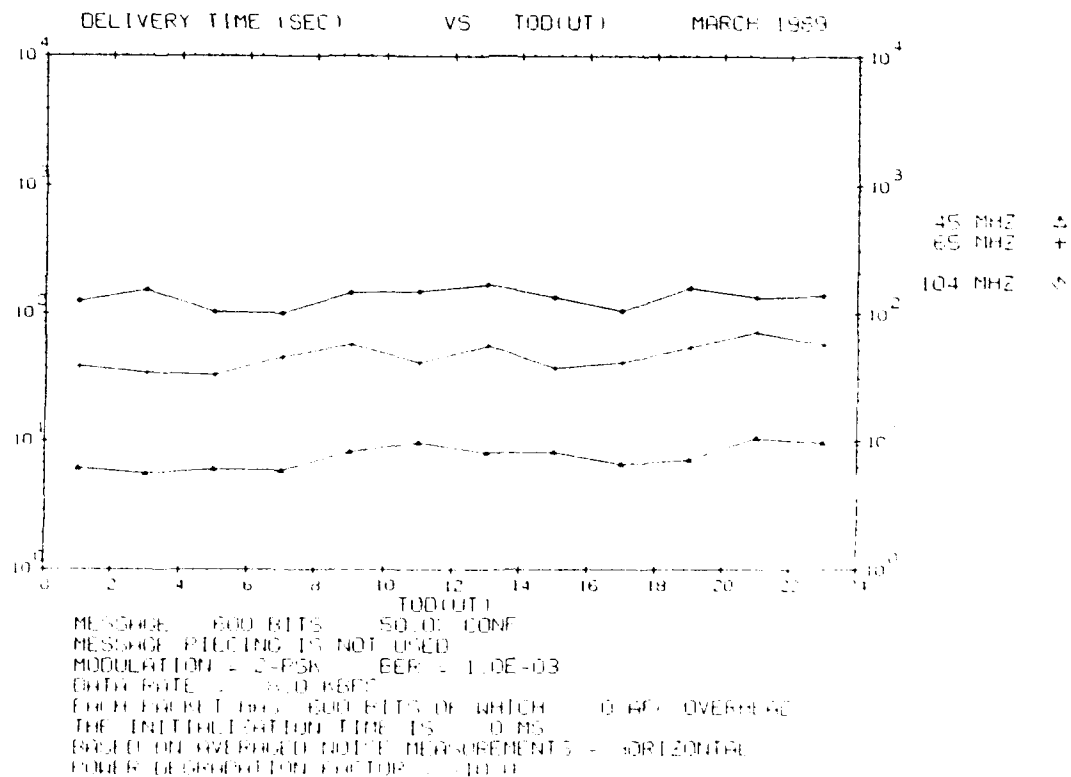


Figure E30. Same as Figure E25 but for Trails of 400 msec



**Figure E31. Waiting Time vs Time of Day for Trails of 50 msec Duration for March 1989. The transmitter power is 10,000 W**



**Figure E32. Same as Figure E31 but for Trails of 75 msec**

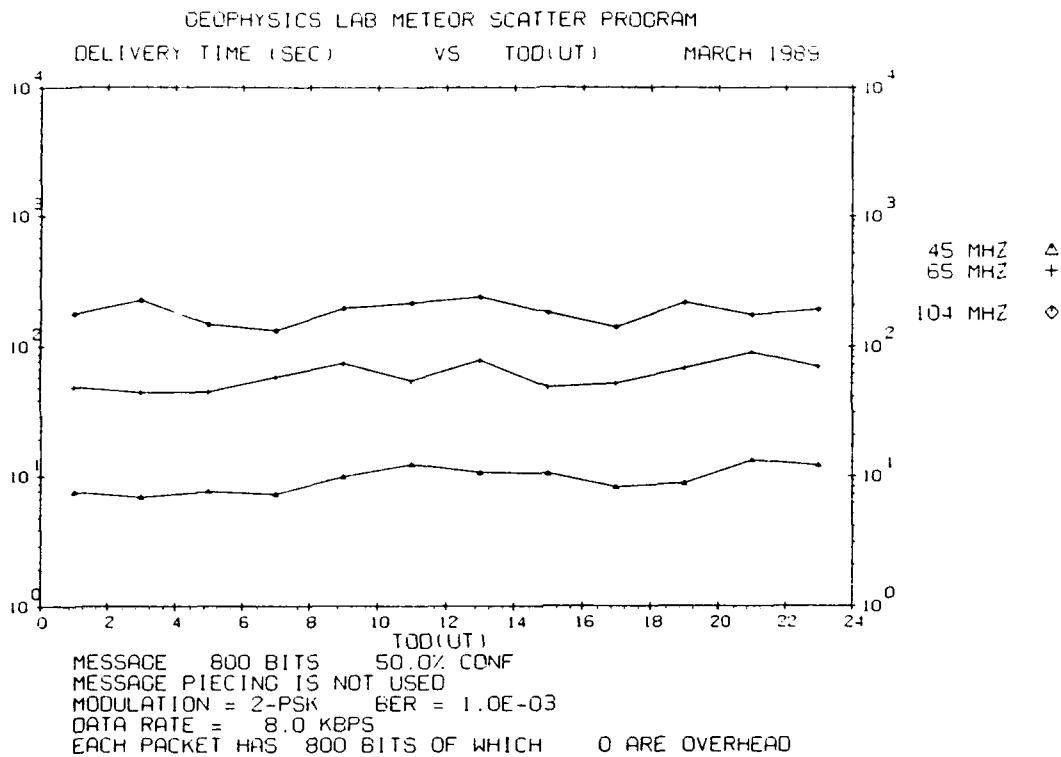


Figure E33. Same as Figure E31 but for Trails of 100 msec

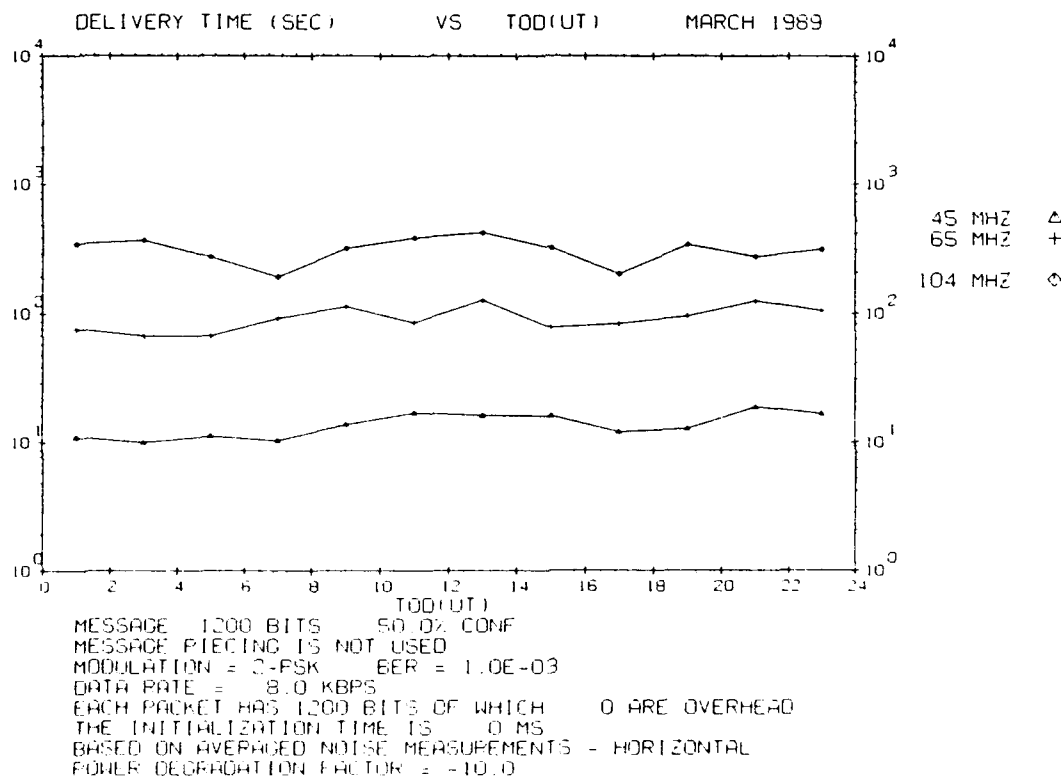


Figure E34. Same as Figure E31 but for Trails of 150 msec



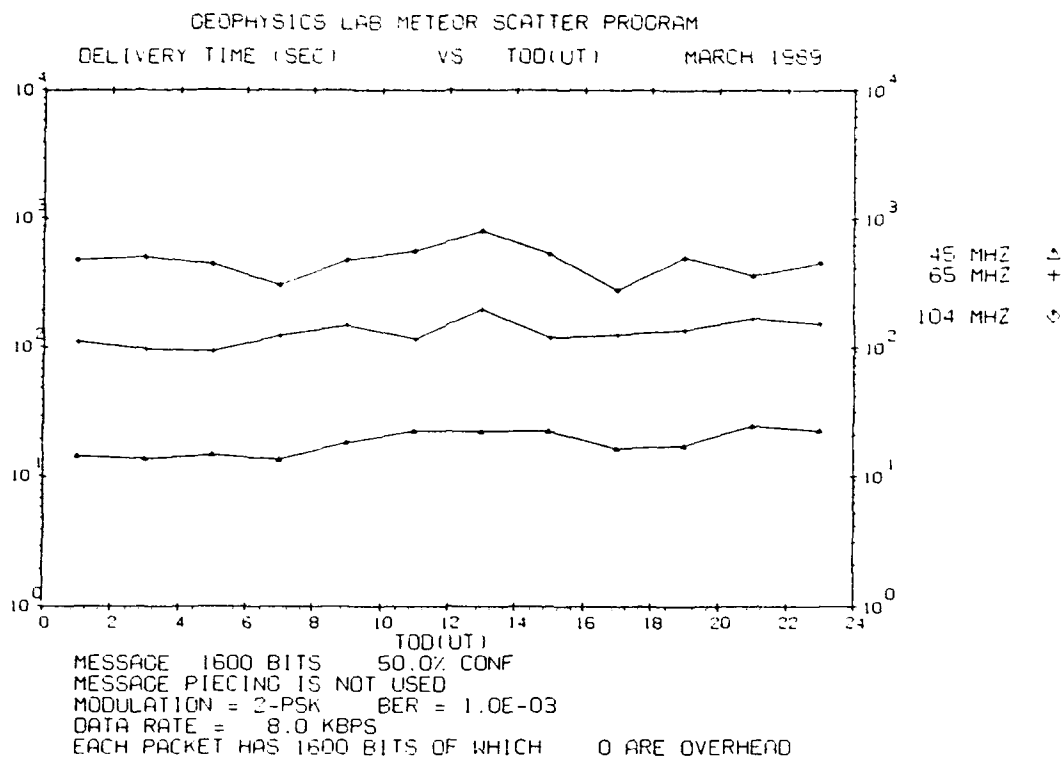


Figure E35. Same as Figure E31 but for Trails of 200 msec

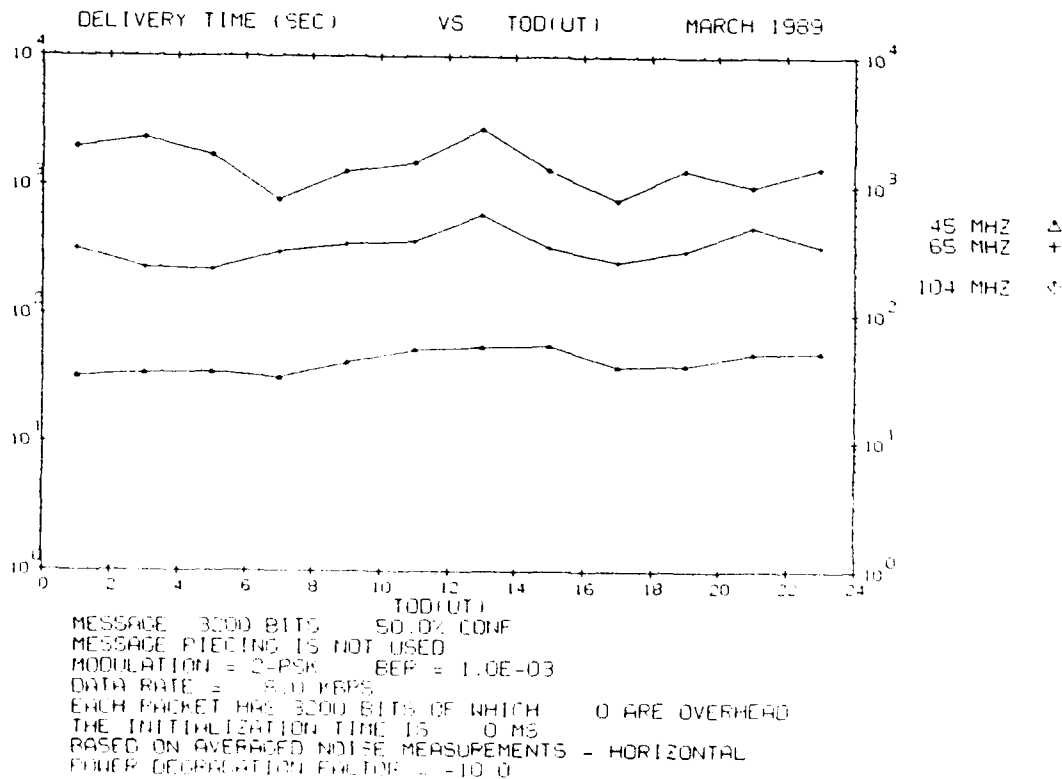
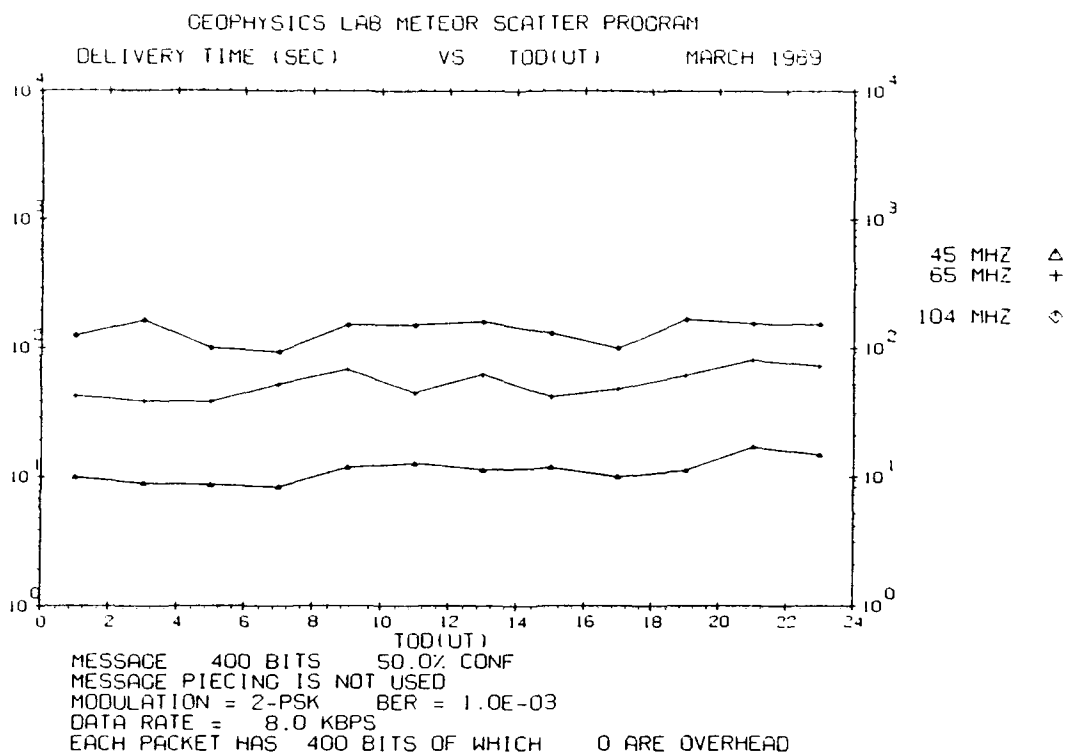
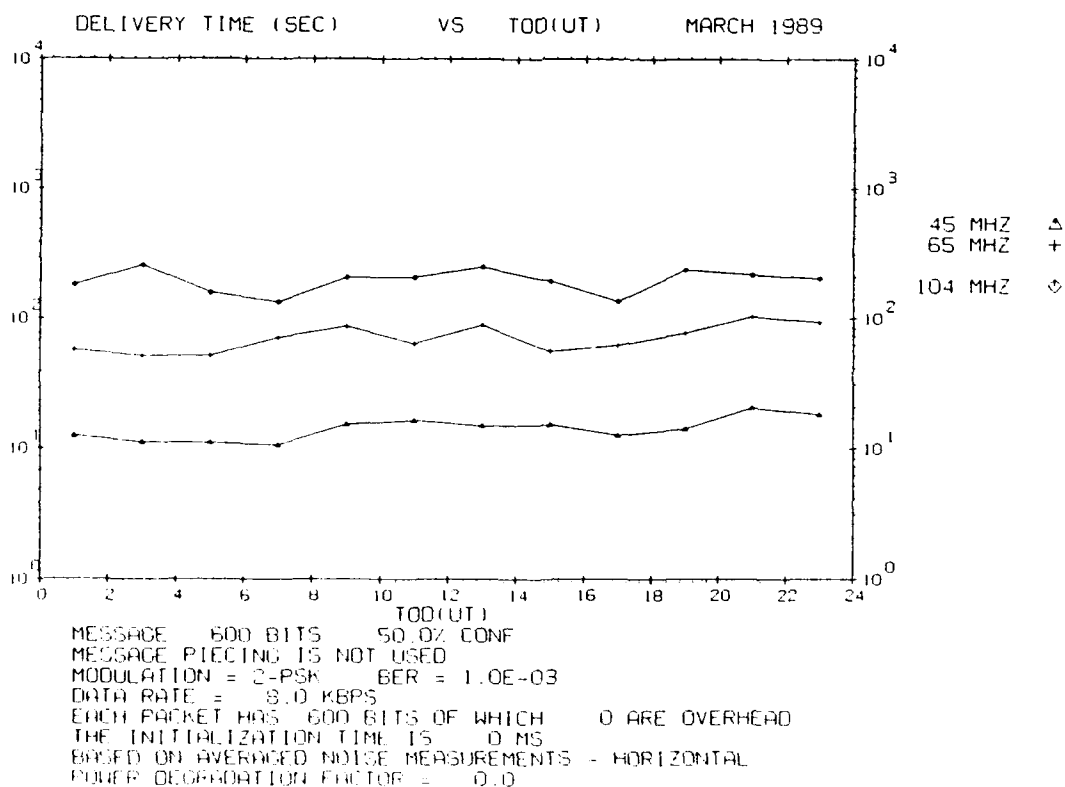


Figure E36. Same as Figure E31 but for Trails of 400 msec



**Figure E37. Waiting Time vs Time of Day for Trails of 50 msec Duration for March 1989. The transmitter power is 1,000 W**



**Figure E38. Same as Figure E37 but for Trails of 75 msec**

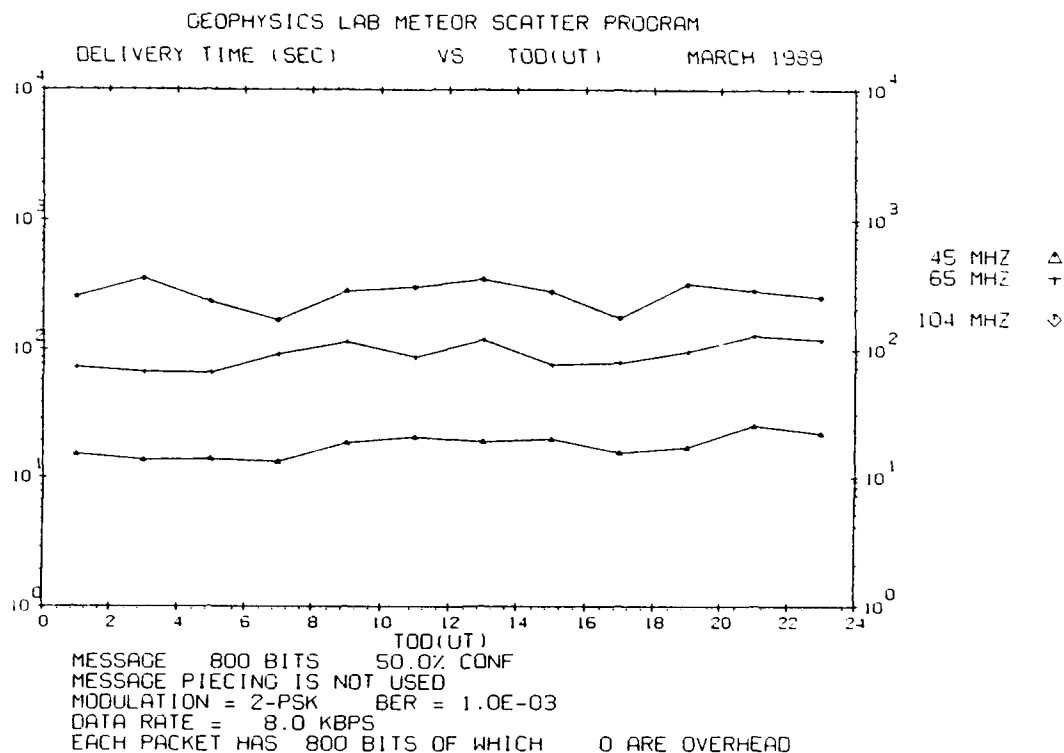


Figure E39. Same as Figure E37 but for Trails of 100 msec

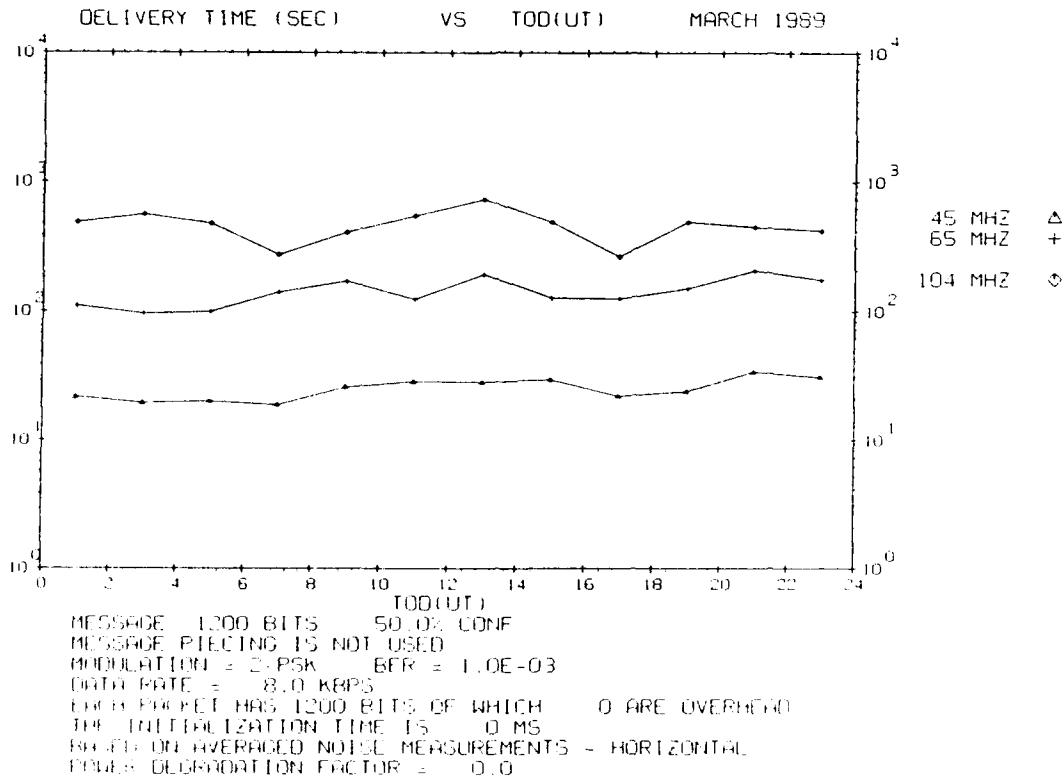


Figure E40. Same as Figure E37 but for Trails of 150 msec

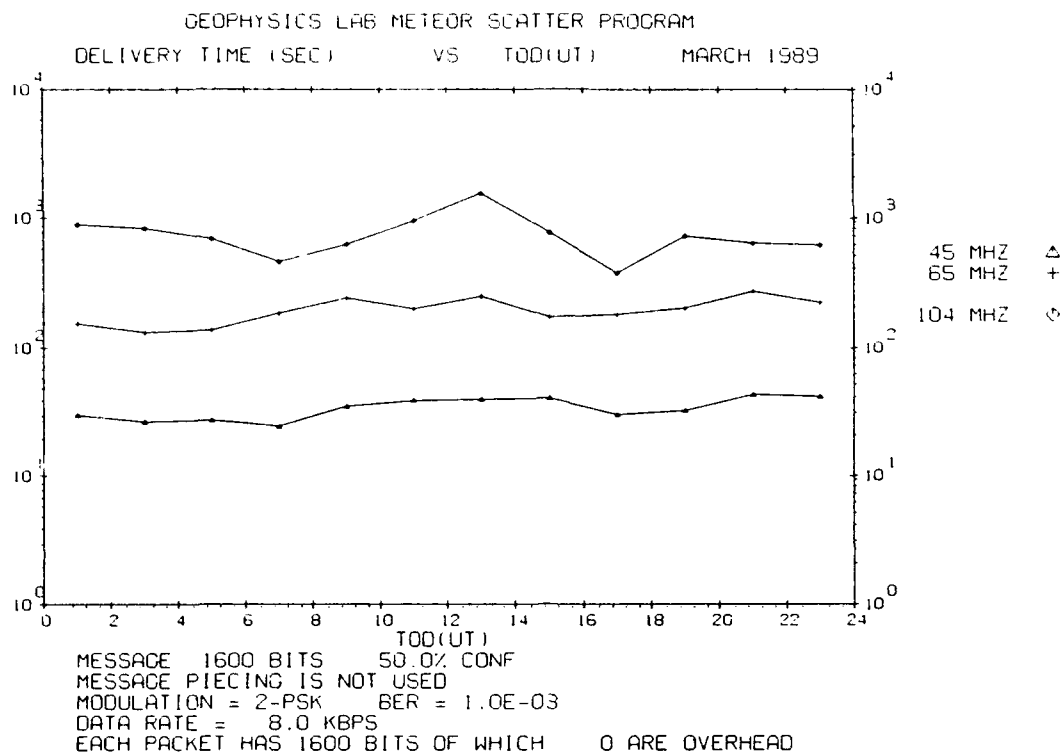


Figure E41. Same as Figure E37 but for Trails of 200 msec

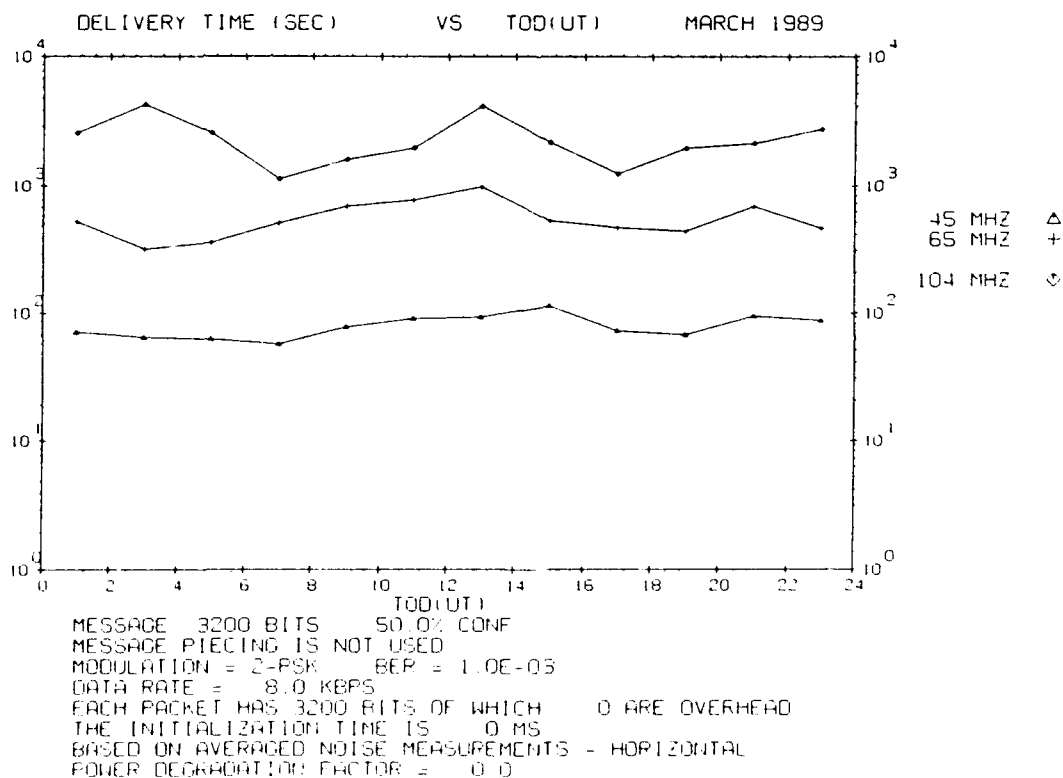
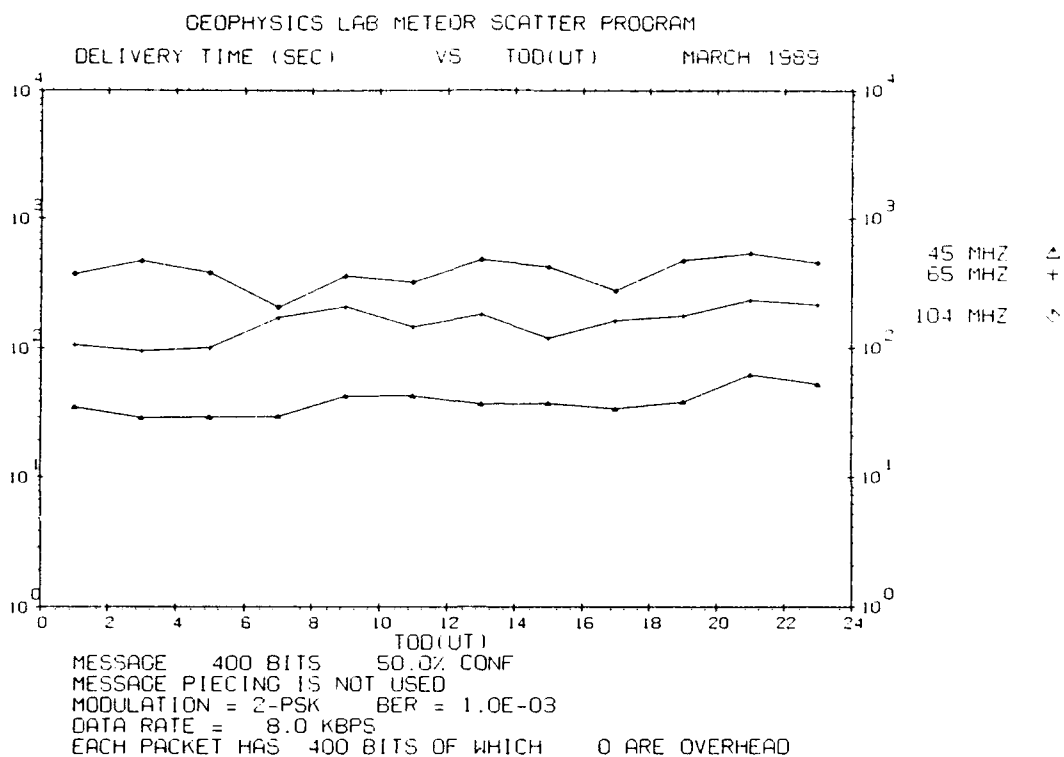
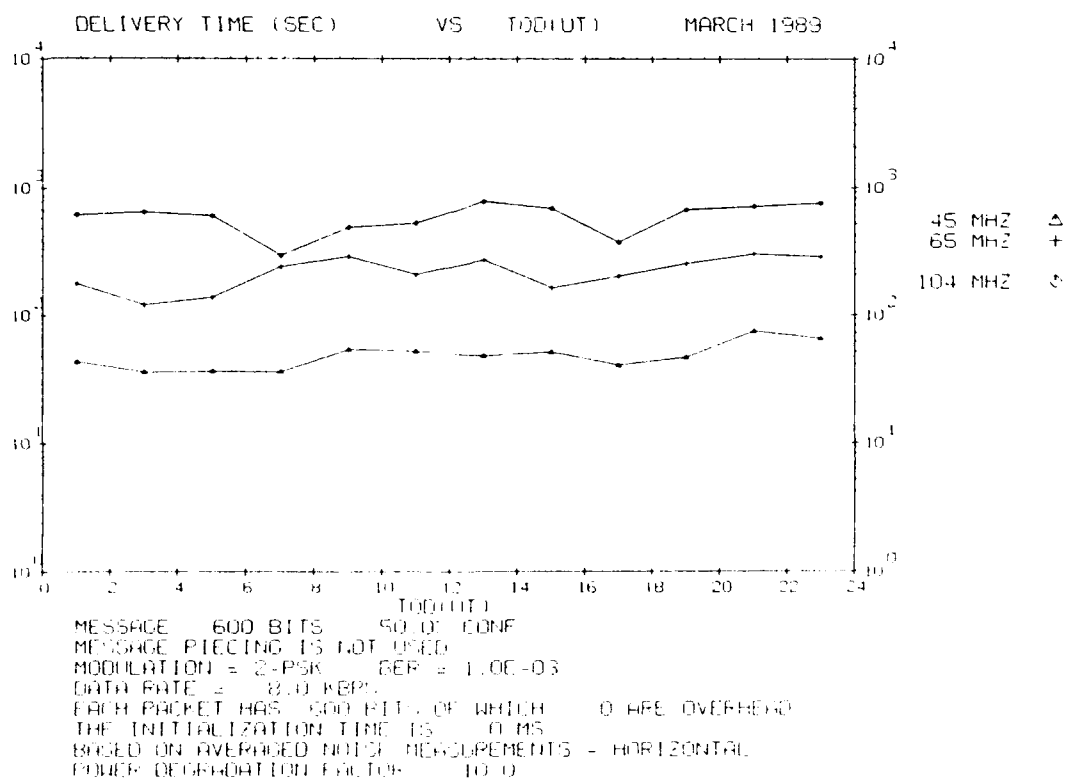


Figure E42. Same as Figure E37 but for Trails of 400 msec



**Figure E43. Waiting Time vs Time of Day for Trails of 50 msec Duration for March 1989. The transmitter power is 100 W**



**Figure E44. Same as Figure E43 but for Trails of 75 msec**

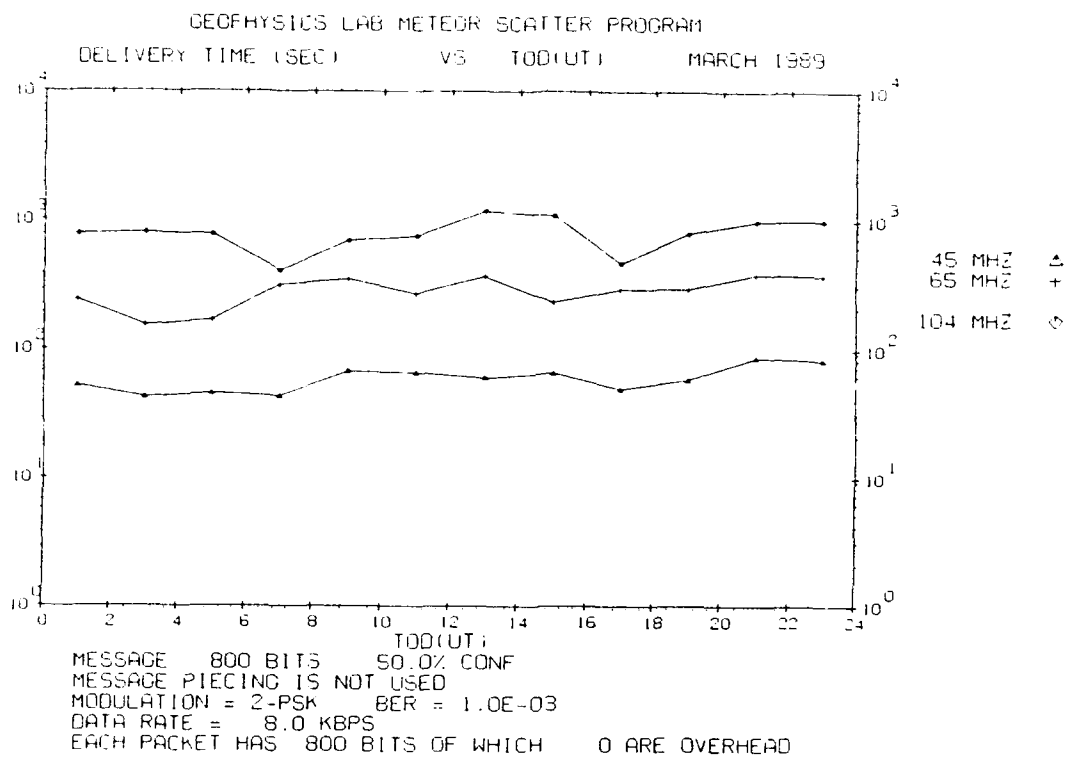


Figure E45. Same as Figure E43 but for Trails of 100 msec

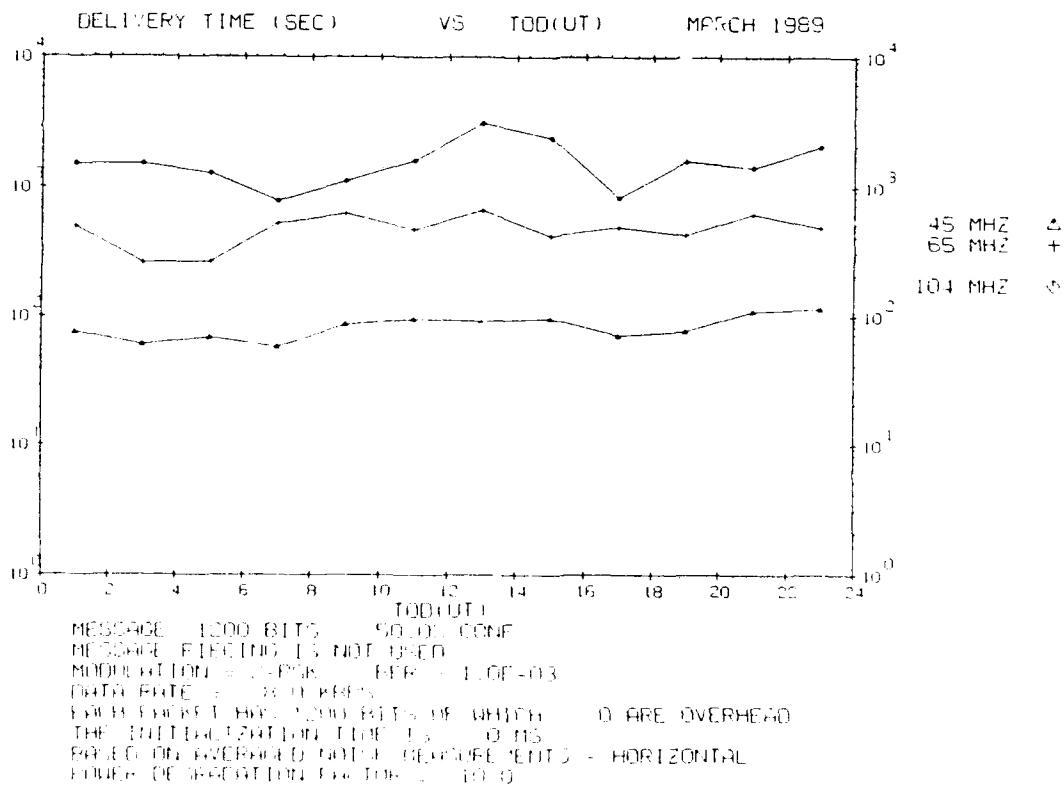


Figure E46. Same as Figure E43 but for Trails of 150 msec

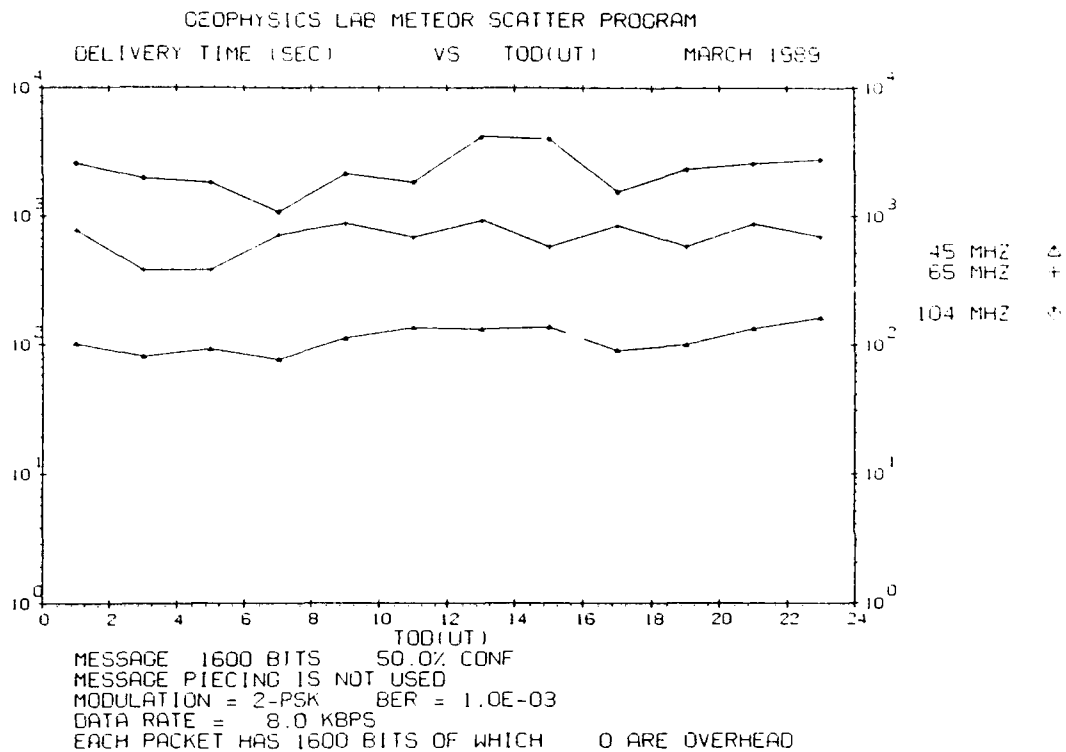


Figure E47. Same as Figure E43 but for Trails of 200 msec

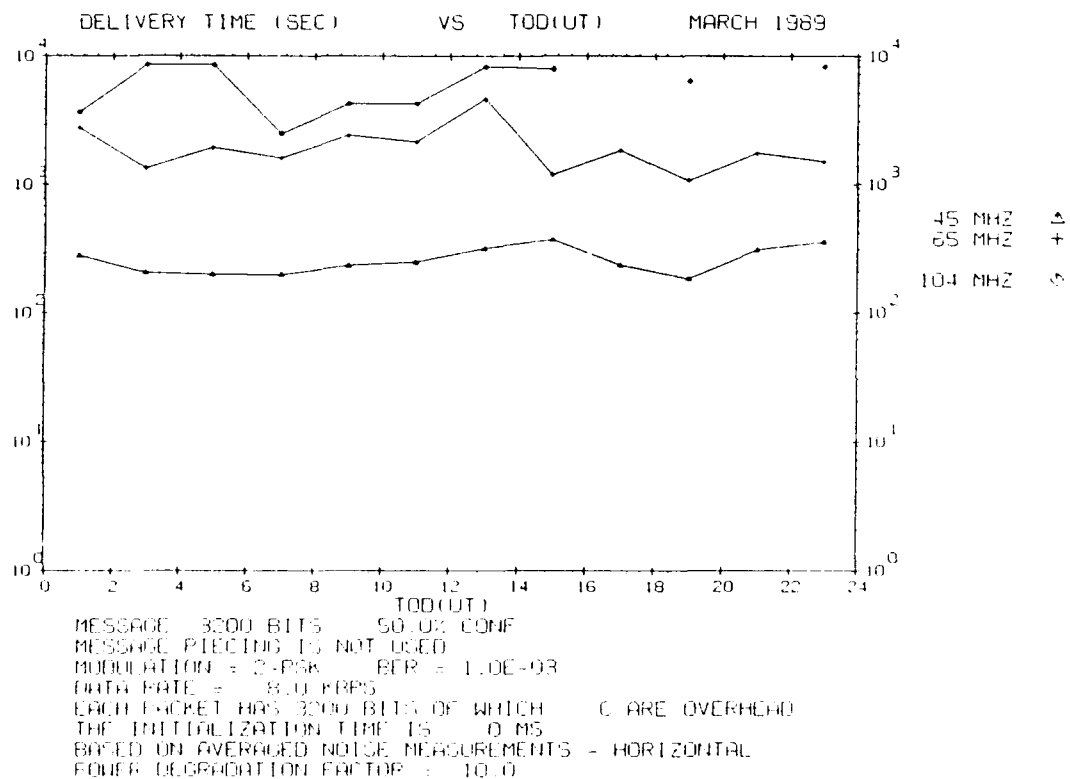
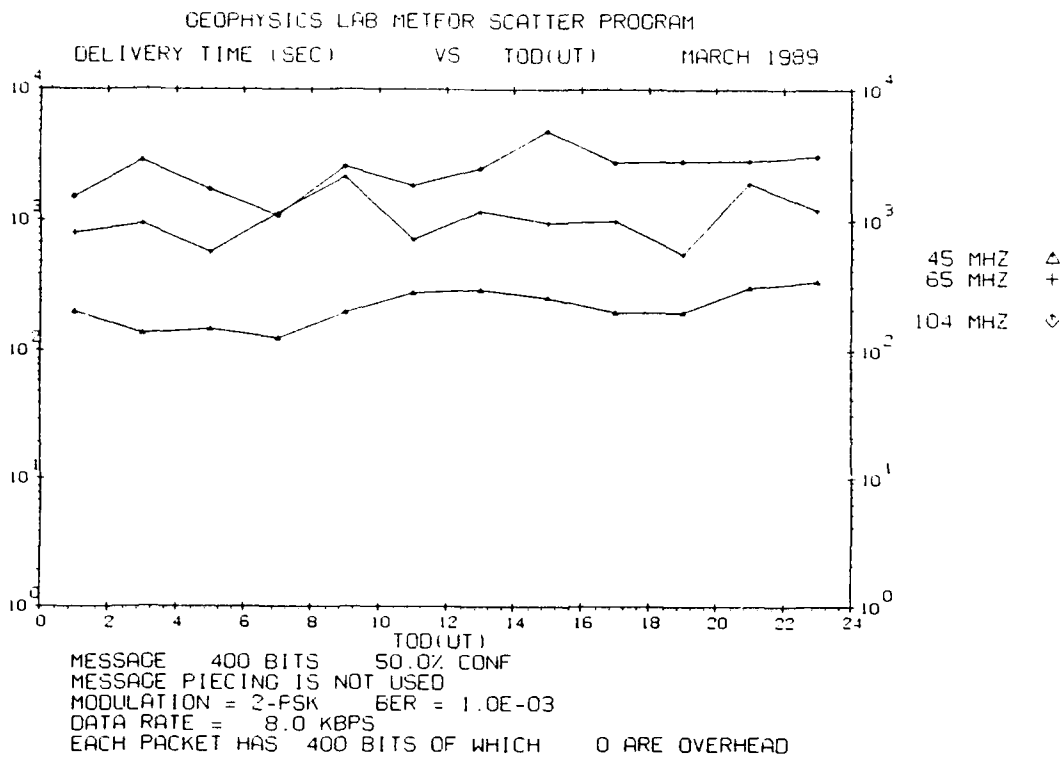
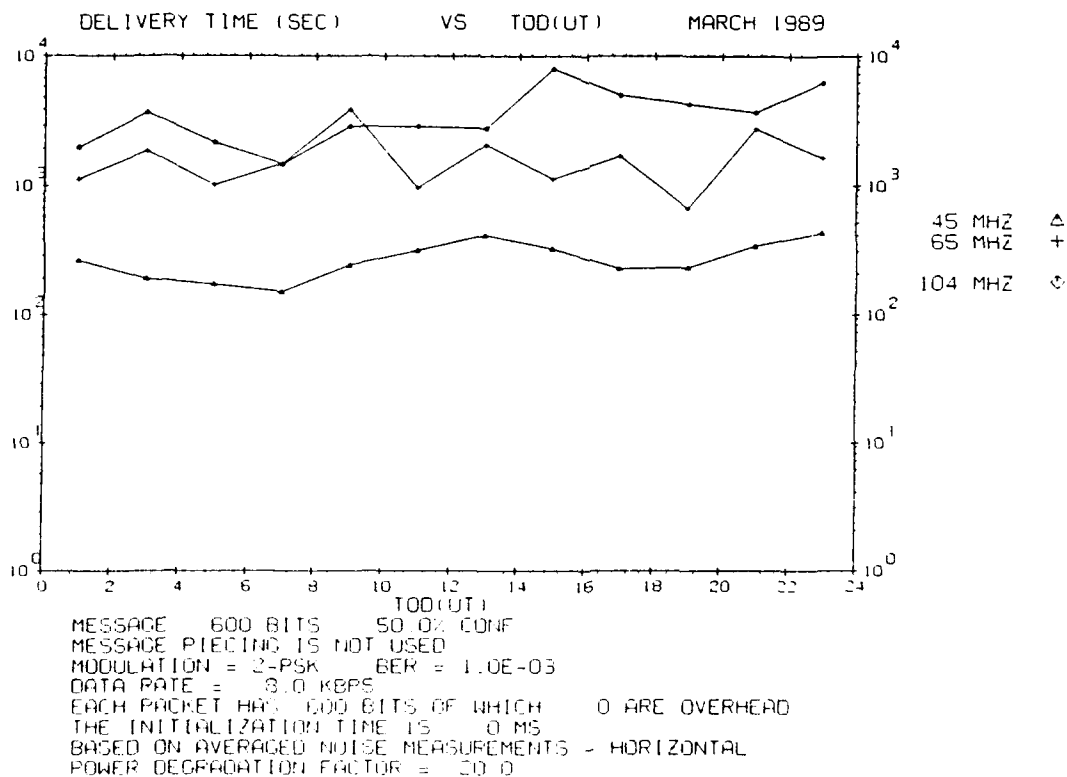


Figure E48. Same as Figure E43 but for Trails of 400 msec



**Figure E49. Waiting Time vs Time of Day for Trails of 50 msec Duration for March 1989. The transmitter power is 10 W**



**Figure E50. Same as Figure E49 but for Trails of 75 msec**



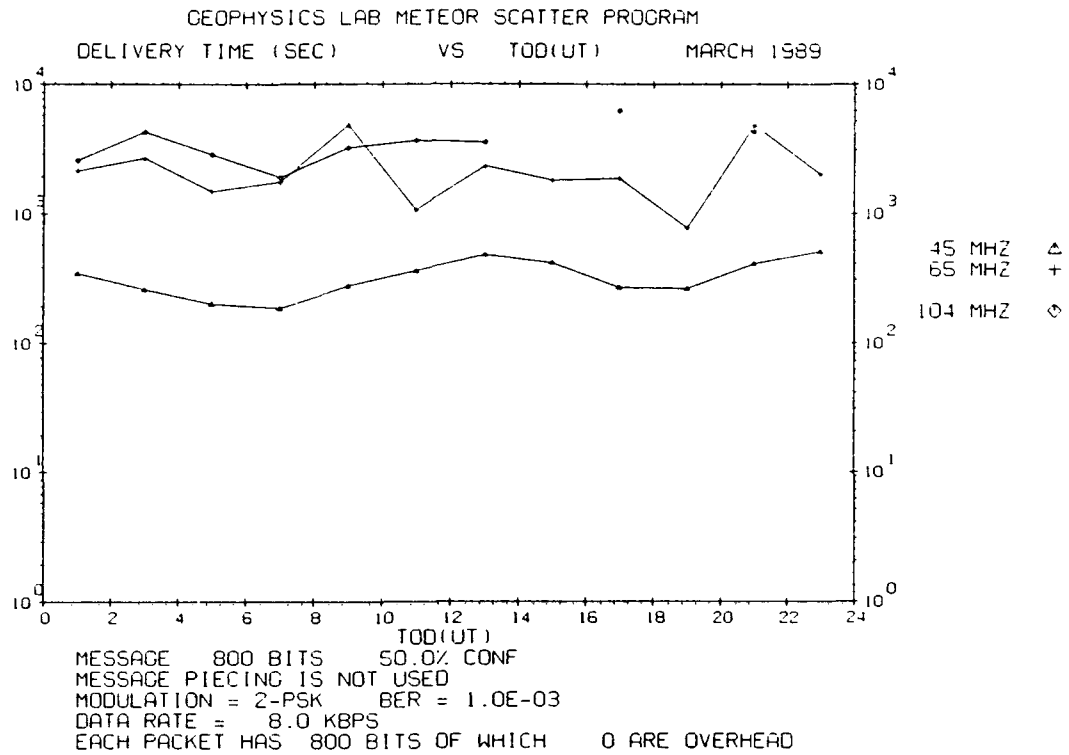


**Figure E51. Same as Figure E49 but for Trails of 100 msec**

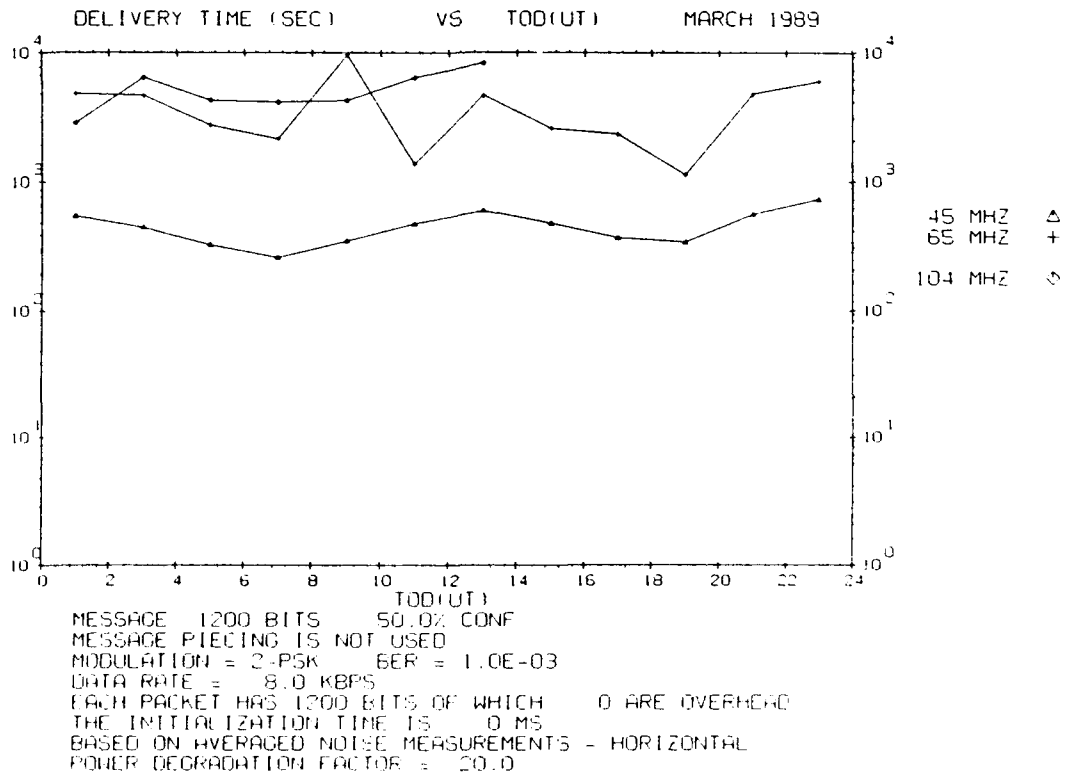


**Figure E52. Same as Figure E49 but for Trails of 150 msec**

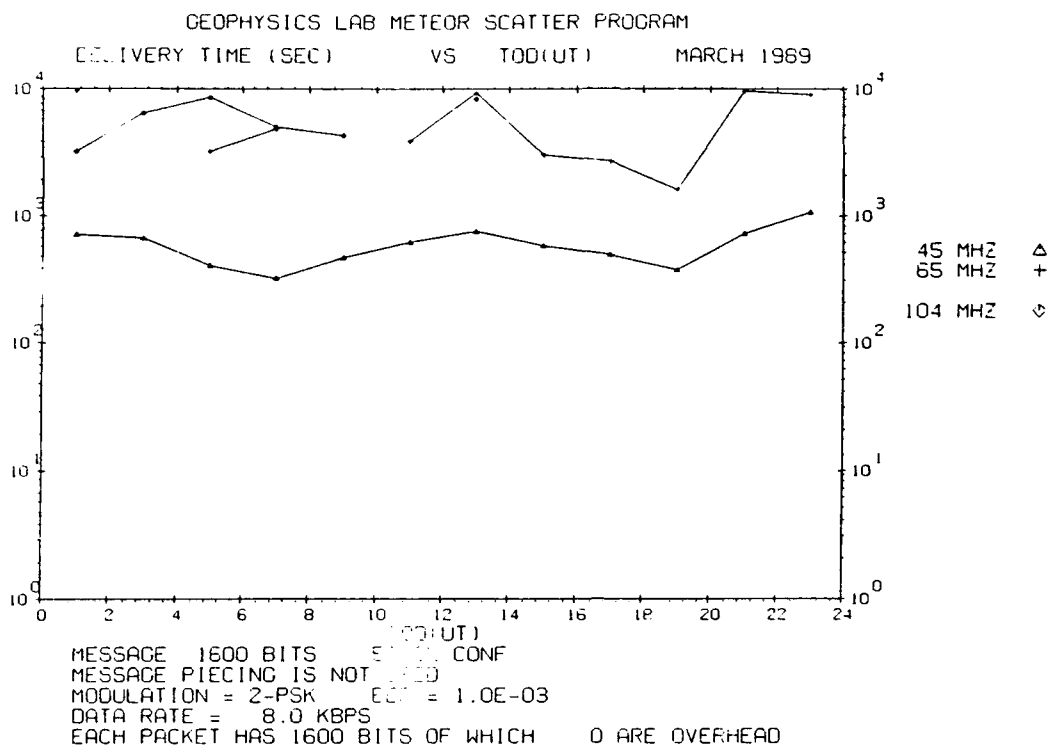


Figure E53. Same as Figure E49 but for Trails of 200 msec

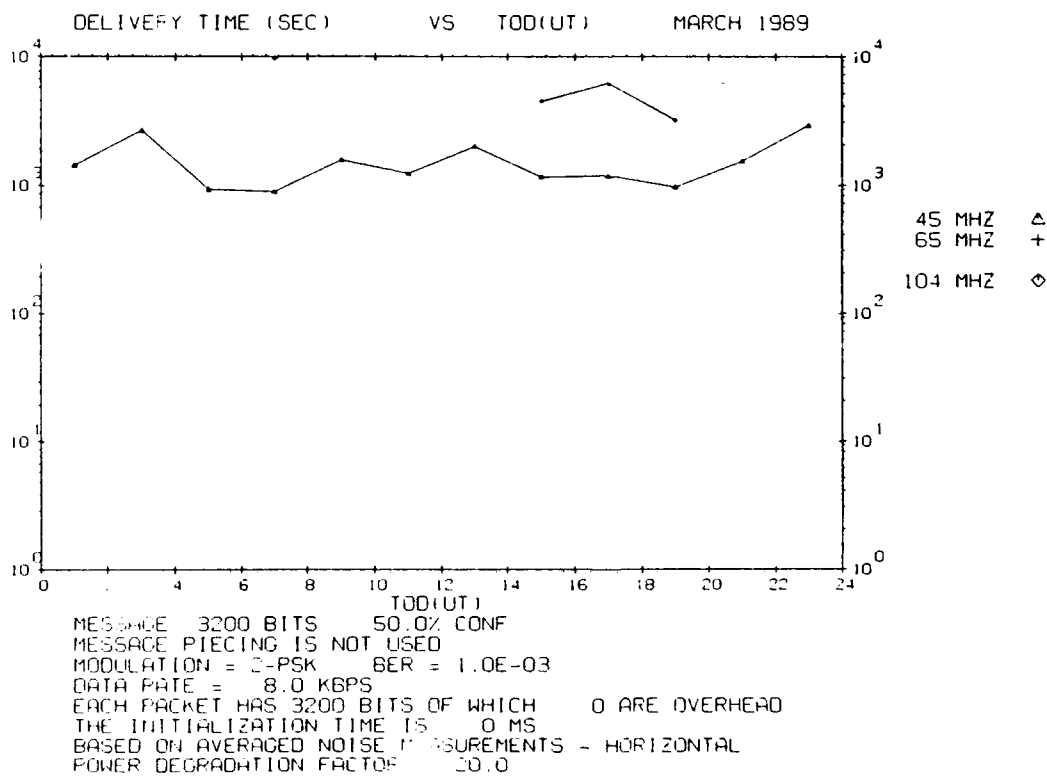
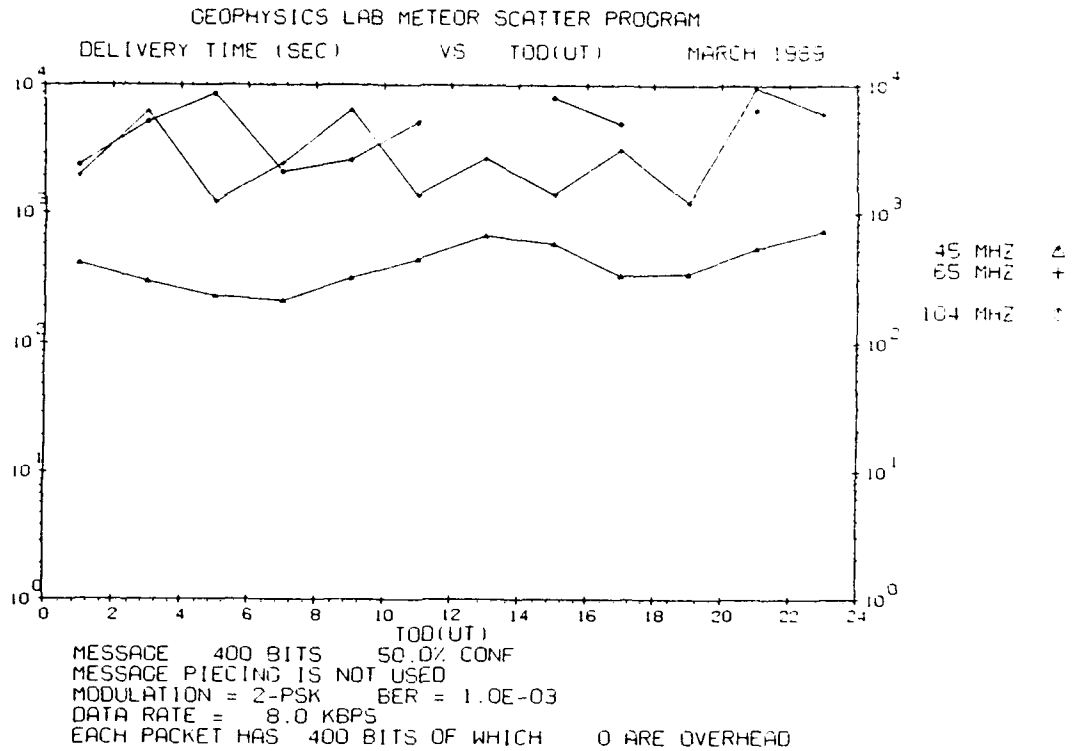
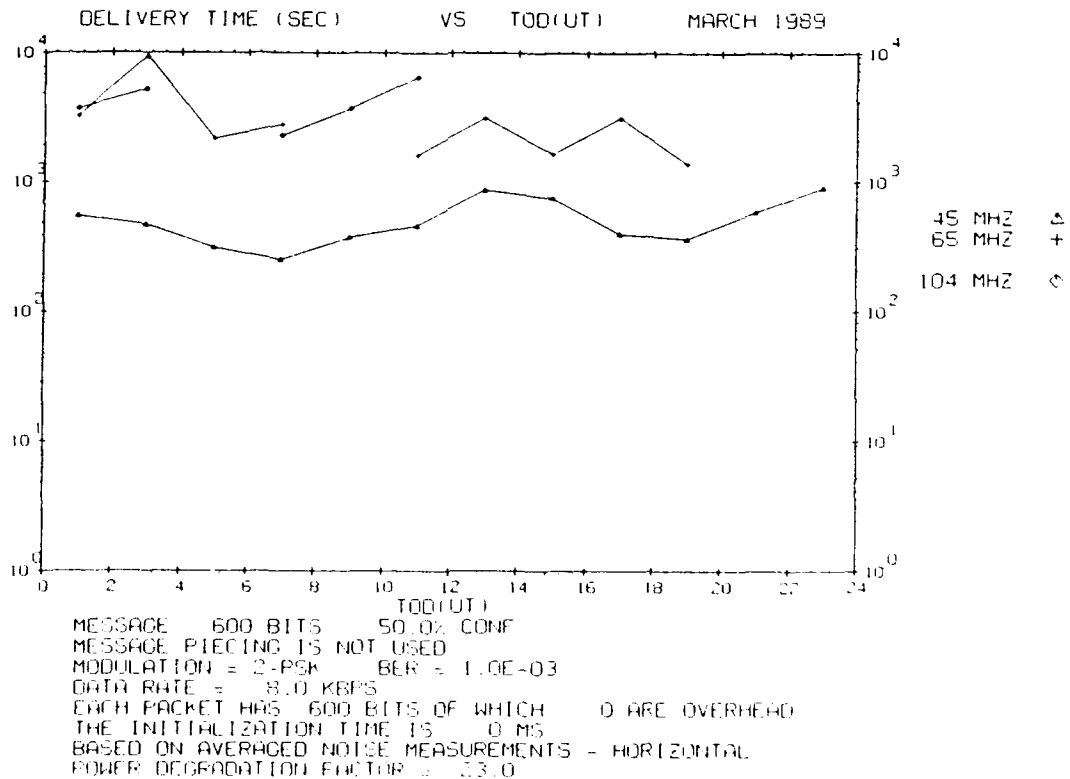


Figure E54. Same as Figure E49 but for Trails of 400 msec



**Figure E55. Waiting Time vs Time of Day for Trails of 50 msec Duration for March 1989. The transmitter power is 5 W**



**Figure E56. Same as Figure E55 but for Trails of 75 msec**

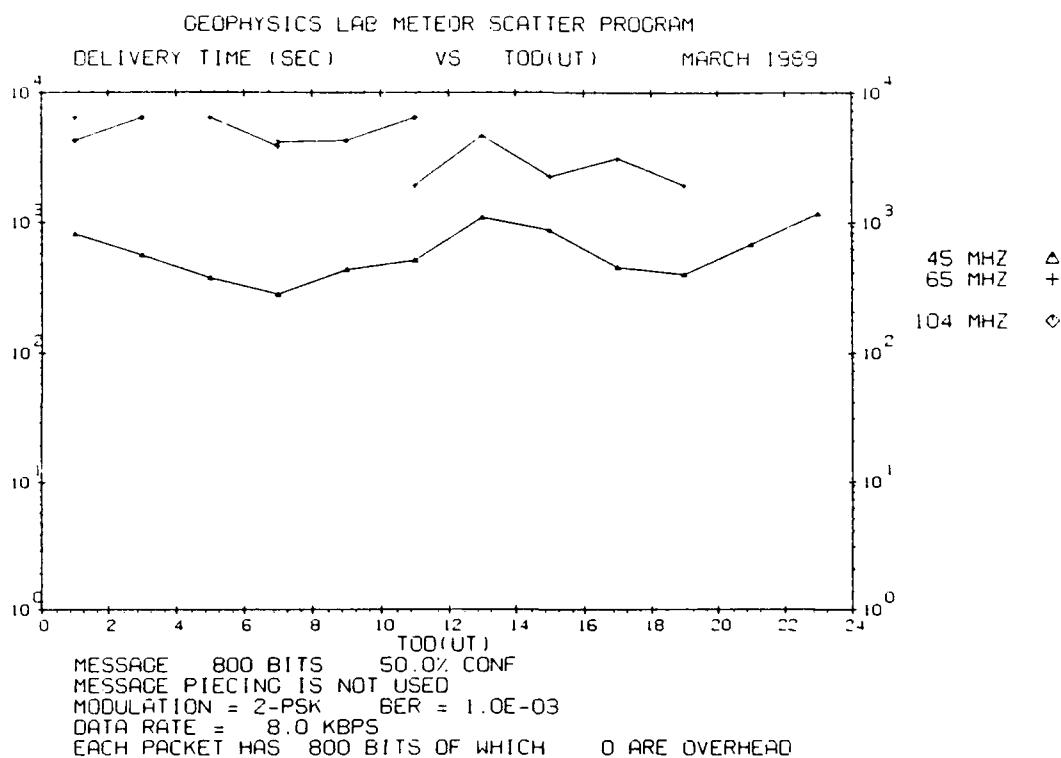


Figure E57. Same as Figure E55 but for Trails of 100 msec

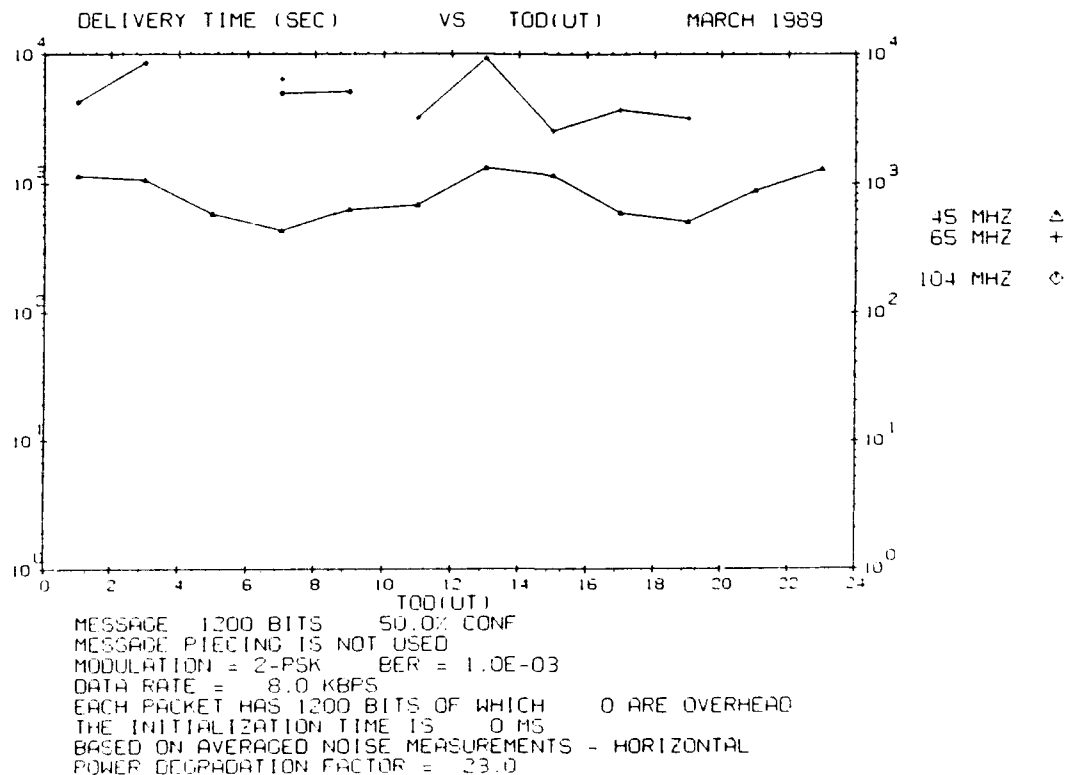


Figure E58. Same as Figure E55 but for Trails of 150 msec

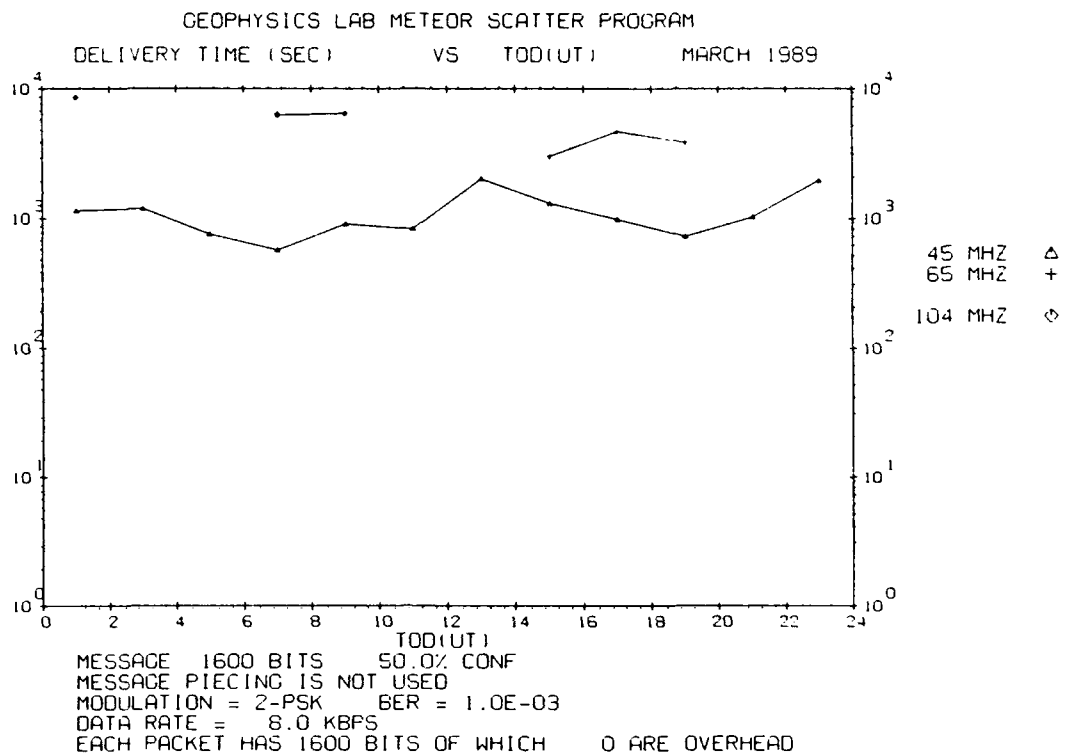


Figure E59. Same as Figure E55 but for Trails of 200 msec

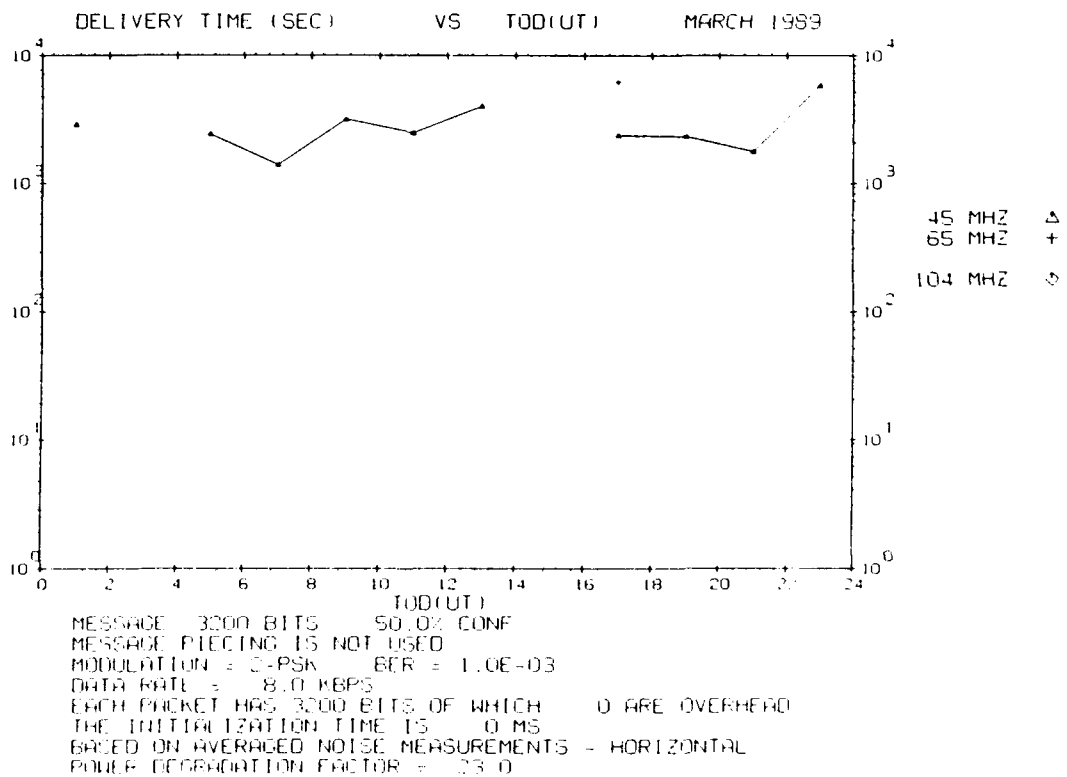
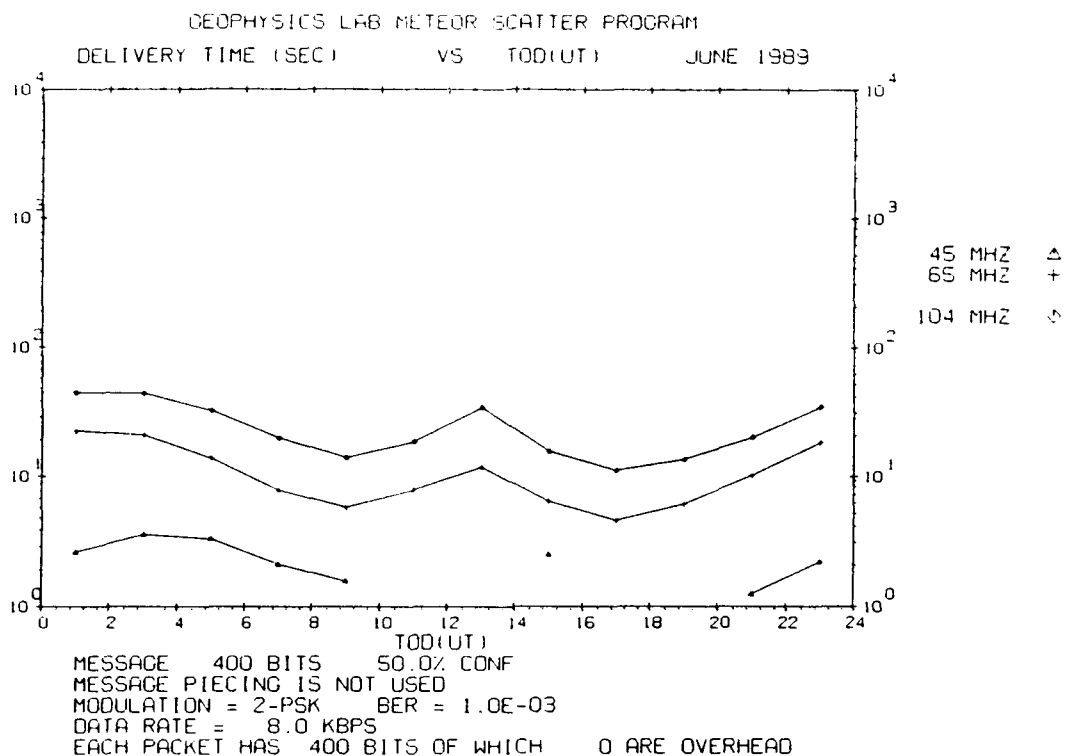
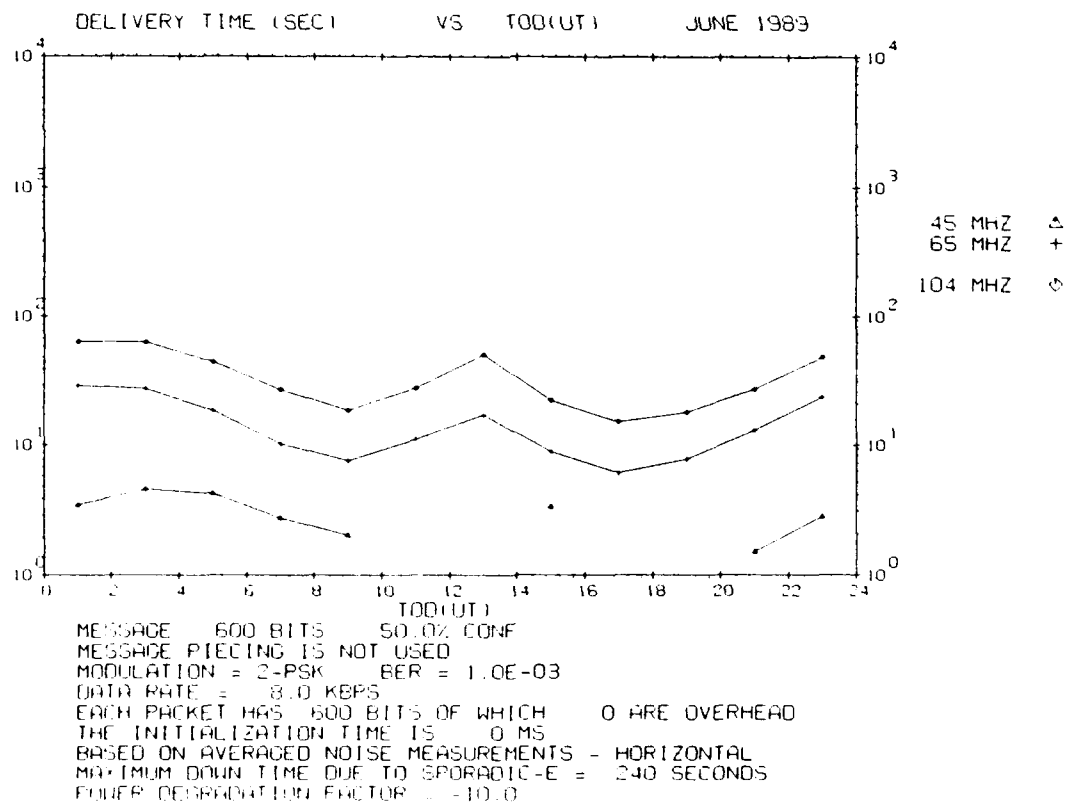


Figure E60. Same as Figure E55 but for Trails of 400 msec



**Figure E61. Waiting Time vs Time of Day for Trails of 50 msec Duration for June 1989. The transmitter power is 10,000 W**



**Figure E62. Same as Figure E61 but for Trails of 75 msec**

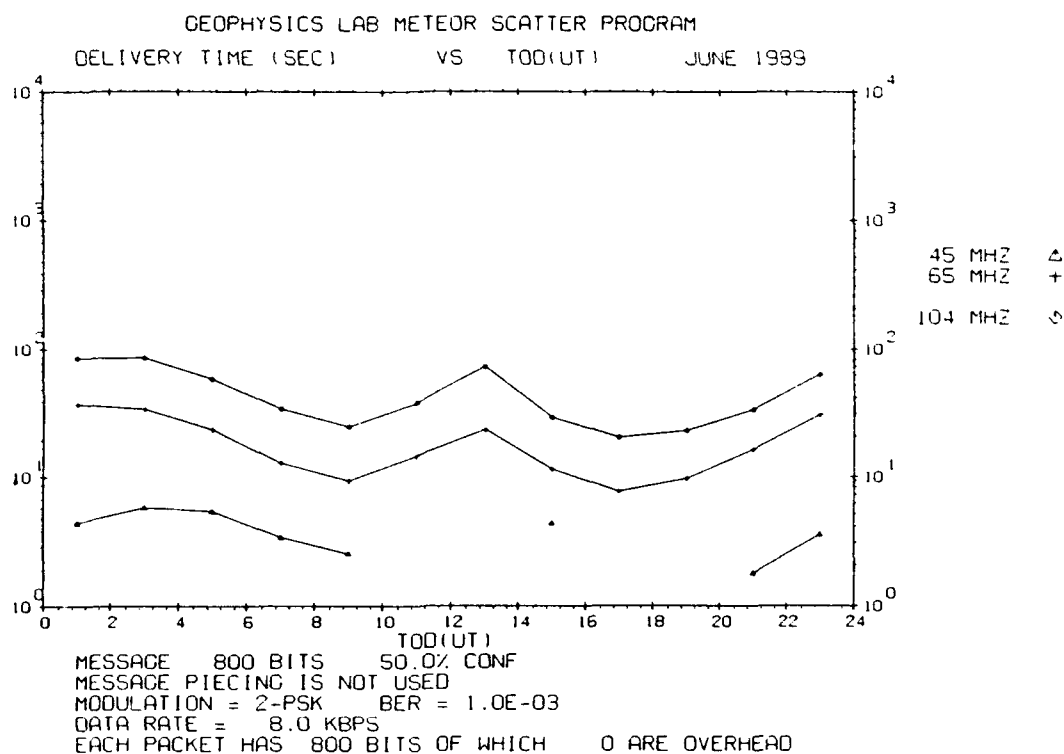


**Figure E63.** Same as Figure E61 but for Trails of 100 msec

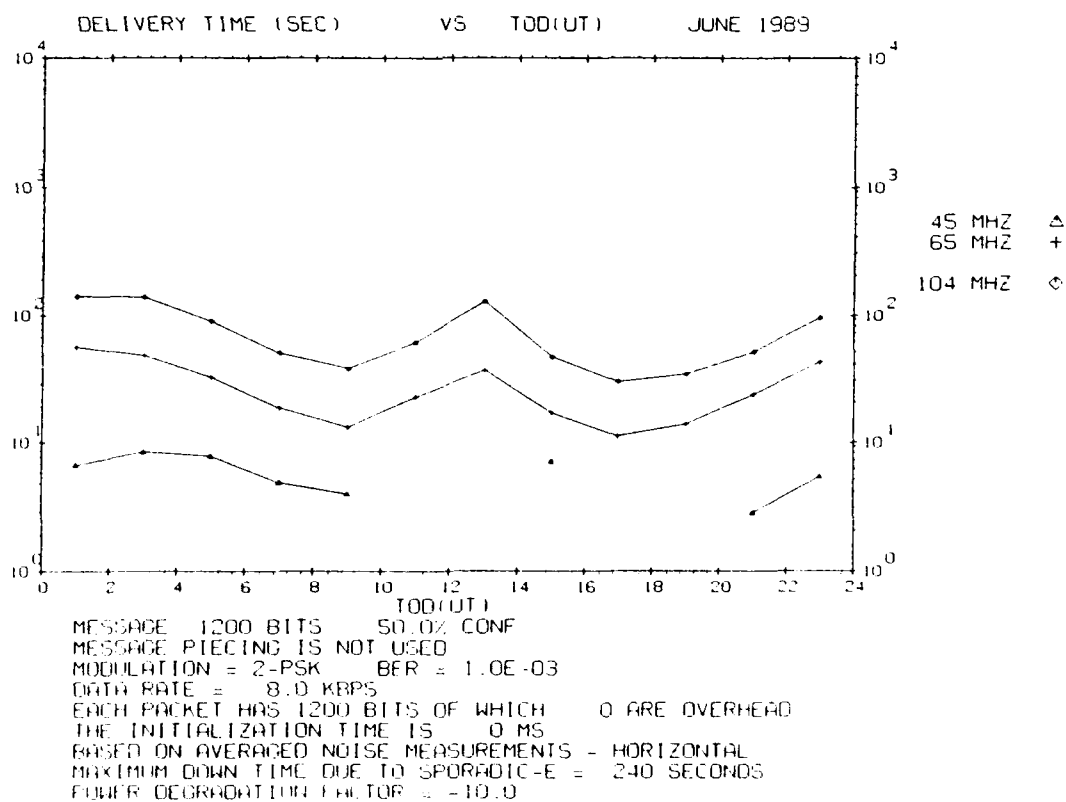


**Figure E64.** Same as Figure E61 but for Trails of 150 msec

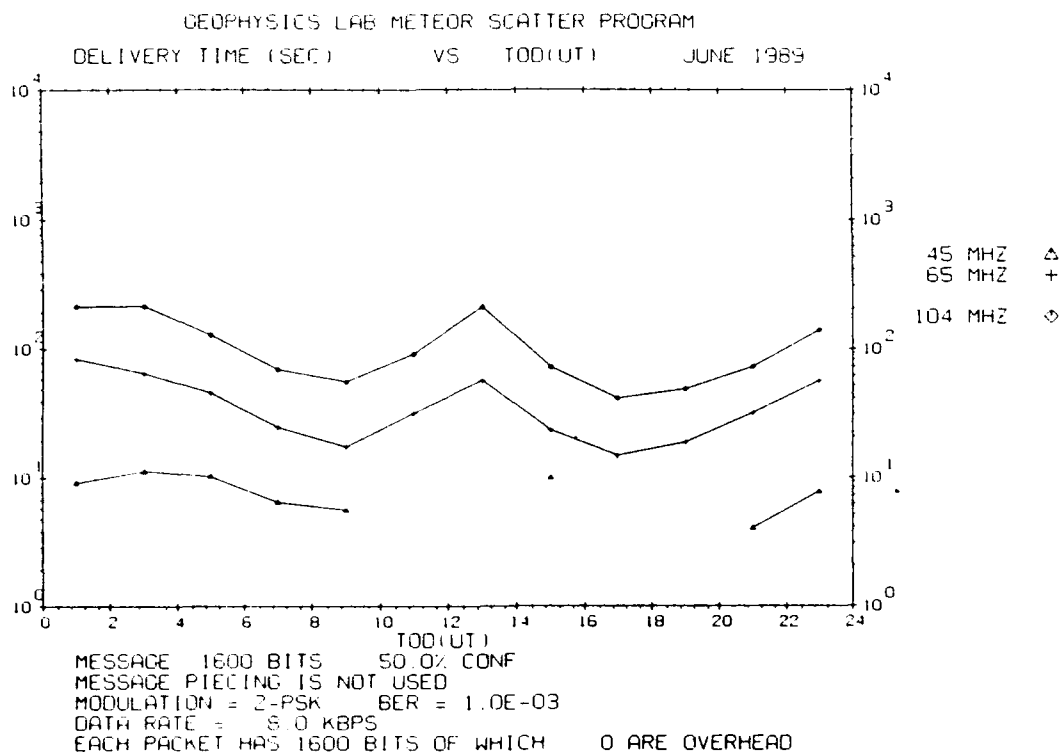


Figure E65. Same as Figure E61 but for Trails of 200 msec

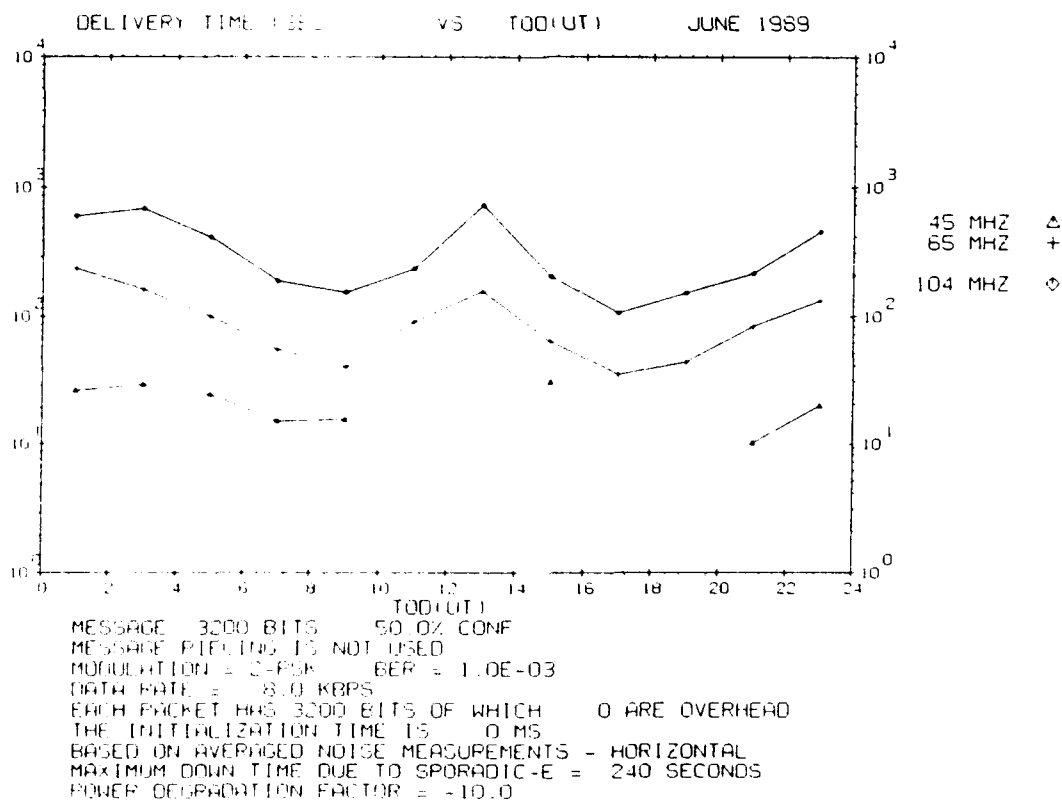
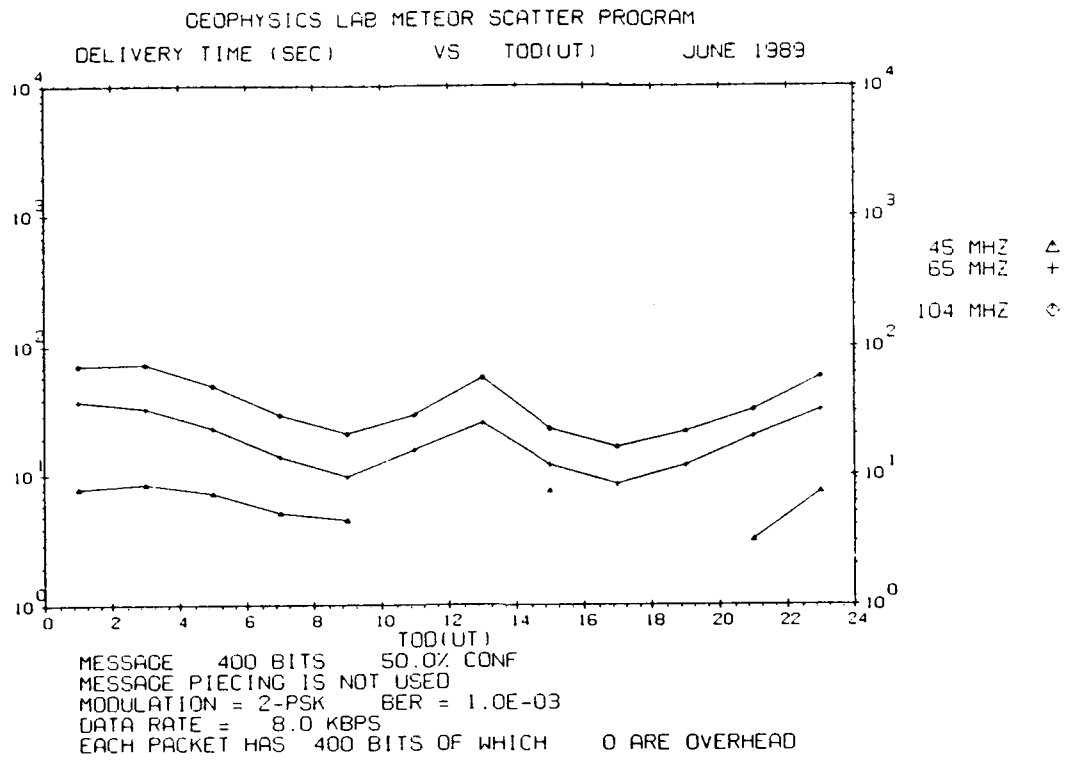
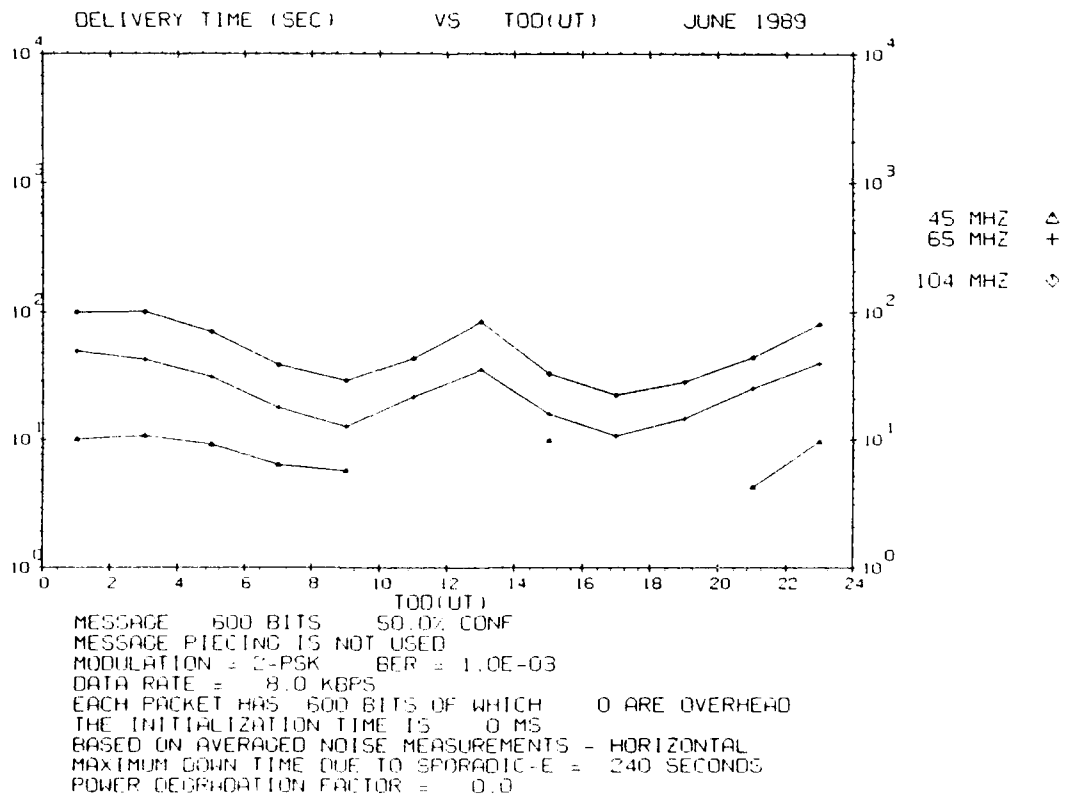


Figure E66. Same as Figure E61 but for Trails of 400 msec





**Figure E67. Waiting Time vs Time of Day for Trails of 50 msec Duration for June 1989. The transmitter power is 1,000 W**



**Figure E68. Same as Figure E67 but for Trails of 75 msec**

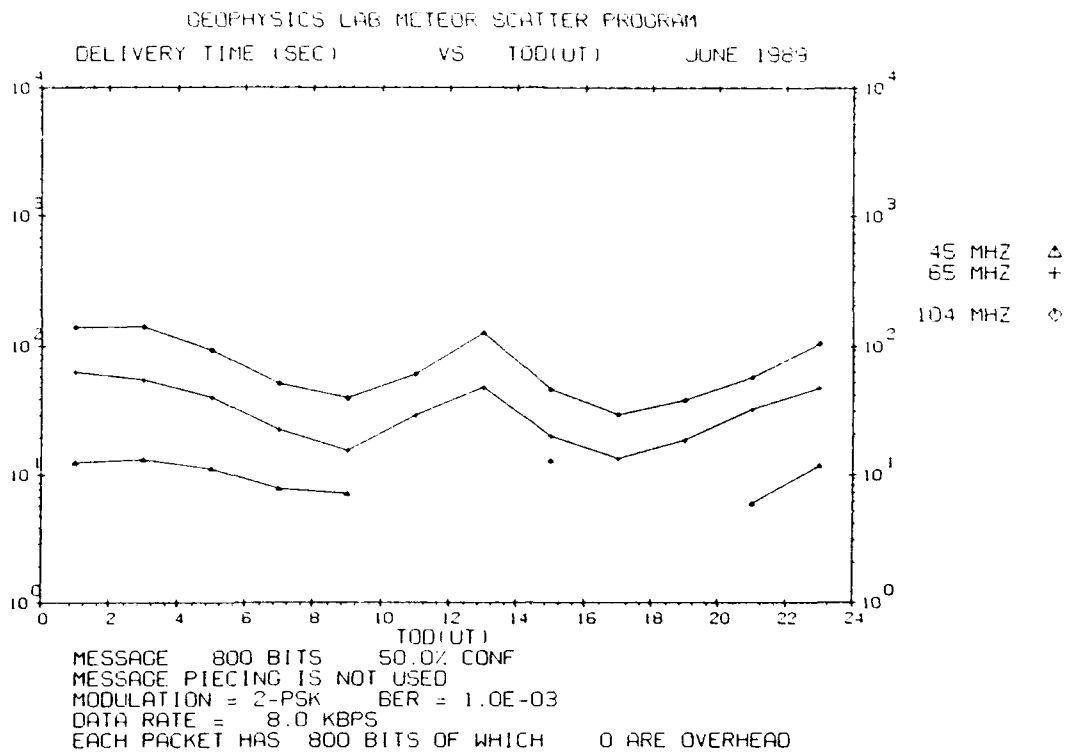


Figure E69. Same as Figure E67 but for Trails of 100 msec

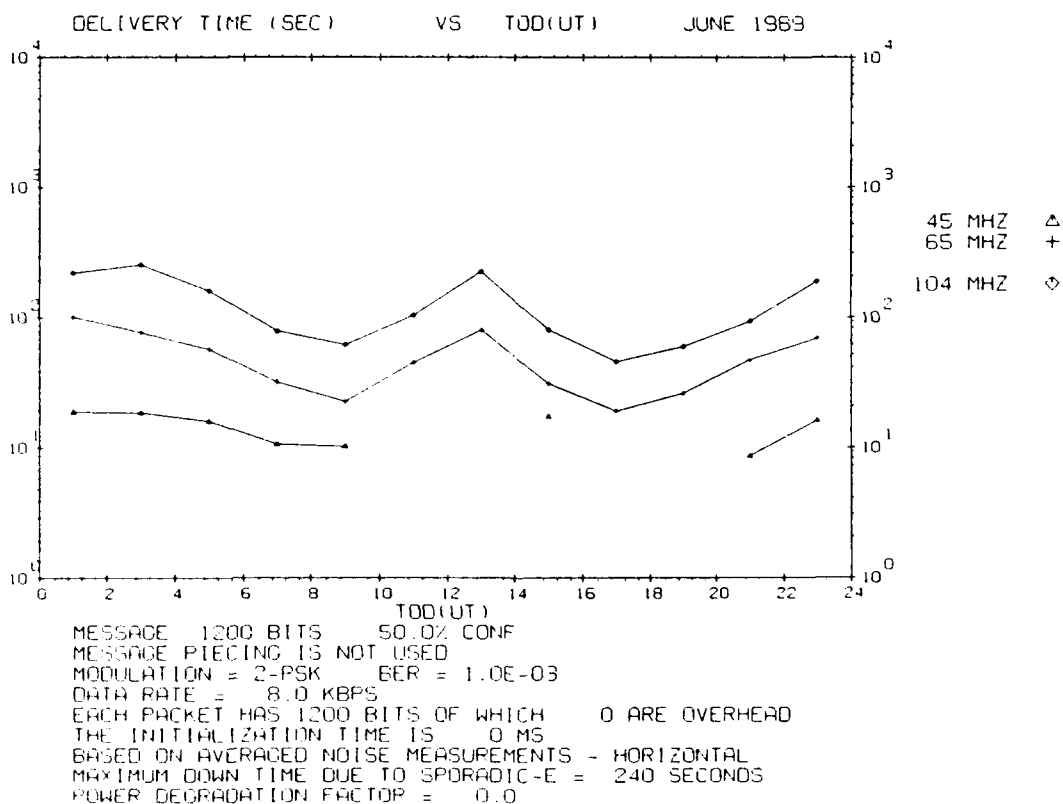


Figure E70. Same as Figure E67 but for Trails of 150 msec

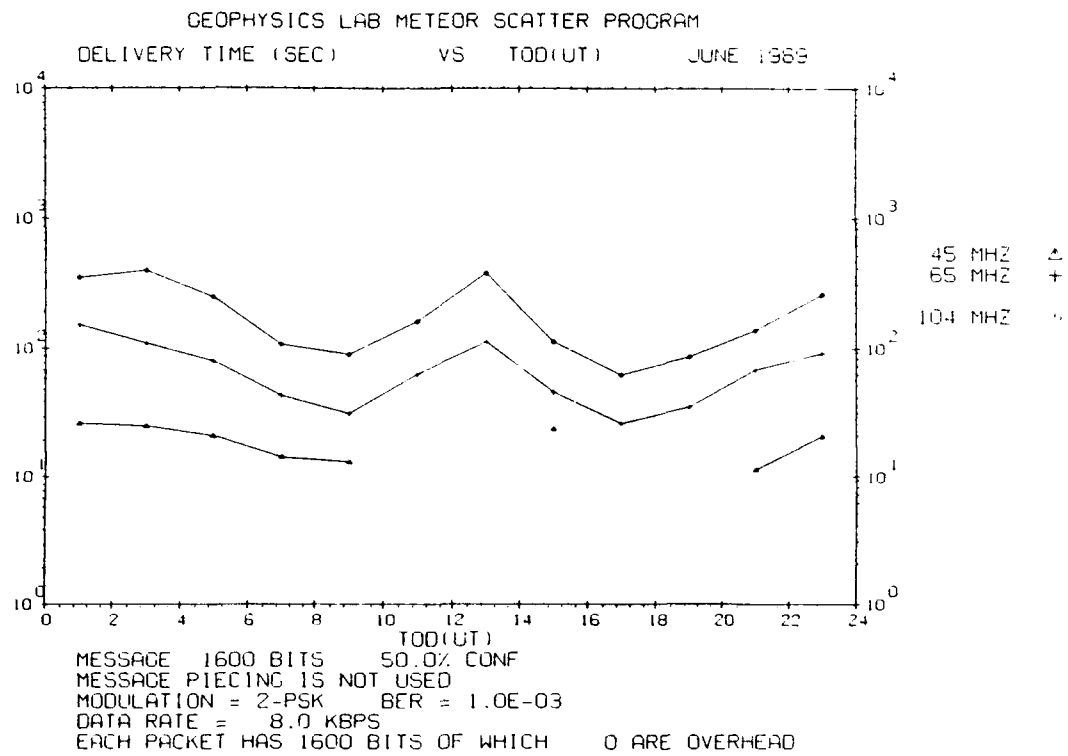


Figure E71. Same as Figure E67 but for Trails of 200 msec

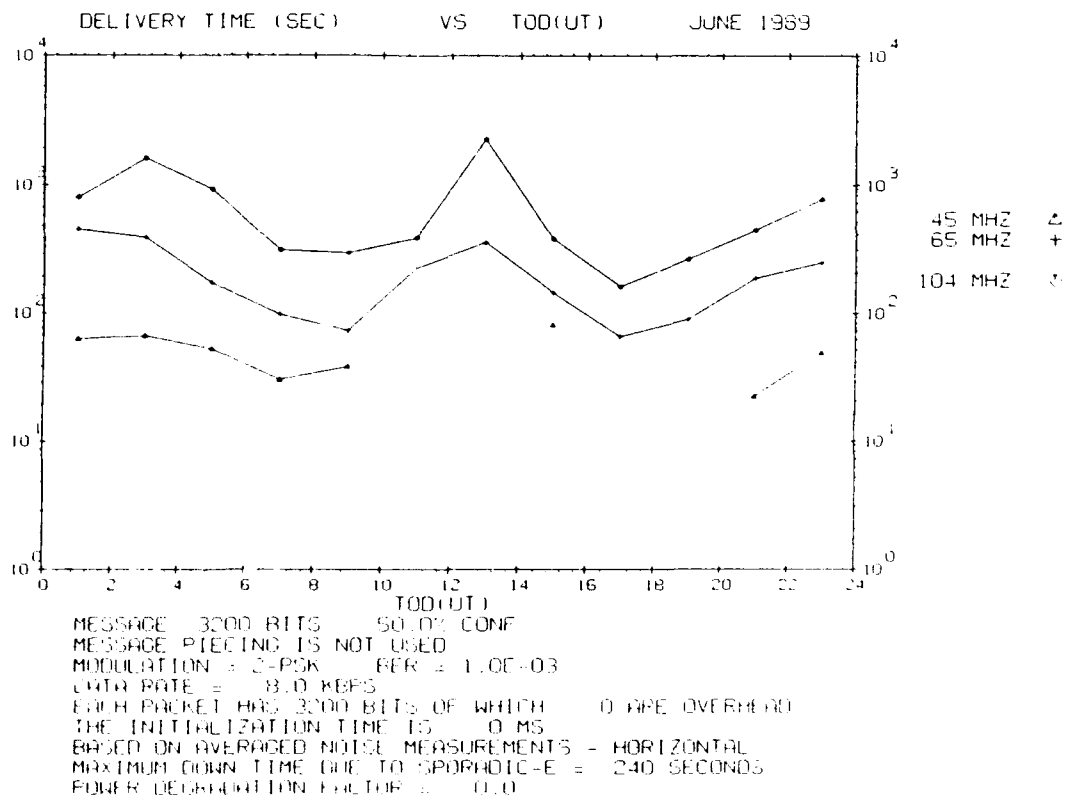
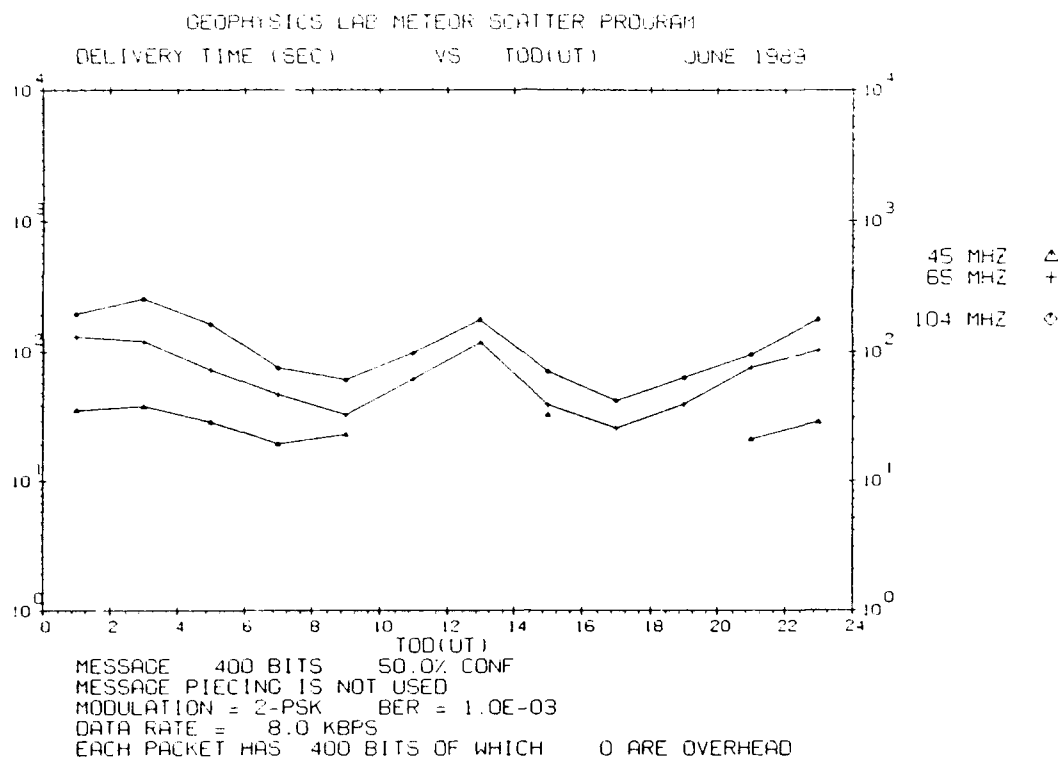
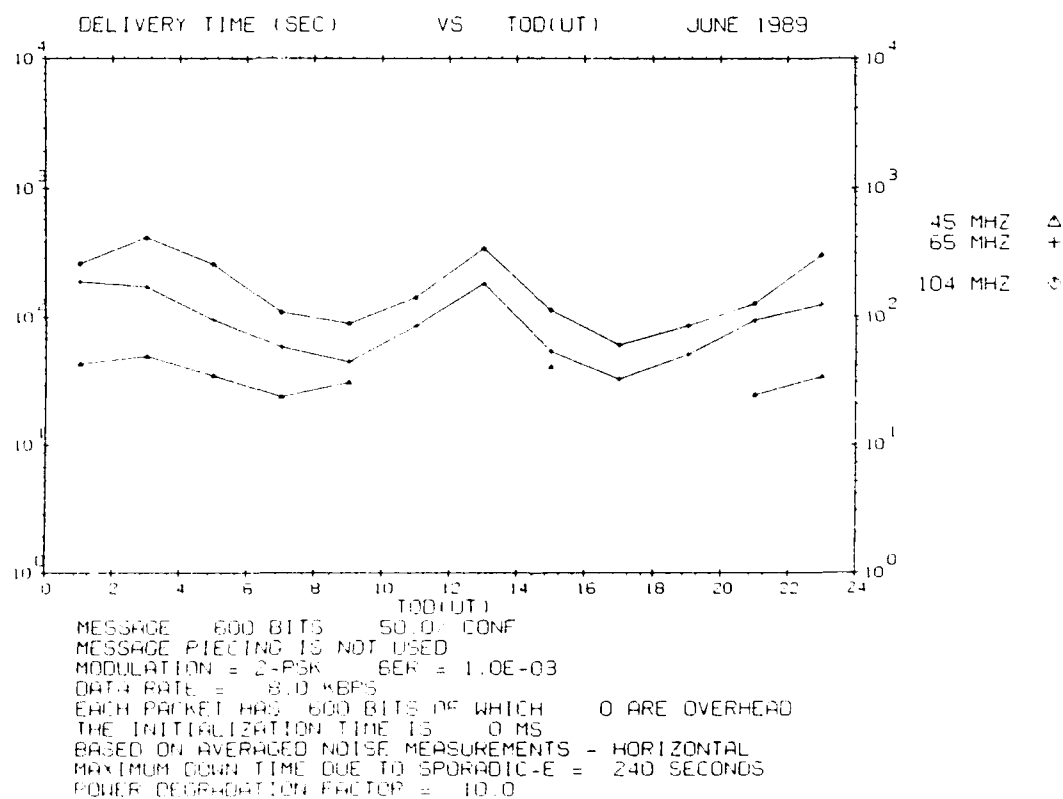


Figure E72. Same as Figure E67 but for Trails of 400 msec



**Figure E73. Waiting Time vs Time of Day for Trails of 50 msec Duration for June 1989. The transmitter power is 100 W**



**Figure E74. Same as Figure E73 but for Trails of 75 msec**

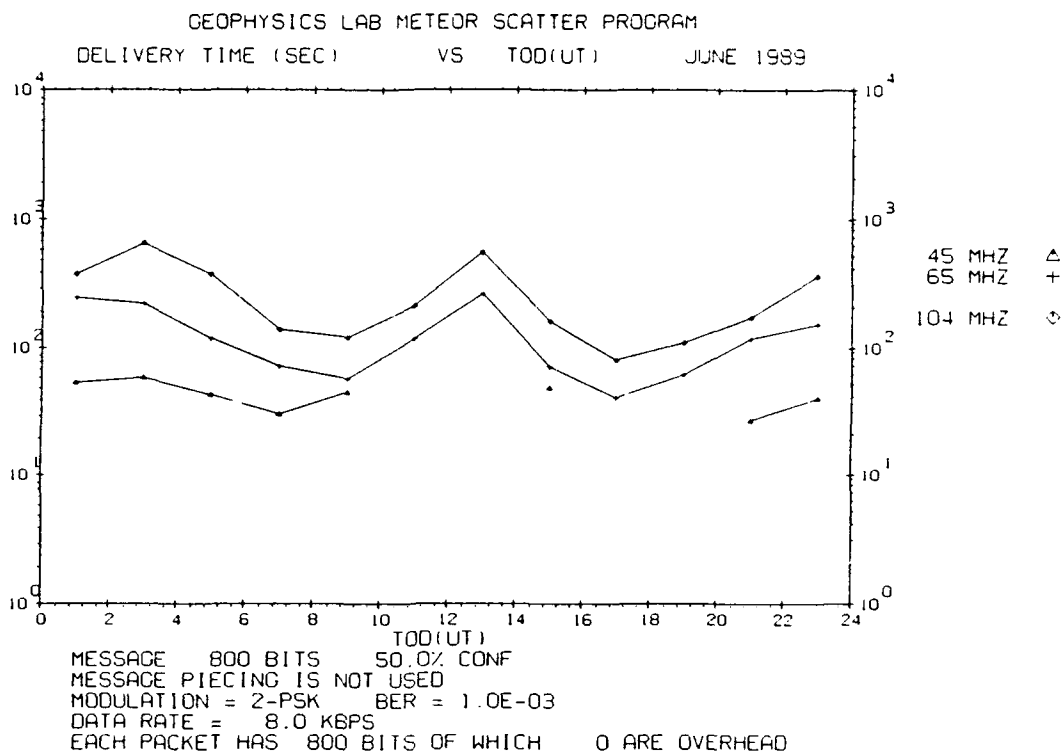


Figure E75. Same as Figure E73 but for Trails of 100 msec

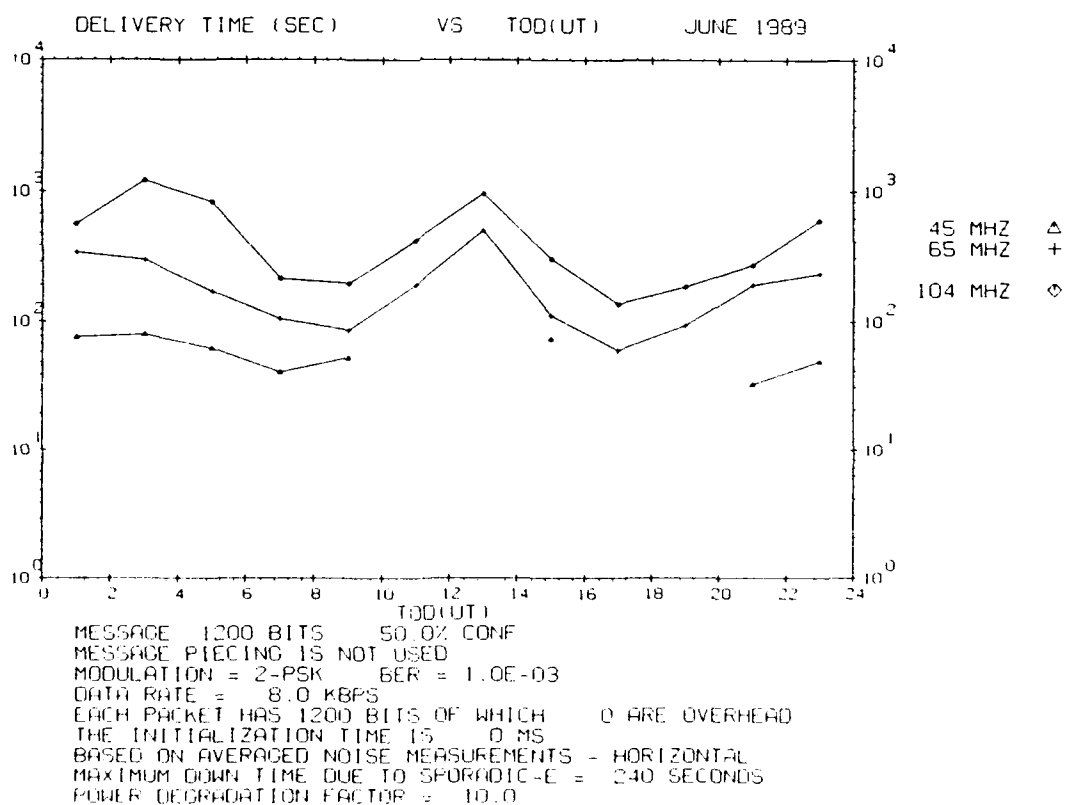


Figure E76. Same as Figure E73 but for Trails of 150 msec

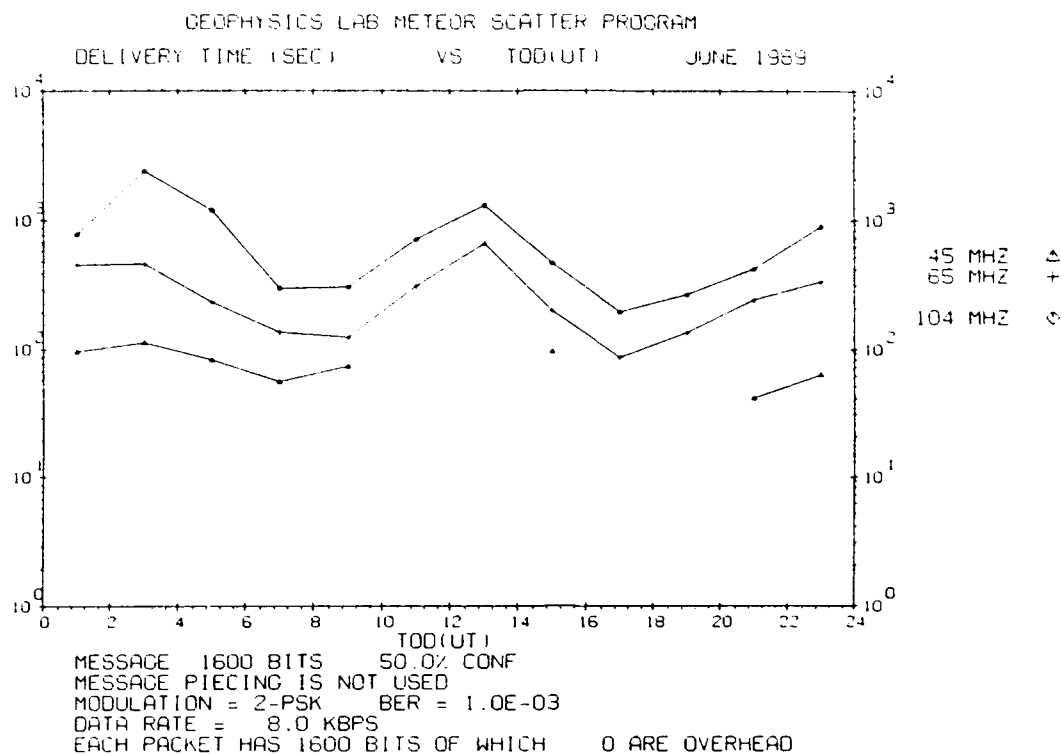


Figure E77. Same as Figure E73 but for Trails of 200 msec

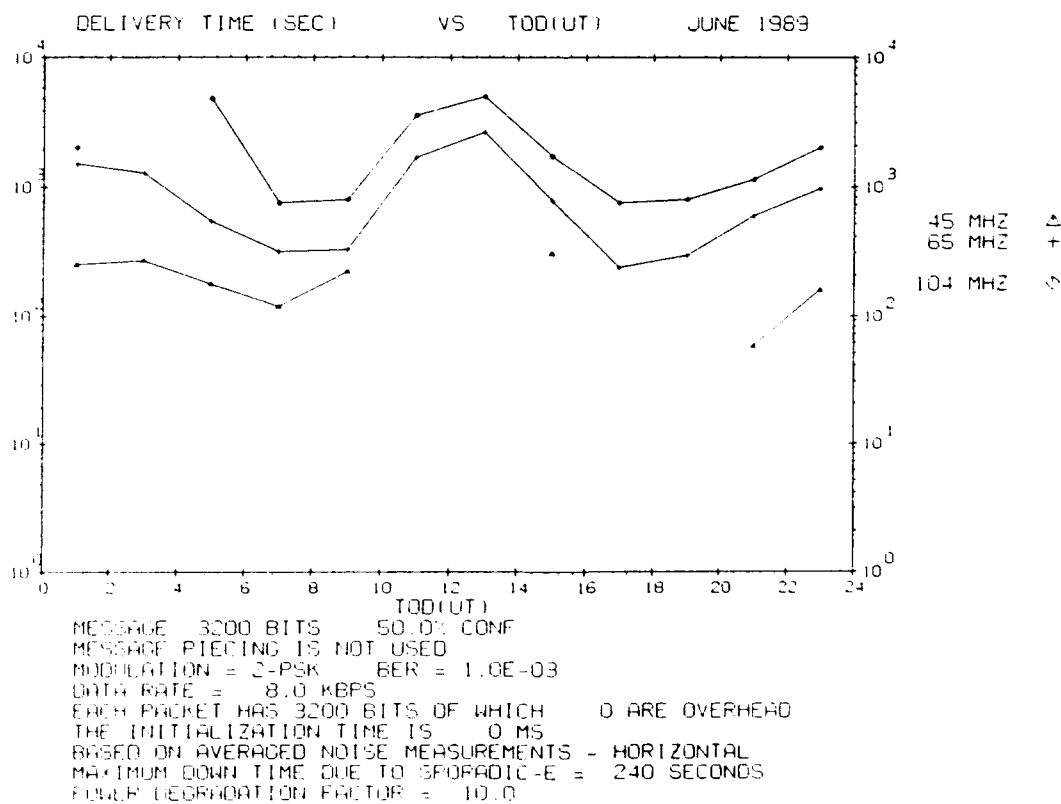
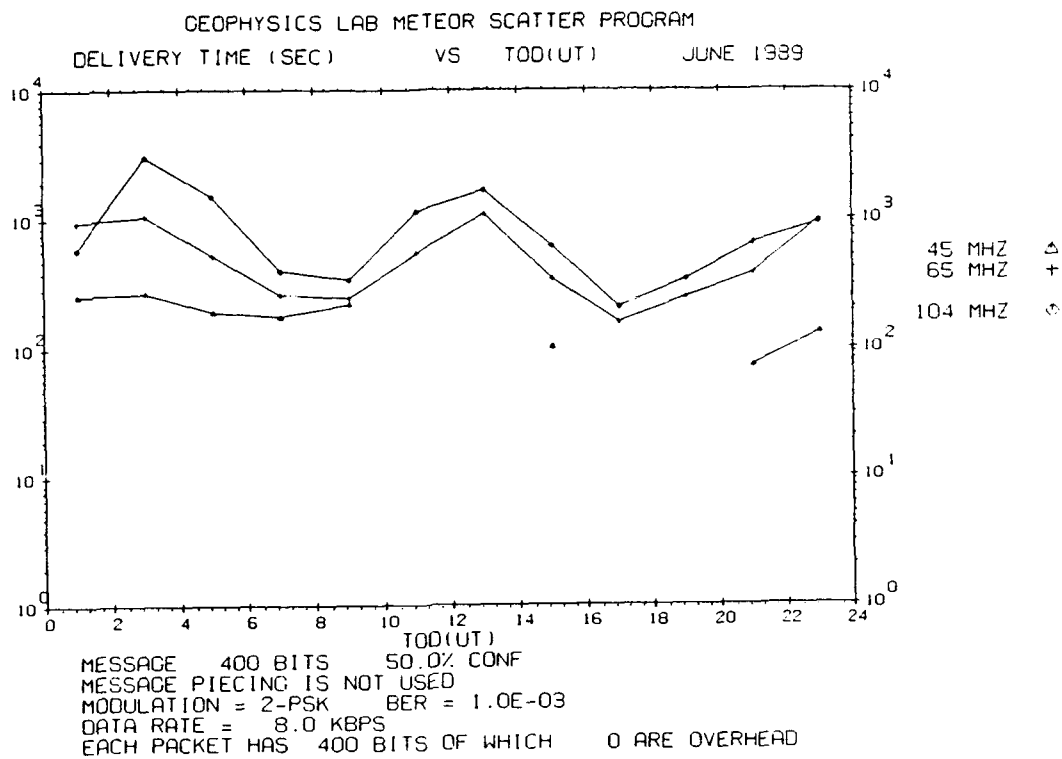
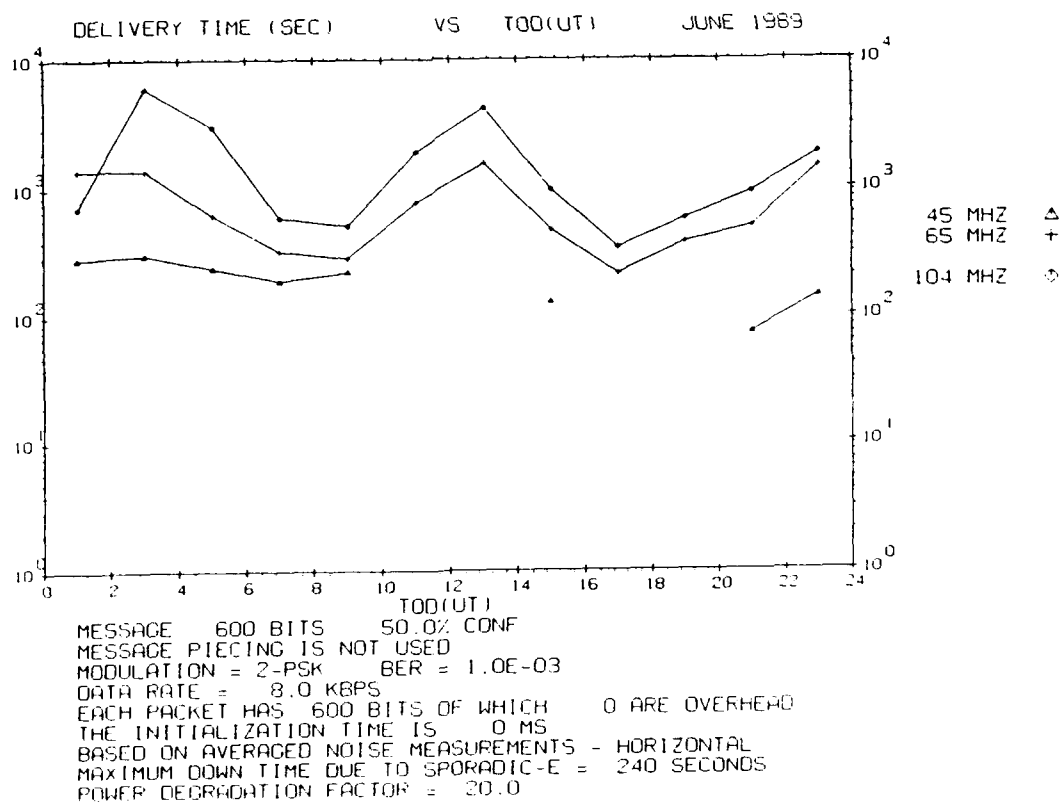


Figure E78. Same as Figure E73 but for Trails of 400 msec



**Figure E79. Waiting Time vs Time of Day for Trails of 50 msec Duration for June 1989. The transmitter power is 10 W**



**Figure E80. Same as Figure E79 but for Trails of 75 msec**

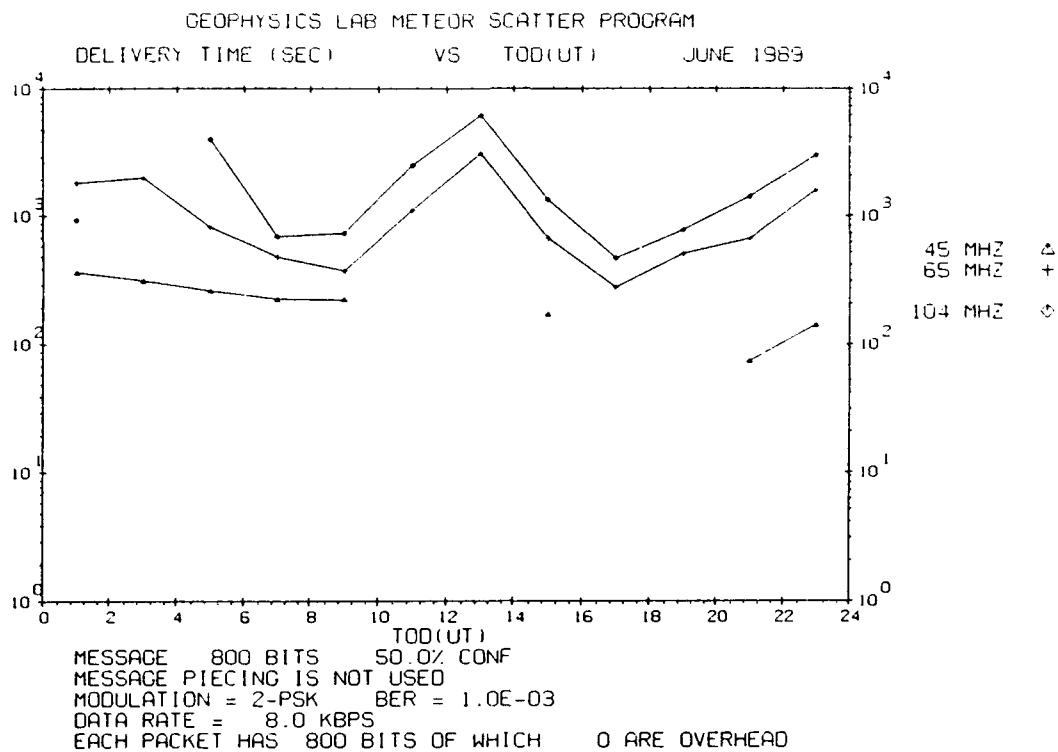


Figure E81. Same as Figure E79 but for Trails of 100 msec

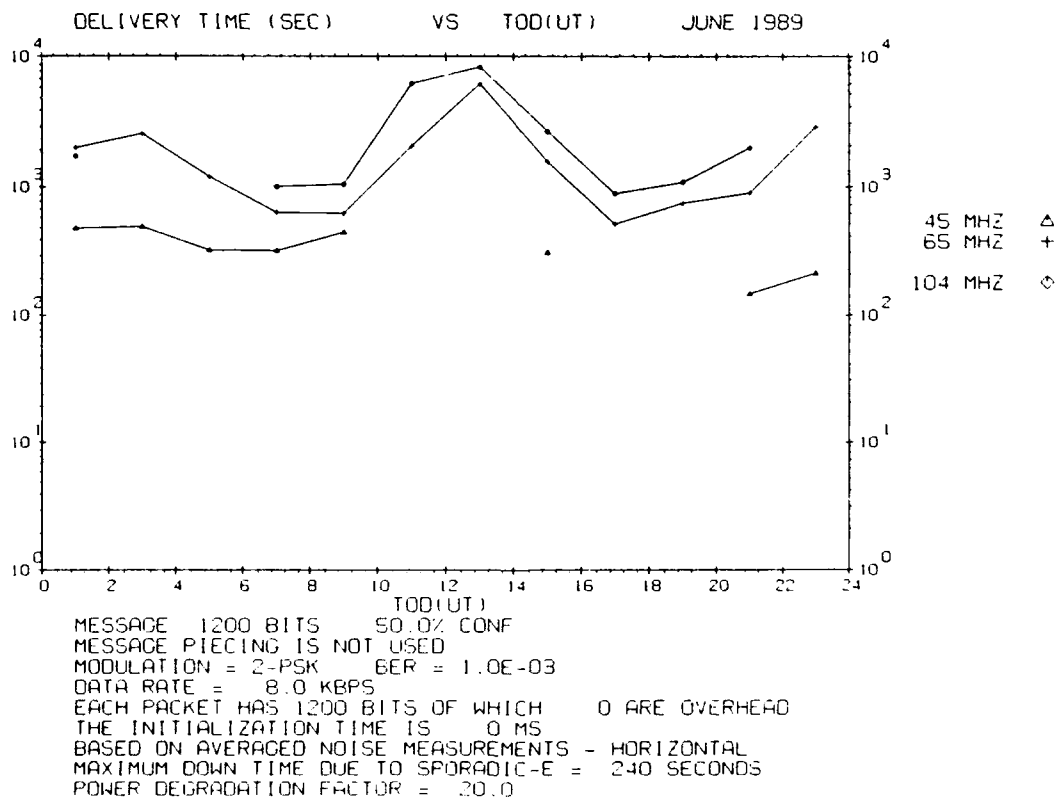


Figure E82. Same as Figure E79 but for Trails of 150 msec



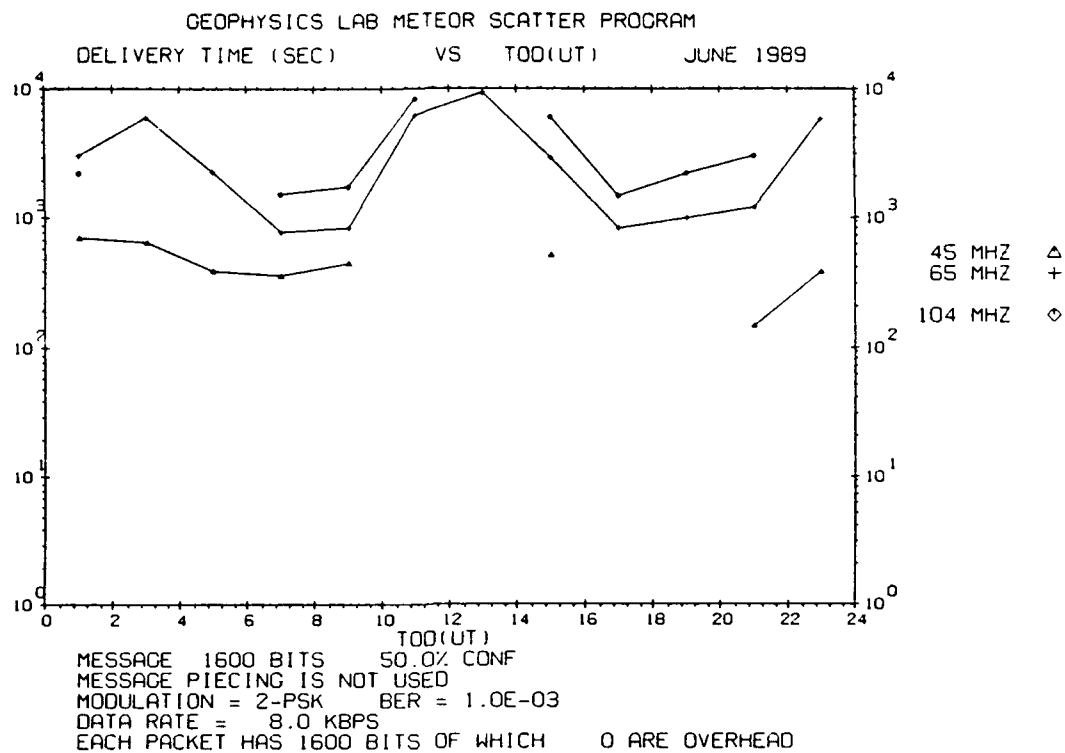


Figure E83. Same as Figure E79 but for Trails of 200 msec

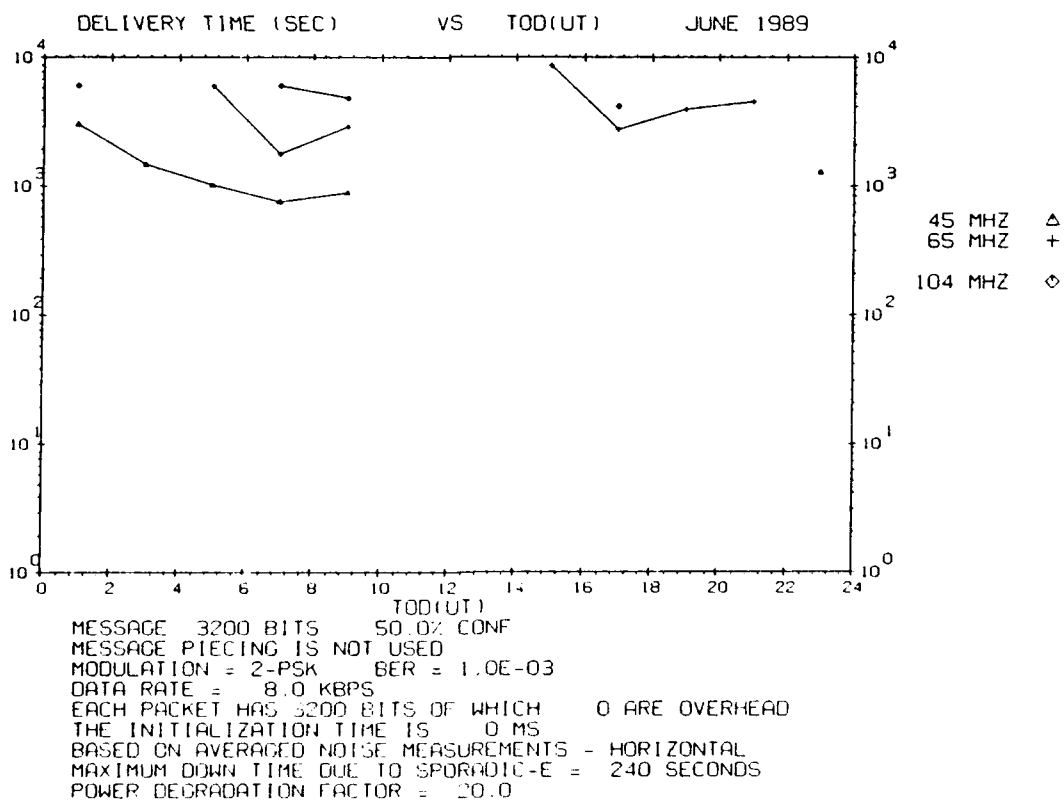
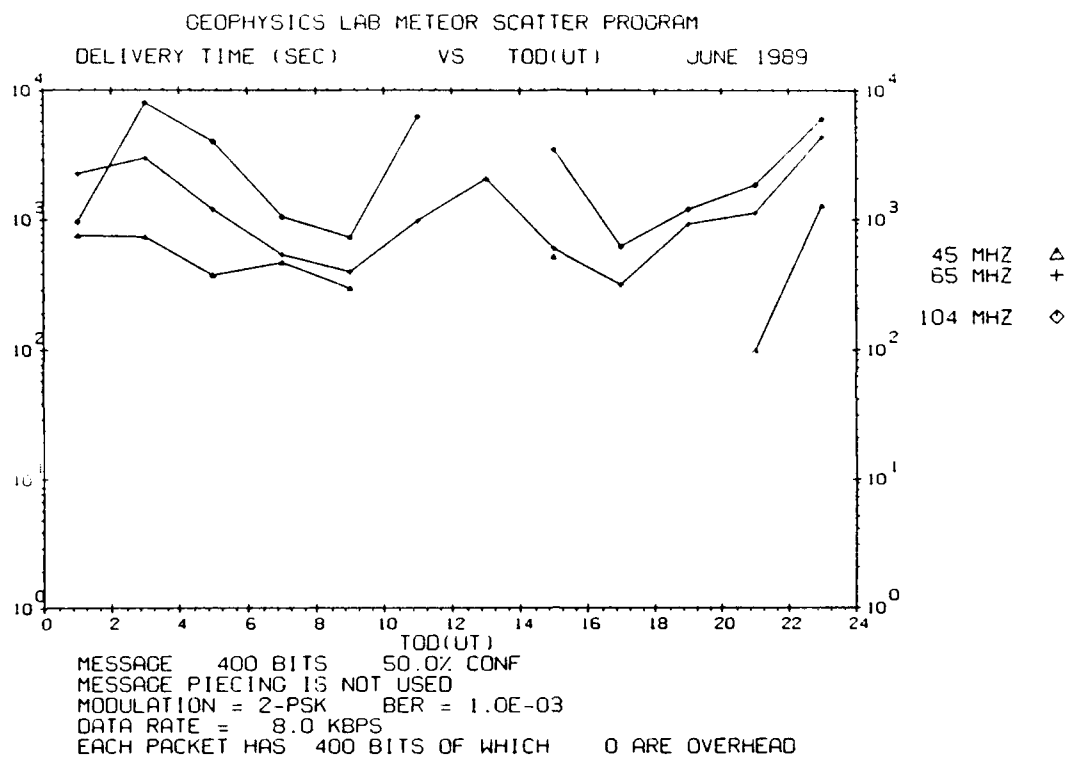
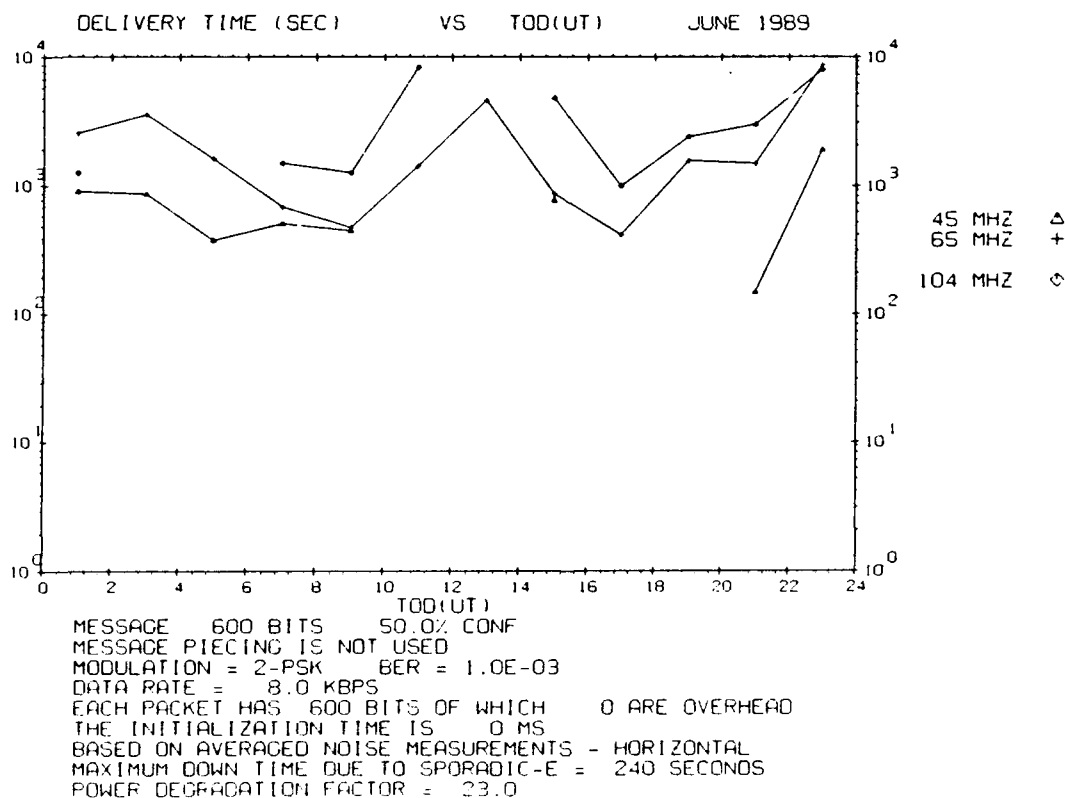


Figure E84. Same as Figure E79 but for Trails of 400 msec



**Figure E85. Waiting Time vs Time of Day for Trails of 50 msec Duration for June 1989. The transmitter power is 5 W**



**Figure E86. Same as Figure E85 but for Trails of 75 msec**

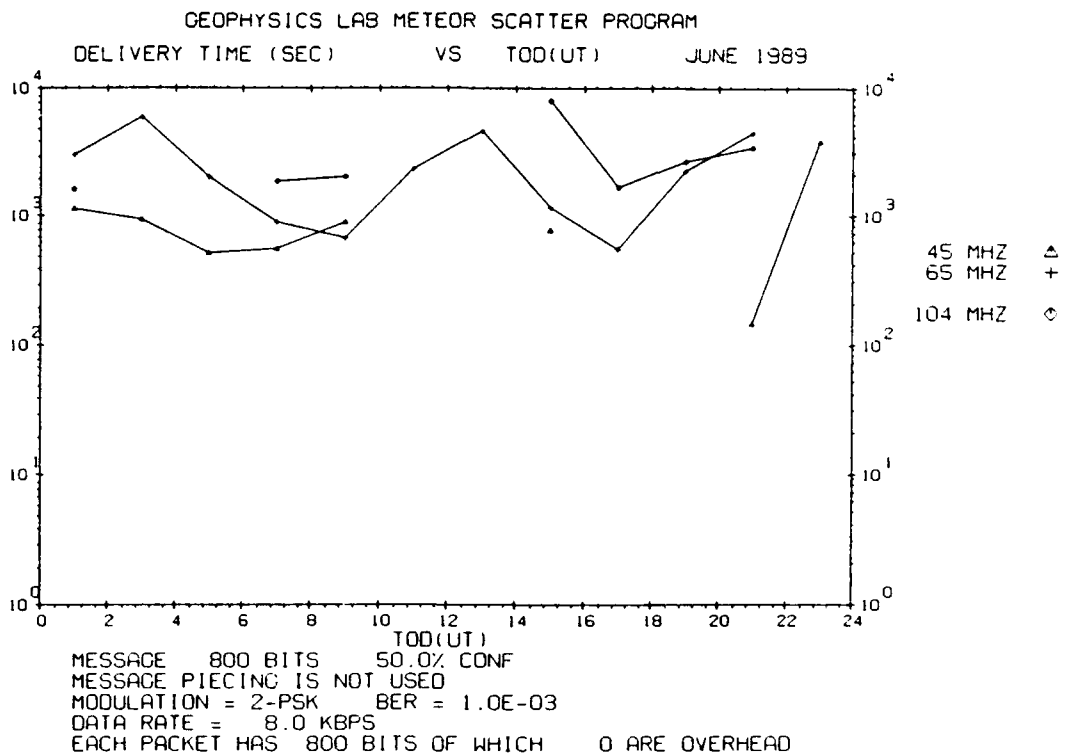


Figure E87. Same as Figure E85 but for Trails of 100 msec

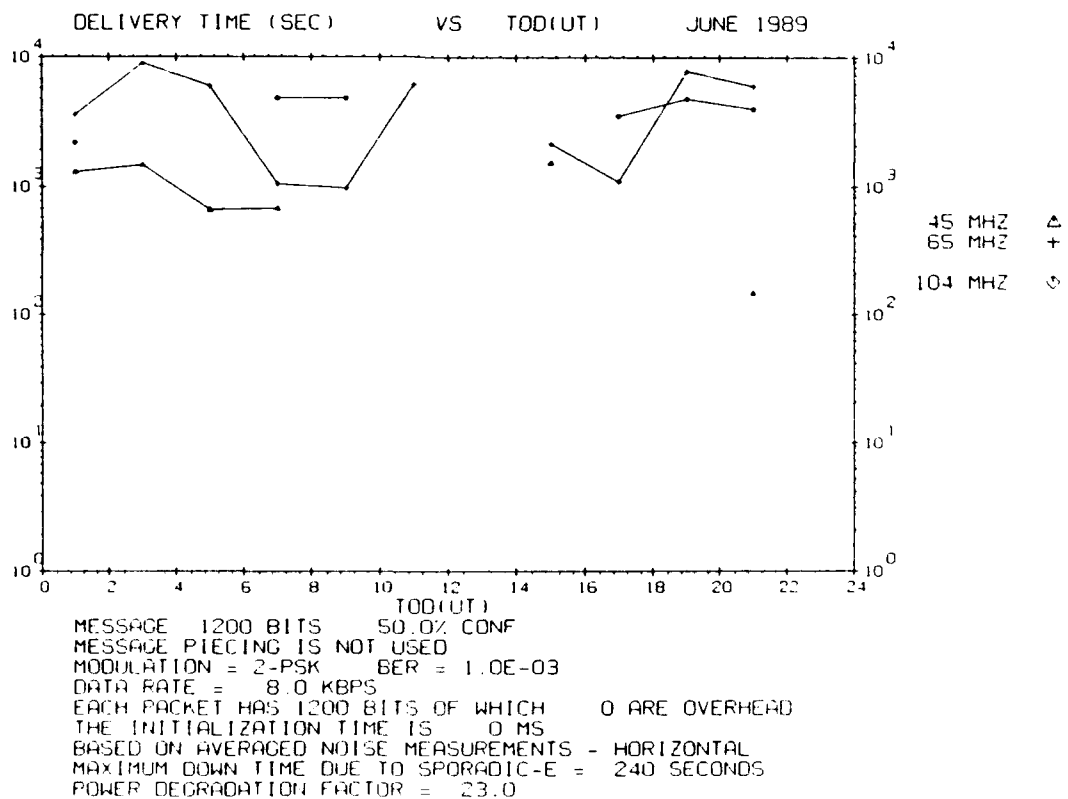


Figure E88. Same as Figure E85 but for Trails of 150 msec

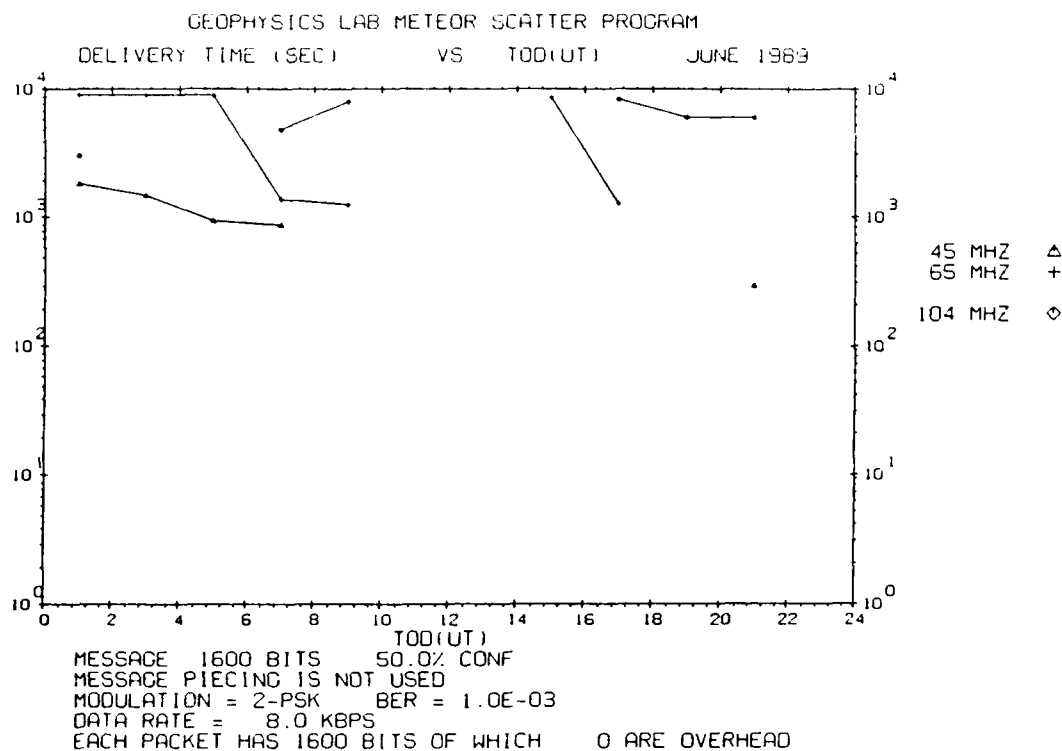


Figure E89. Same as Figure E85 but for Trails of 200 msec

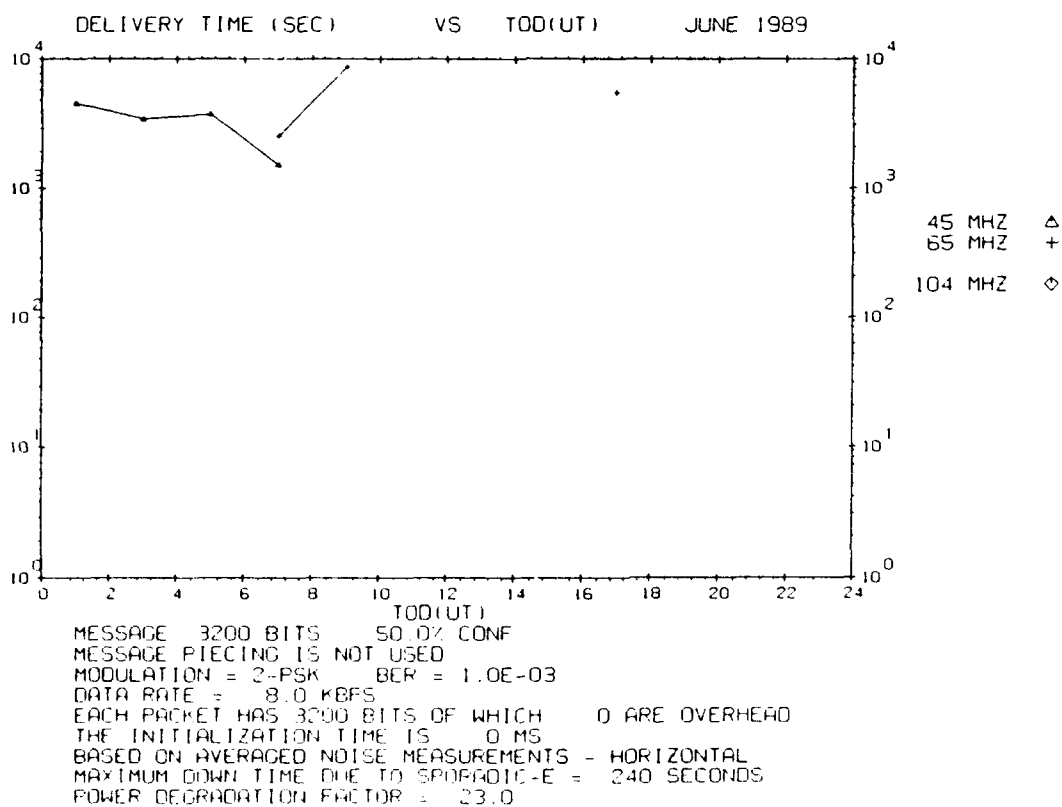
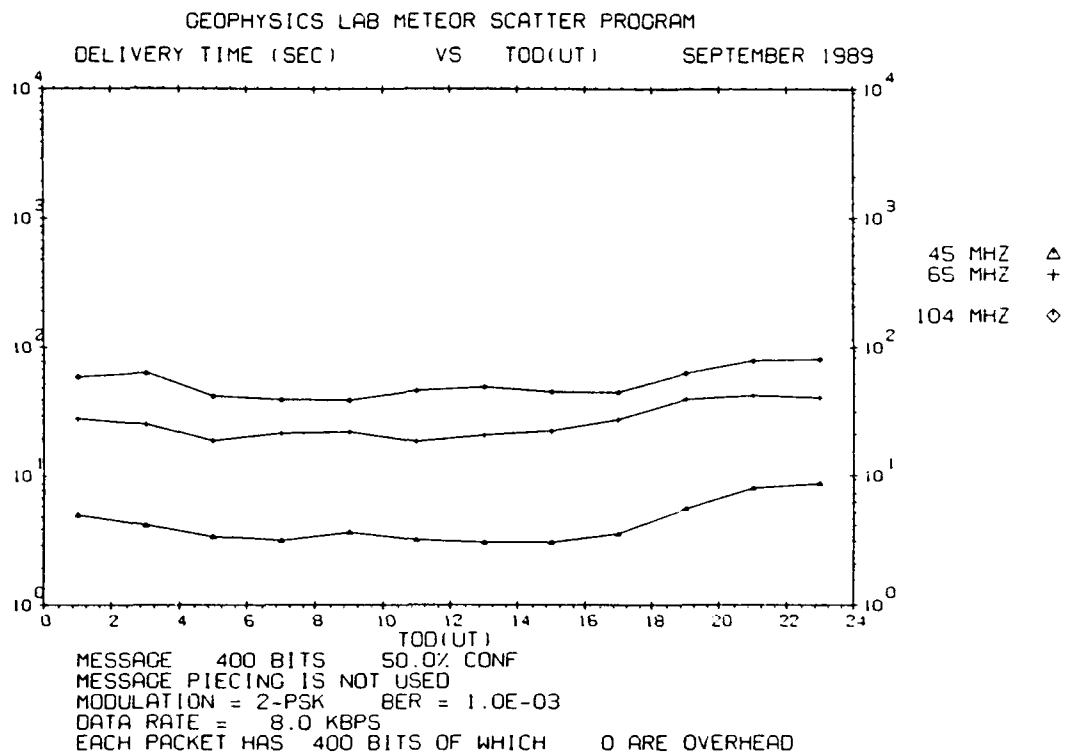
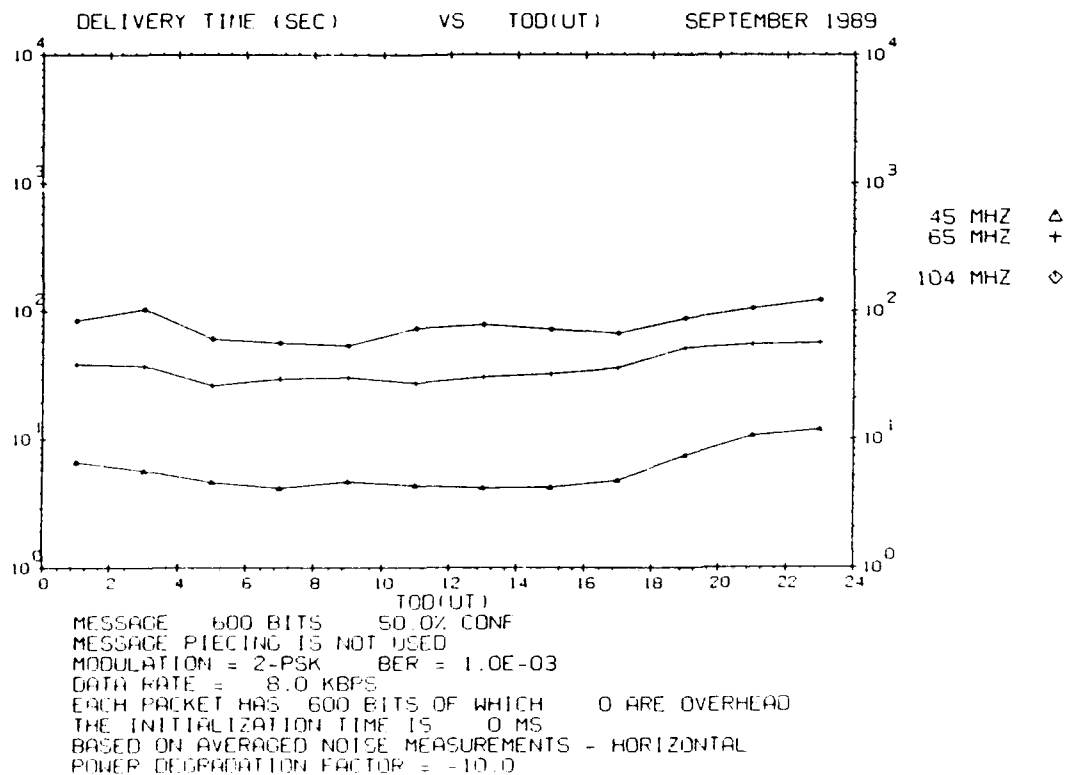


Figure E90. Same as Figure E85 but for Trails of 400 msec



**Figure E91. Waiting Time vs Time of Day for Trails of 50 msec Duration for September 1989. The transmitter power is 10,000 W**



**Figure E92. Same as Figure E91 but for Trails of 75 msec**

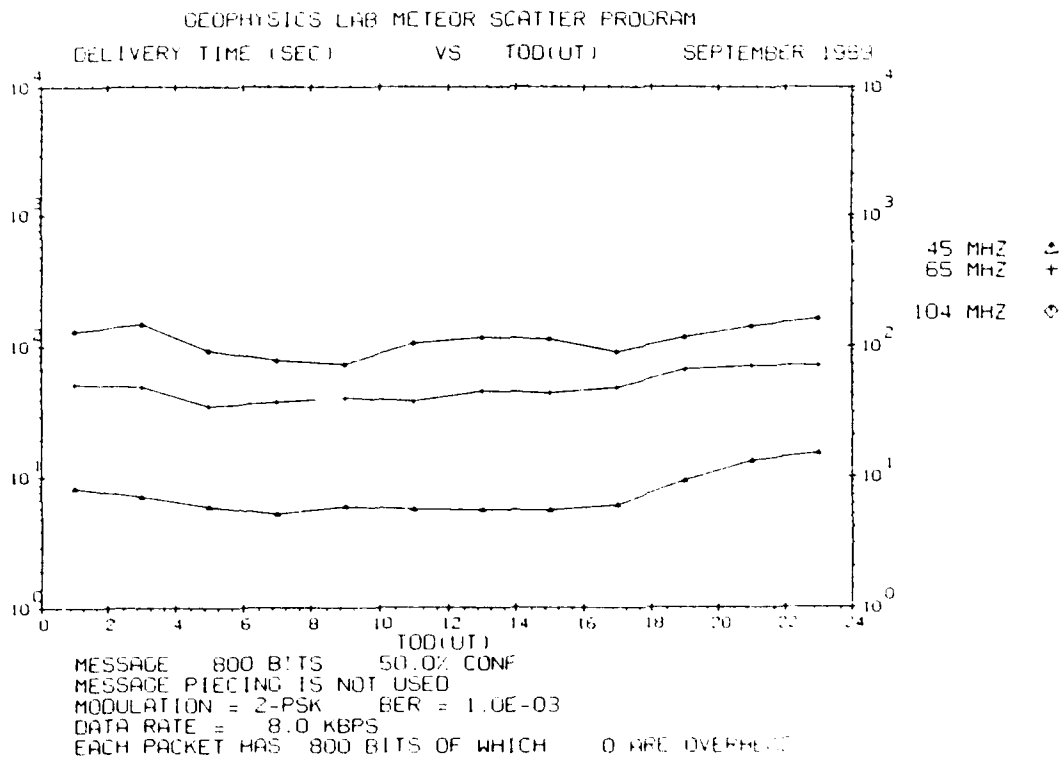


Figure E93. Same as Figure E91 but for Trails of 100 msec

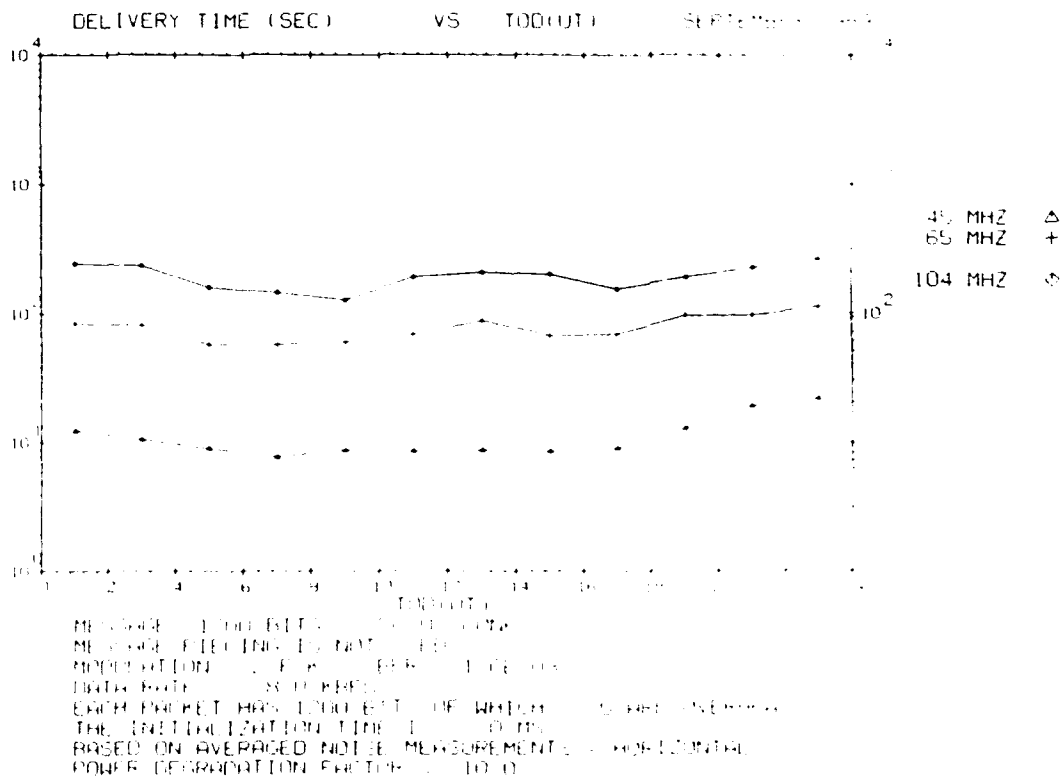
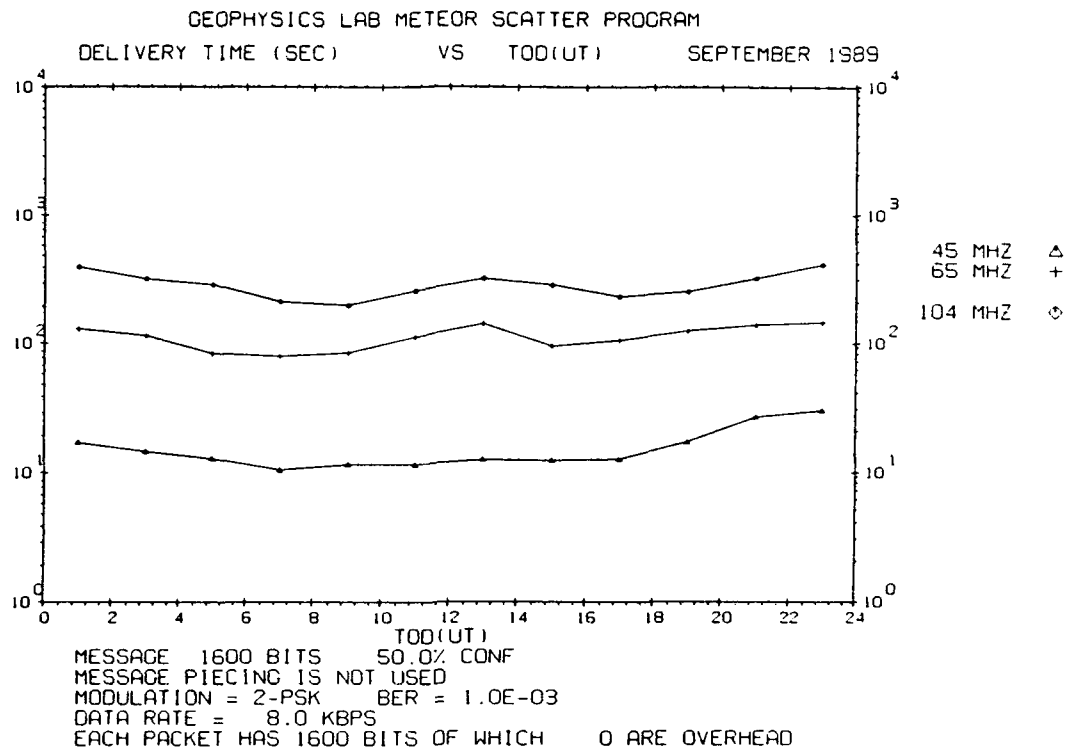
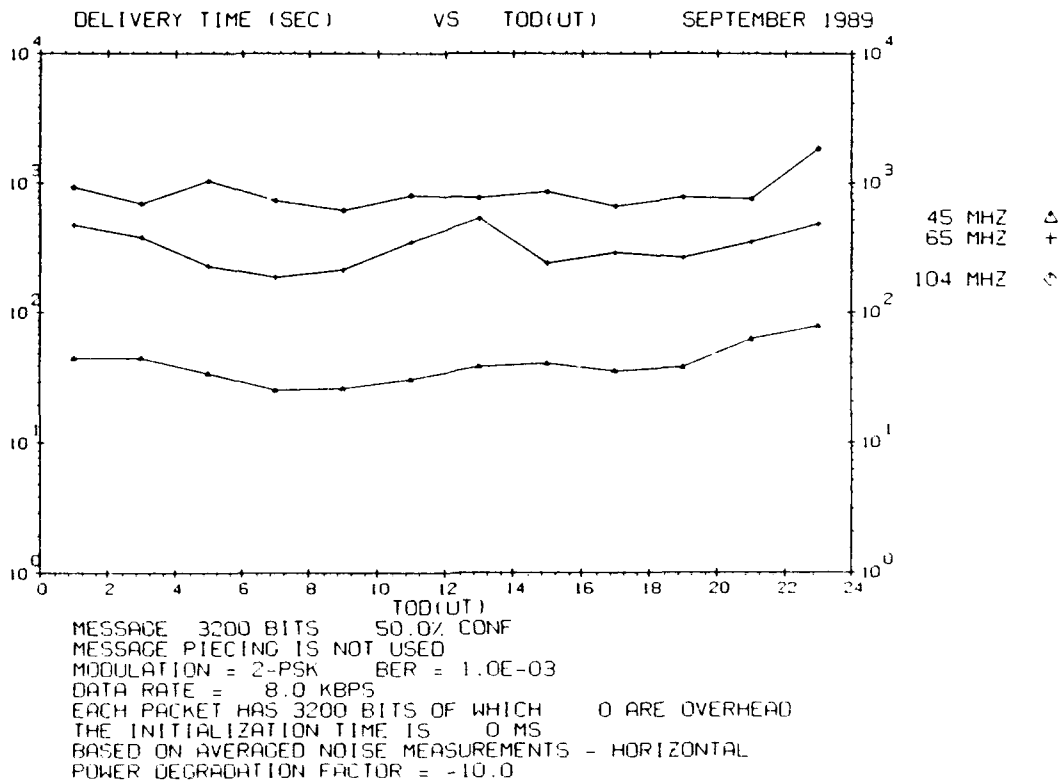


Figure E94. Same as Figure E91 but for Trails of 150 msec



**Figure E95.** Same as Figure E91 but for Trails of 200 msec



**Figure E96.** Same as Figure E91 but for Trails of 400 msec

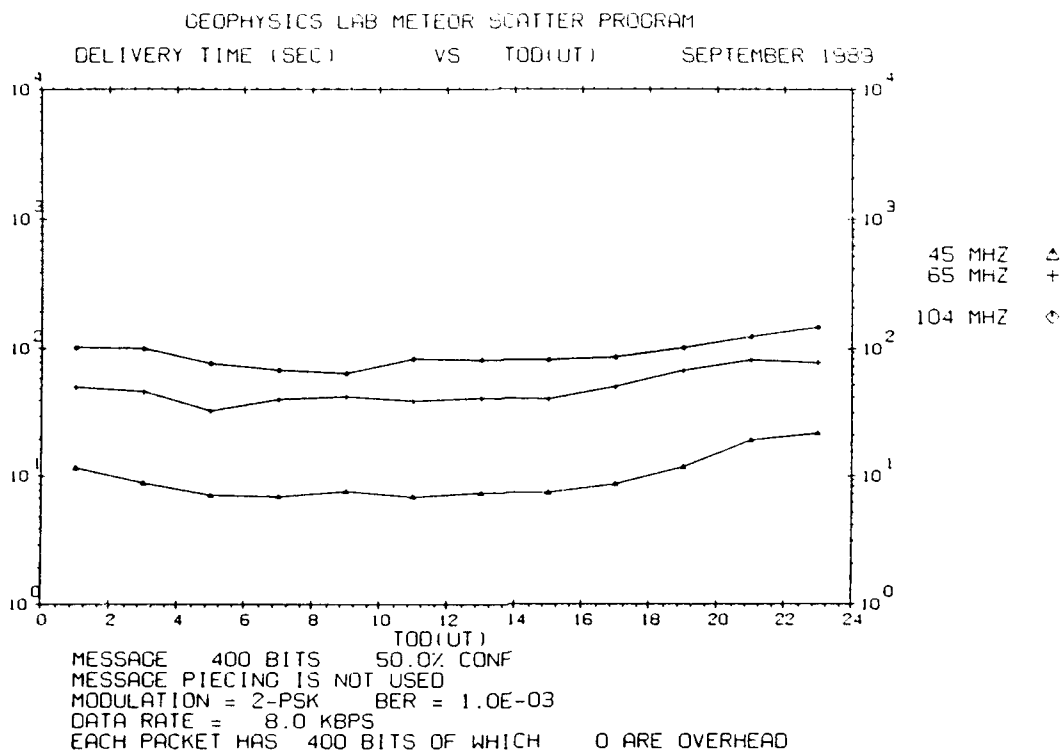


**Figure E97. Waiting Time vs Time of Day for Trails of 50 msec Duration for September 1989. The transmitter power is 1,000 W**

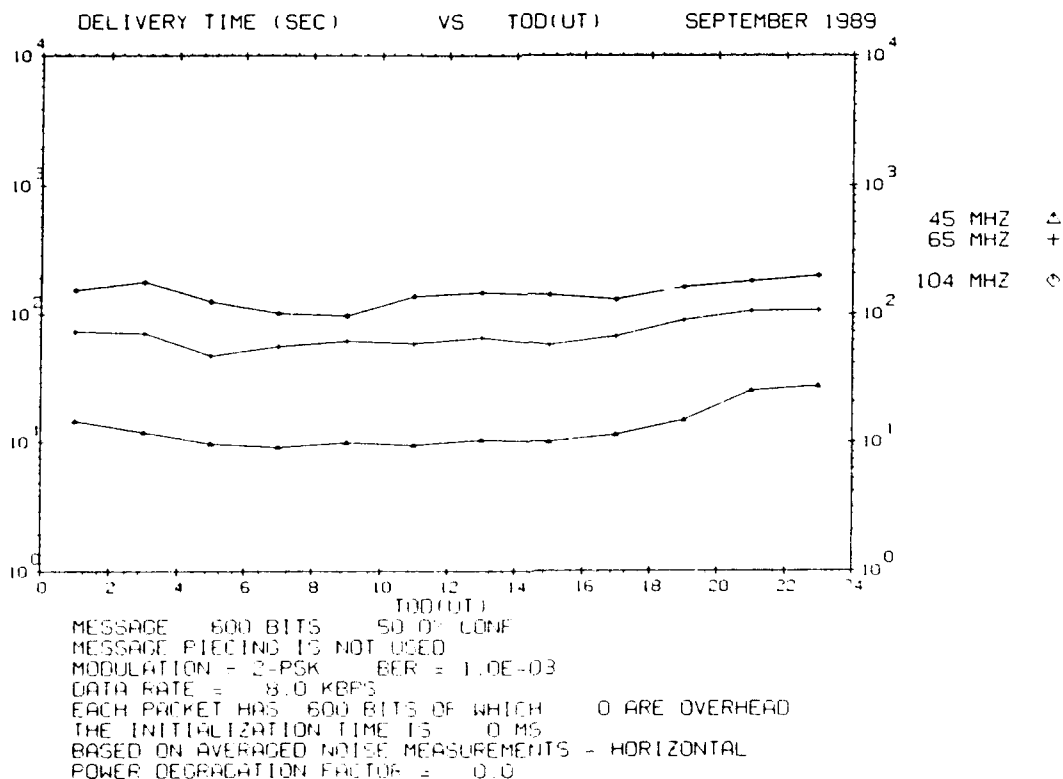


**Figure E98. Same as Figure E97 but for Trails of 75 msec**



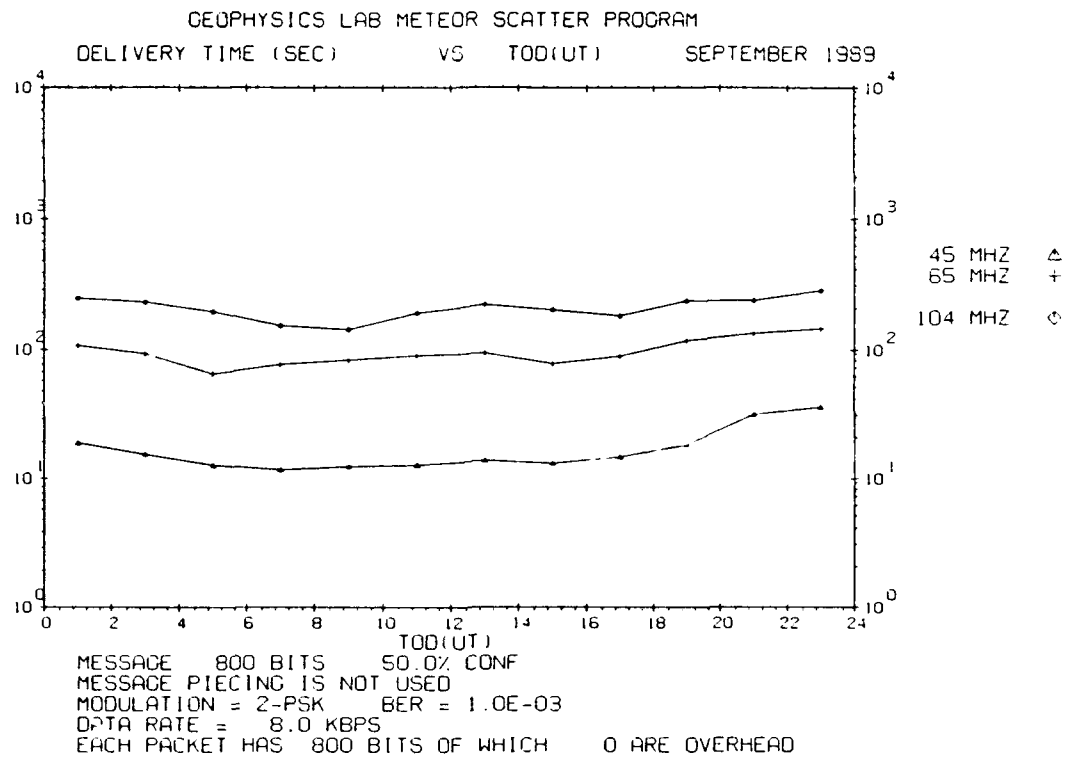


Figure E99. Same as Figure E97 but for Trails of 100 msec

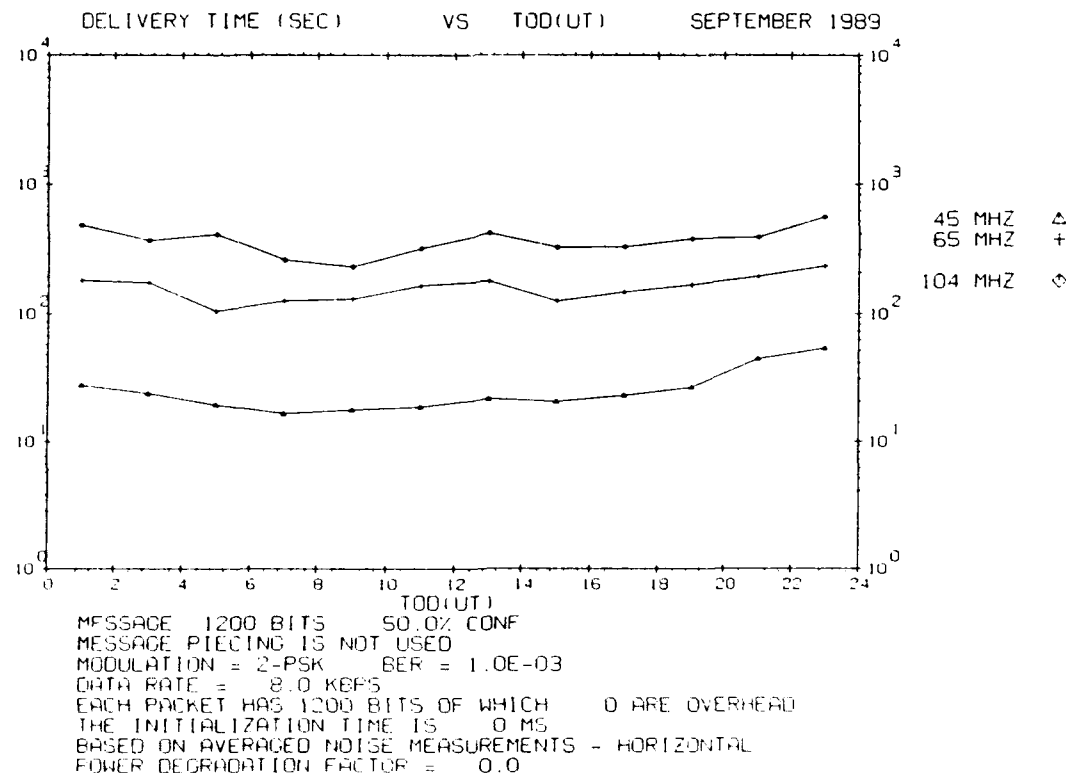


Figure E100. Same as Figure E97 but for Trails of 150 msec

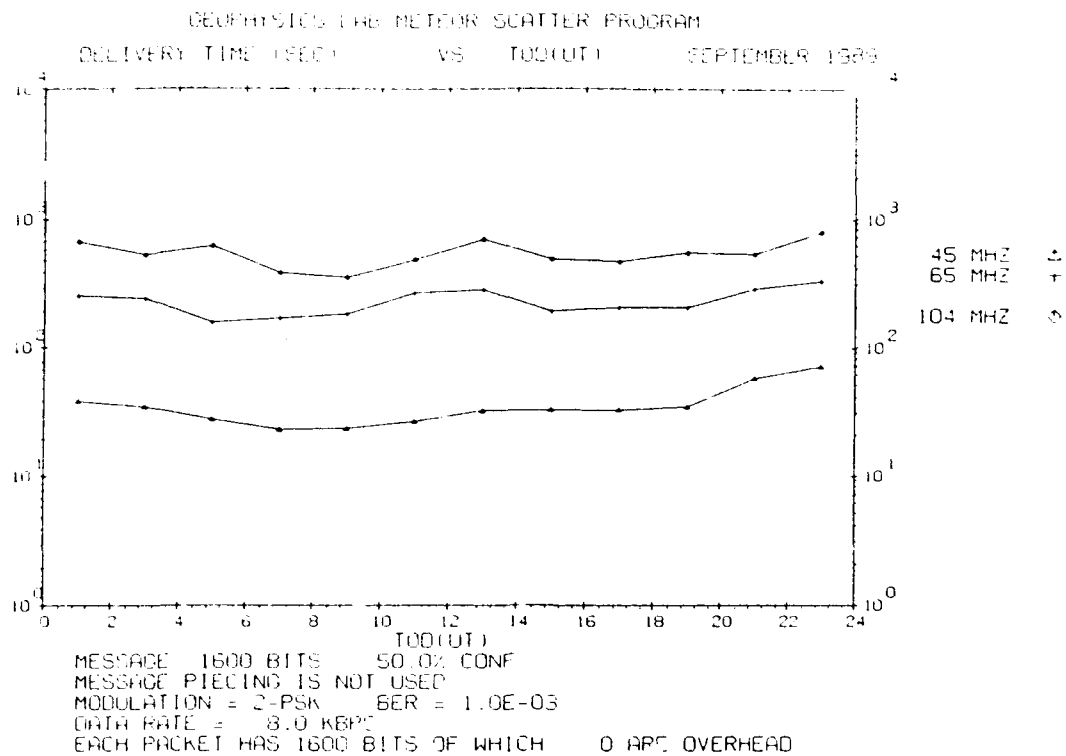


Figure E101. Same as Figure E97 but for Trails of 200 msec

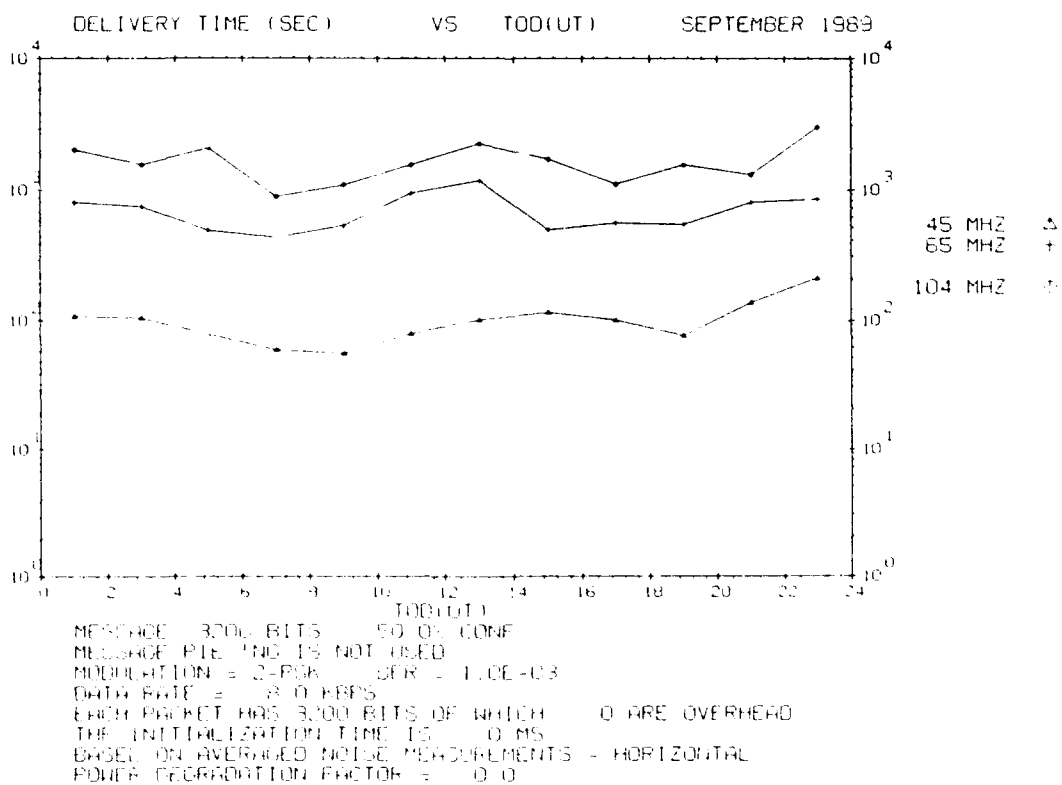
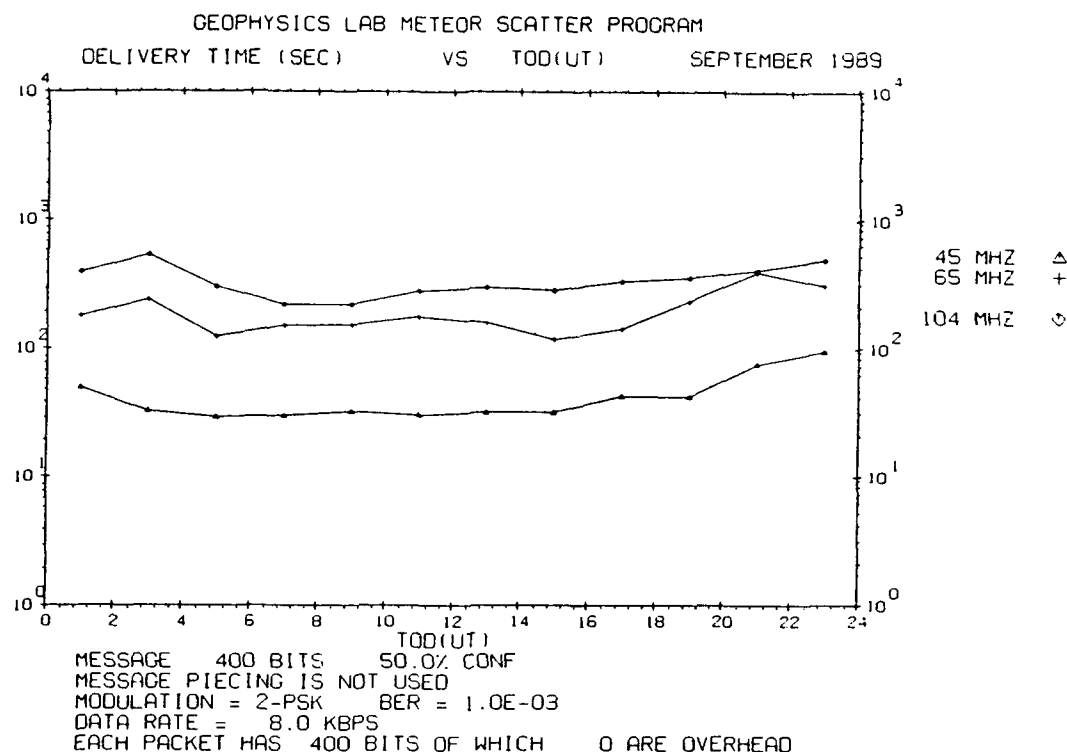
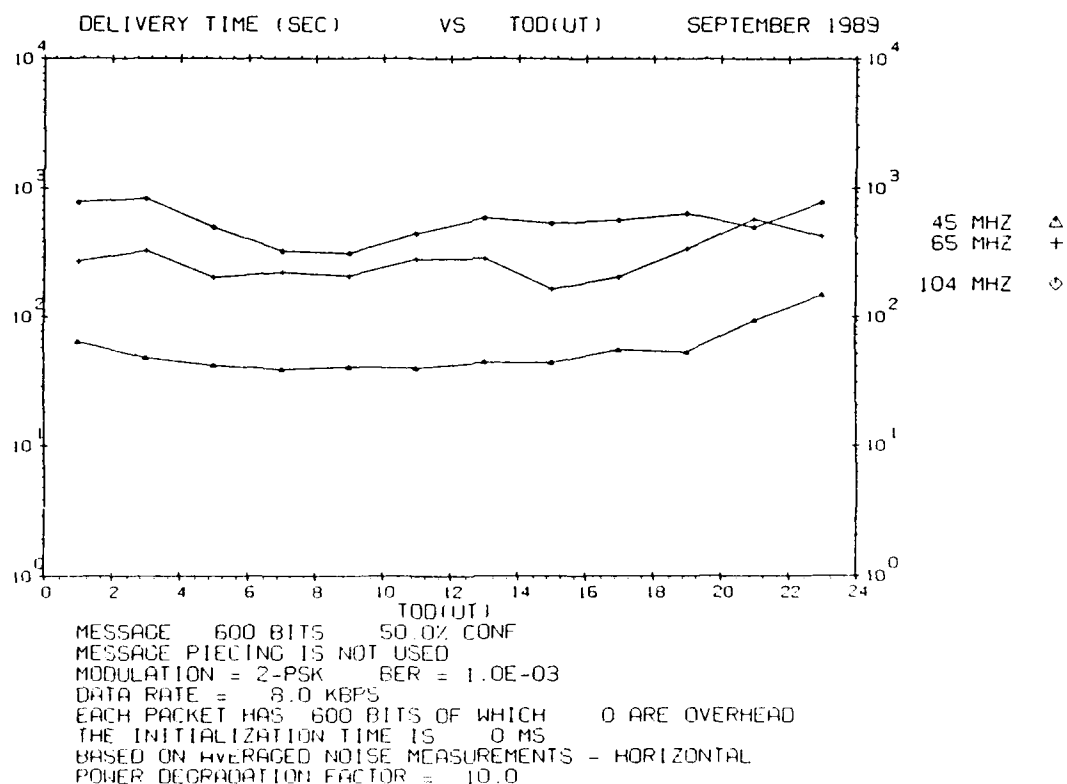


Figure E102. Same as Figure E97 but for Trails of 400 msec



**Figure E103. Waiting Time vs Time of Day for Trails of 50 msec Duration for September 1989. The transmitter power is 100 W**



**Figure E104. Same as Figure E103 but for Trails of 75 msec**

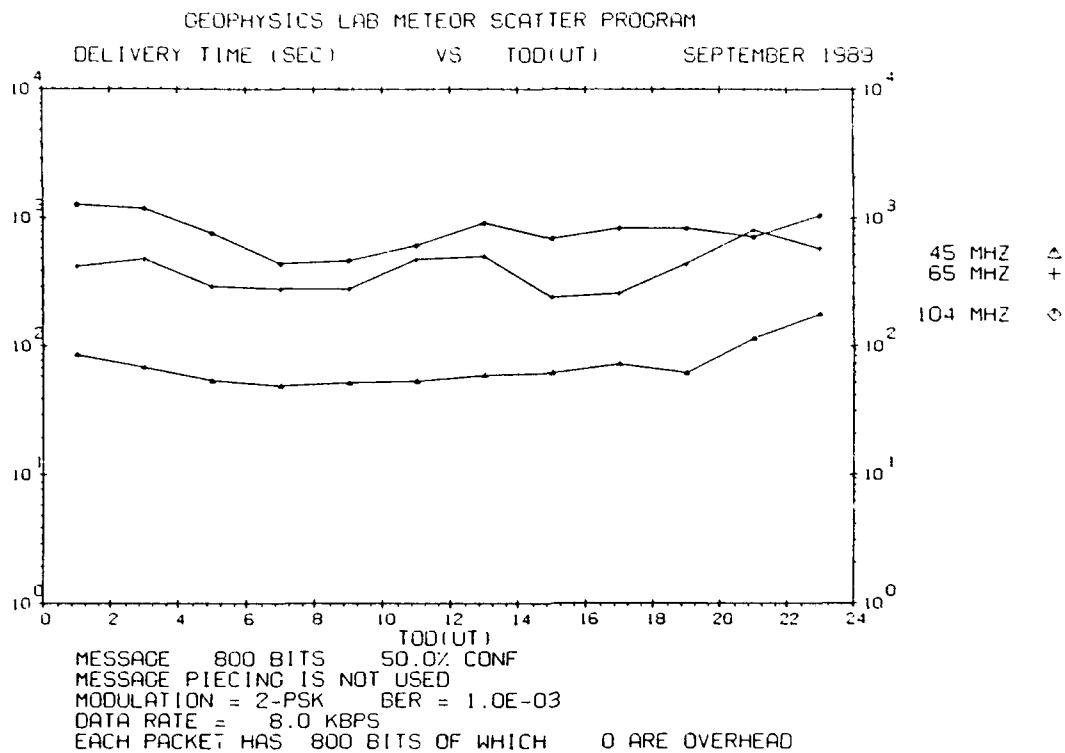


Figure E105. Same as Figure E103 but for Trails of 100 msec

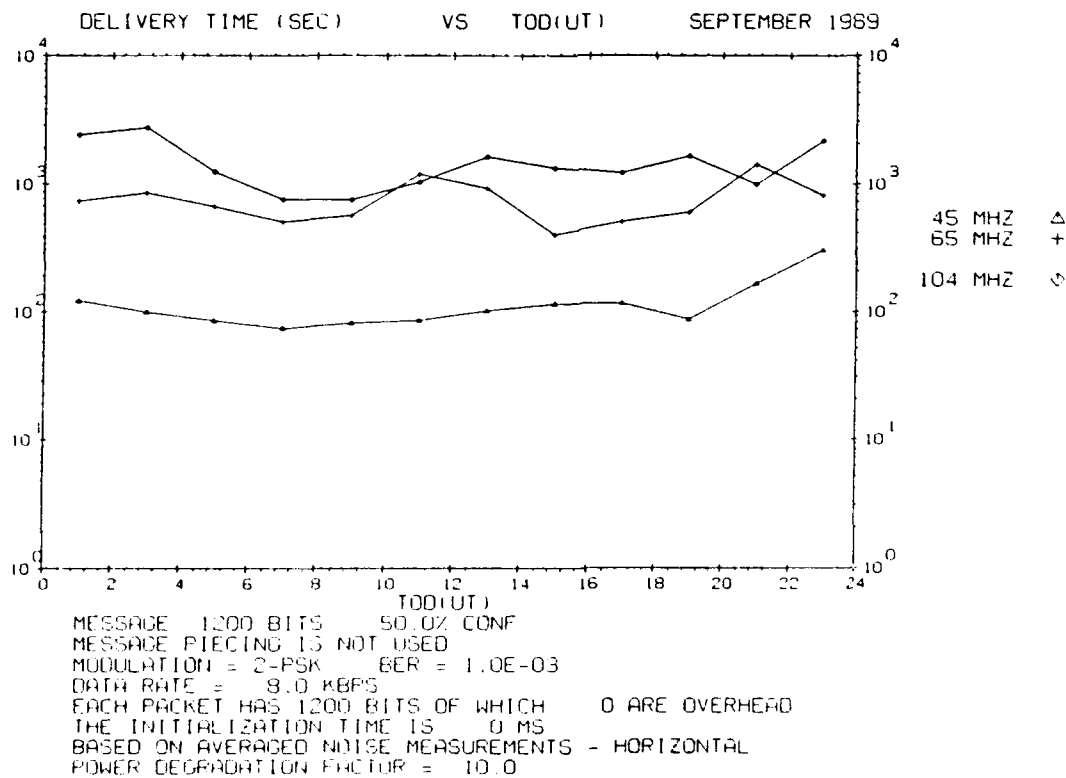


Figure E106. Same as Figure E103 but for Trails of 150 msec

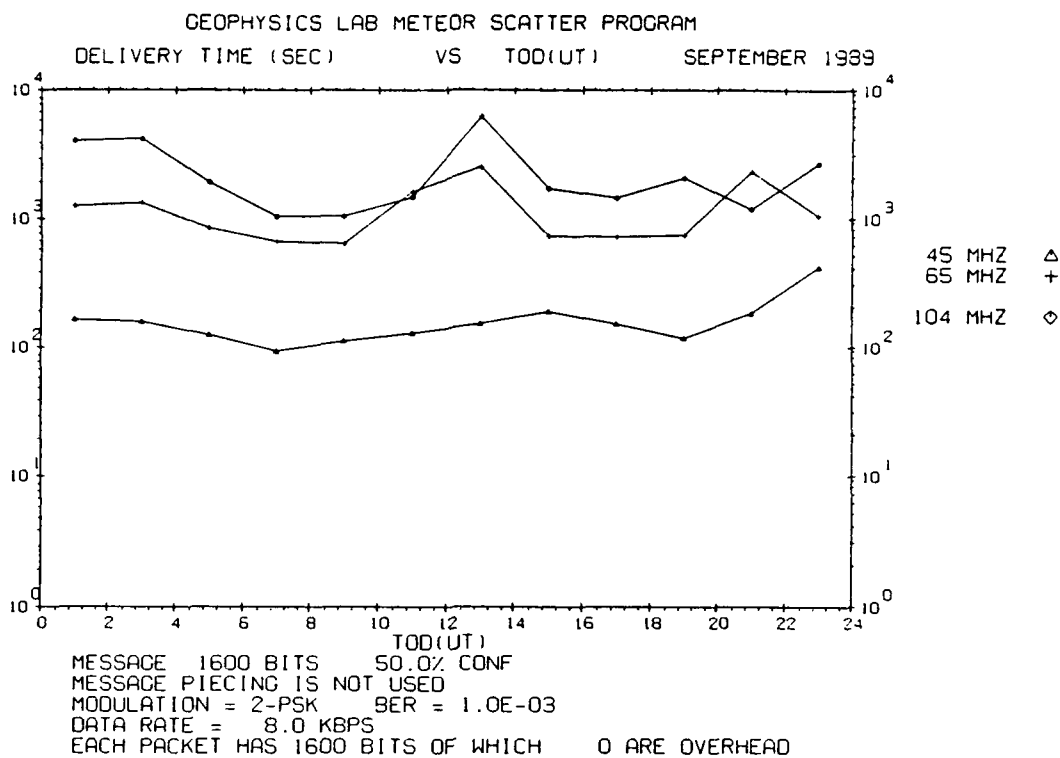


Figure E107. Same as Figure E103 but for Trails of 200 msec

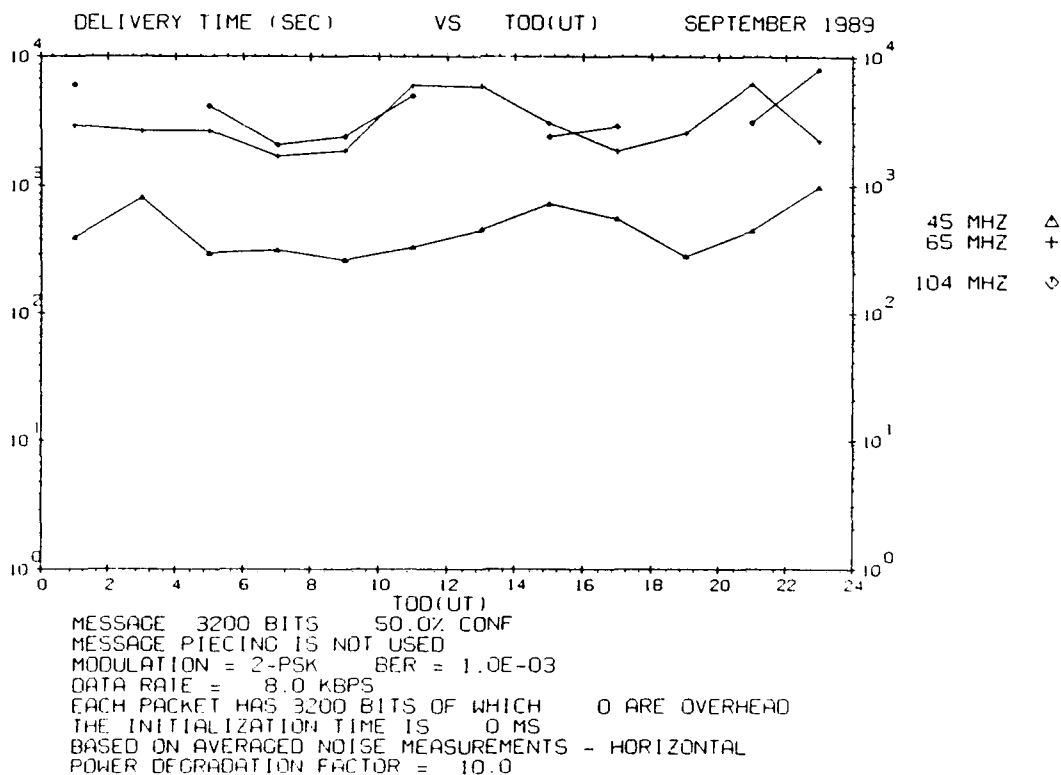
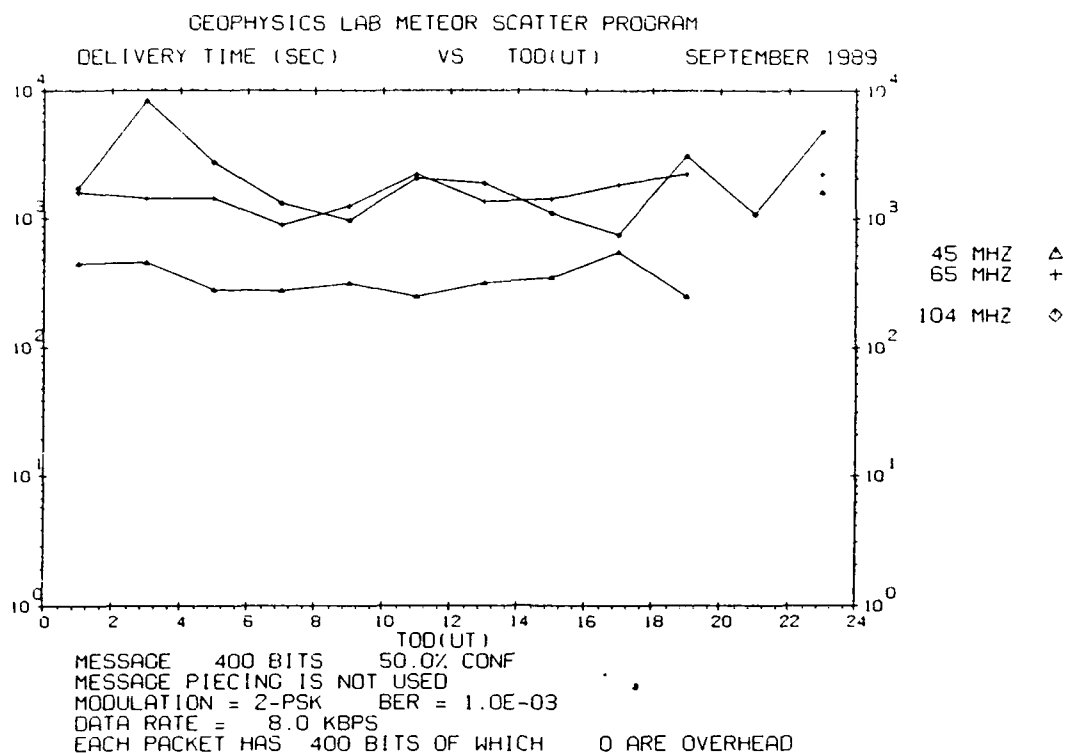
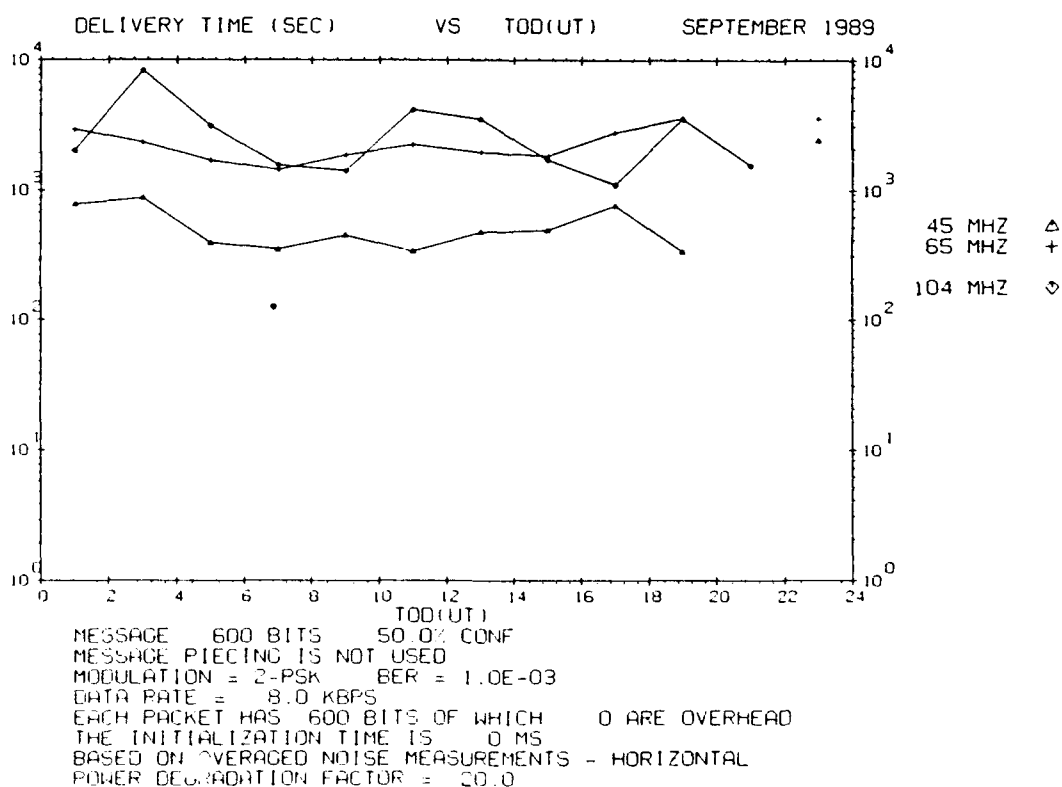


Figure E108. Same as Figure E103 but for Trails of 400 msec



**Figures E109. Waiting Time vs Time of Day for Trails of 50 msec Duration for September 1989. The transmitter power is 10 W**



**Figure E110. Same as Figure E109 but for Trails of 75 msec**

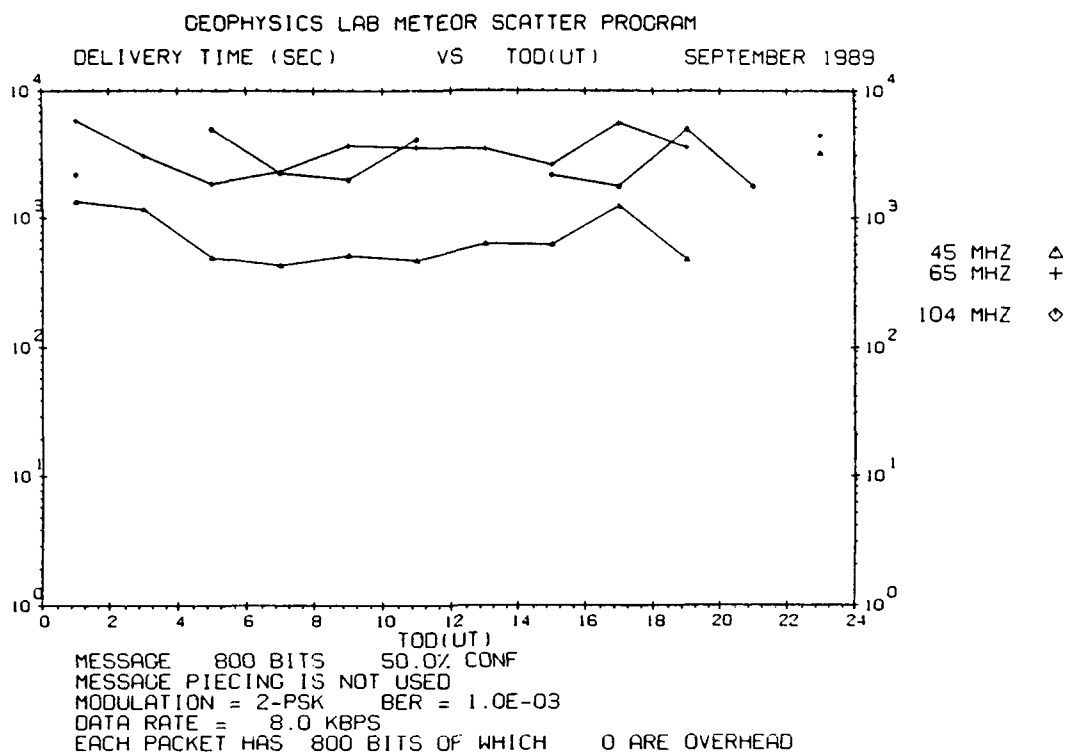


**Figure E111.** Same as Figure E109 but for Trails of 100 msec

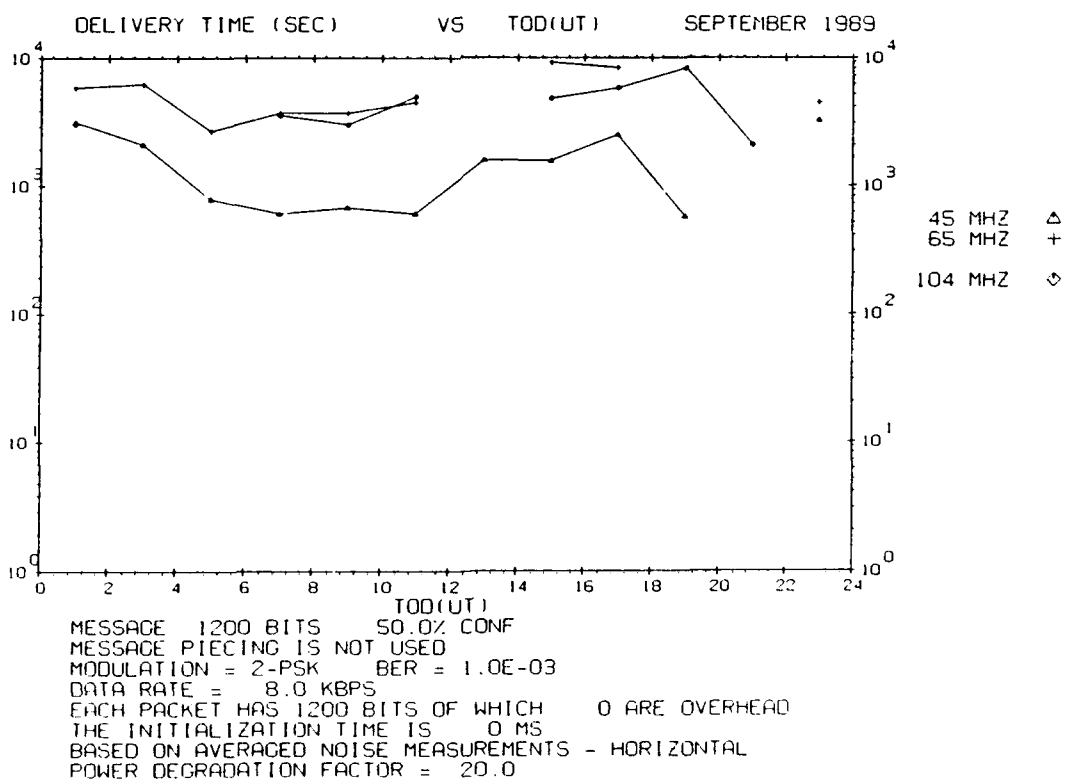


**Figure E112.** Same as Figure E109 but for Trails of 150 msec

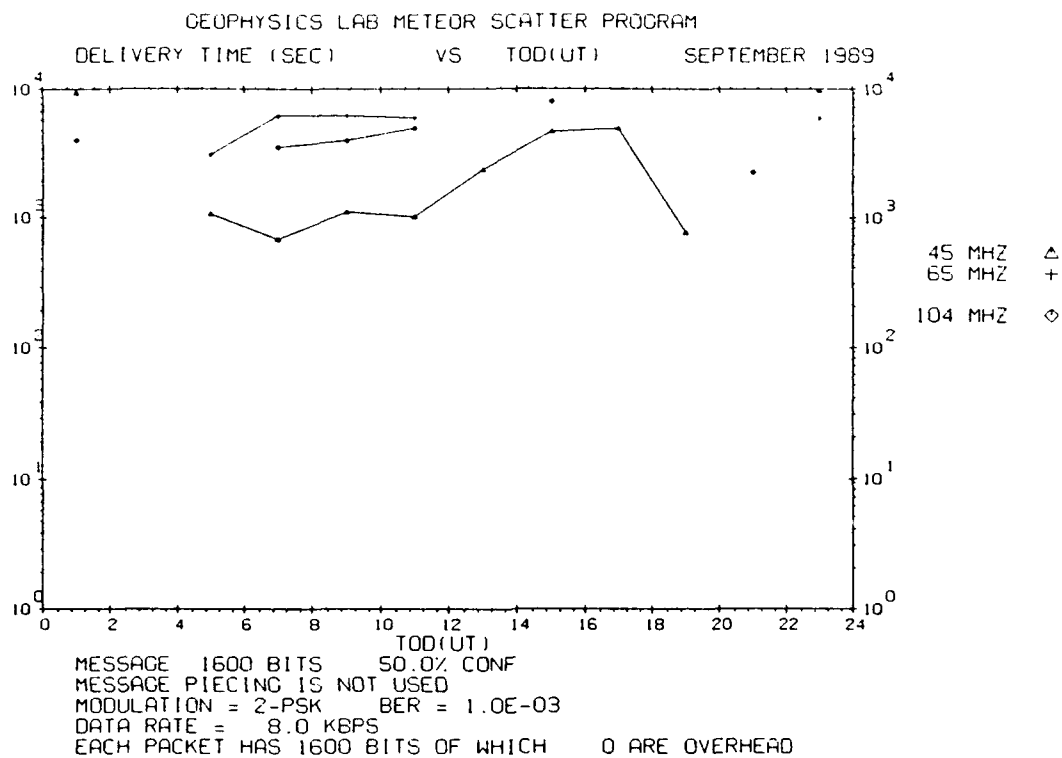


Figure E113. Same as Figure E109 but for Trails of 200 msec

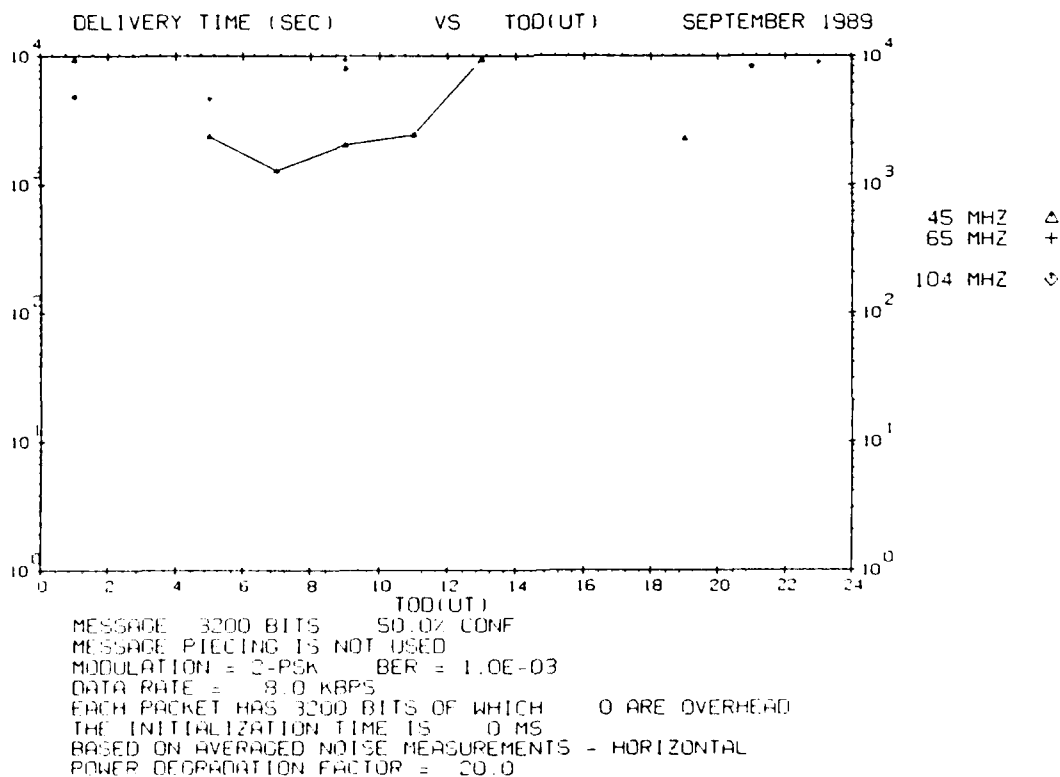
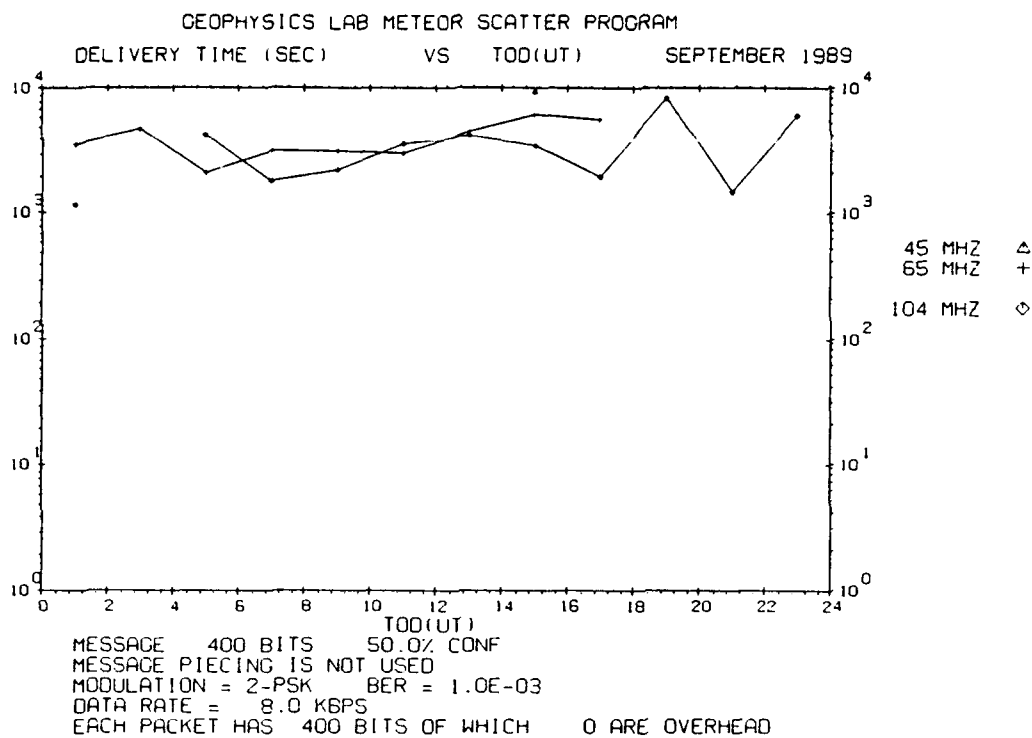
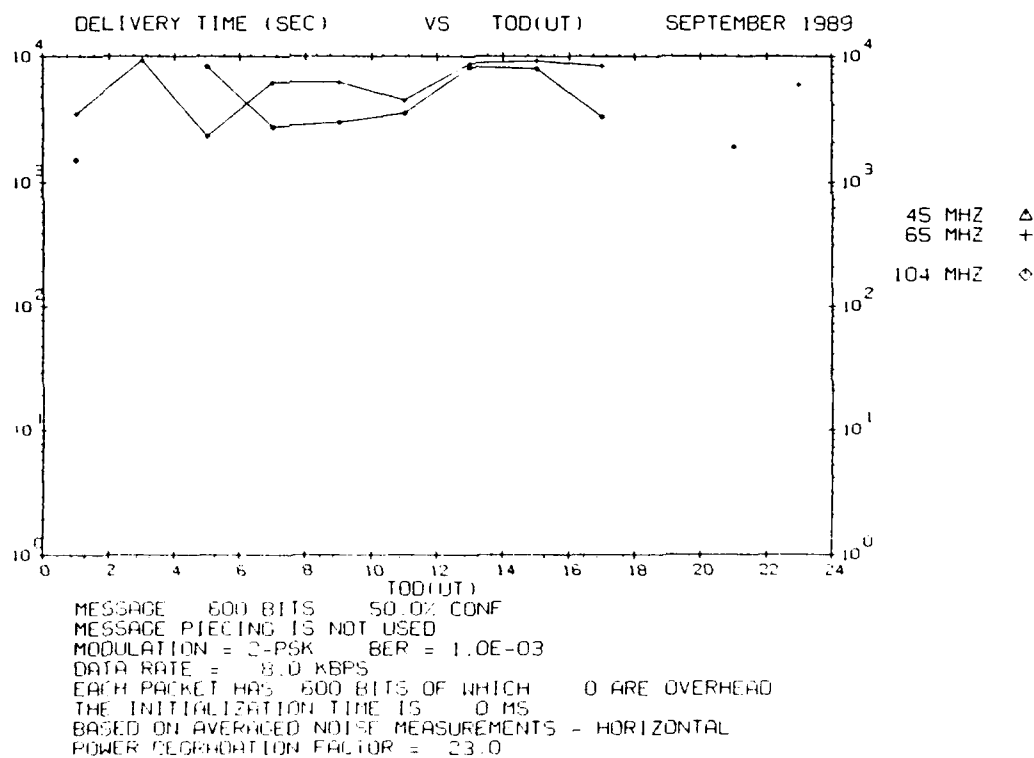


Figure E114. Same as Figure E109 but for Trails of 400 msec





**Figure E115. Waiting Time vs Time of Day for Trails of 50 msec Duration for September 1989. The transmitter power is 5 W**



**Figure E116. Same as Figure E115 but for Trails of 75 msec**

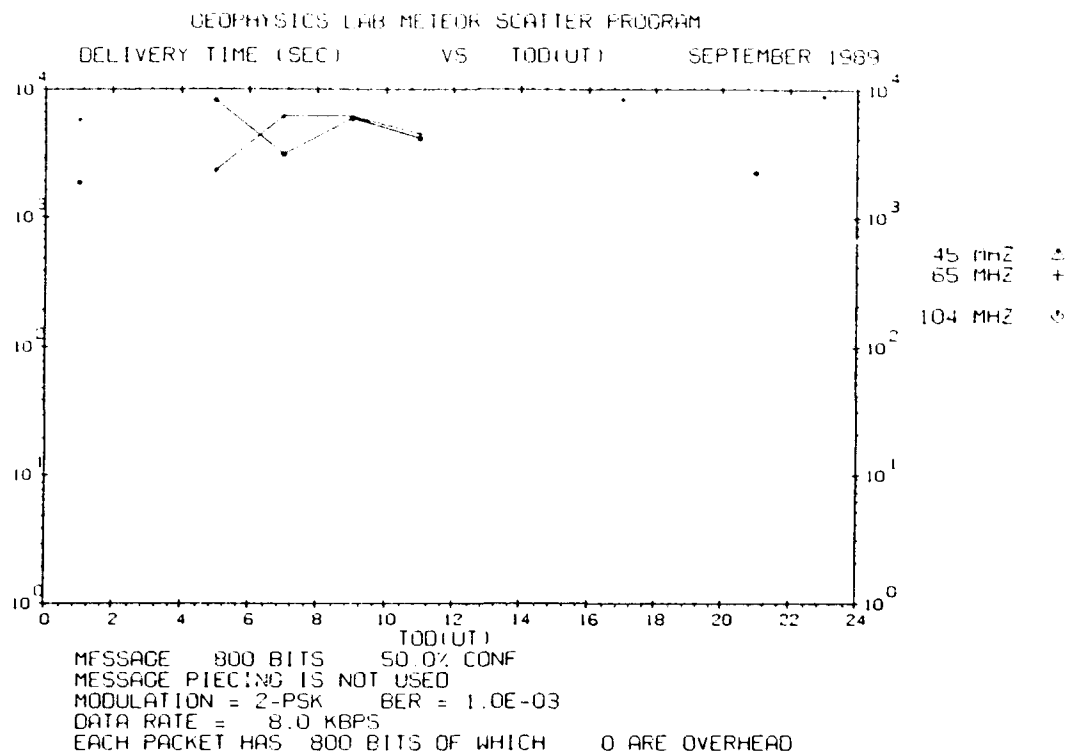


Figure E117. Same as Figure E115 but for Trails of 100 msec

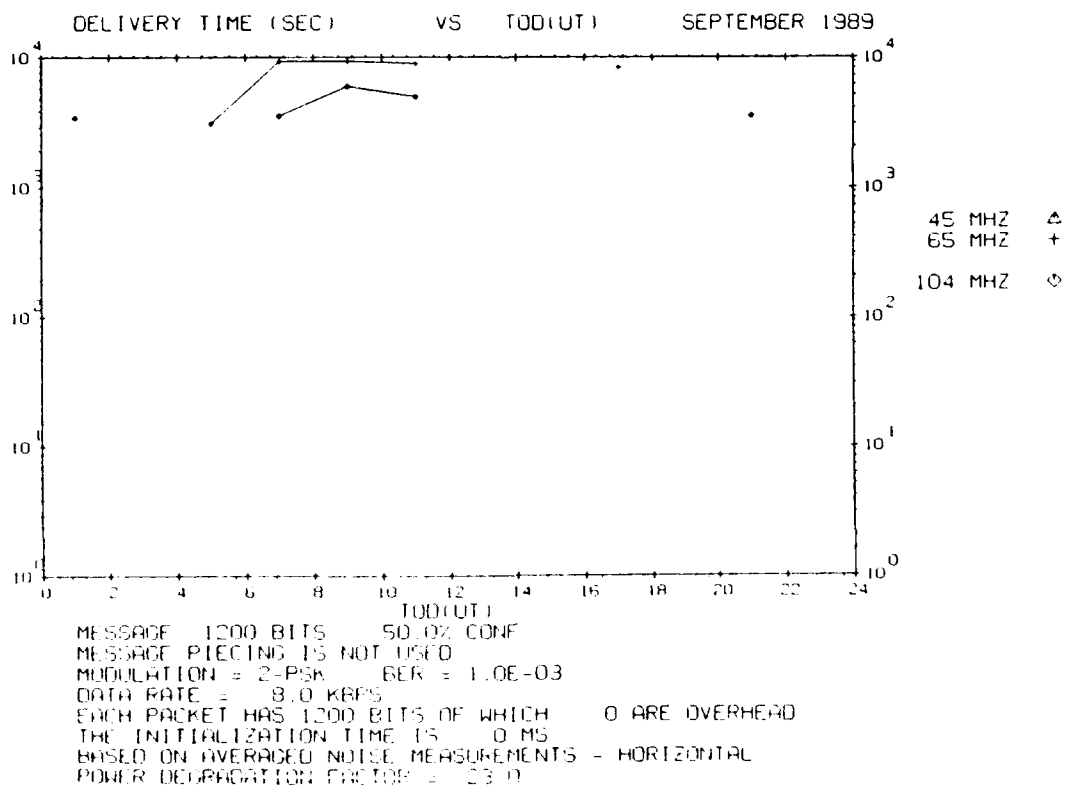


Figure E118. Same as Figure E115 but for Trails of 150 msec

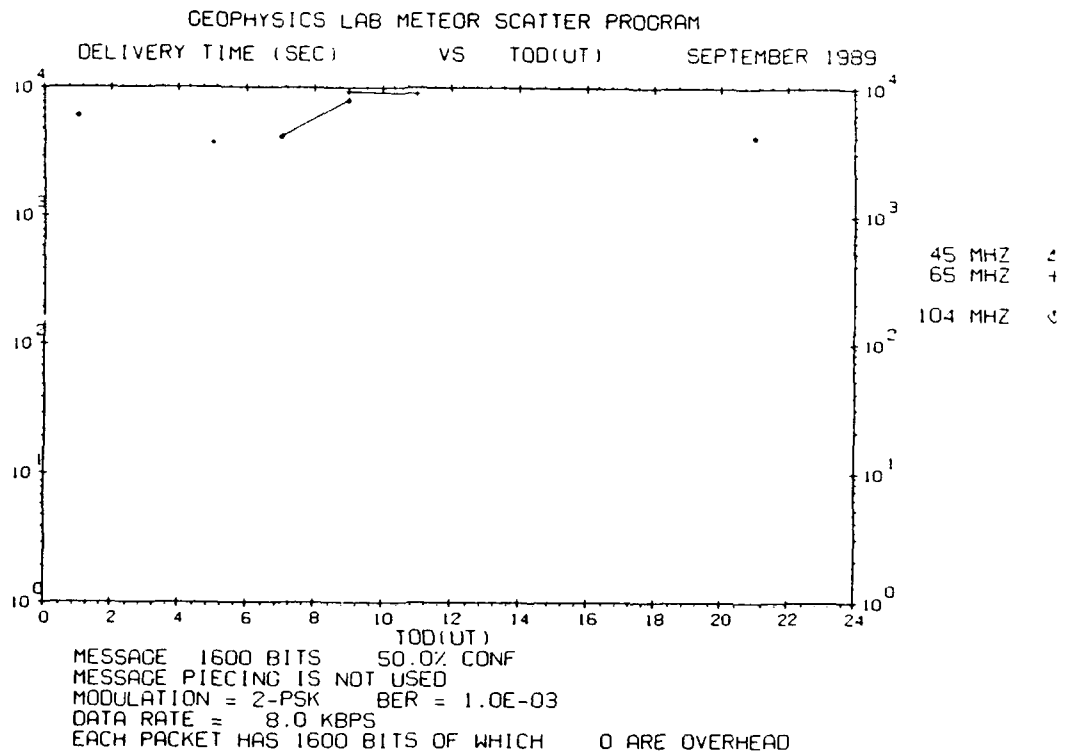


Figure E119. Same as Figure E115 but for Trails of 200 msec

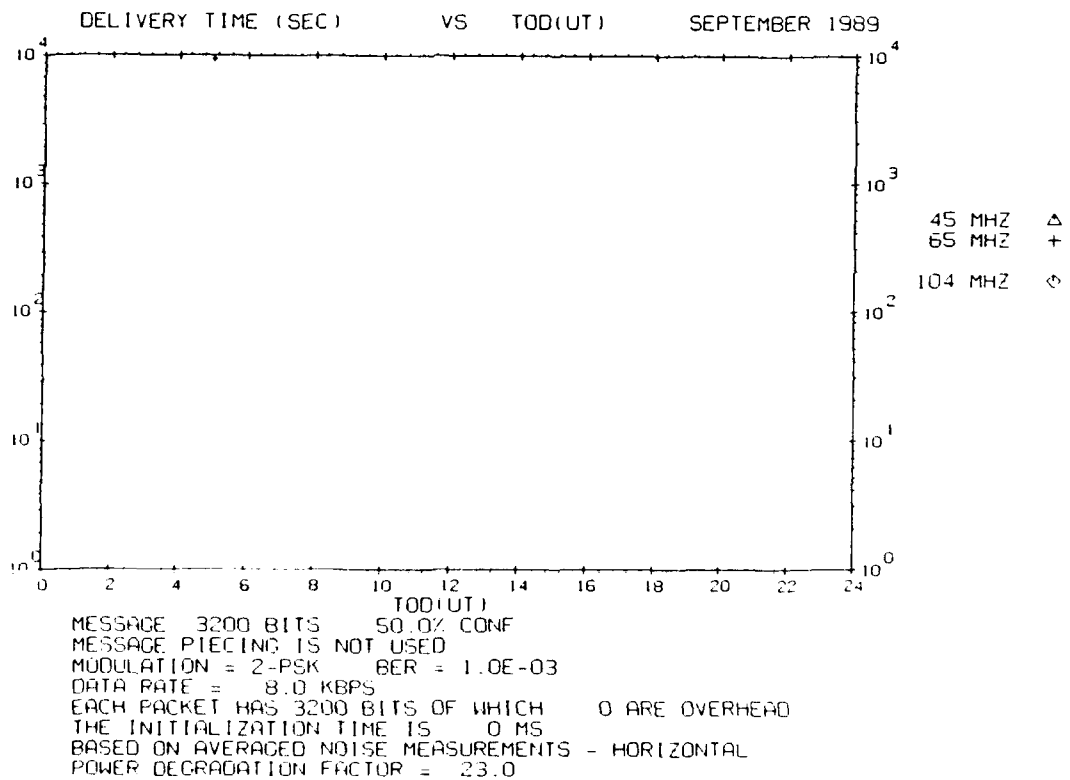
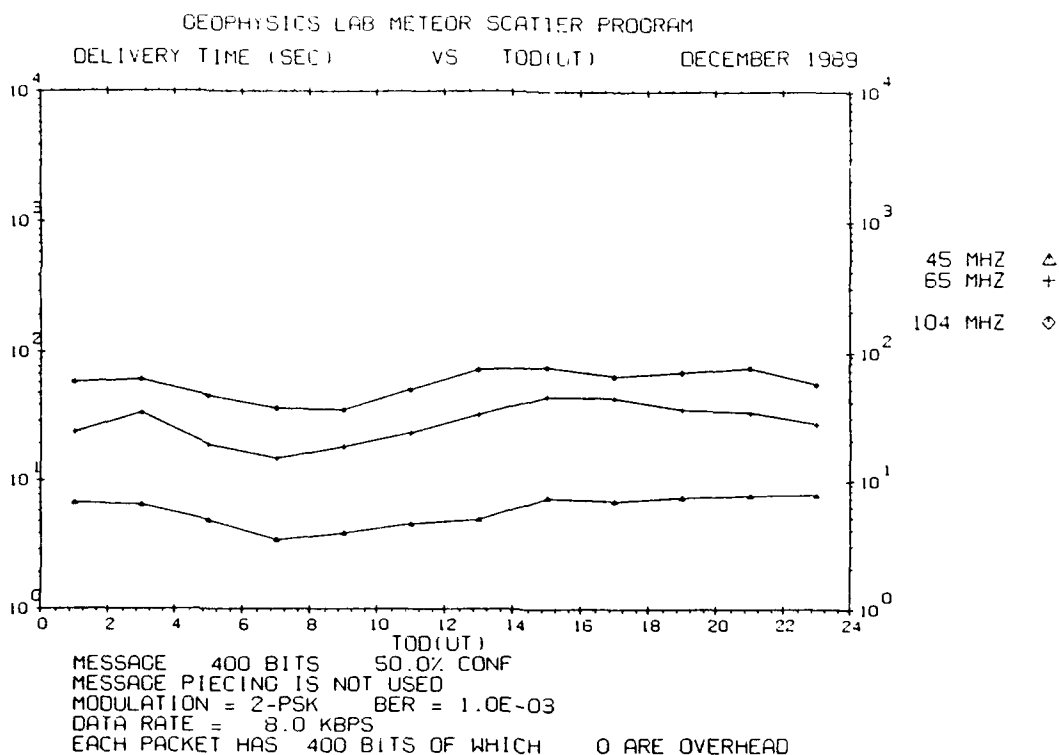
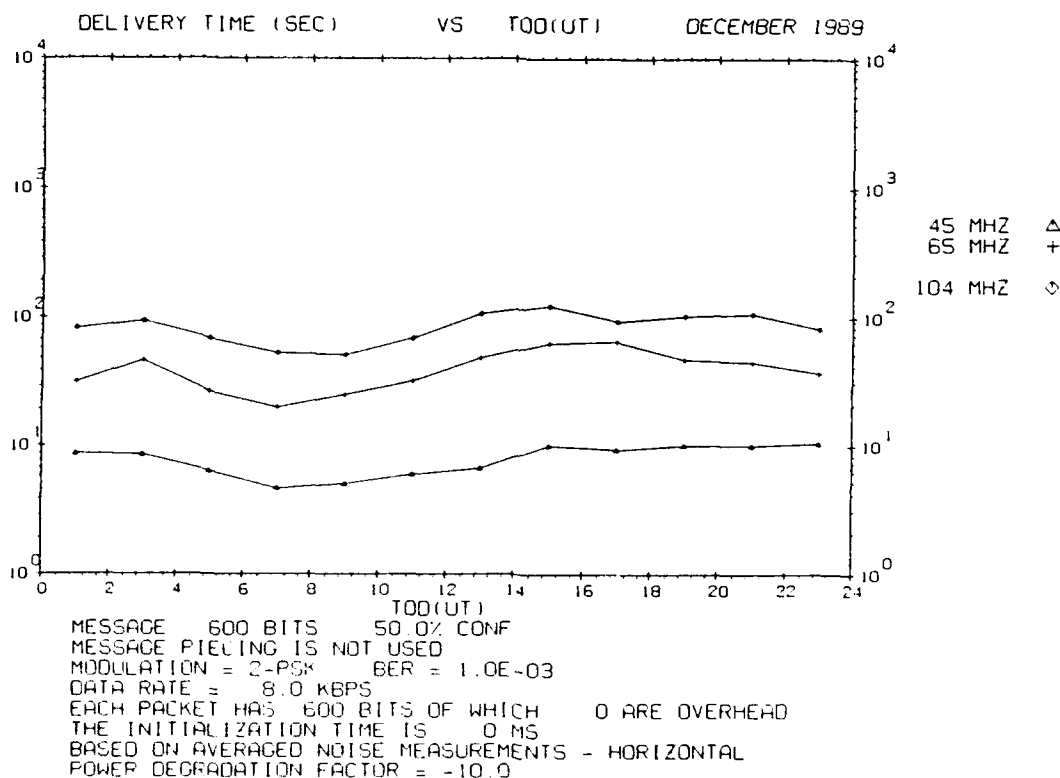


Figure E120. Same as Figure E115 but for Trails of 400 msec



**Figure E121. Waiting Time vs Time of Day for Trails of 50 msec Duration for December 1989. The transmitter power is 10,000 W**



**Figure E122. Same as Figure E121 but for Trails of 75 msec**

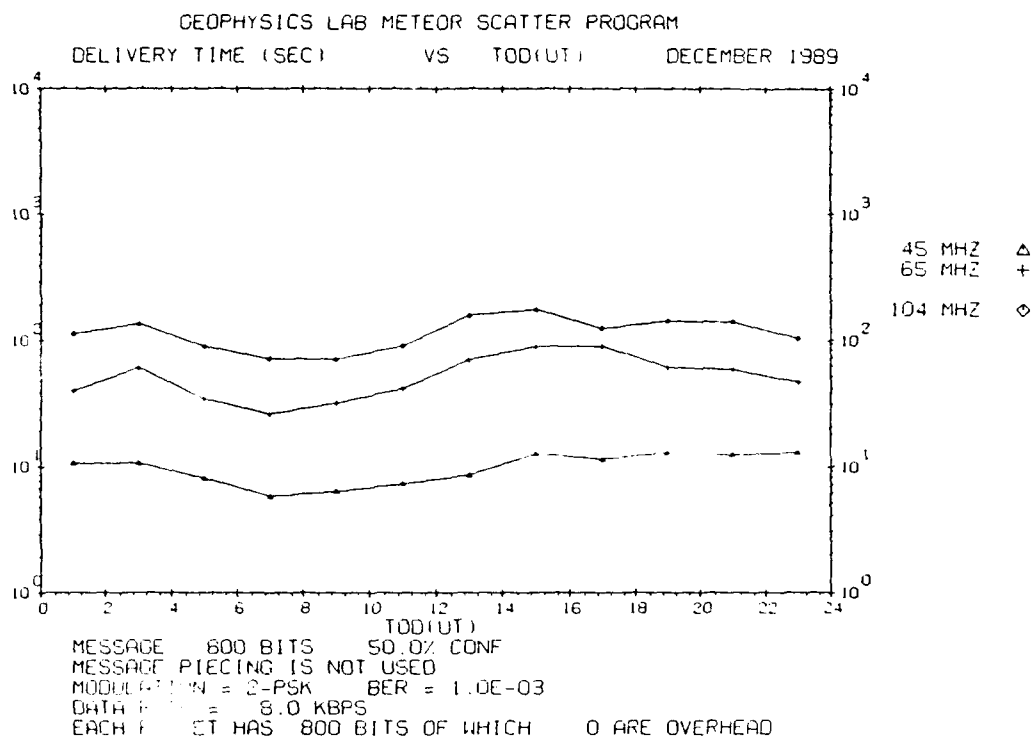


Figure E123. Same as Figure E121 but for Trails of 100 msec

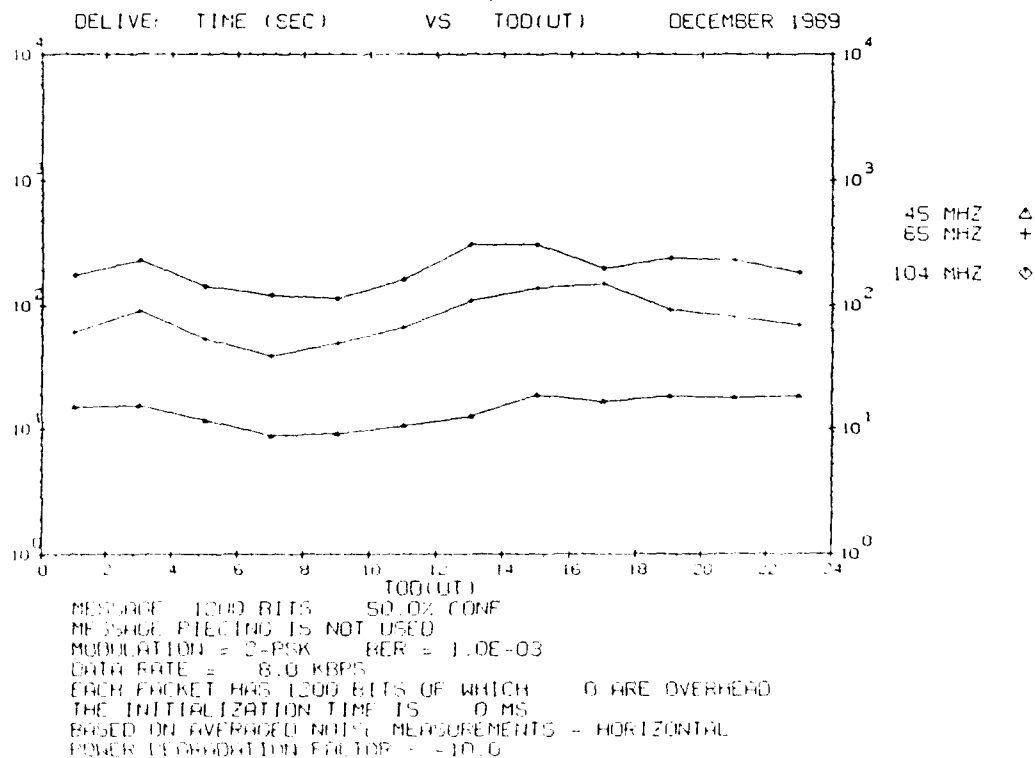


Figure E124. Same as Figure E121 but for Trails of 150 msec

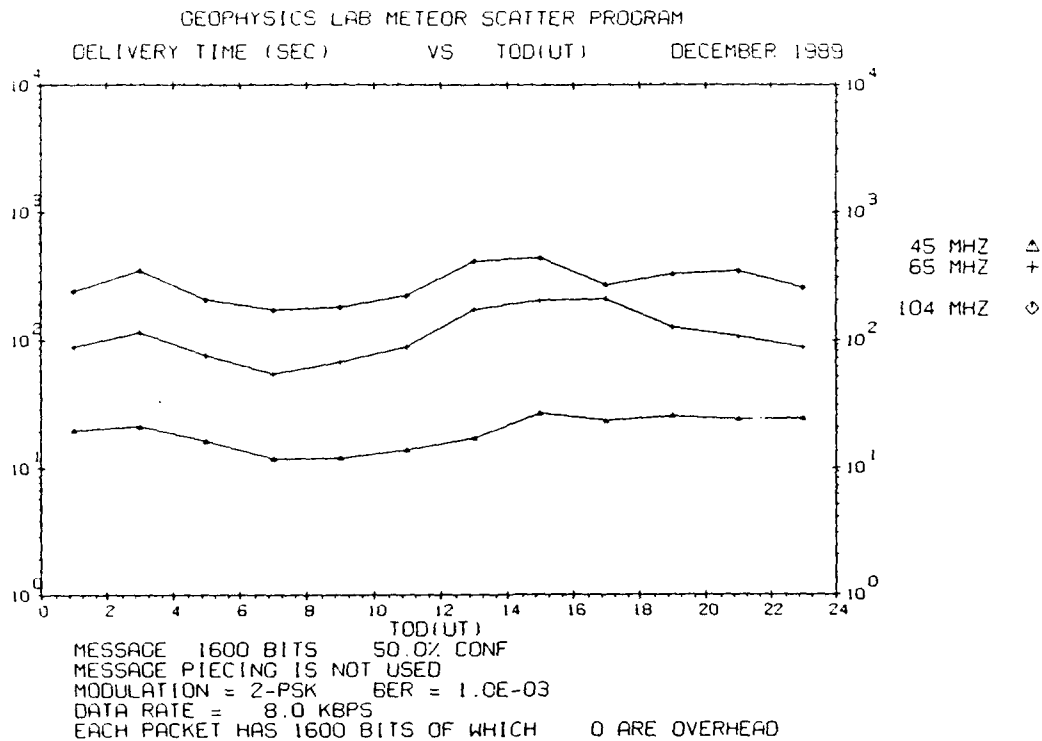


Figure E125. Same as Figure E121 but for Trails of 200 msec

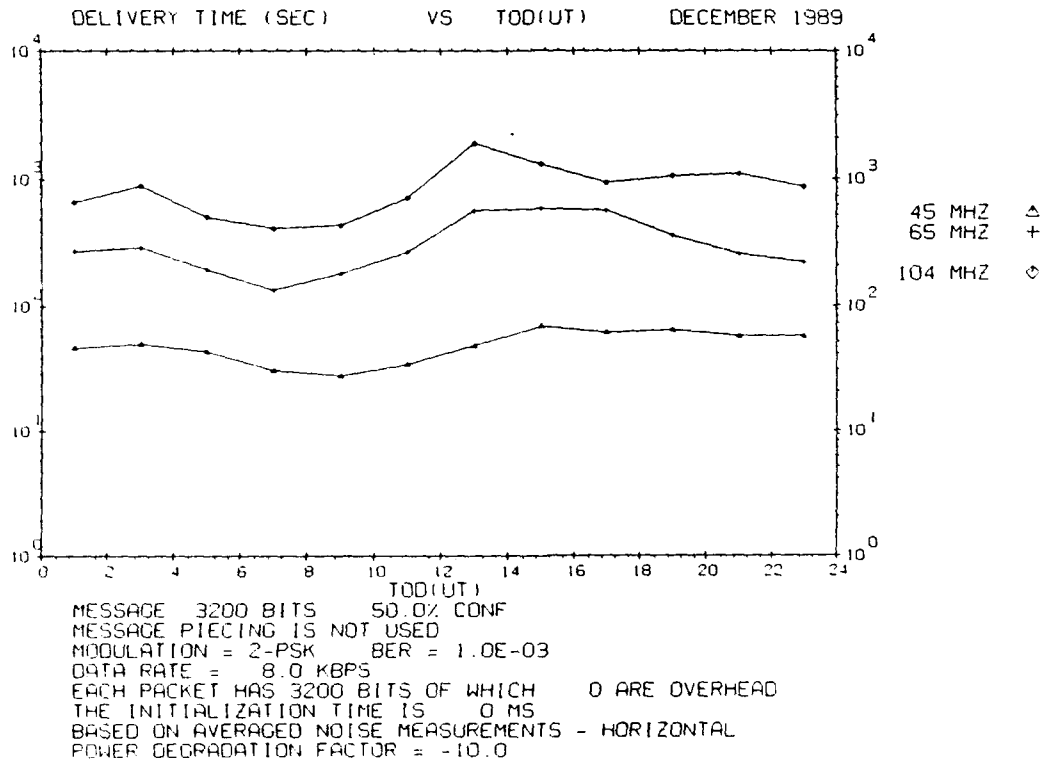
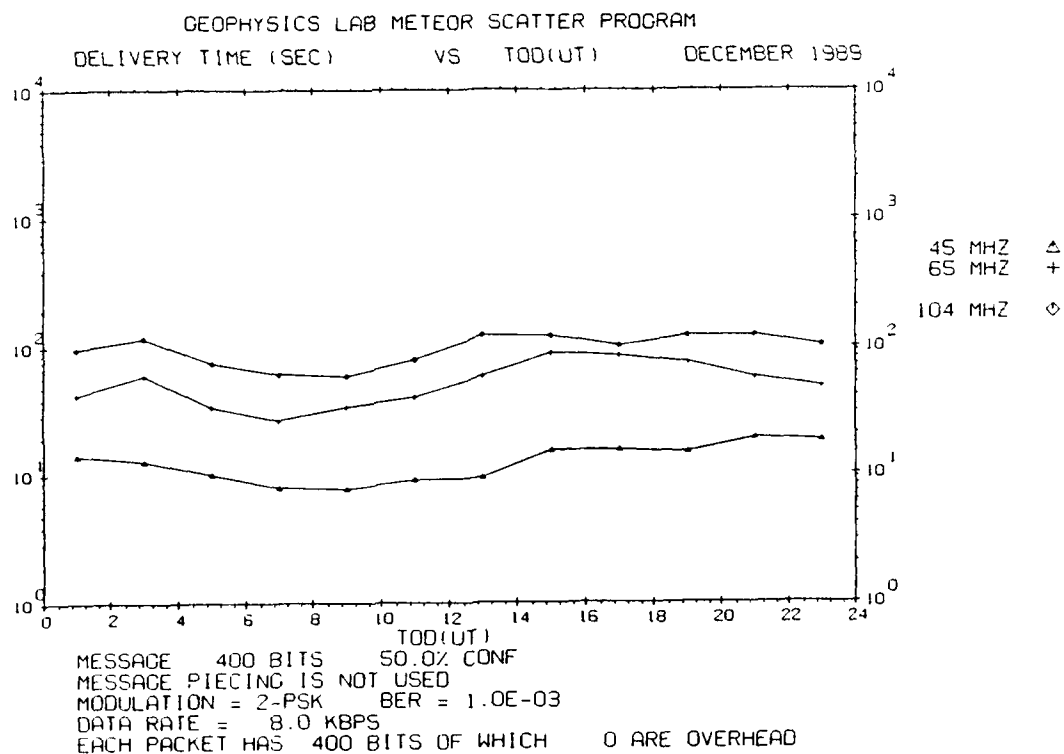
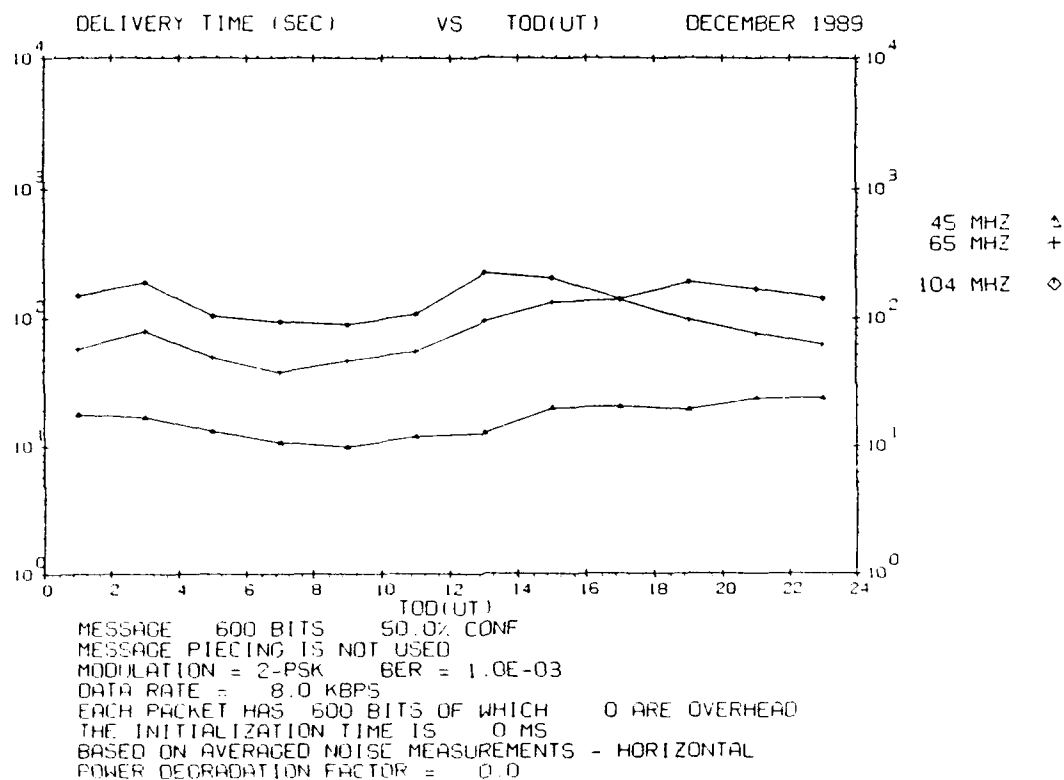


Figure E126. Same as Figure E121 but for Trails of 400 msec



**Figure E127. Waiting Time vs Time of Day for Trails of 50 msec Duration for December 1989. The transmitter power is 1,000 W**



**Figure E128. Same as Figure E127 but for Trails of 75 msec**

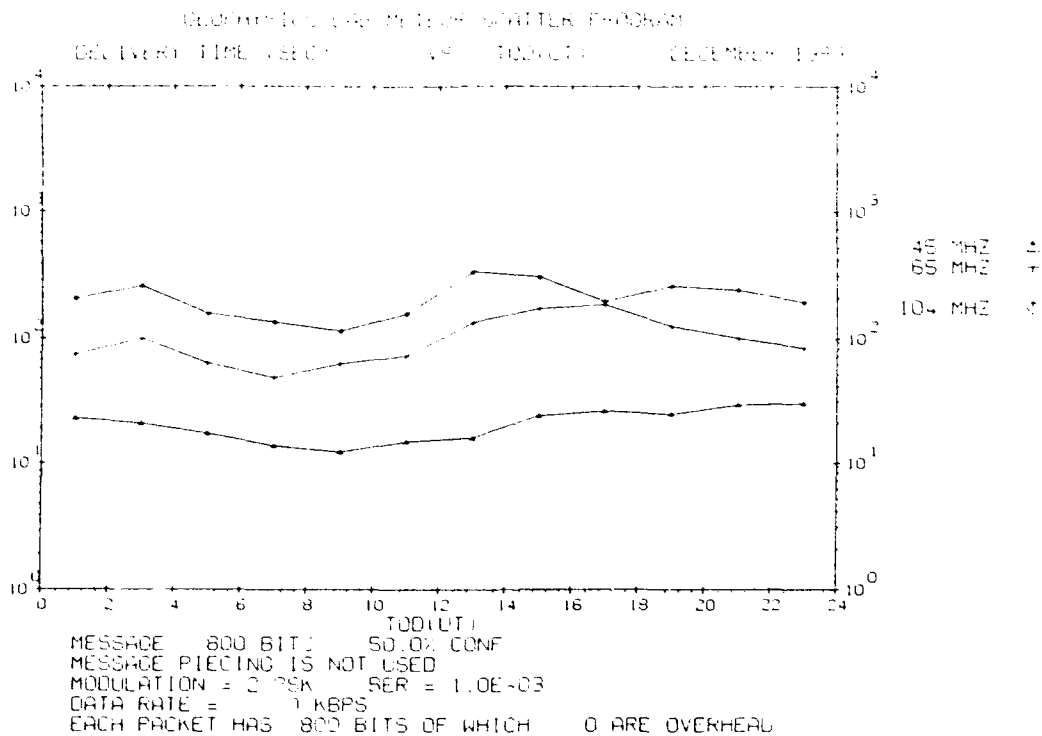


Figure E129. Same as Figure E127 but for Trails of 100 msec

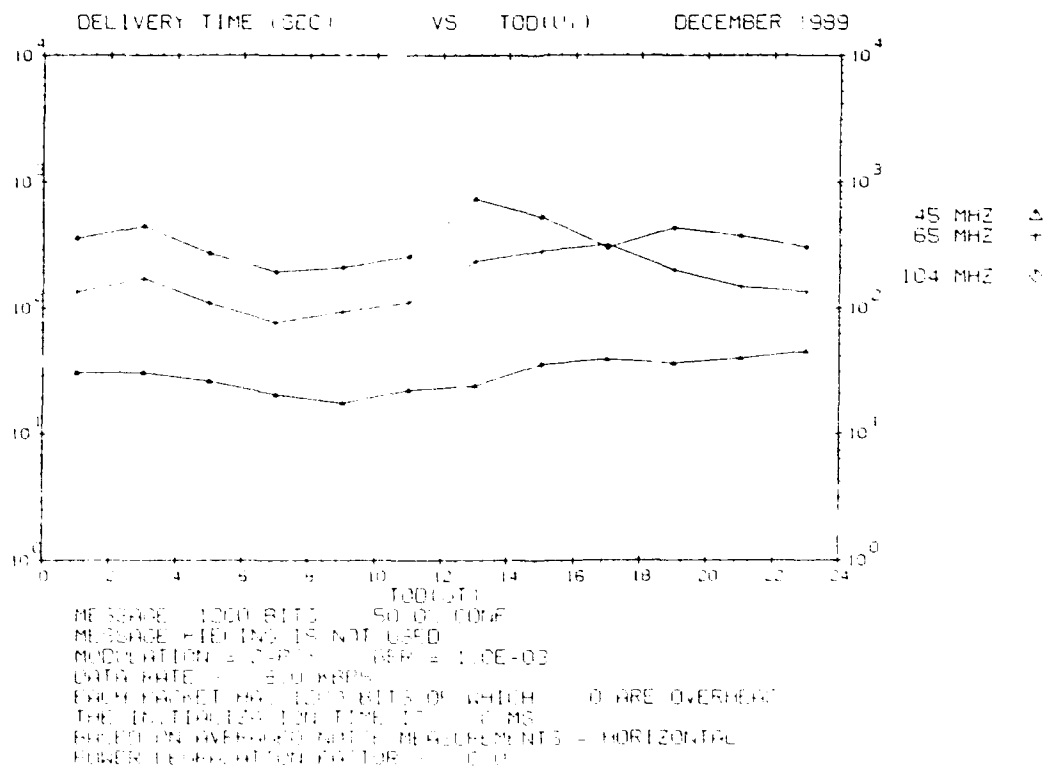


Figure E130. Same as Figure E127 but for Trails of 150 msec



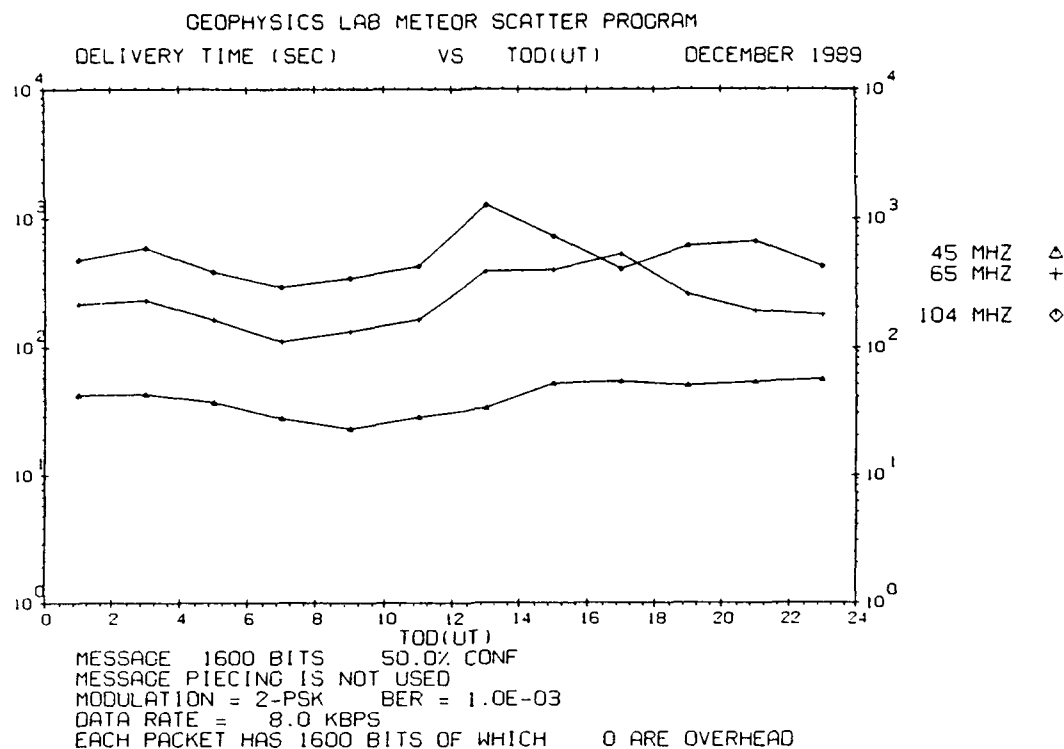


Figure E131. Same as Figure E127 but for Trails of 200 msec

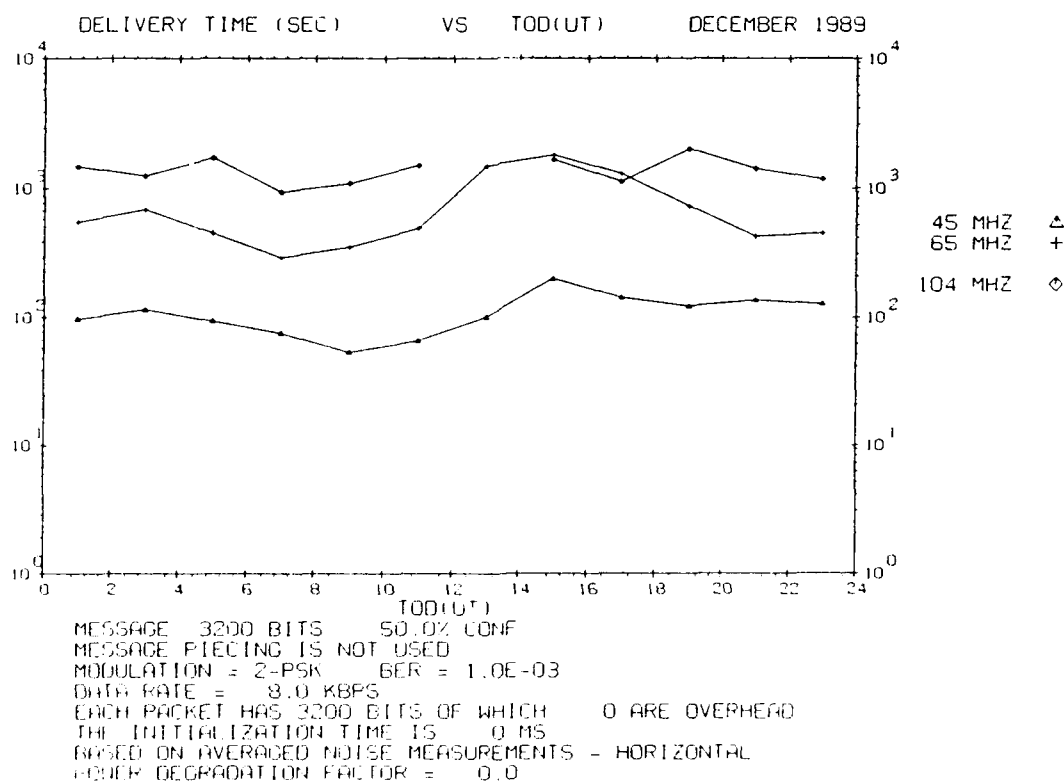
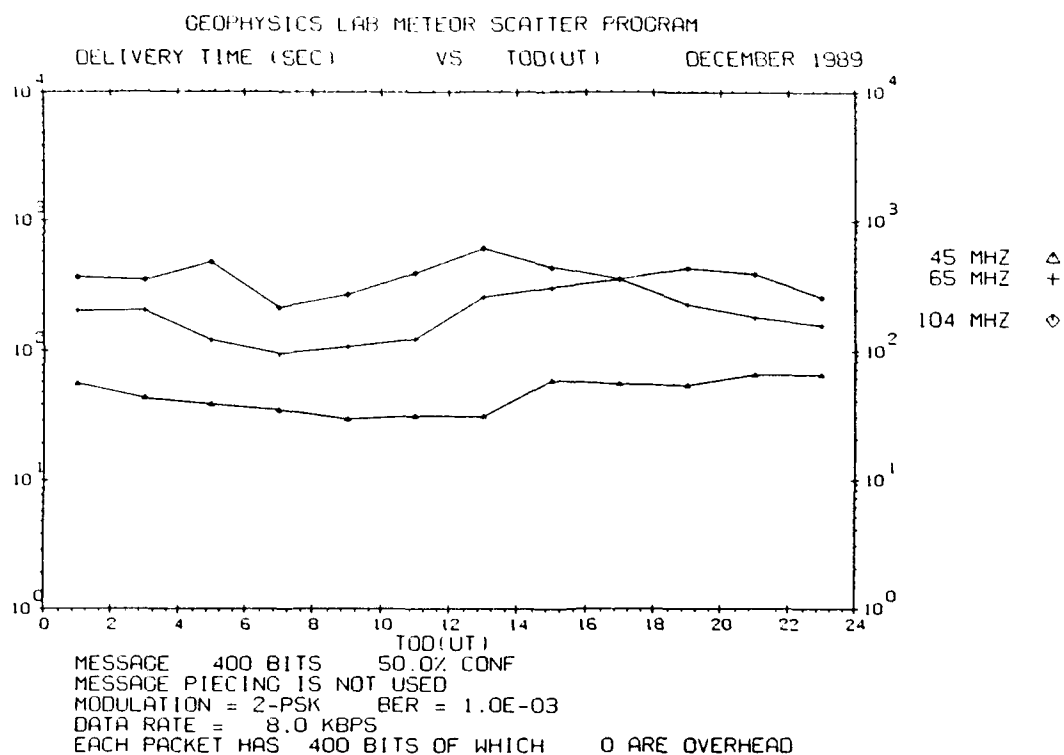
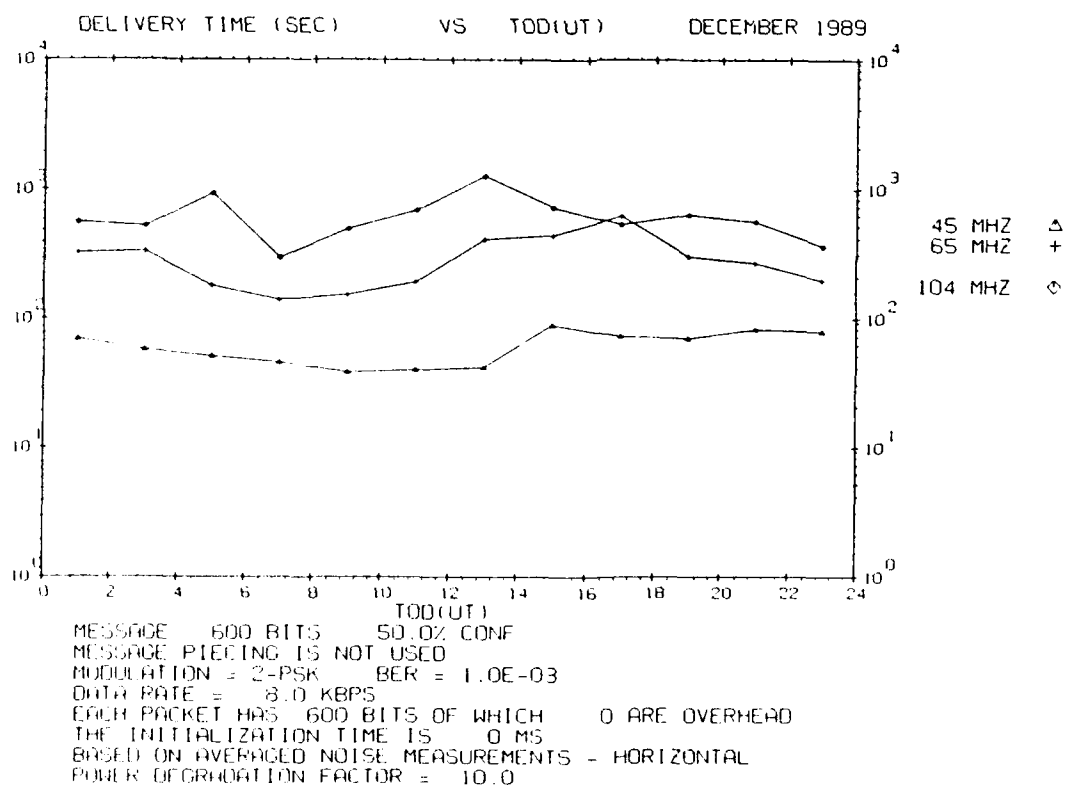


Figure E132. Same as Figure E127 but for Trails of 400 msec



**Figure E133. Waiting Time vs Time of Day for Trails of 50 msec Duration for December 1989. The transmitter power is 100 W**



**Figure E134. Same as Figure E133 but for Trails of 75 msec**

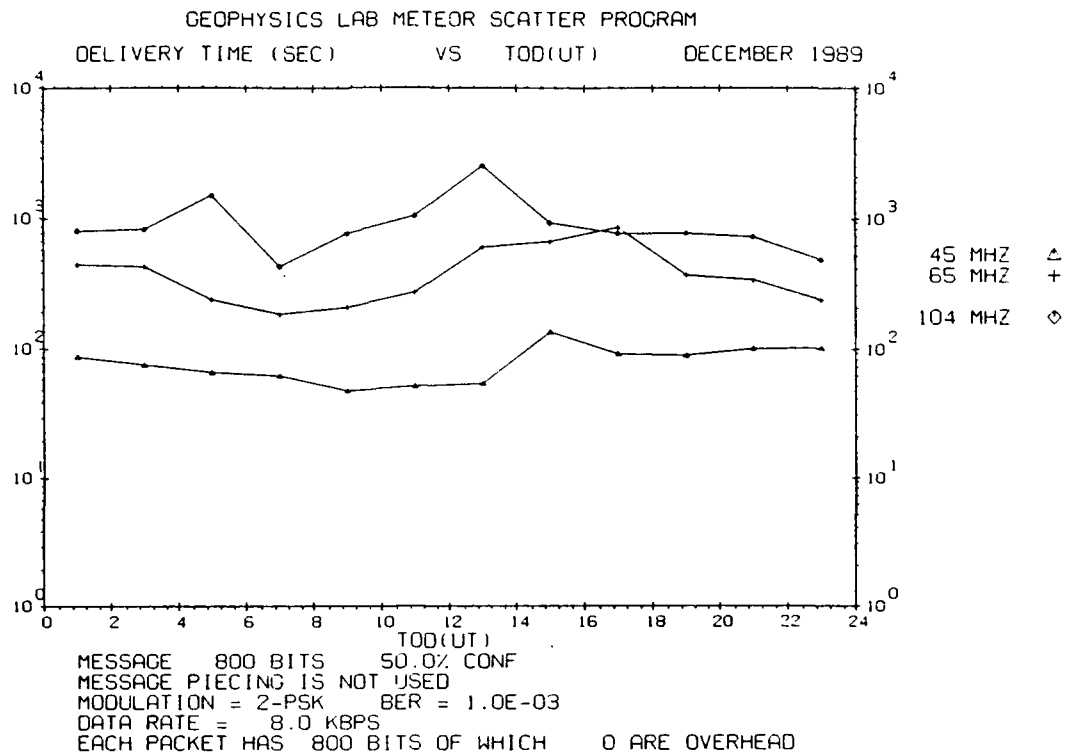


Figure E135. Same as Figure E133 but for Trails of 100 msec

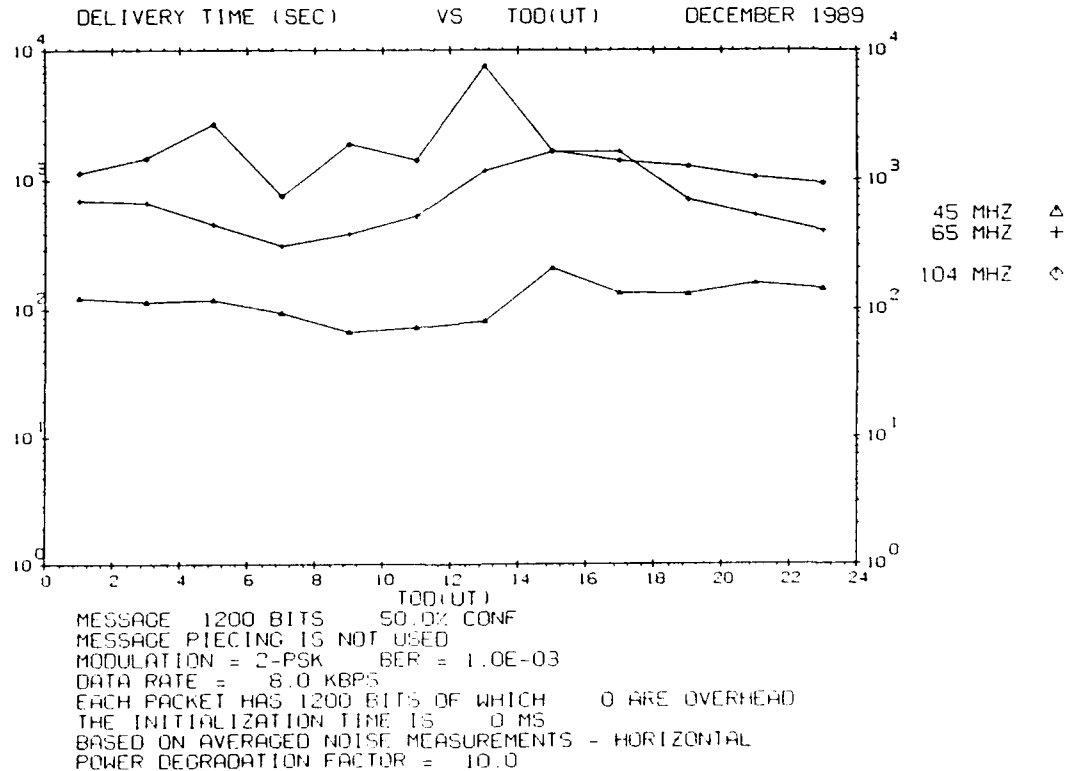


Figure E136. Same as Figure E133 but for Trails of 150 msec

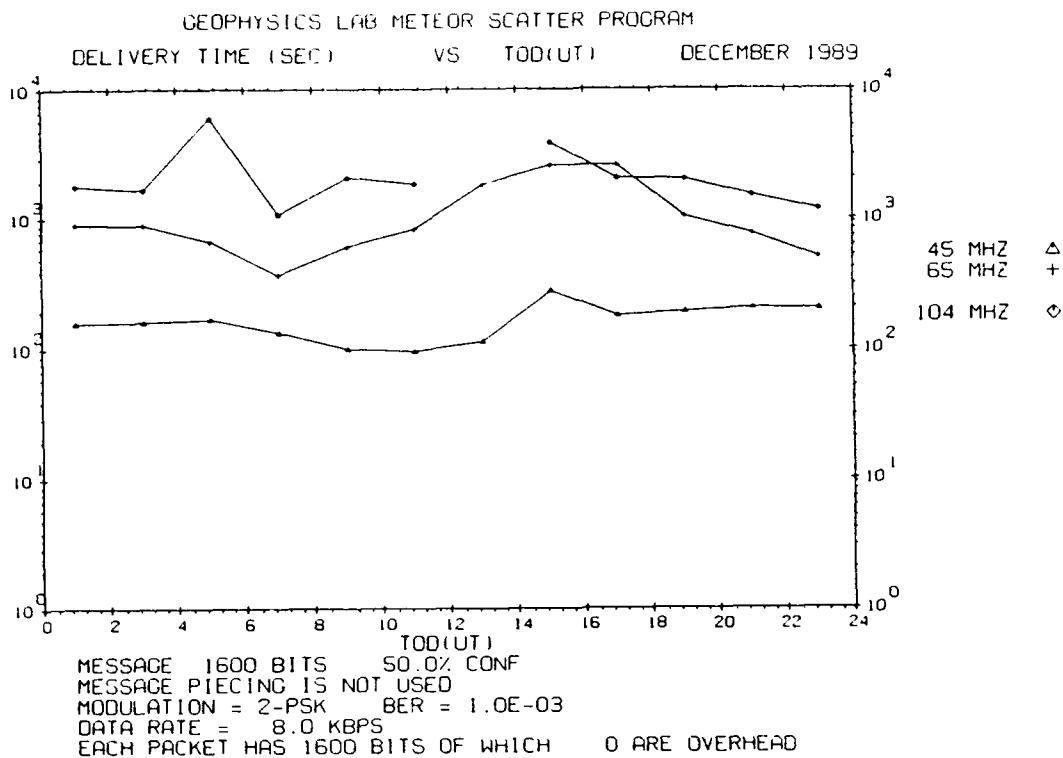


Figure E137. Same as Figure E133 but for Trails of 200 msec

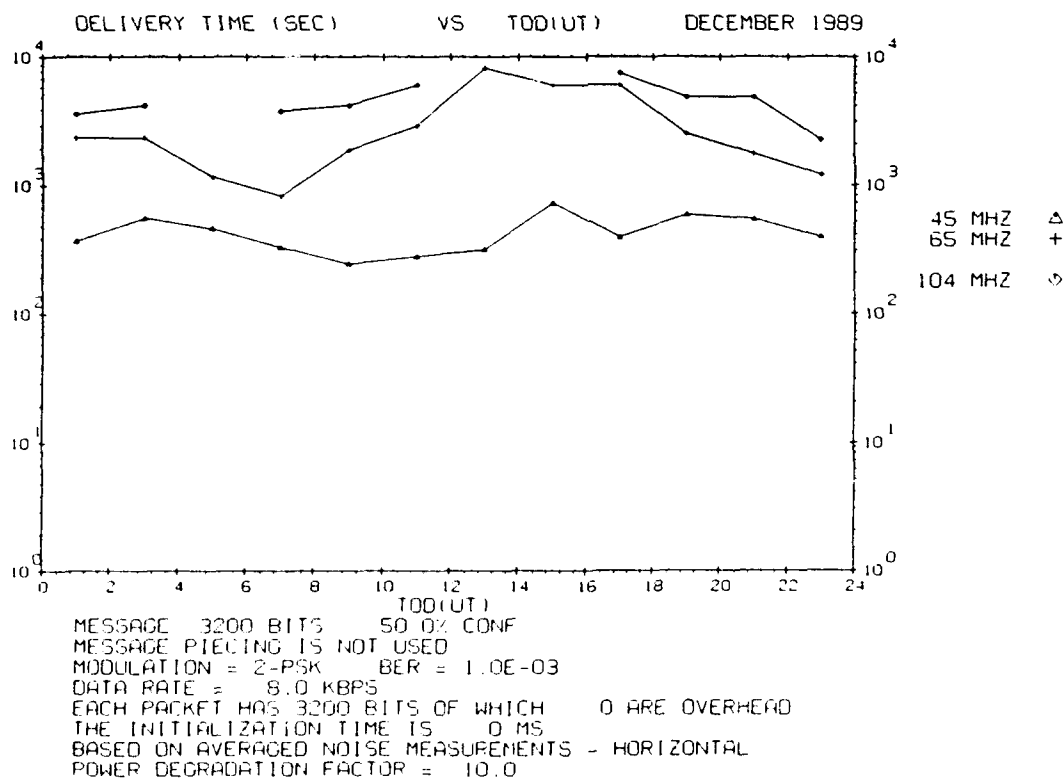
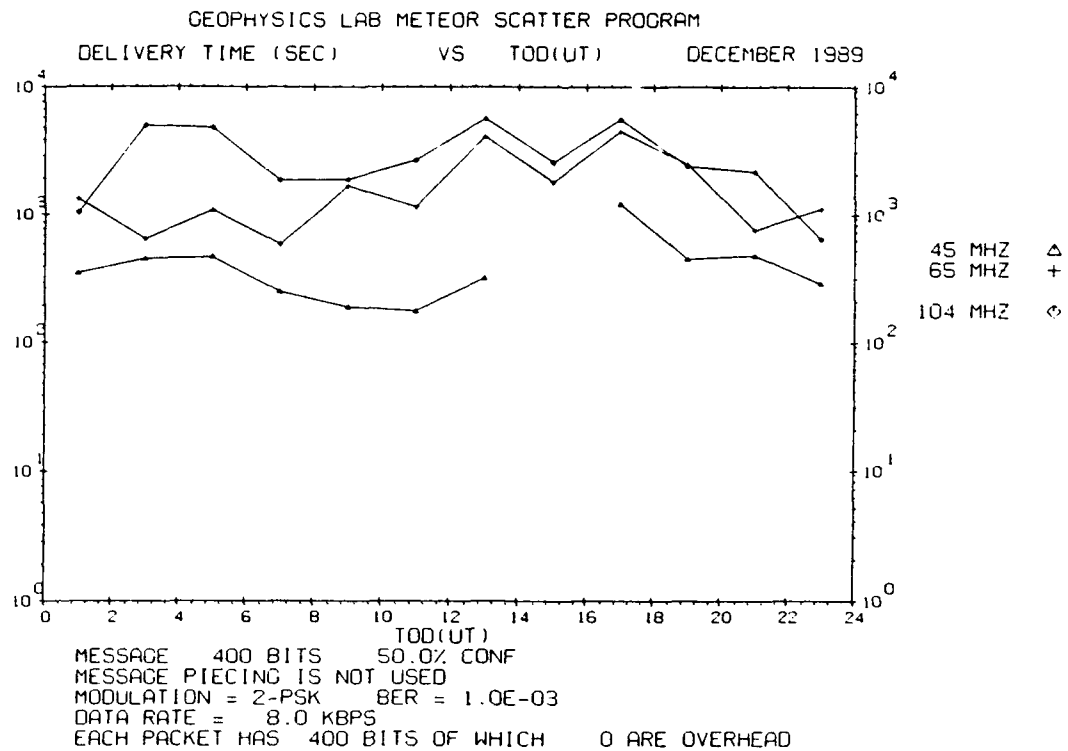
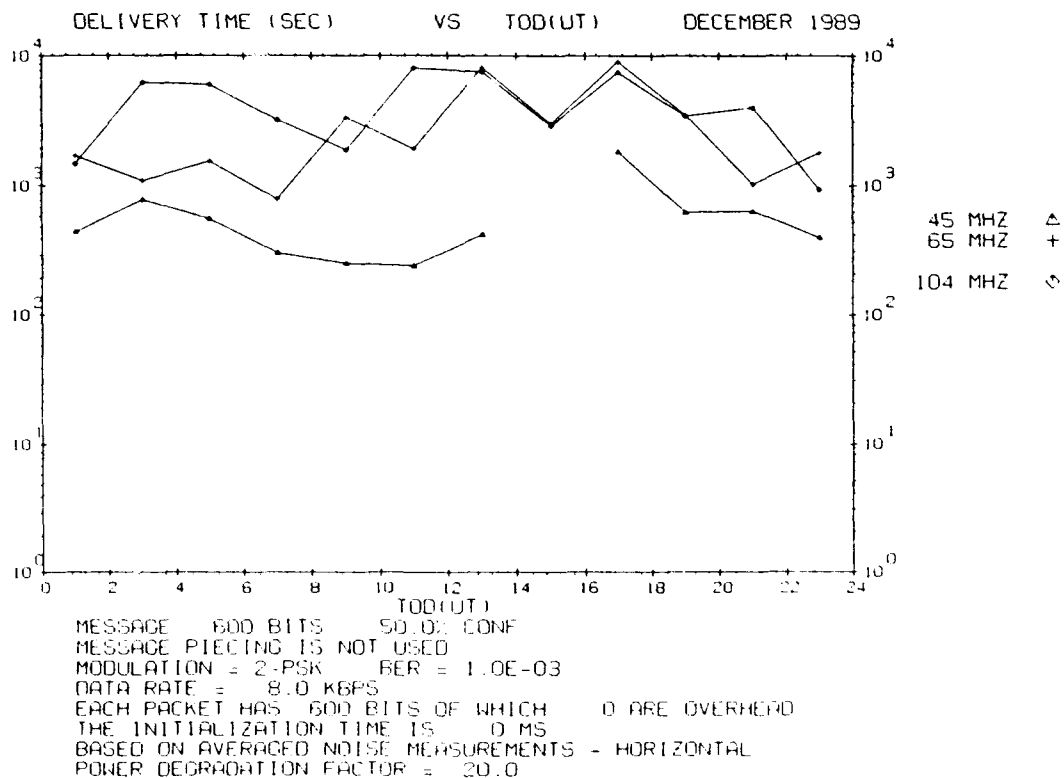


Figure E138. Same as Figure E133 but for Trails of 400 msec



**Figure E139. Waiting Time vs Time of Day for Trails of 50 msec duration for December 1989. The transmitter power is 10 W**



**Figure E140. Same as Figure E139 but for Trails of 75 msec**

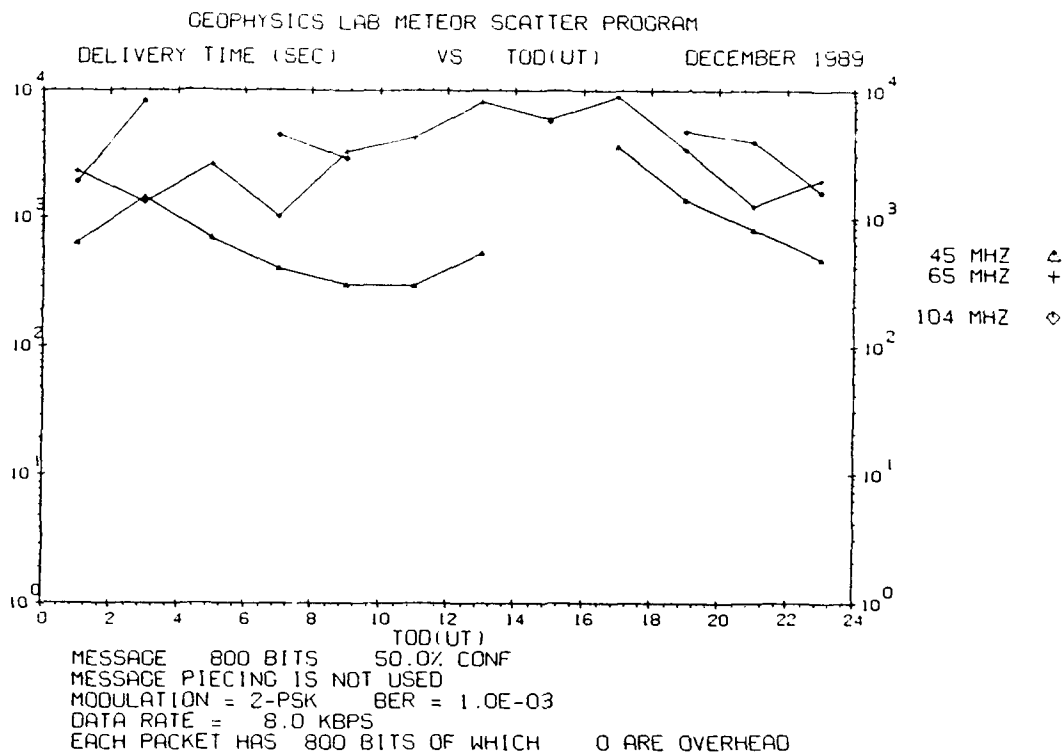


Figure E141. Same as Figure E139 but for Trails of 100 msec

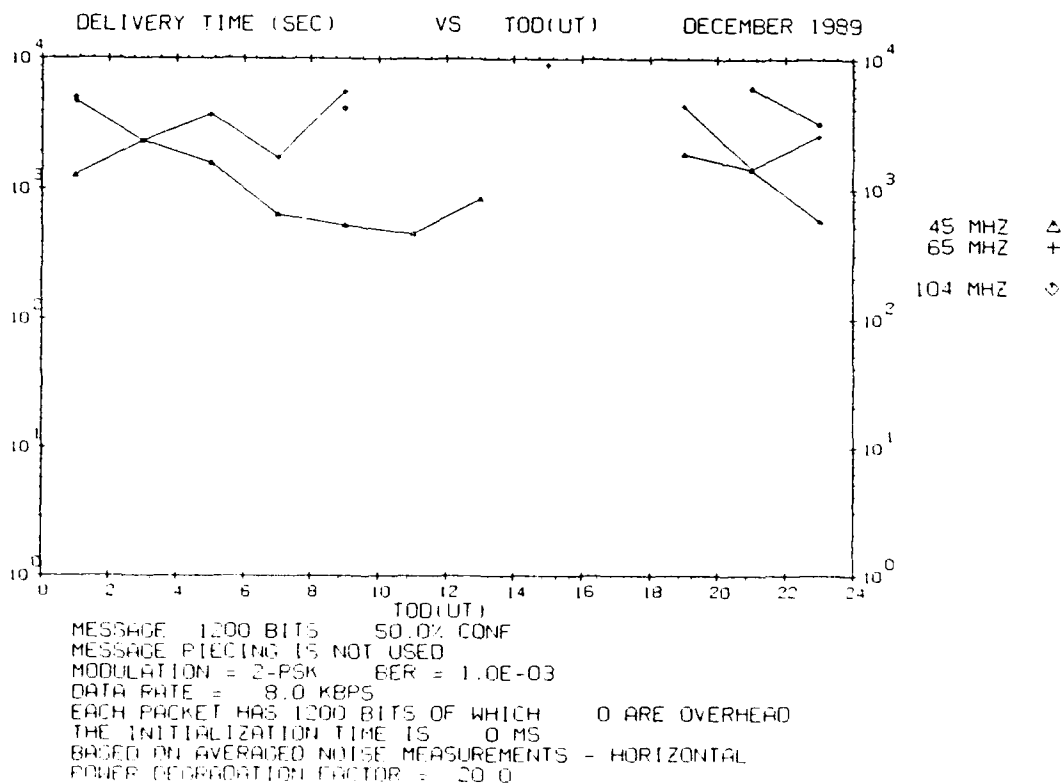


Figure E142. Same as Figure E139 but for Trails of 150 msec

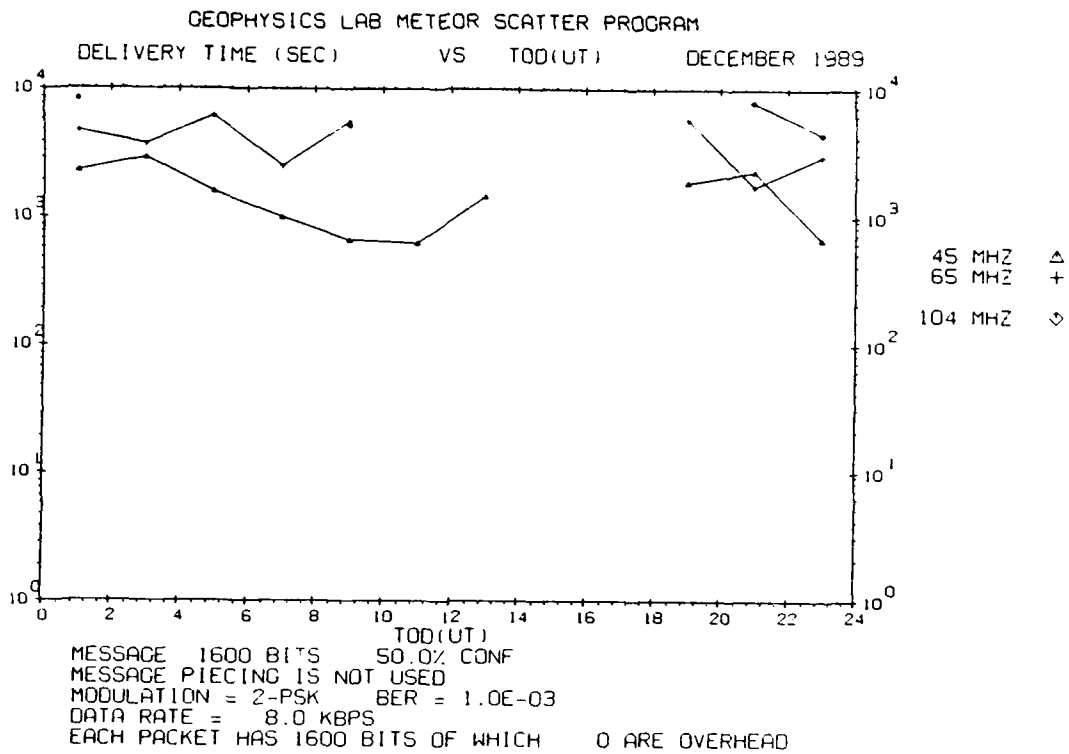


Figure E143. Same as Figure E139 but for Trails of 200 msec

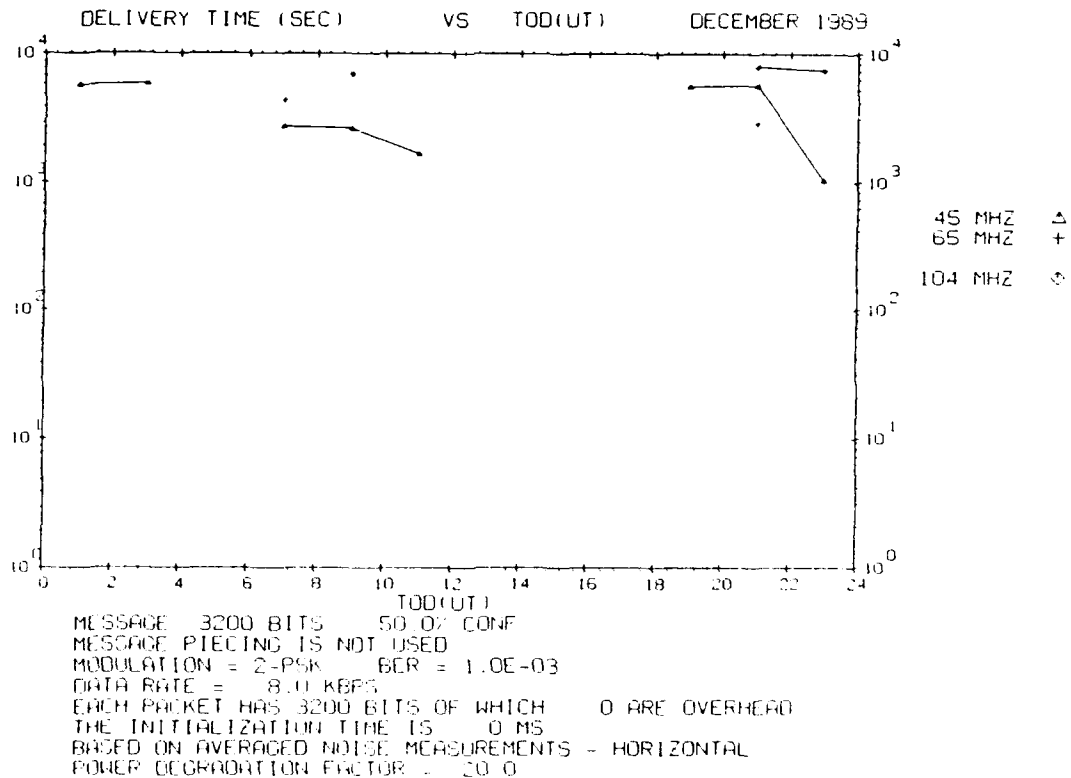
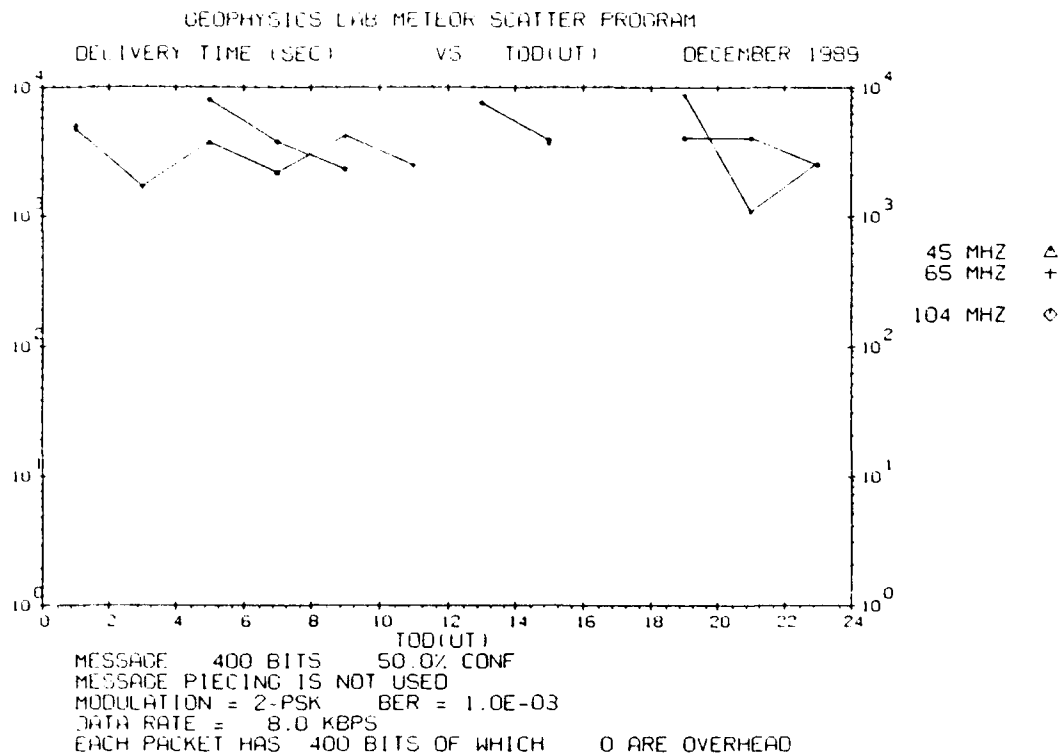
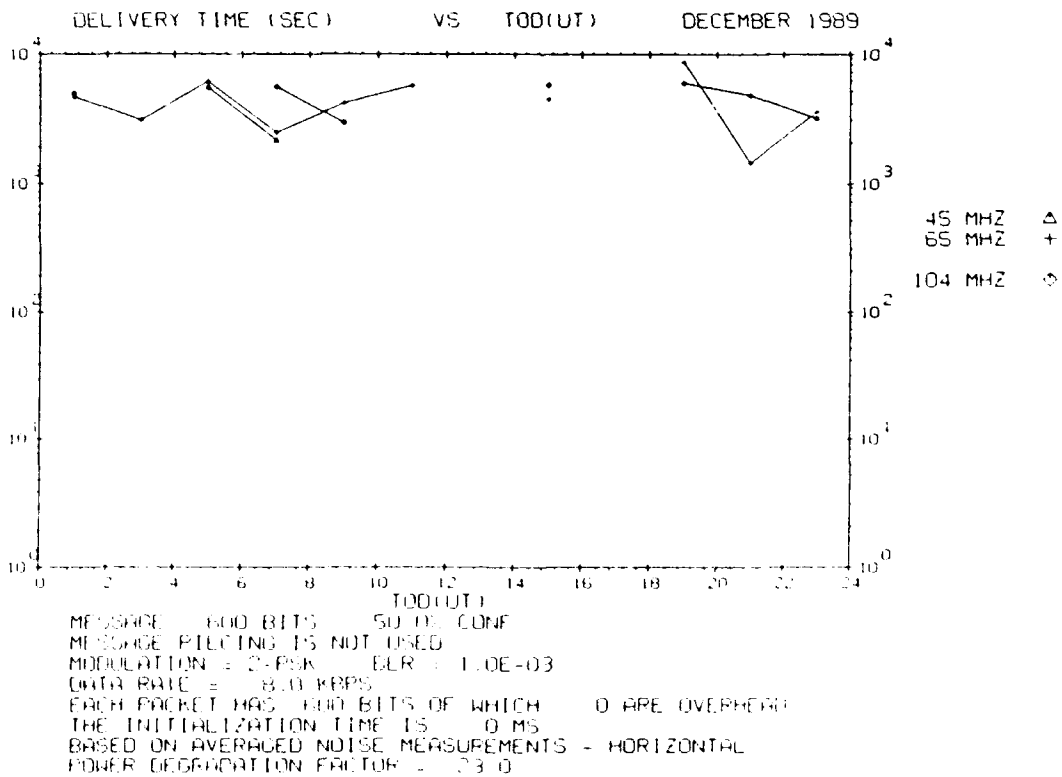


Figure E144. Same as Figure E139 but for Trails of 400 msec



**Figure E145. Waiting Time vs Time of Day for Trails of 50 msec Duration for December 1989. The transmitter power is 5 W**



**Figure E146. Same as Figure E145 but for Trails of 75 msec**



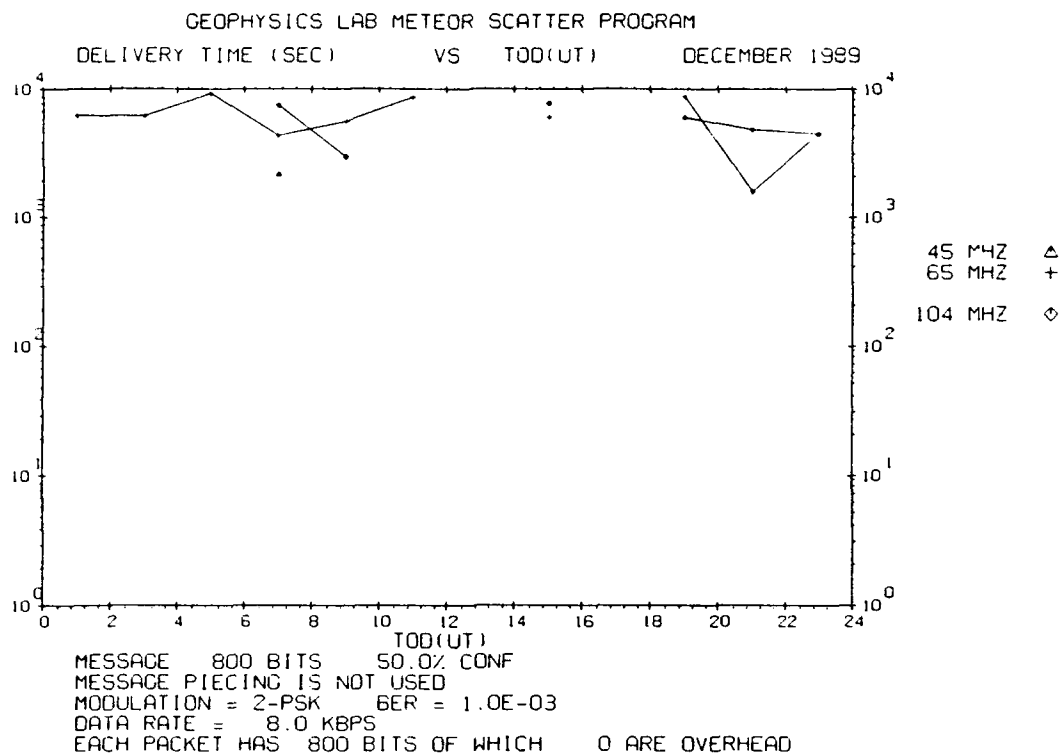


Figure E147. Same as Figure E145 but for Trails of 100 msec

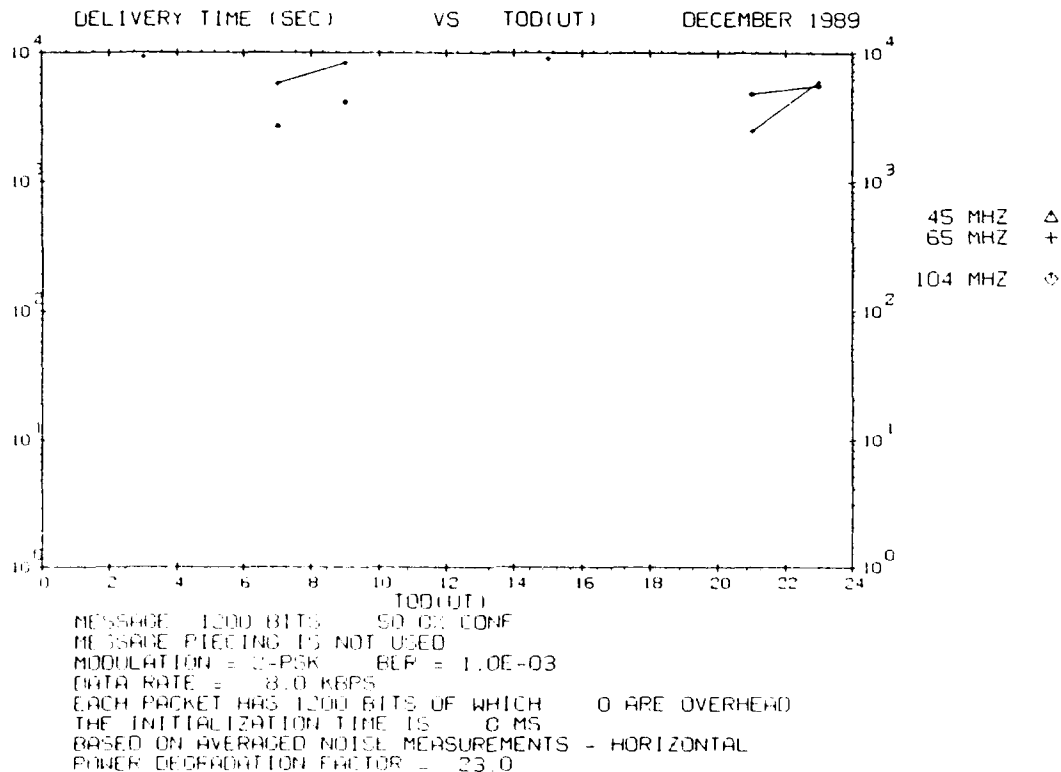
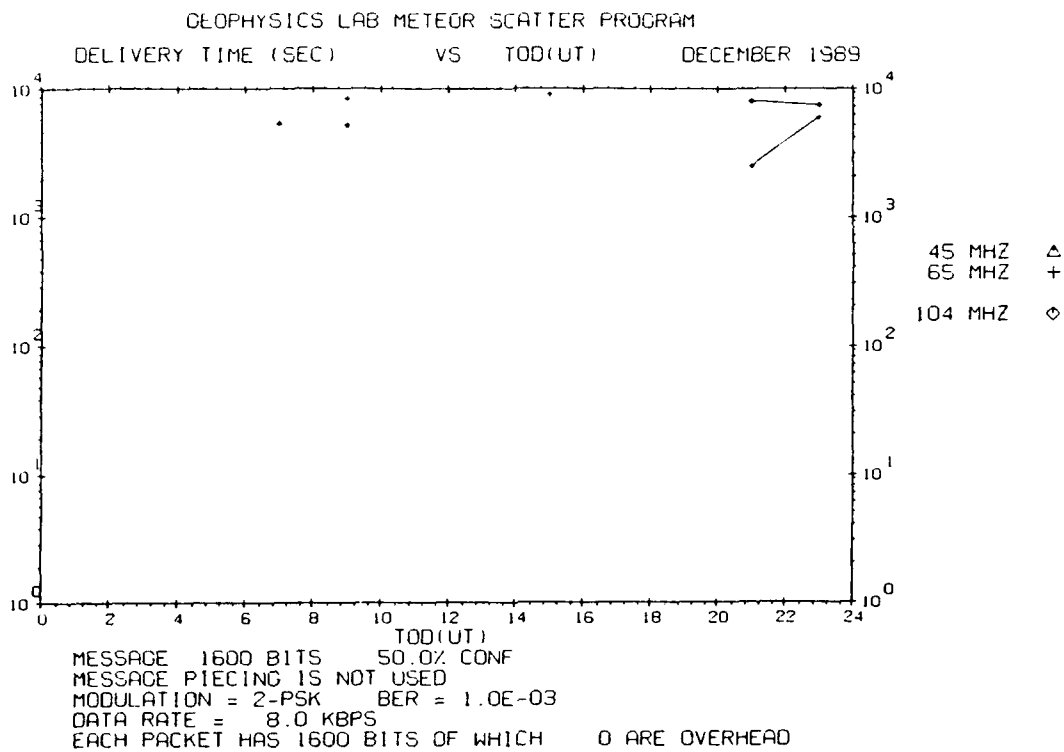
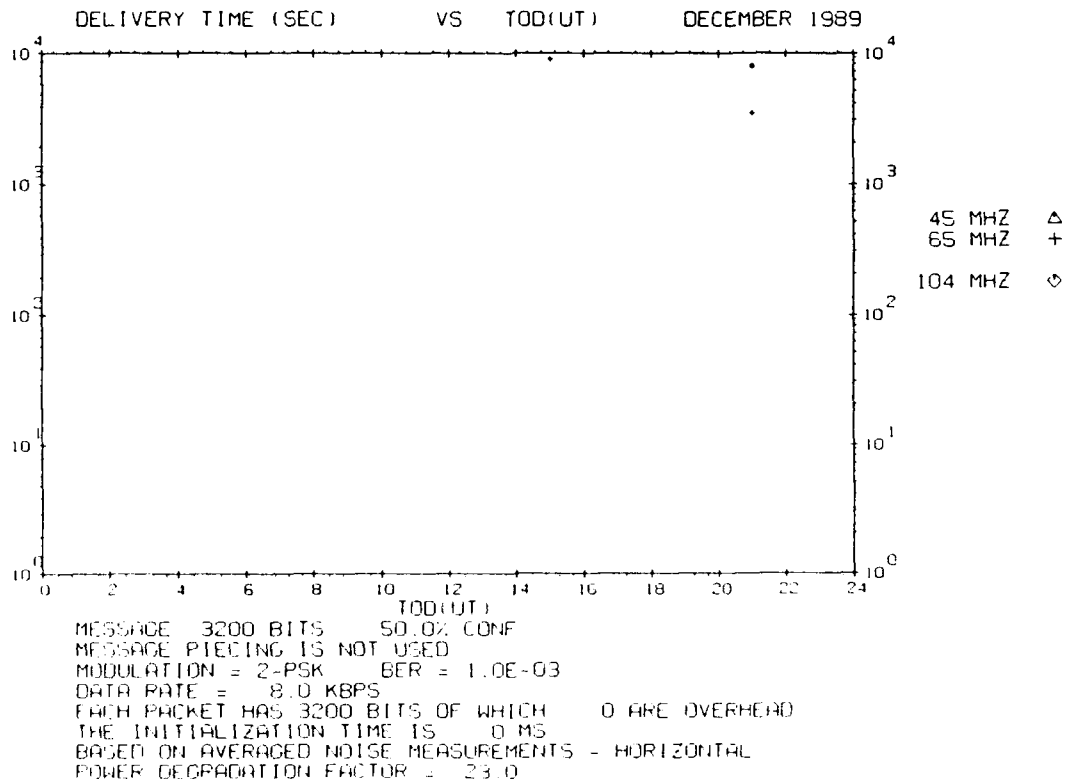


Figure E148. Same as Figure E145 but for Trails of 150 msec



**Figure E149.** Same as Figure E145 but for Trails of 200 msec



**Figure E150.** Same as Figure E145 but for Trails of 400 msec

## **Appendix F**

### **Average Waiting Time Statistics**

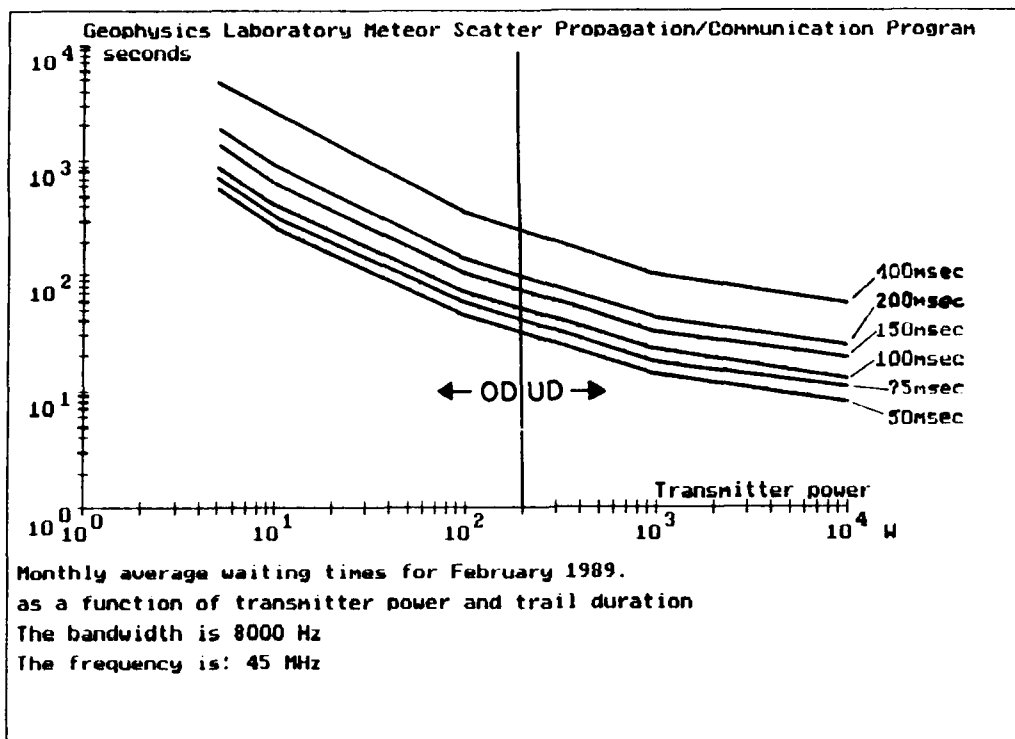


Figure F1. Monthly Average Waiting Time as a Function of Transmitter Power for Trails of 50, 75, 150, 200, 400 msec Duration for the Month of February 1989. The frequency is 45 MHz

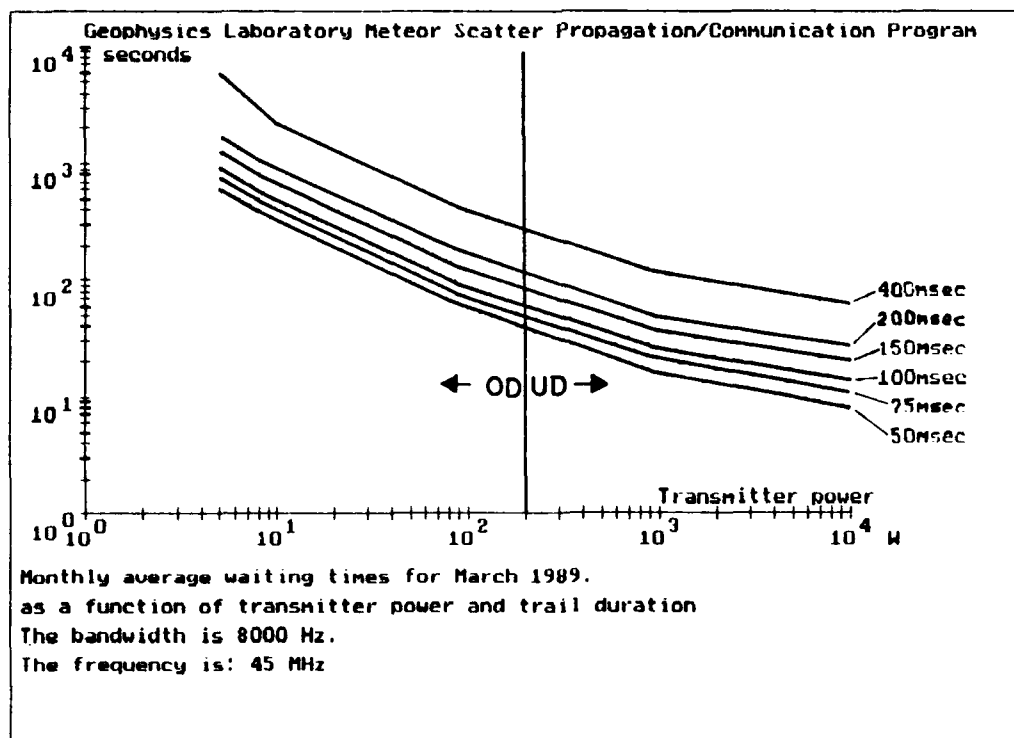


Figure F2. Same as Figure F1 but for March 1989

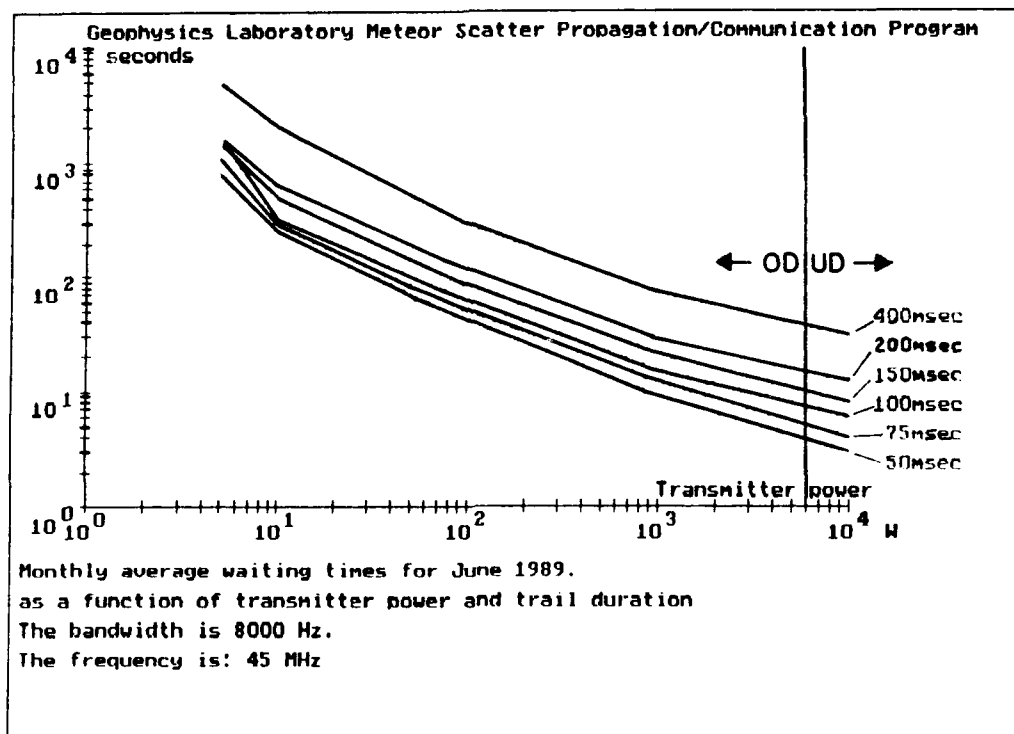


Figure F3. Same as Figure F1 but for June 1989

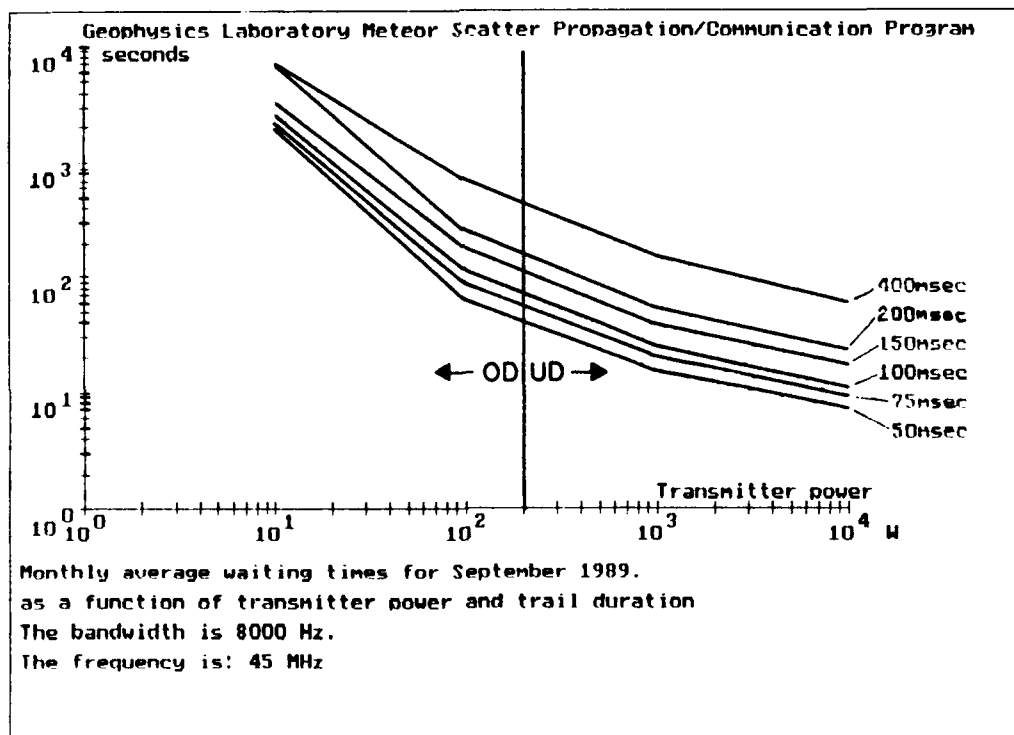


Figure F4. Same as Figure F1 but for September 1989

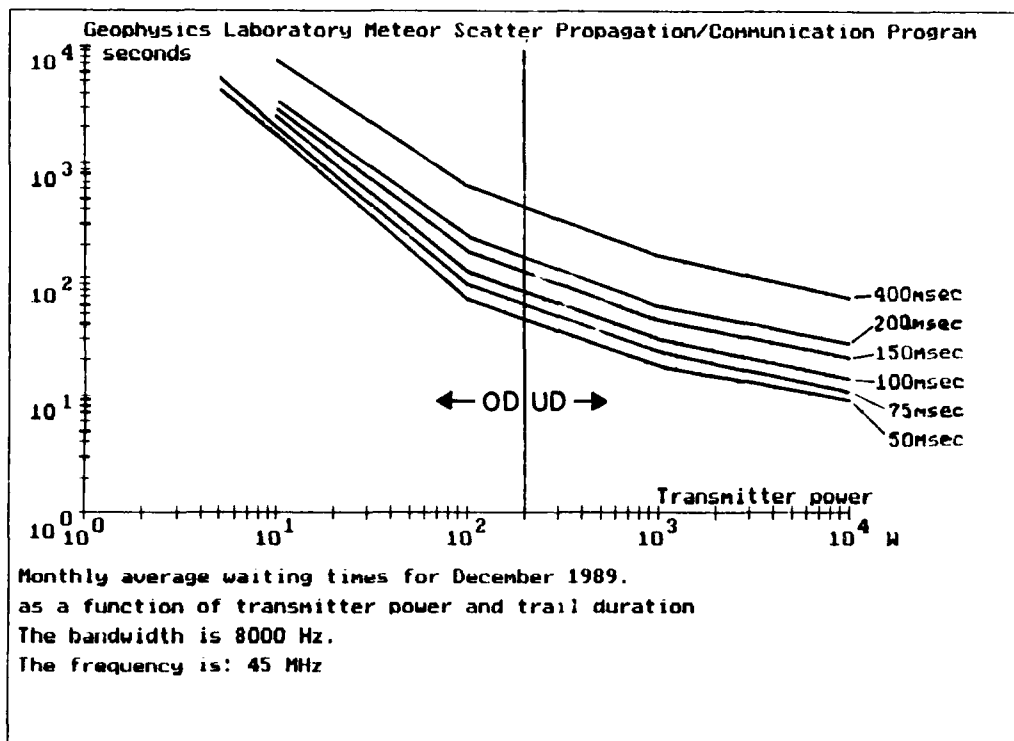


Figure F5. Same as Figure F1 but for December 1989

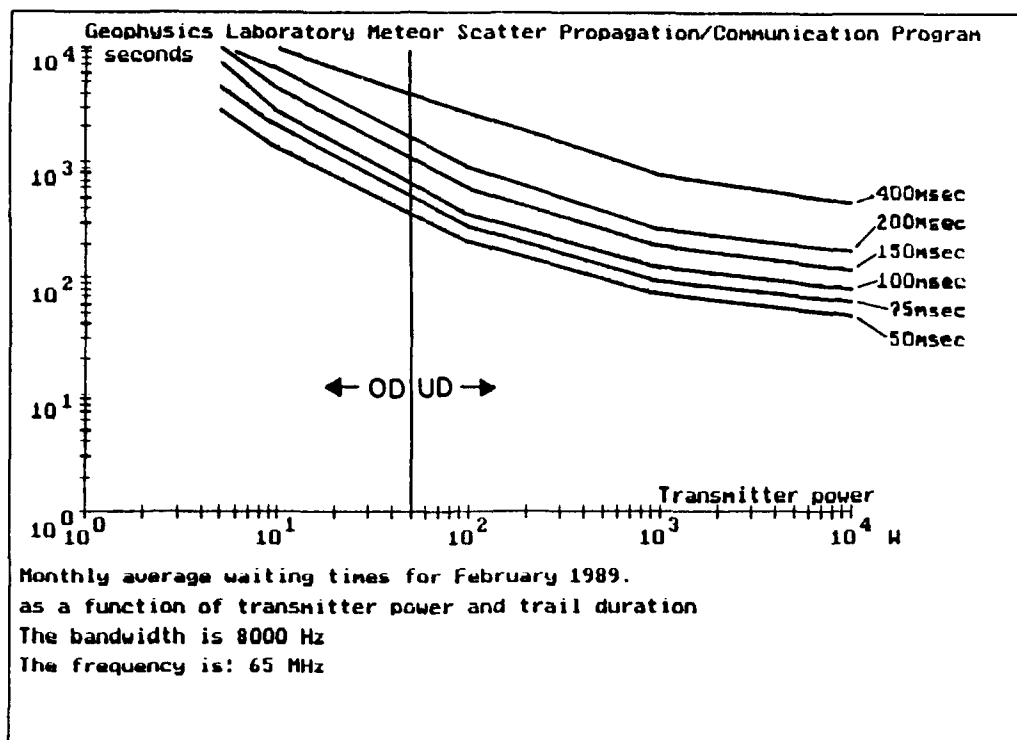


Figure F6. Monthly Average Waiting Time as a Function of Transmitter Power for Trails of 50, 75, 150, 200, 400 msec Duration for the Month of February 1989. The frequency is 65 MHz

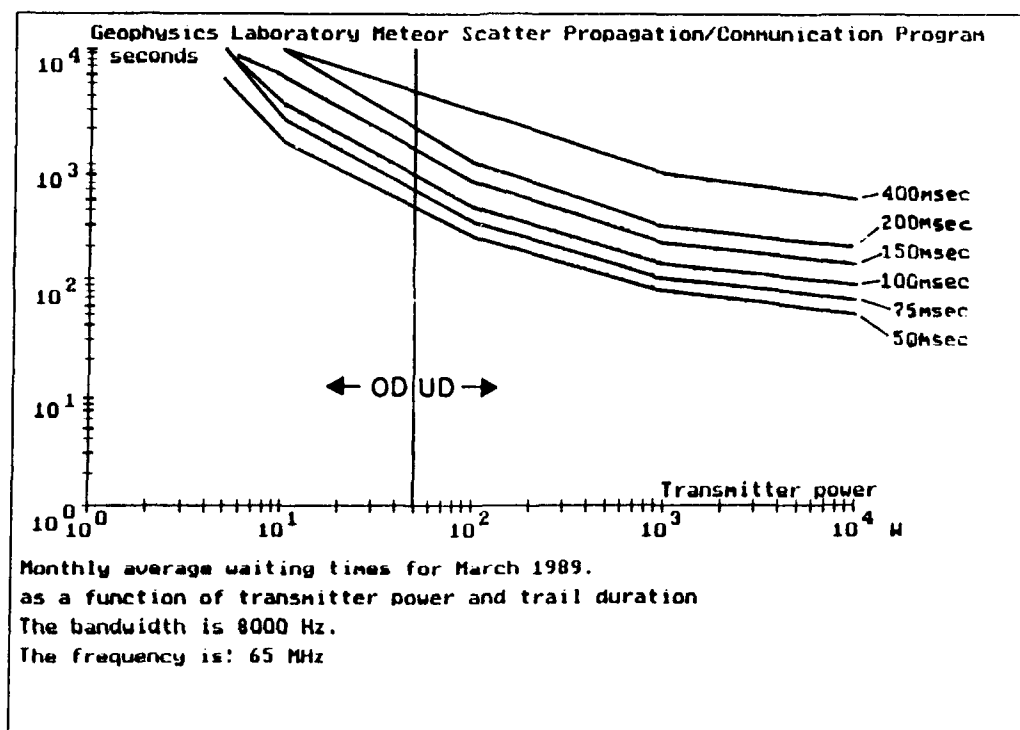


Figure F7. Same as Figure F6 but for March 1989

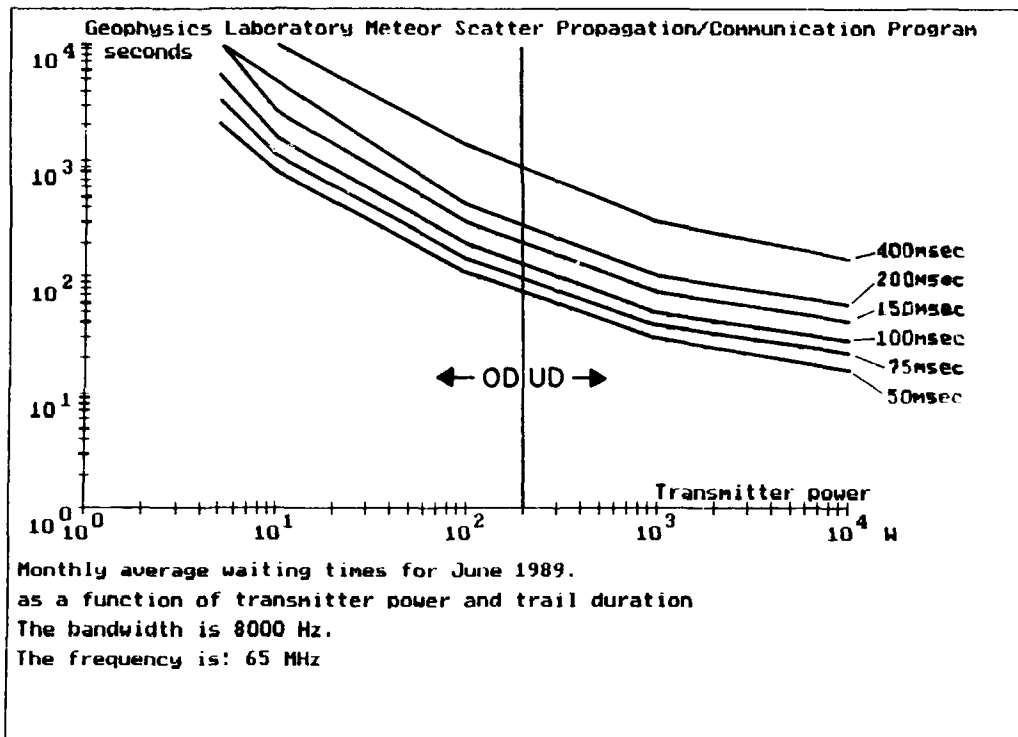


Figure F8. Same as Figure F6 but for June 1989

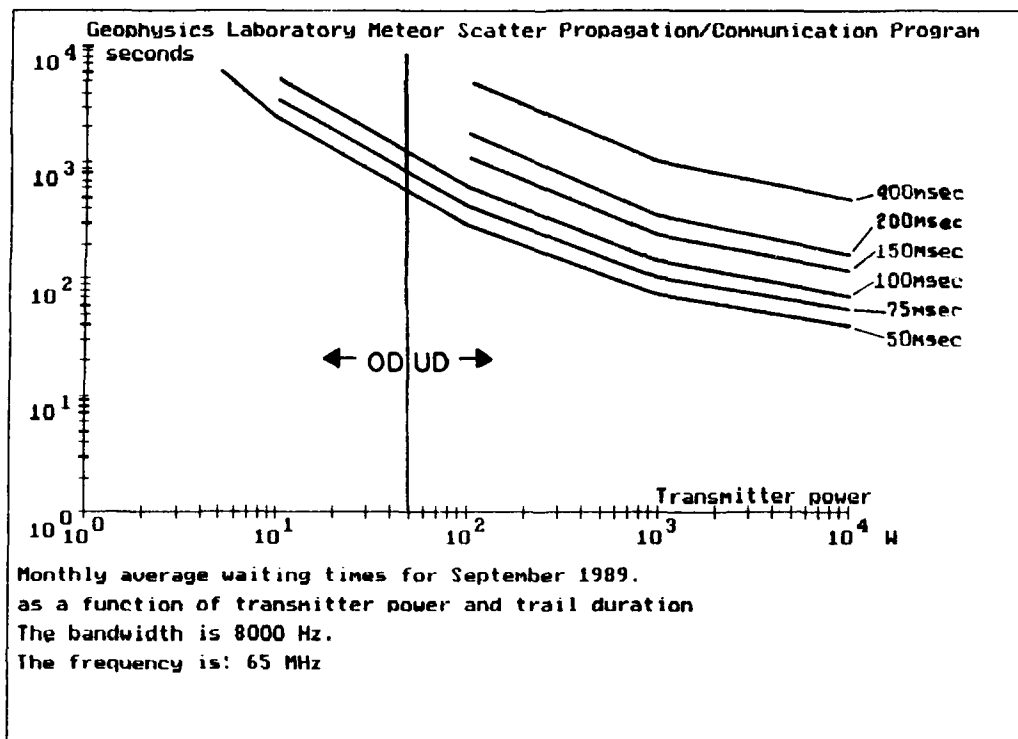


Figure F9. Same as Figure F6 but for September 1989



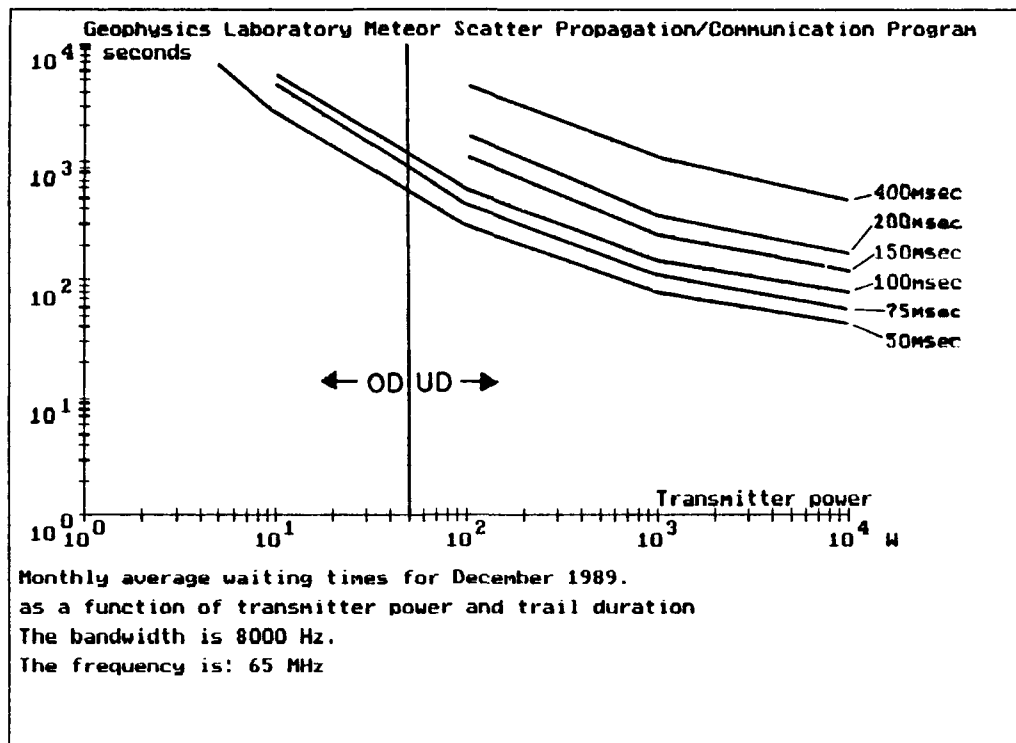


Figure F10. Same as Figure F6 but for December 1989

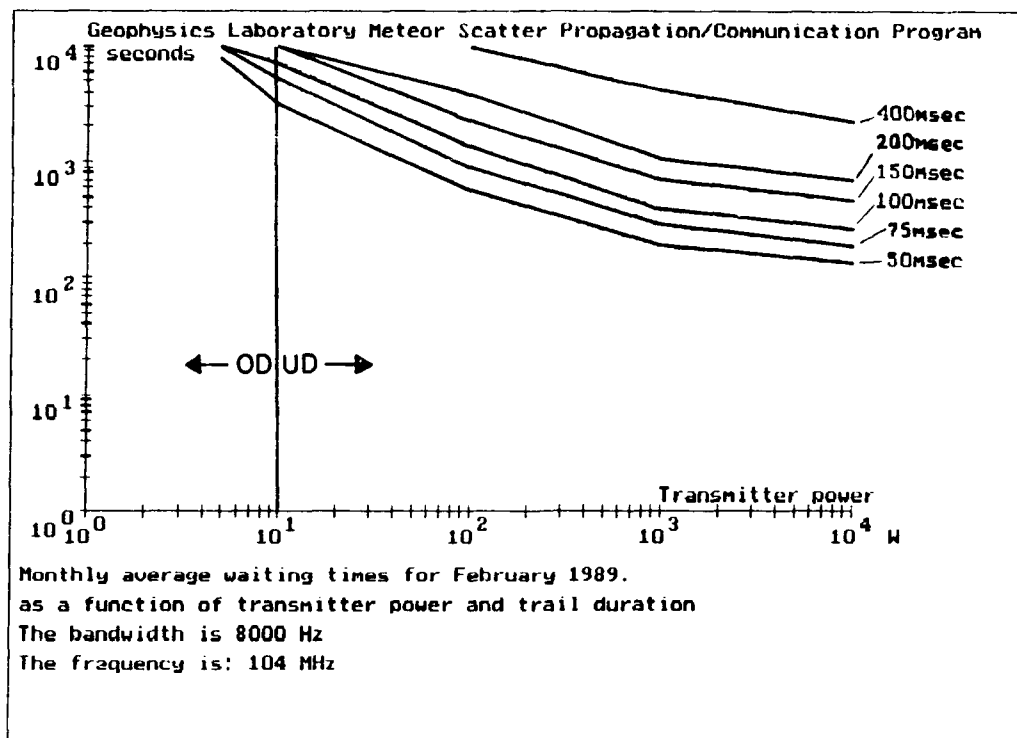


Figure F11. Monthly Average Waiting Time as a Function of Transmitter Power for Trails of 50, 75, 150, 200, 400 msec Duration for the Month of February 1989. The frequency is 104 MHz

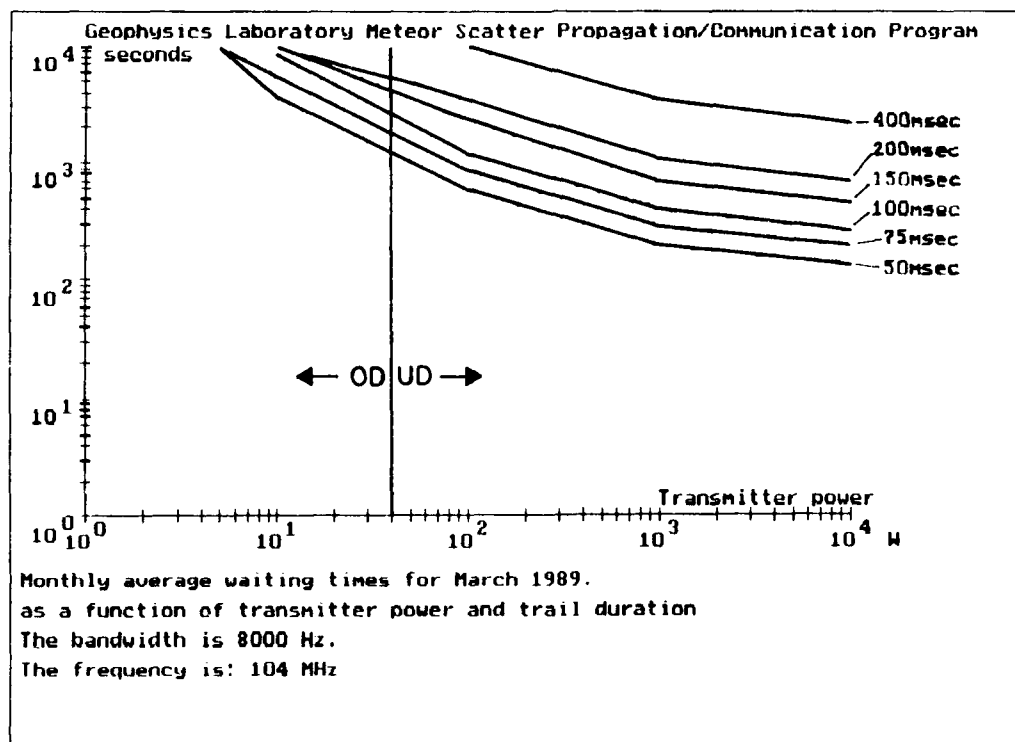


Figure F12. Same as Figure F11 but for March 1989

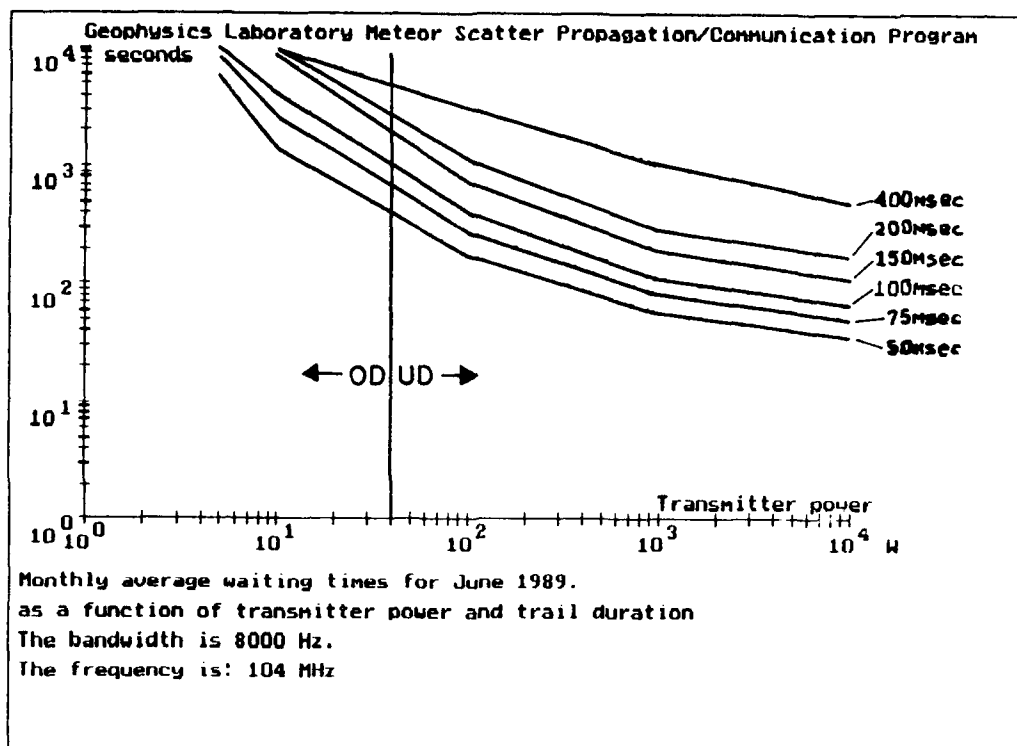


Figure F13. Same as Figure F11 but for June 1989

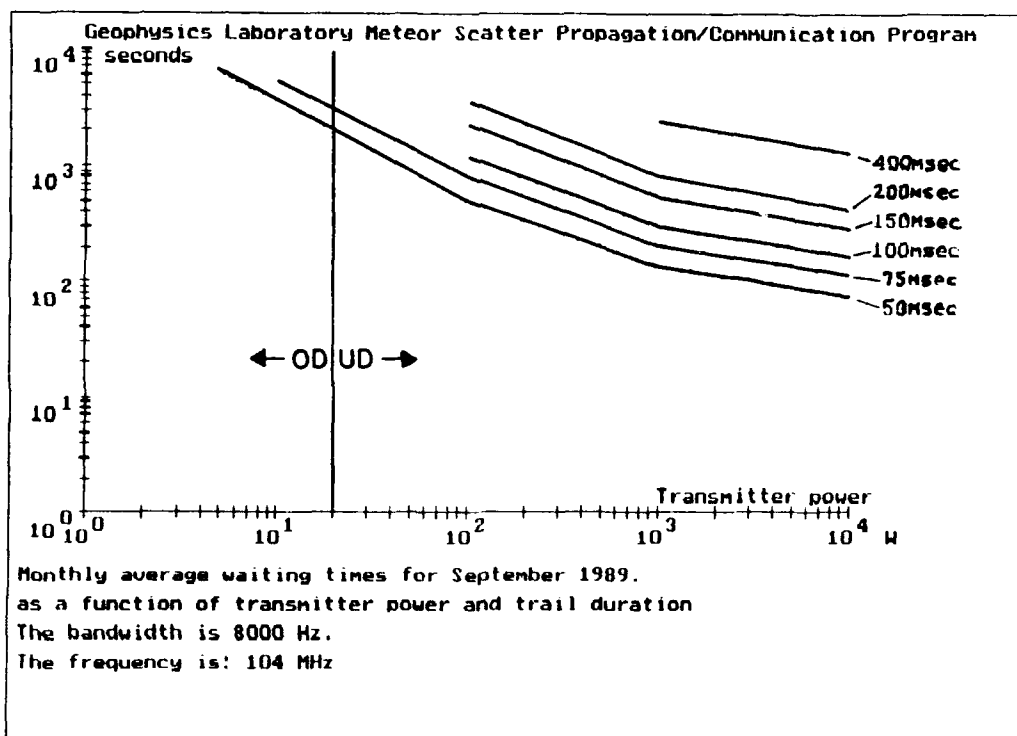


Figure F14. Same as Figure F11 but for September 1989

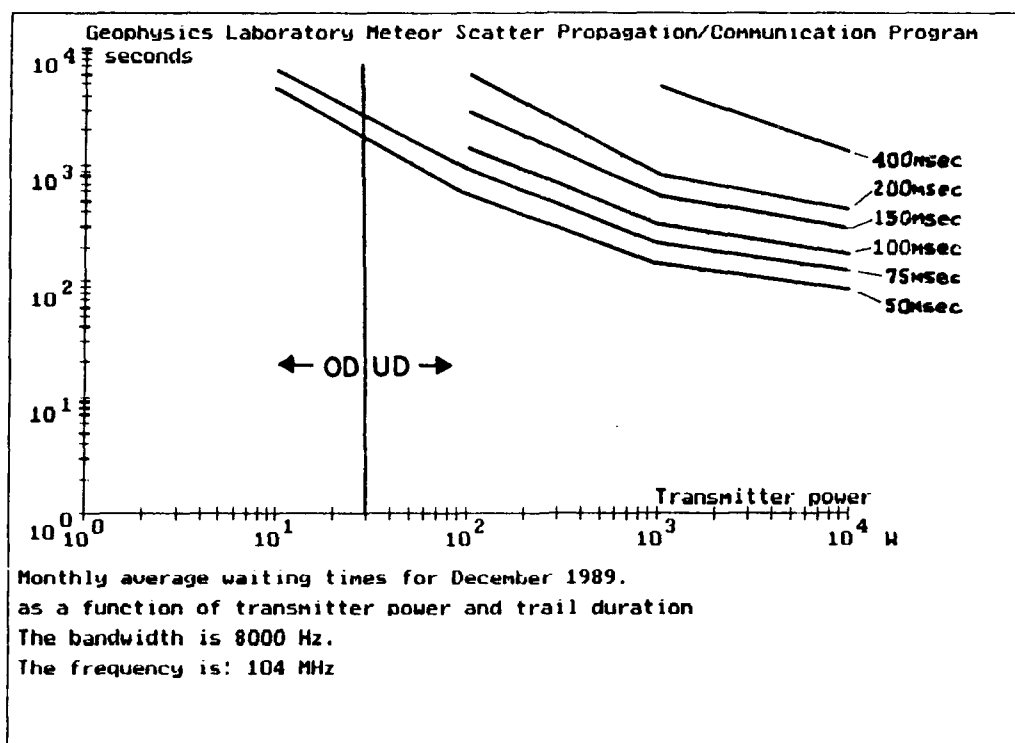


Figure F15. Same as Figure F11 but for December 1989

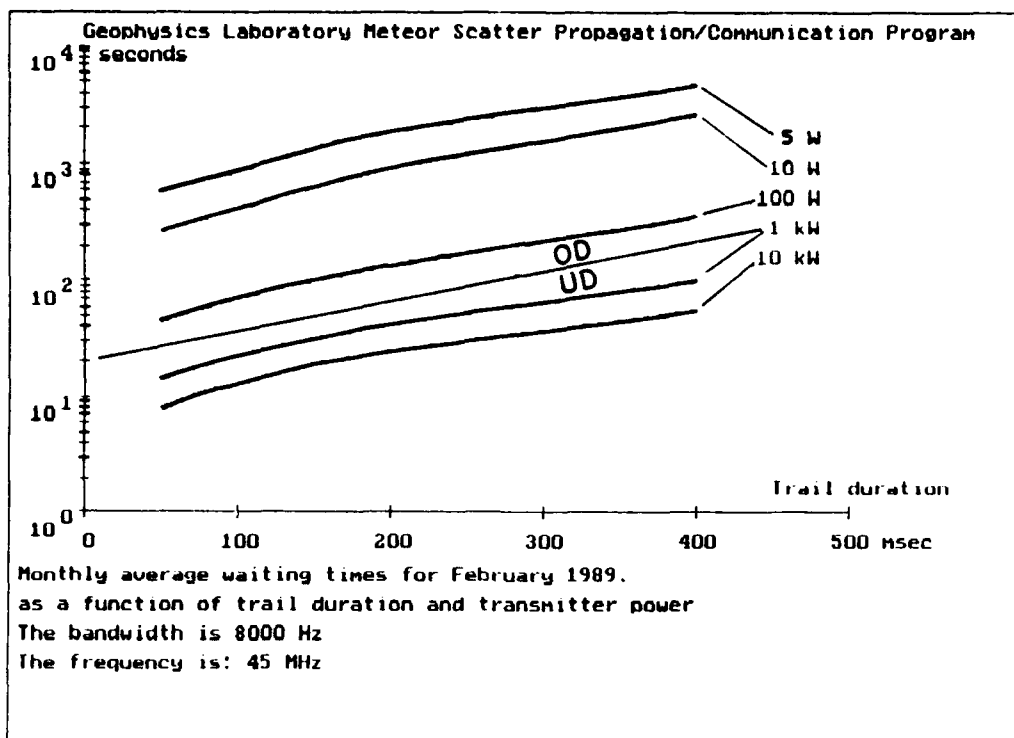


Figure F16. Monthly Average Waiting Time as a Function of Duration for Transmitter Powers of 10 kW, 1kW, 100 W, 10 W, and 5 W for the Month of February 1989. The Frequency is 45 MHz

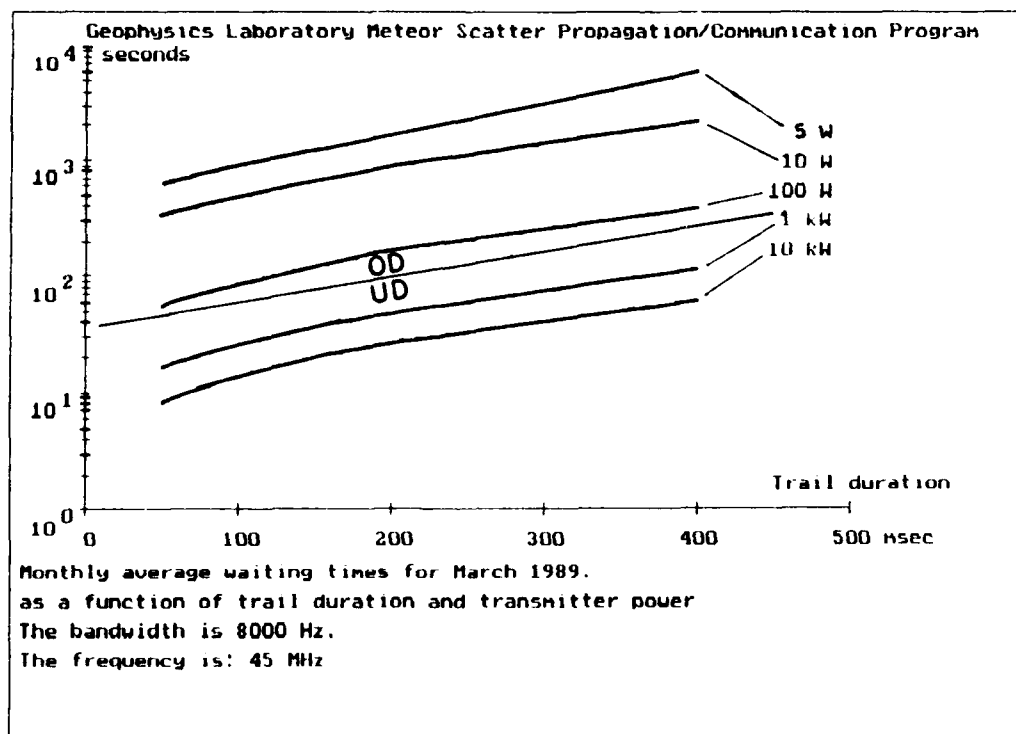


Figure F17. Same as Figure F16 but for March 1989

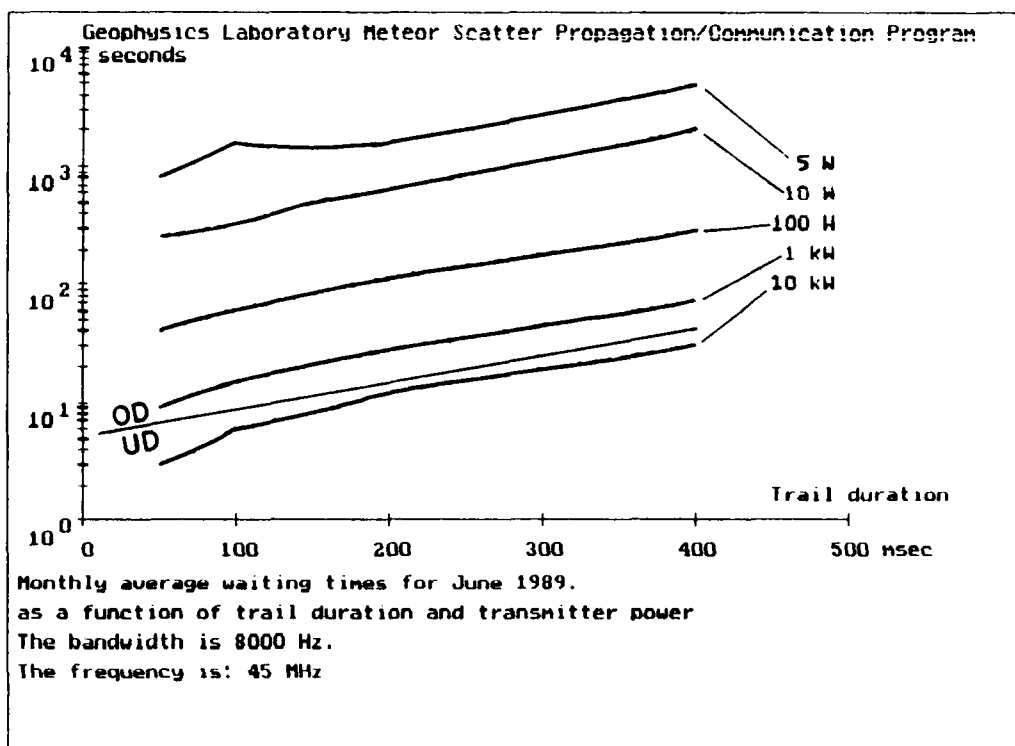


Figure F18. Same as Figure F16 but for June 1989

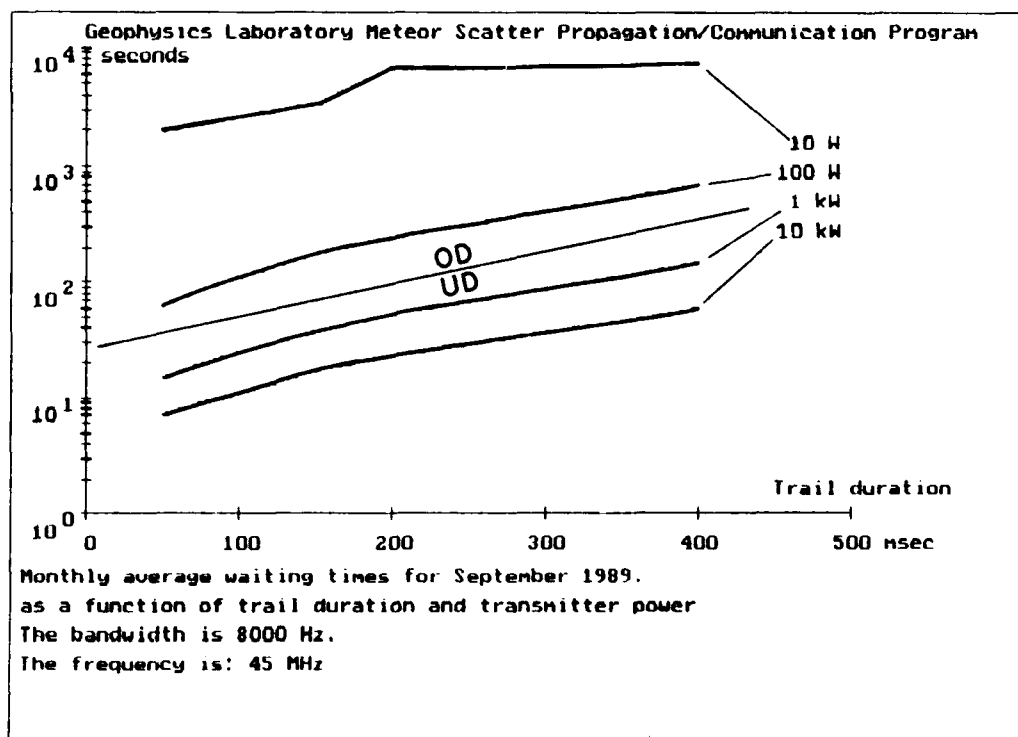


Figure F19. Same as Figure F16 but for September 1989

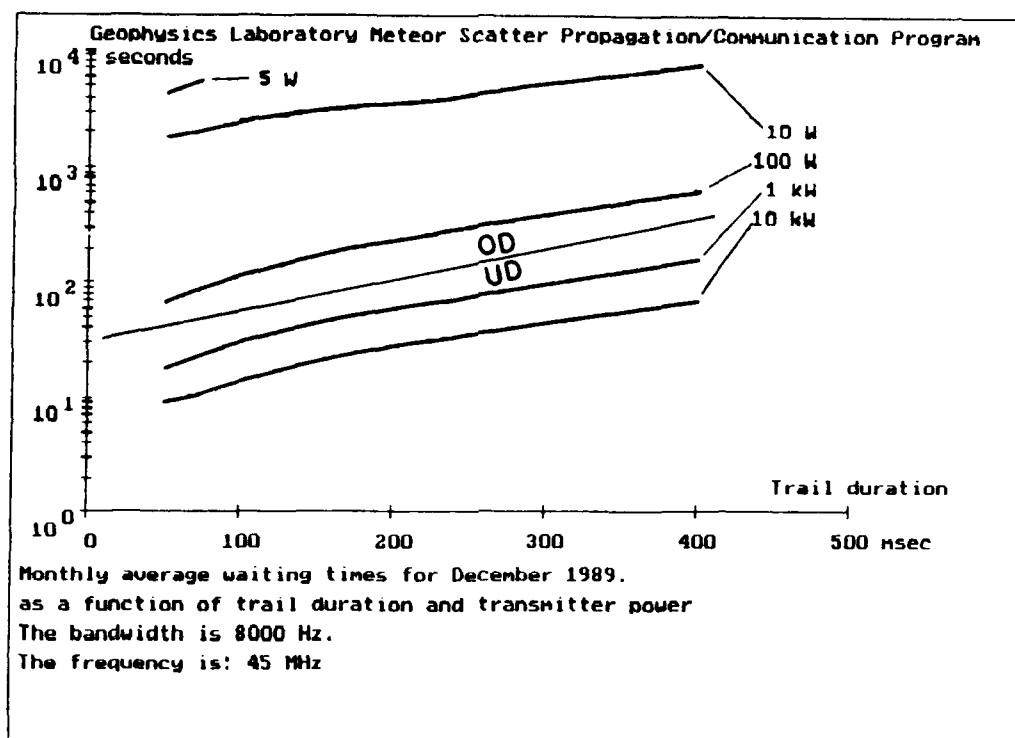


Figure F20. Same as Figure F16 but for December 1989

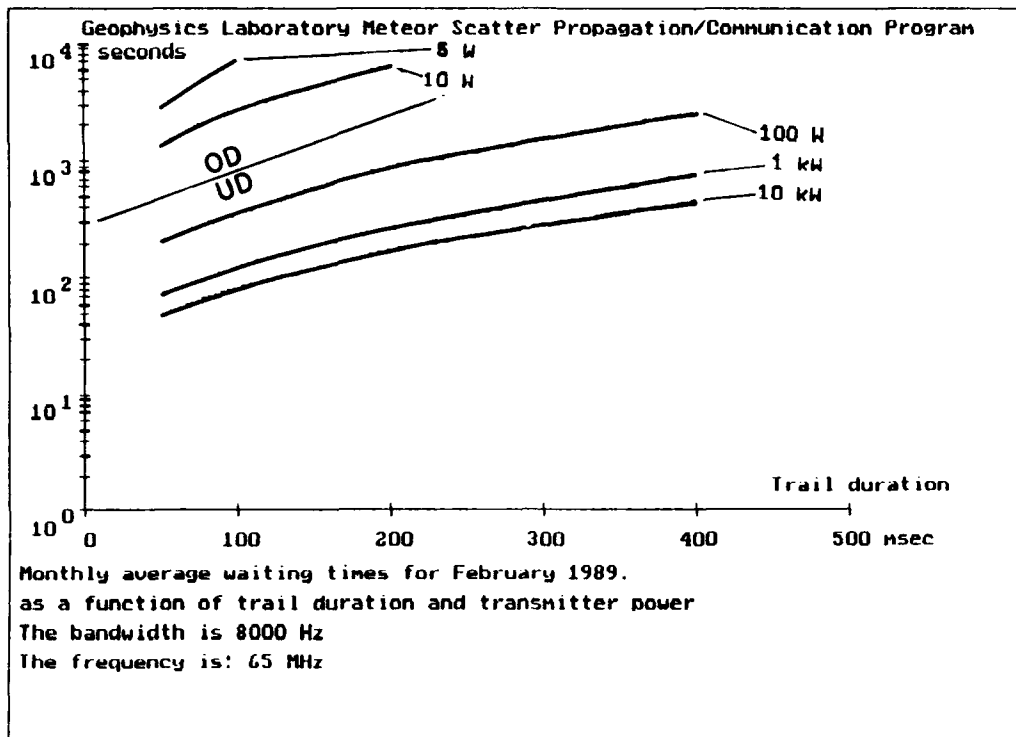


Figure F21. Monthly Average Waiting Time as a Function of Duration for Transmitter Powers of 10 kW, 1kW, 100 W, 10 W, and 5 W for the Month of February 1989. The frequency is 65 MHz

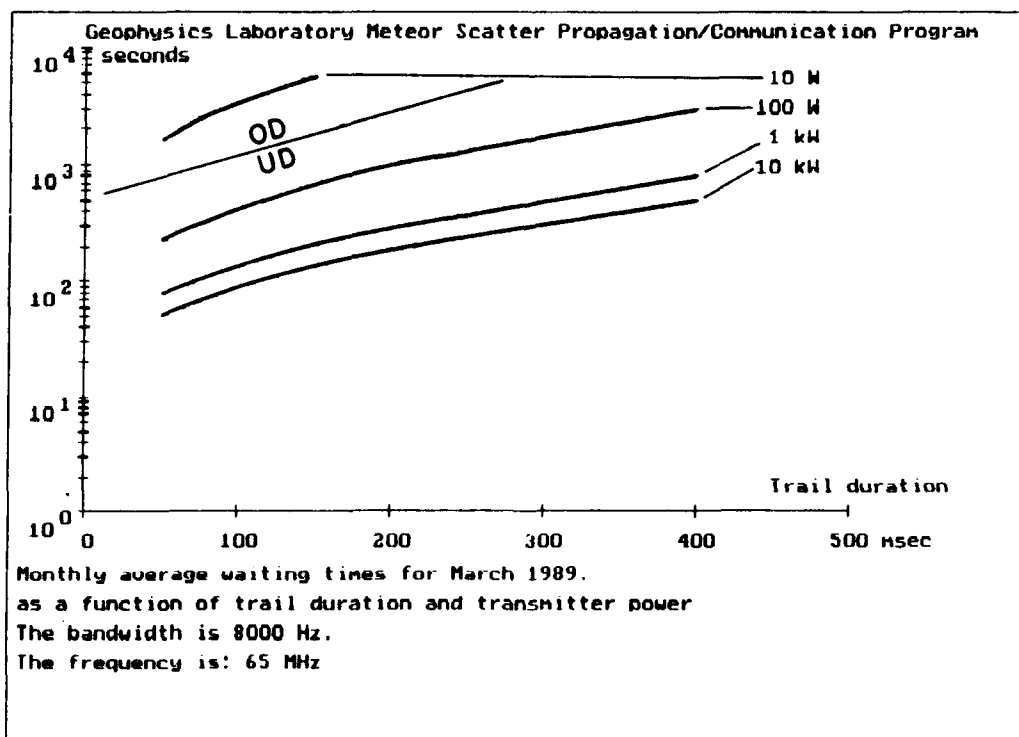


Figure F22. Same as Figure F21 but for March 1989



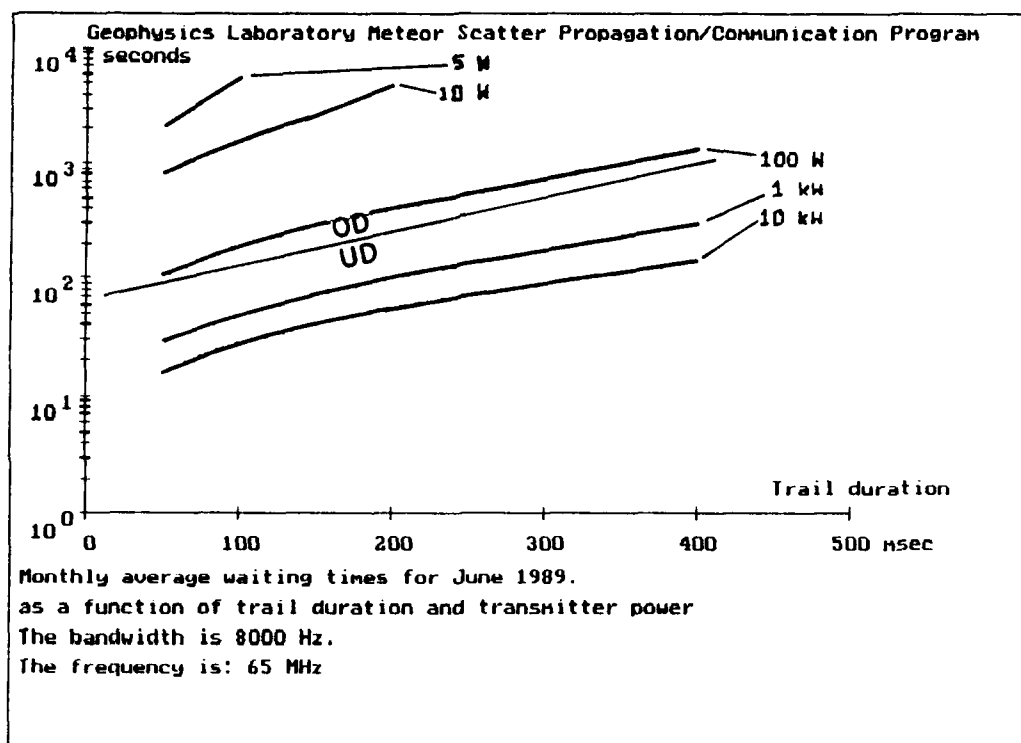


Figure F23. Same as Figure F21 but for June 1989

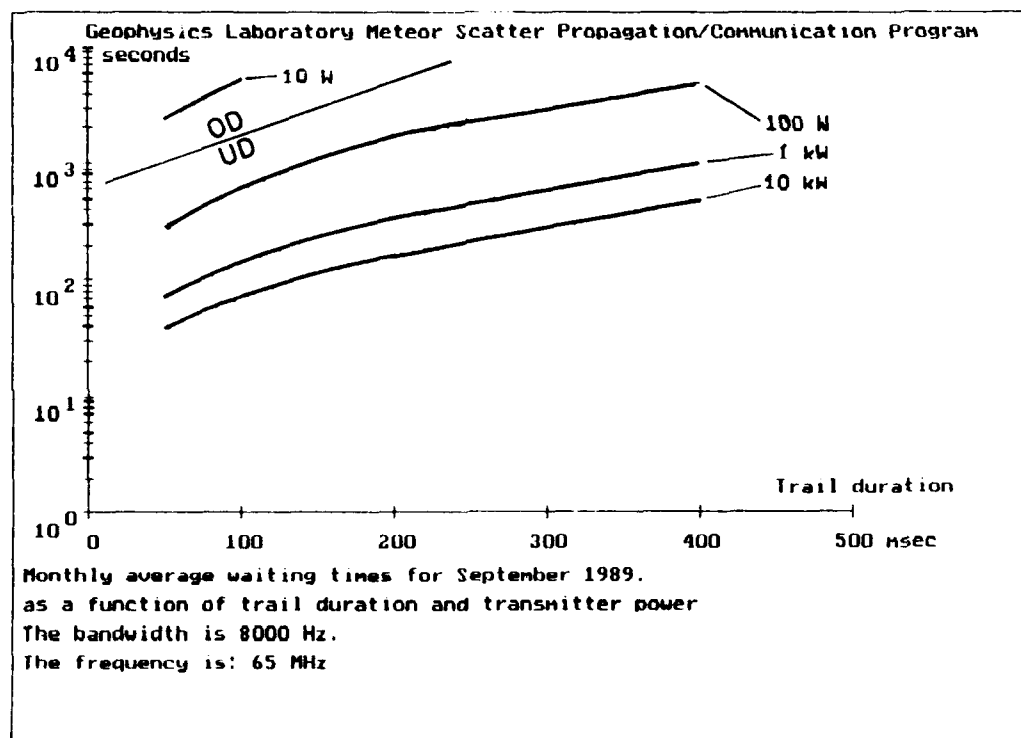


Figure F24. Same as Figure F21 but for September 1989

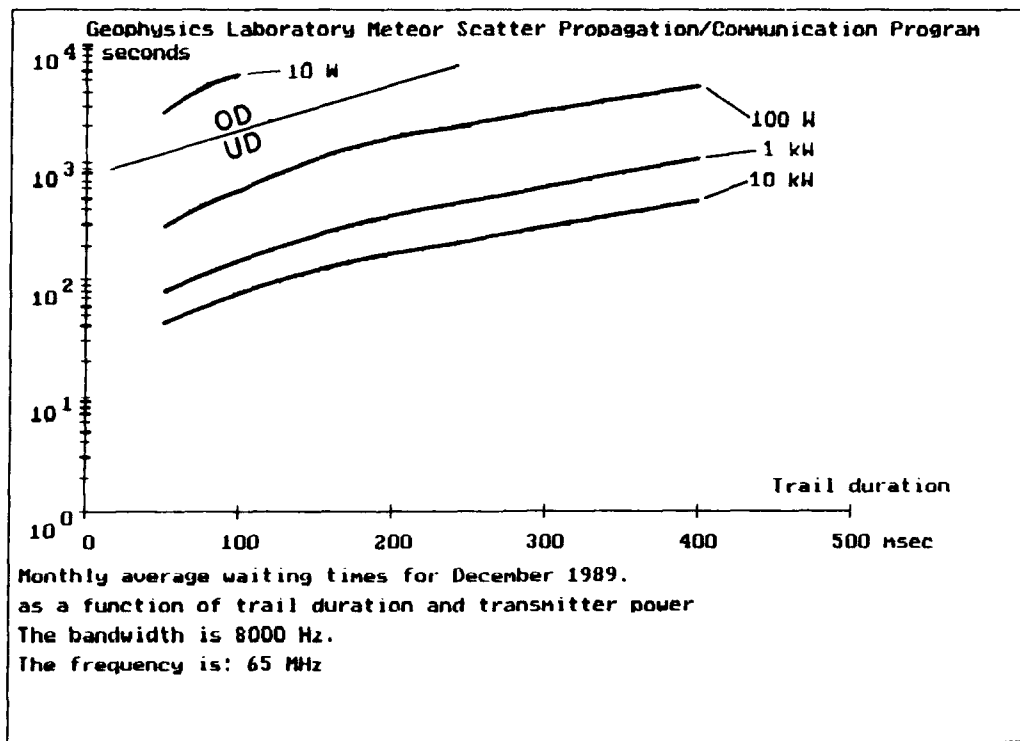


Figure F25. Same as Figure F21 but for December 1989

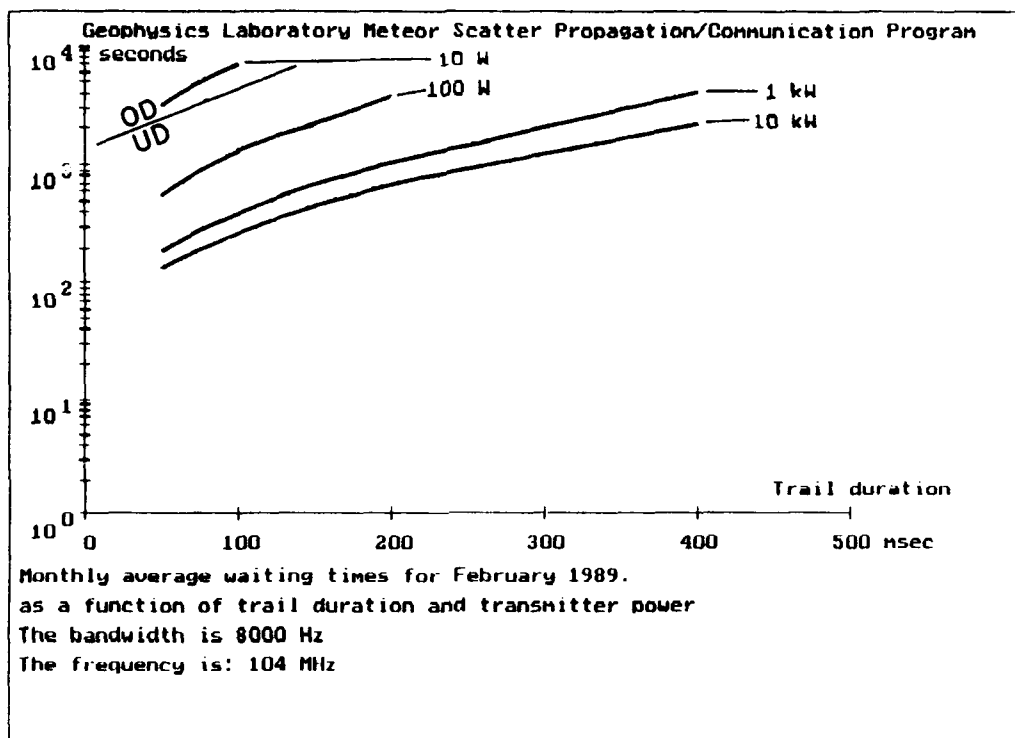


Figure F26. Monthly Average Waiting Time as a Function of Duration for Transmitter Powers of 10 kW, 1 kW, 100 W, 10 W, and 5 W for the Month of February 1989. The frequency is 104 MHz

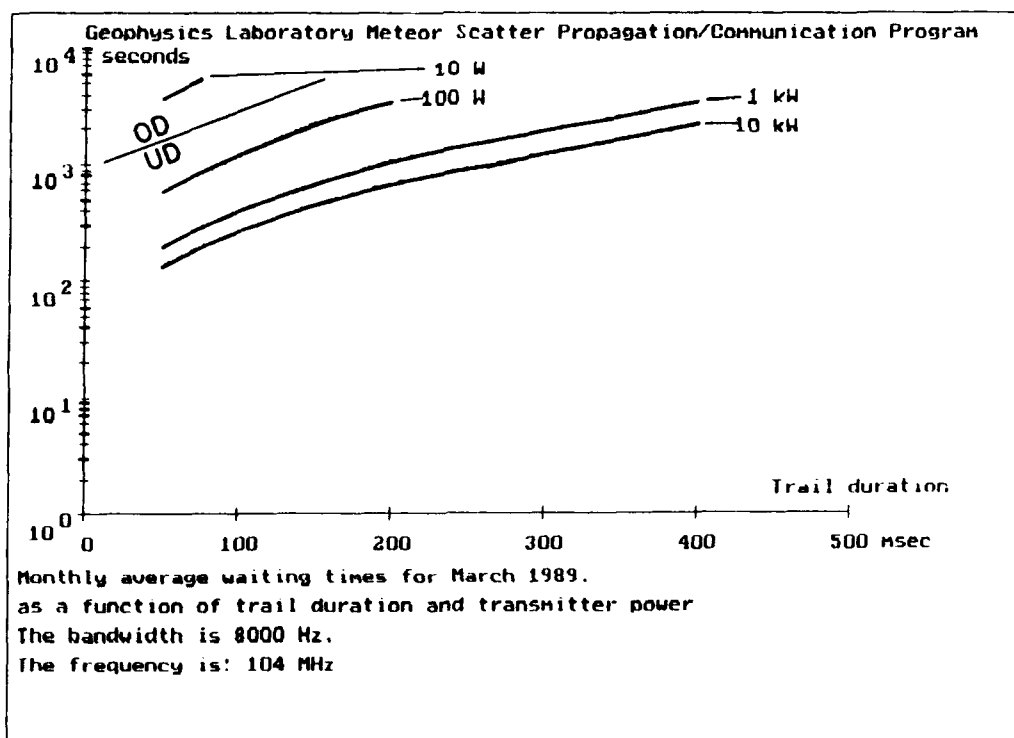


Figure F27. Same as Figure F26 but for March 1989

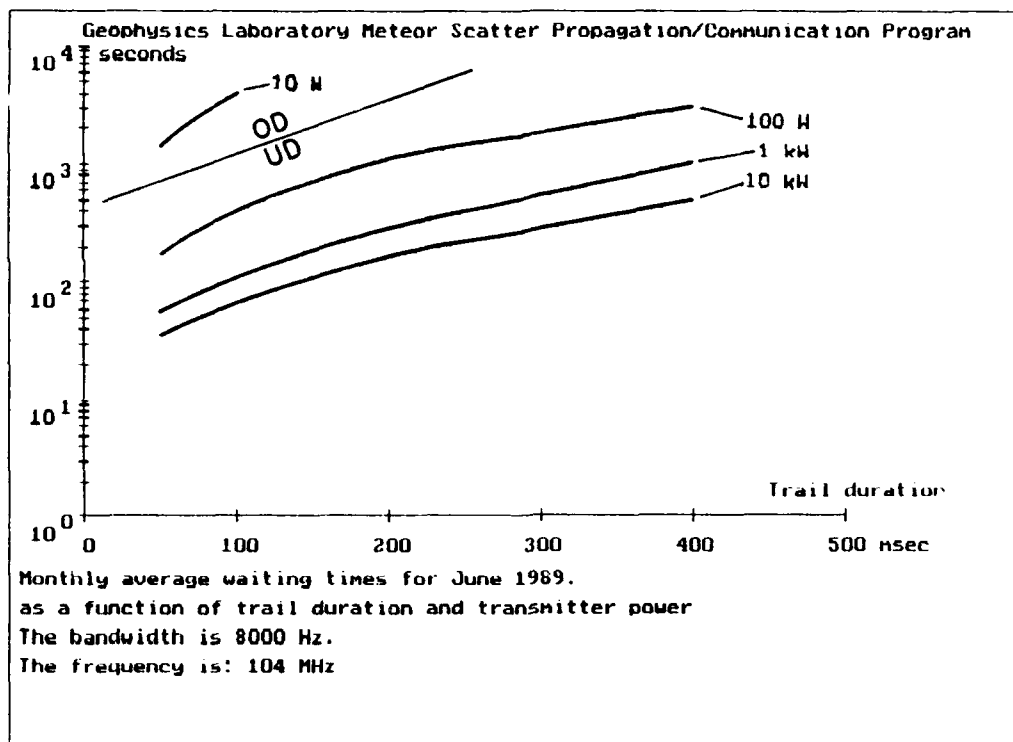


Figure F28. Same as Figure F26 but for June 1989

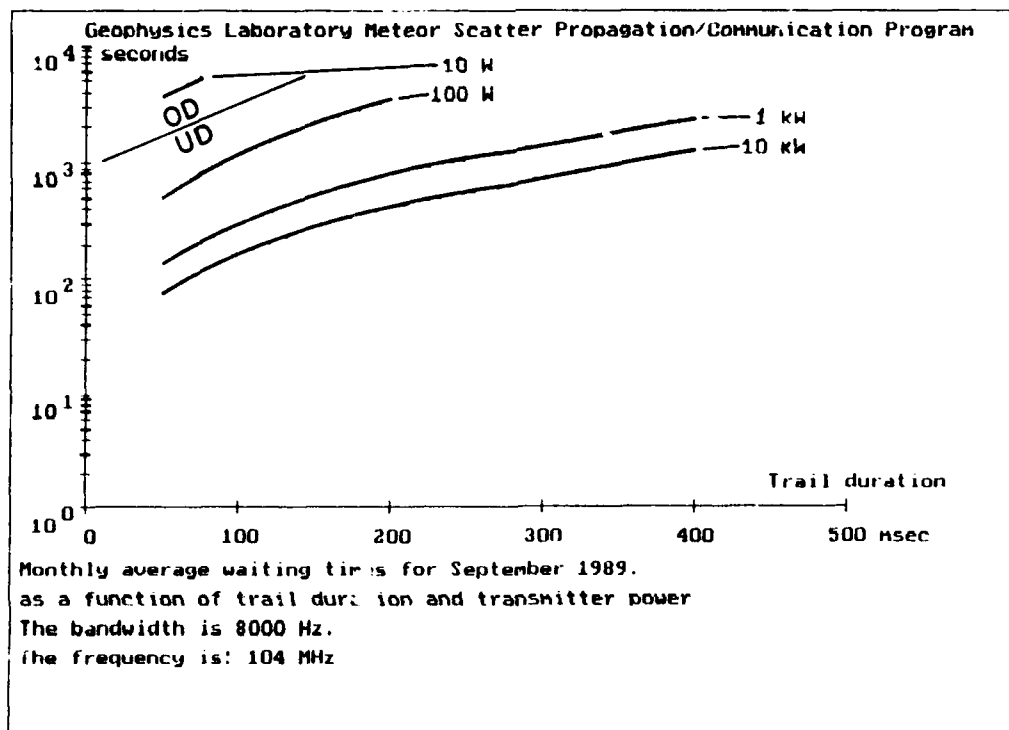


Figure F29. Same as Figure F26 but for September 1989

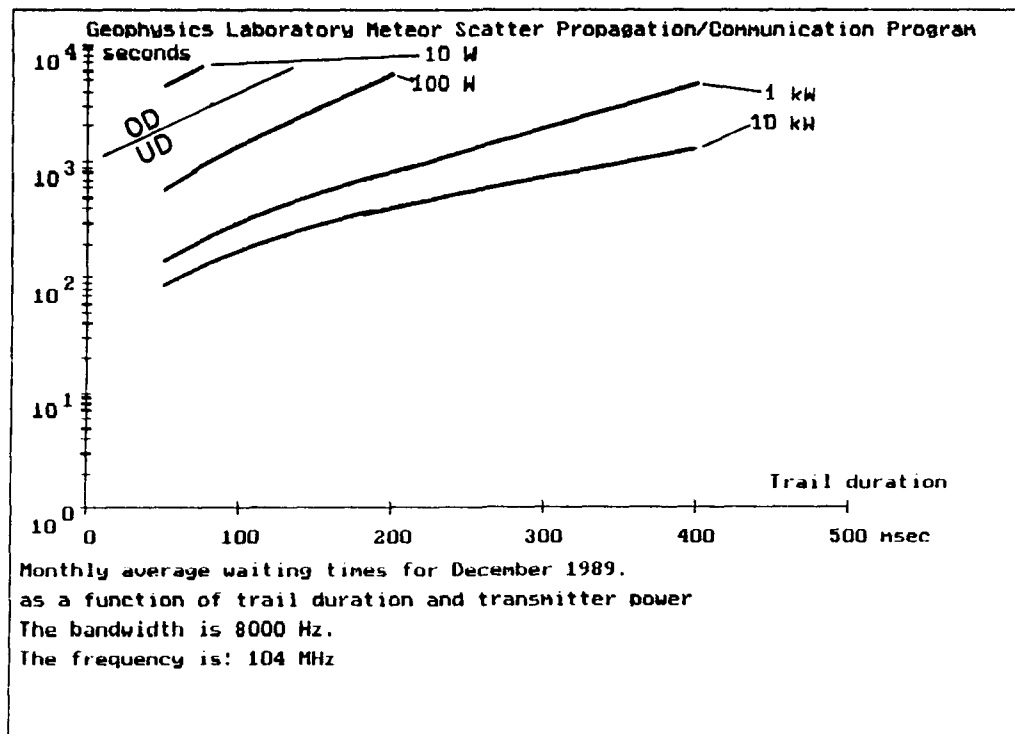


Figure F30. Same as Figure F26 but for December 1989

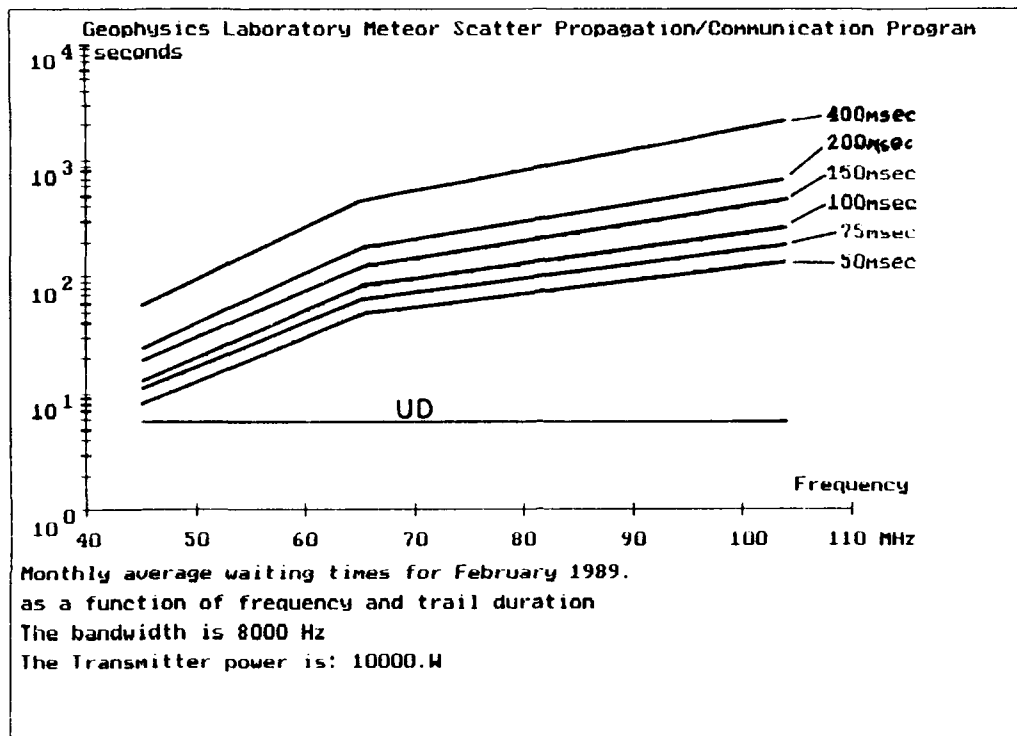


Figure F31. Monthly Average Waiting Times as a Function of Frequency for Trails of 50, 75, 100, 150, 200, 400 msec Duration for the Month of February 1989. The transmitter power is 10 kW

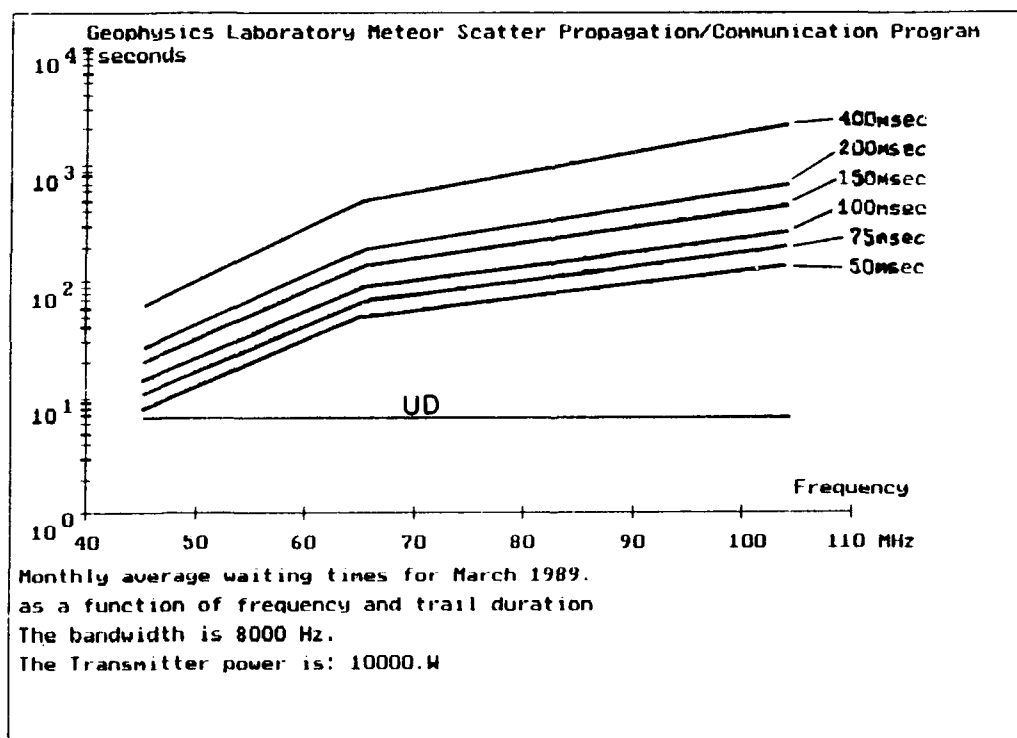


Figure F32. Same as Figure F31 but for March 1989

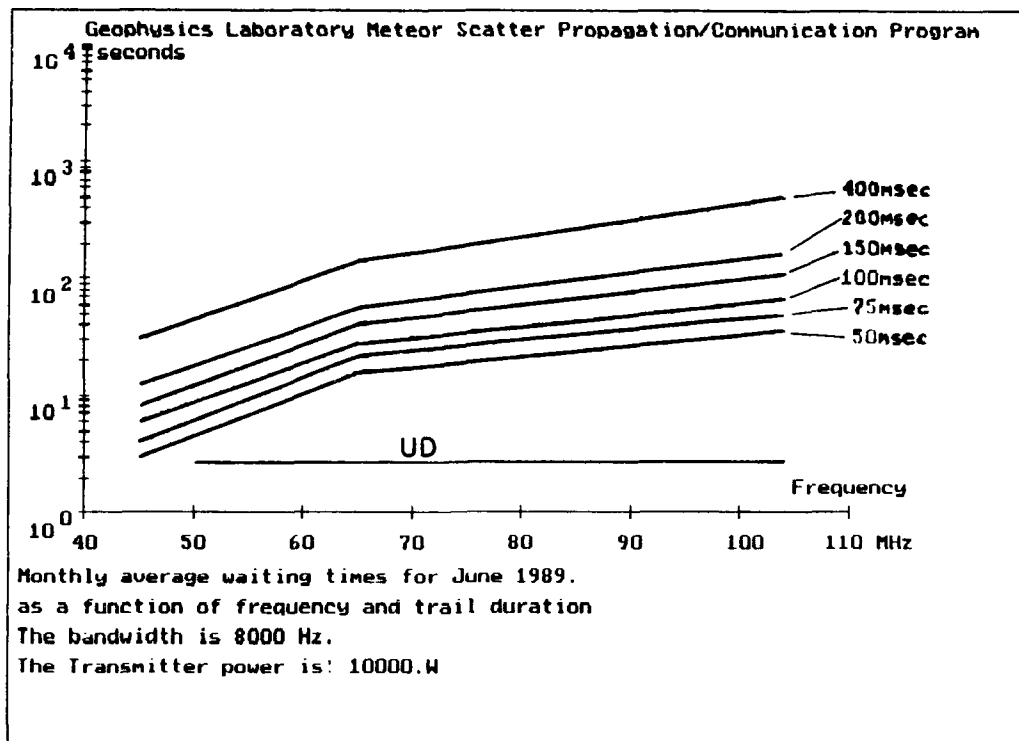


Figure F33. Same as Figure F31 but for June 1989

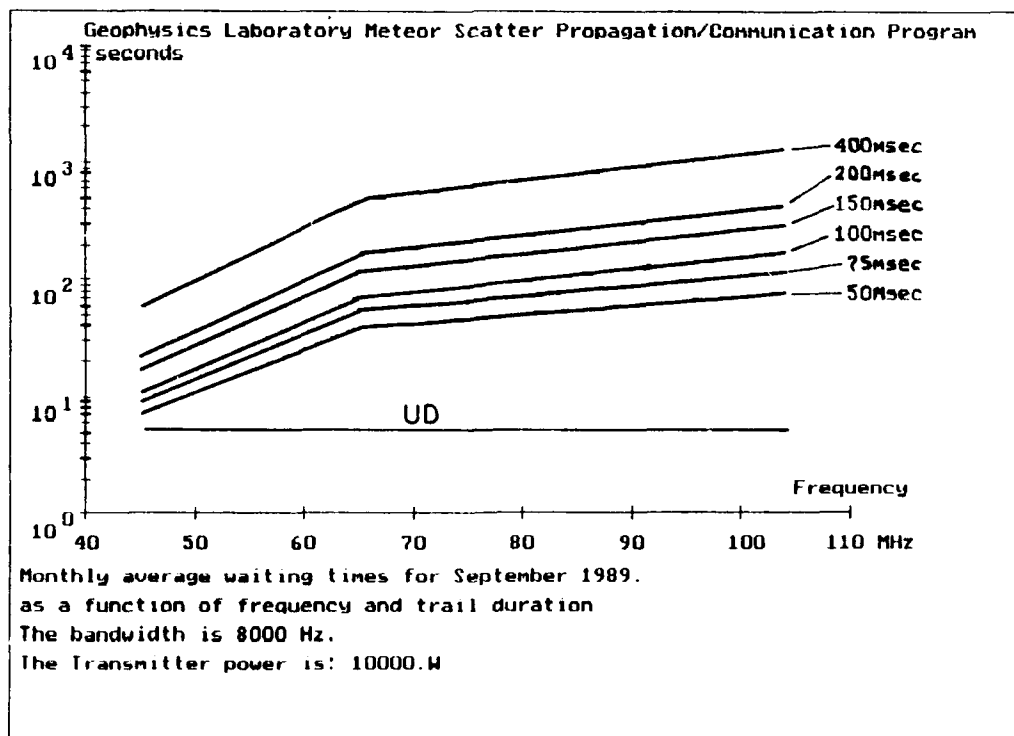


Figure F34. Same as Figure F31 but for September 1989

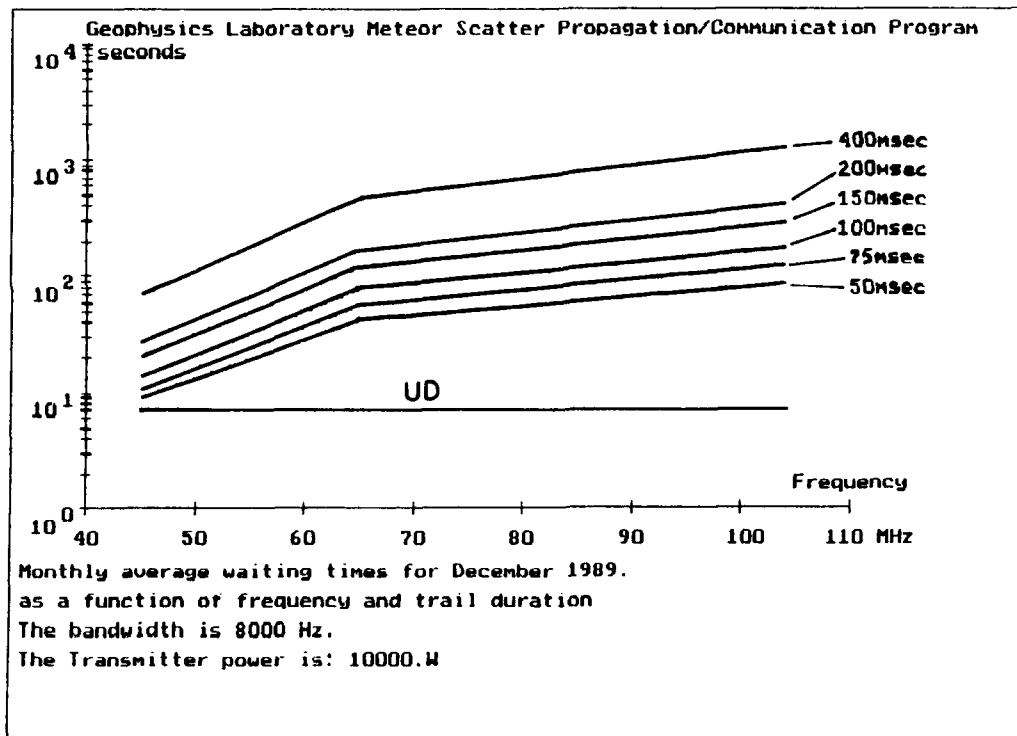


Figure F35. Same as Figure F31 but for December 1989



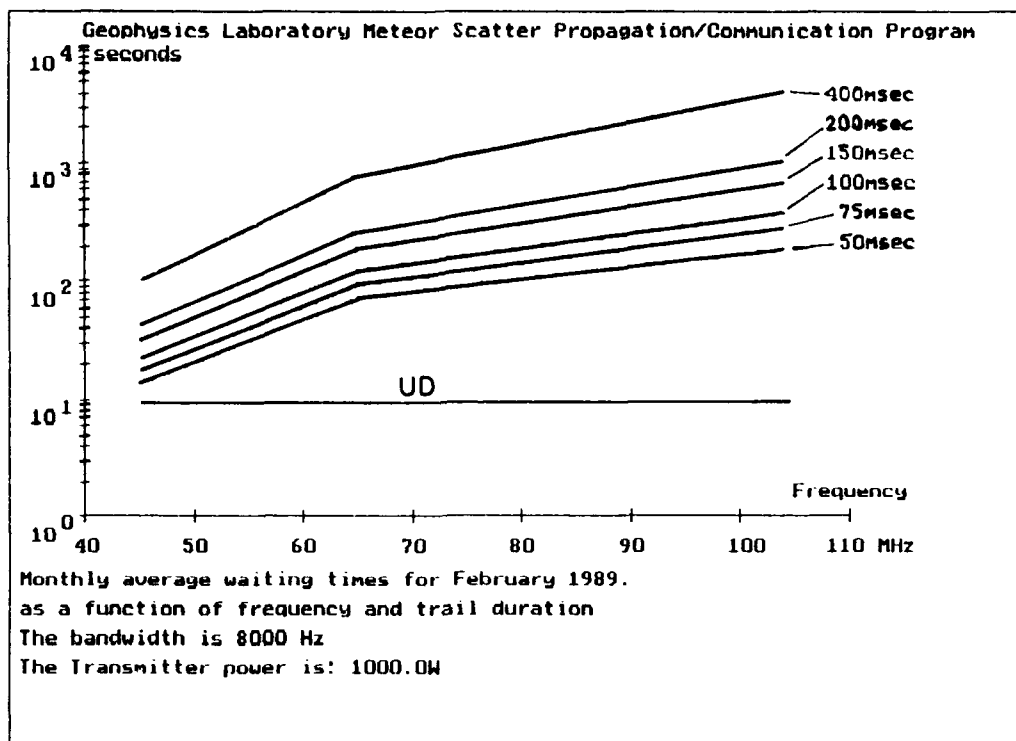


Figure F36. Monthly Average Waiting Times as a Function of Frequency for Trails of 50, 75, 100, 150, 200, 400 msec Duration for the Month of February 1989. The transmitter power is 1 kW

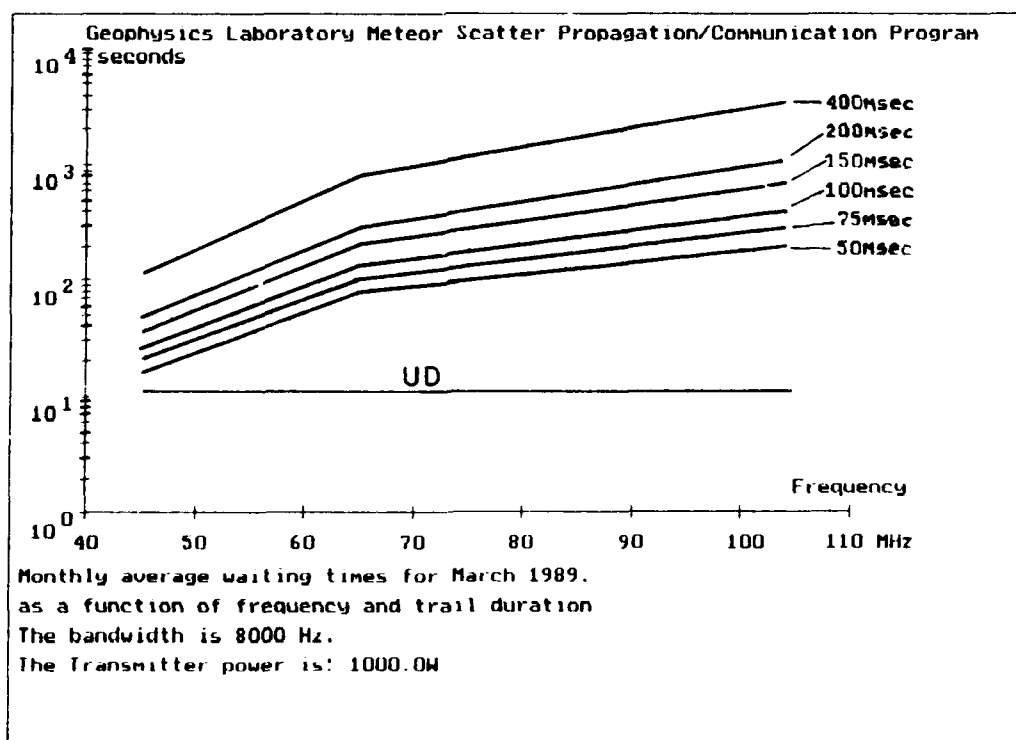


Figure F37. Same as Figure F36 but for March 1989

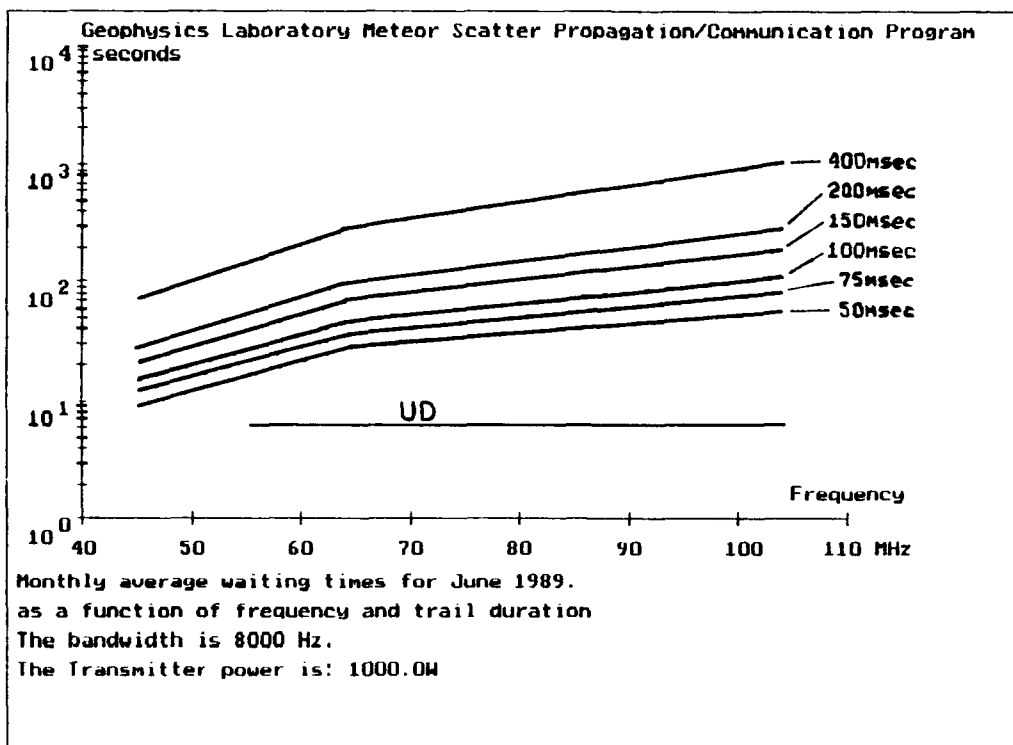


Figure F38. Same as Figure F36 but for June 1989

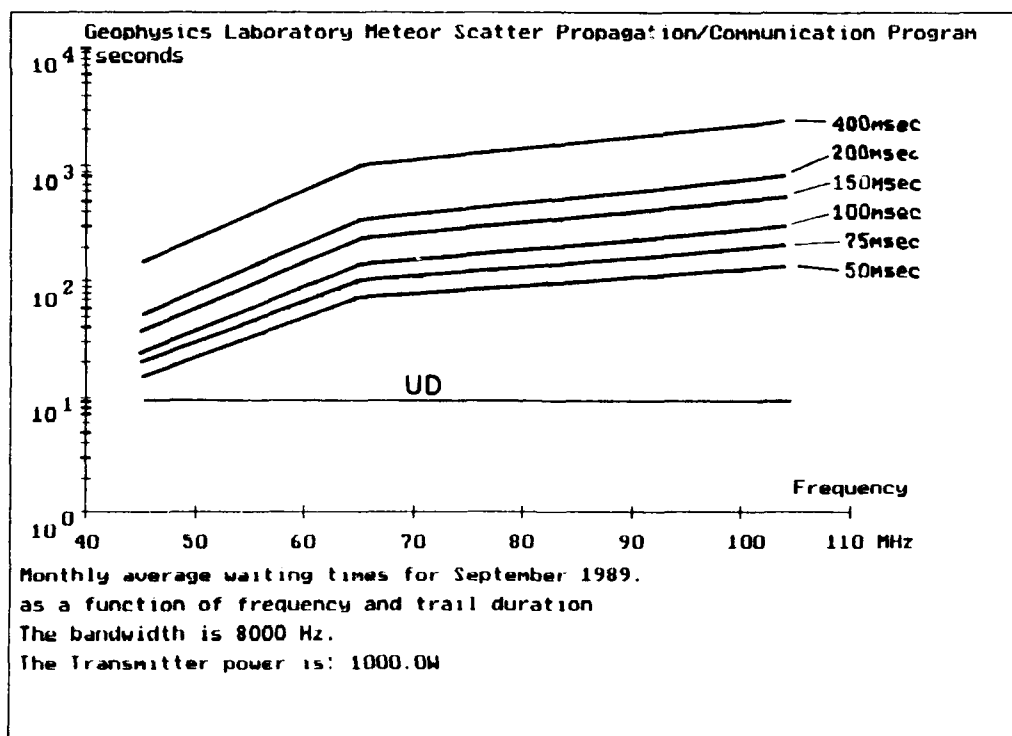


Figure F39. Same as Figure F36 but for September 1989

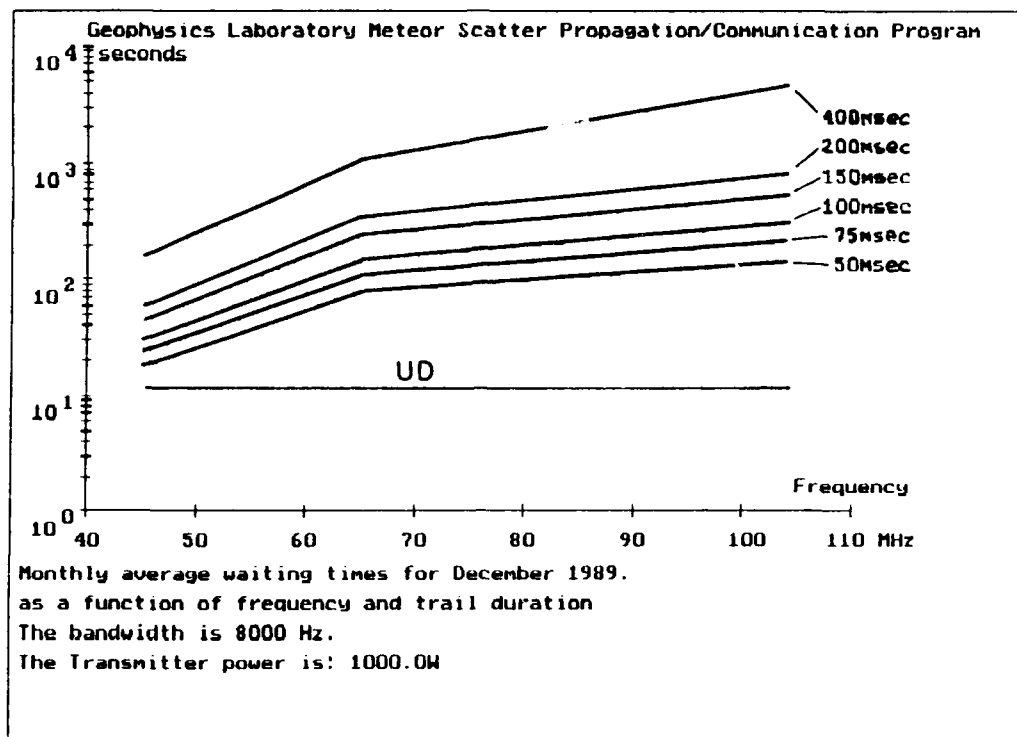


Figure F40. Same as Figure F36 but for December 1989

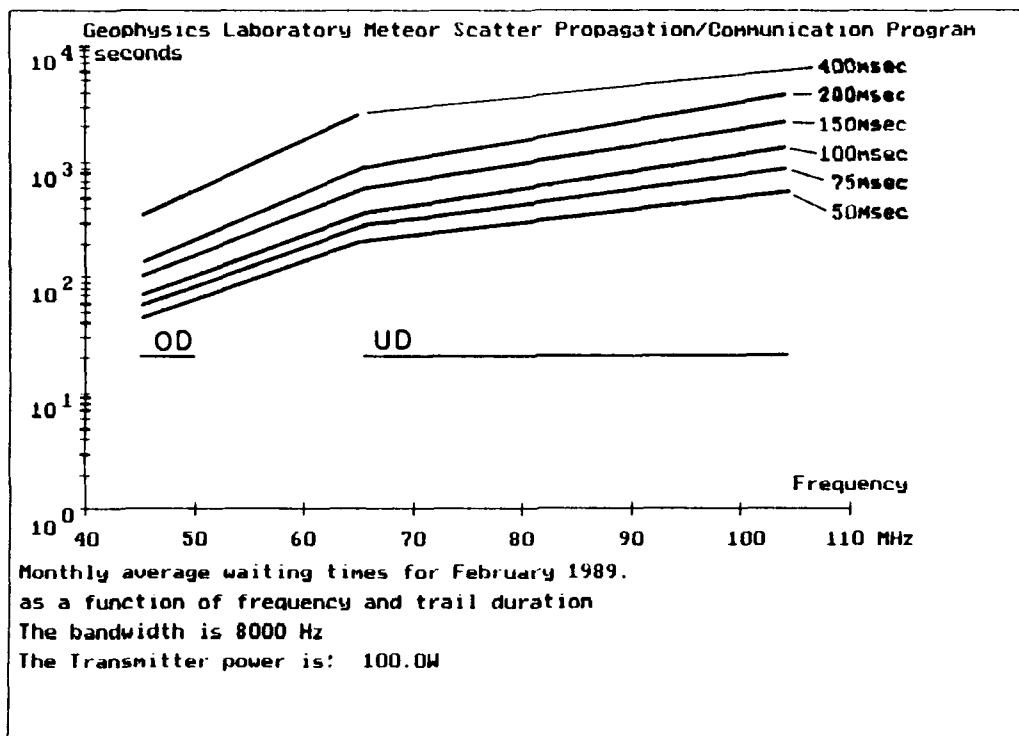


Figure F41. Monthly Average Waiting Times as a Function of Frequency for Trails of 50, 75, 100, 150, 200, 400 msec Duration for the Month of February 1989. The transmitter power is 100 W

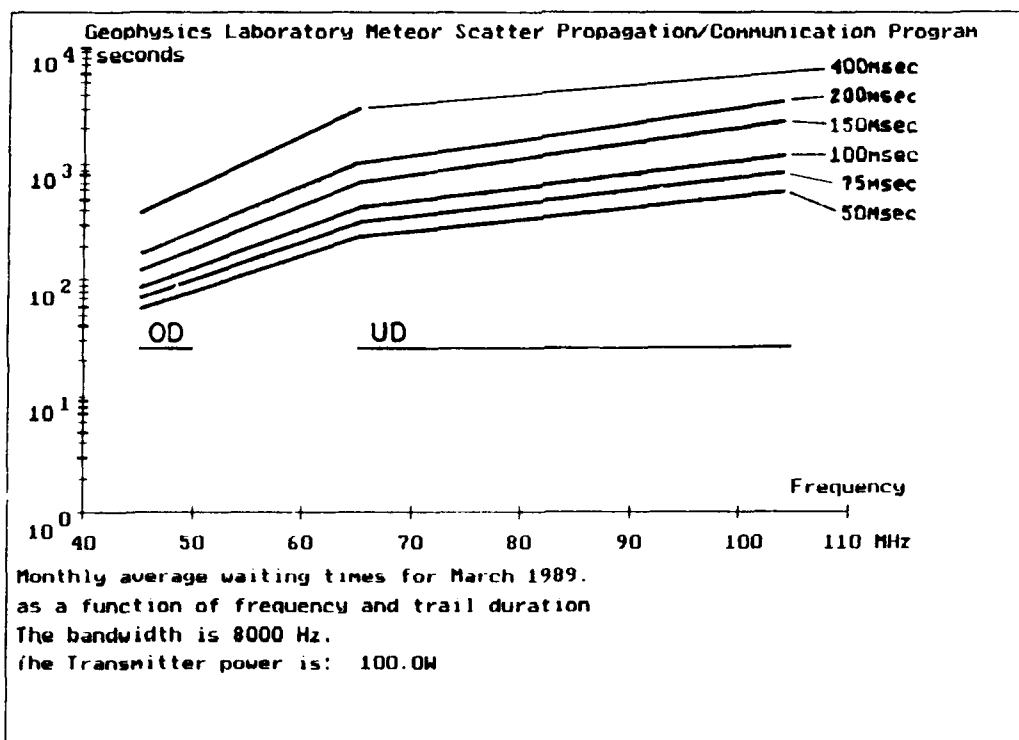


Figure F42. Same as Figure F41 but for March 1989

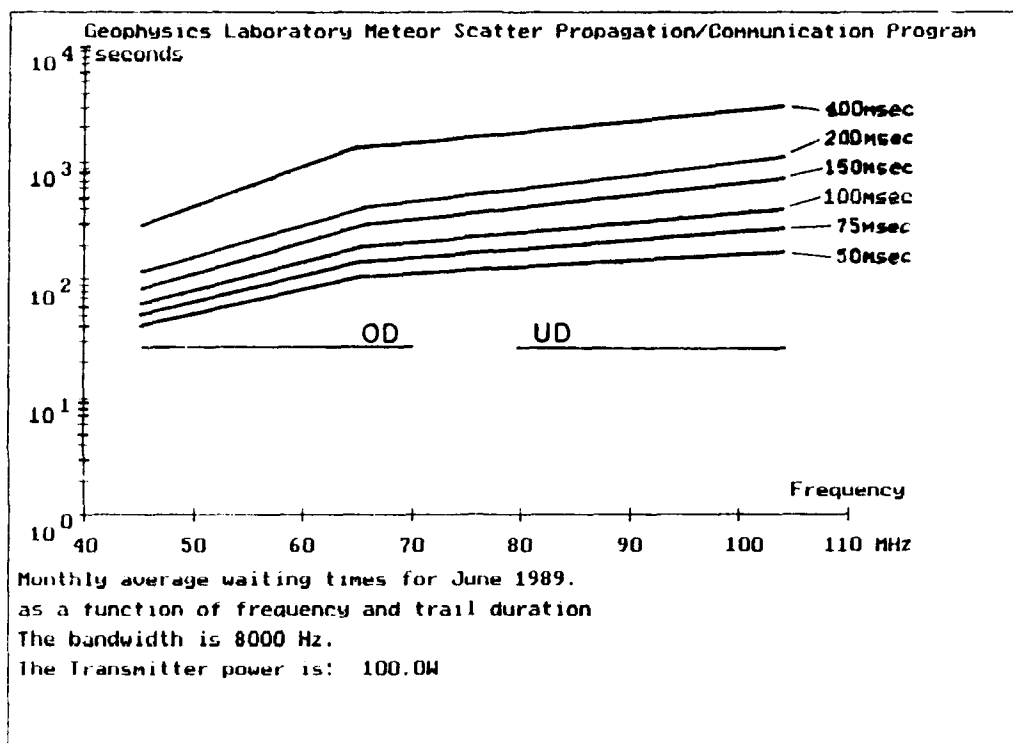


Figure F43. Same as Figure F41 but for June 1989

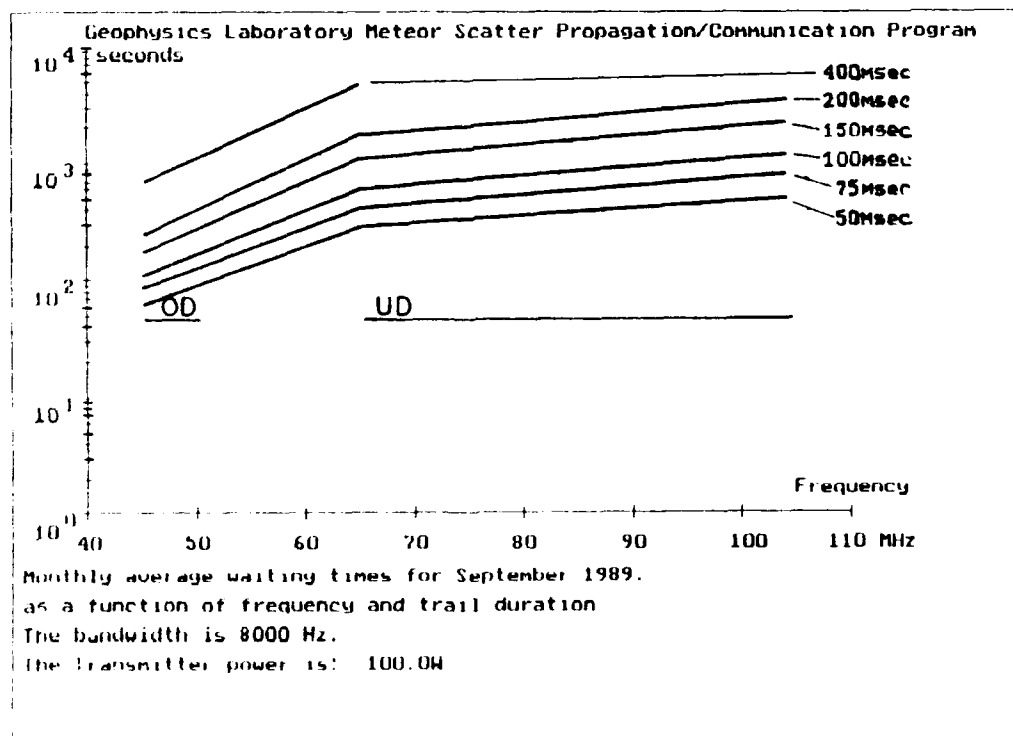


Figure F44. Same as Figure F41 but for September 1989

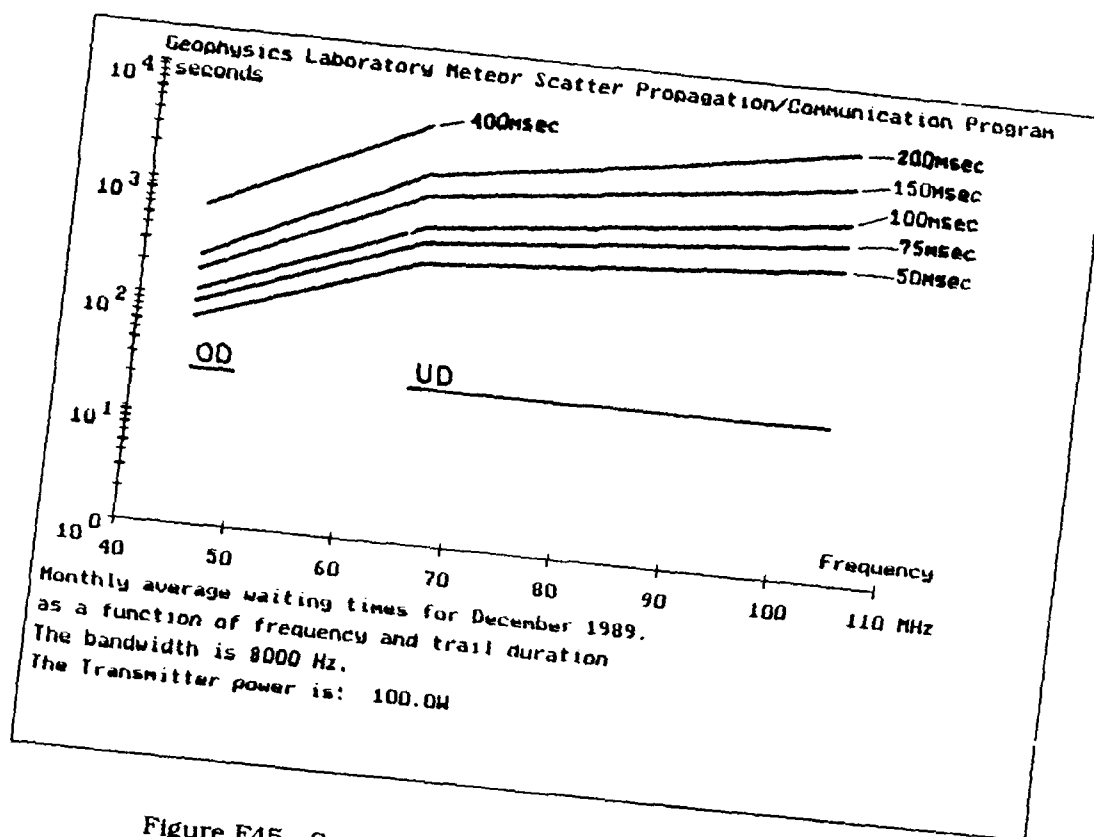


Figure F45. Same as Figure F41 but for December 1989

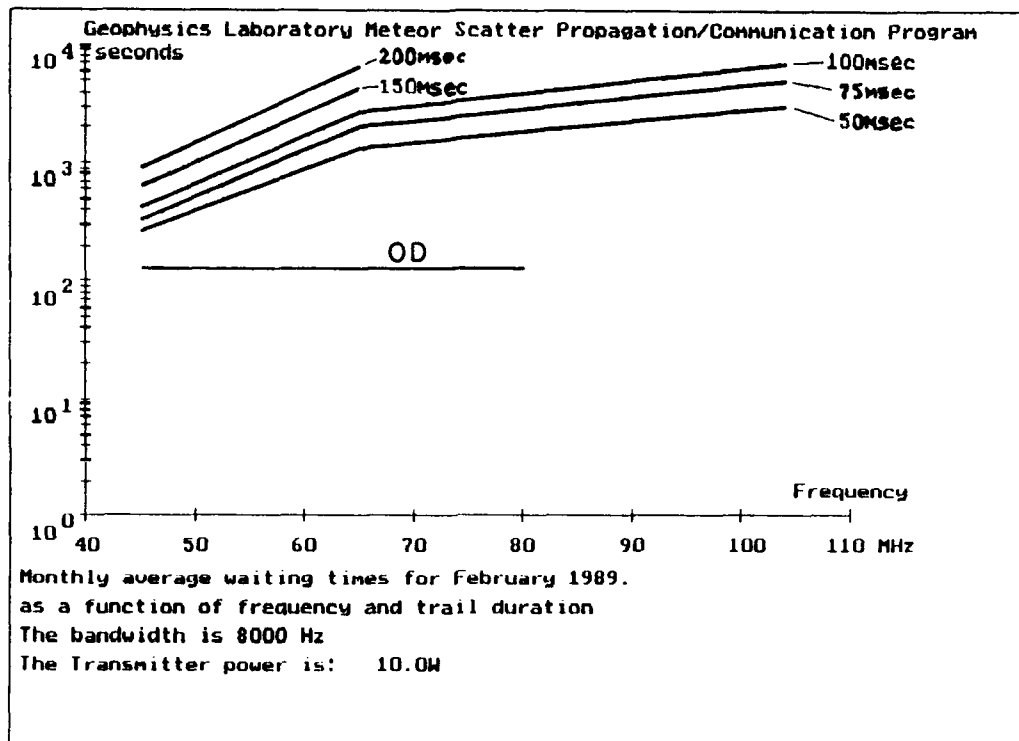


Figure F46. Monthly Average Waiting Times as a Function of Frequency for Trails of 50, 75, 100, 150, 200, 400 msec Duration for the Month of February 1989. The transmitter power is 10 W

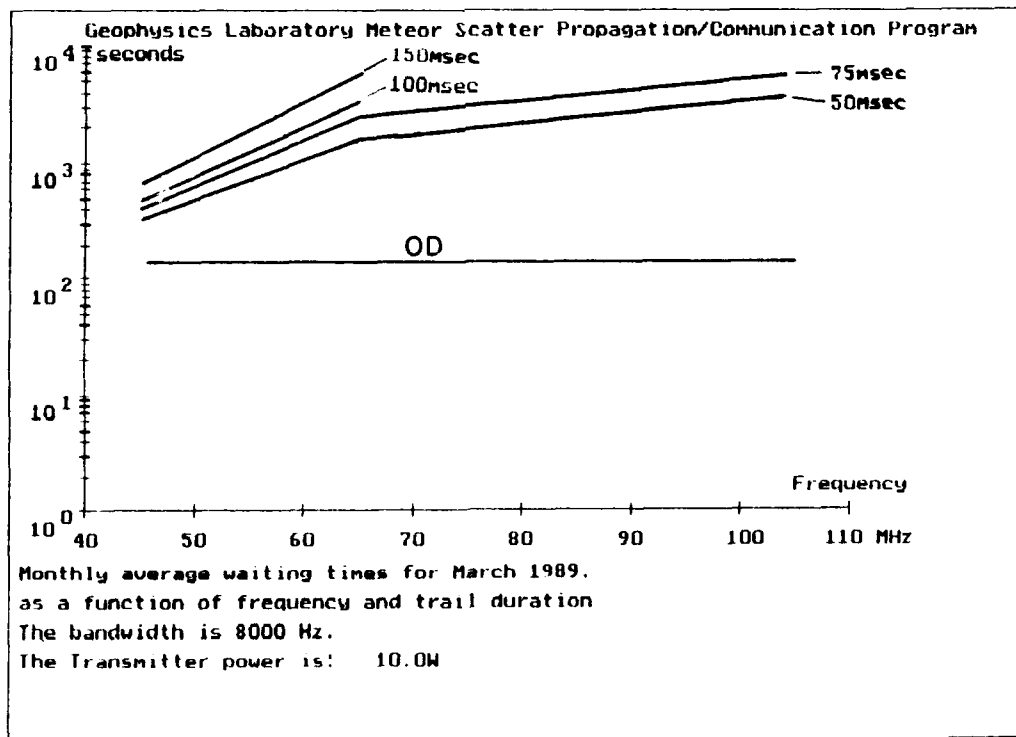


Figure F47. Same as Figure F46 but for March 1989

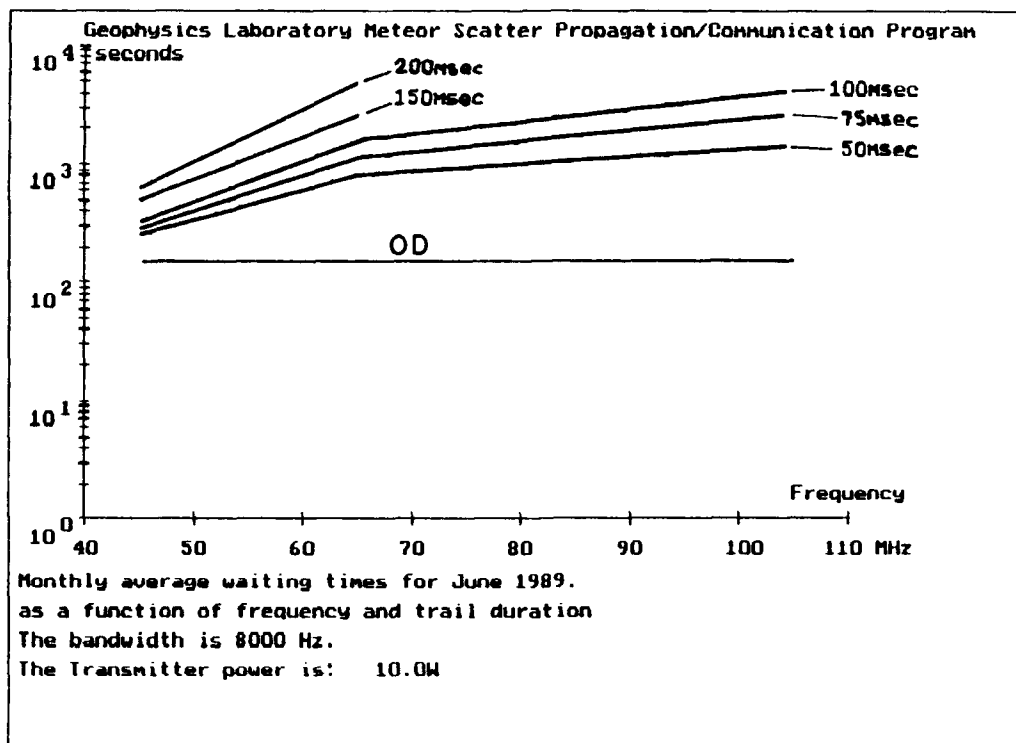


Figure F48. Same as Figure F46 but for June 1989

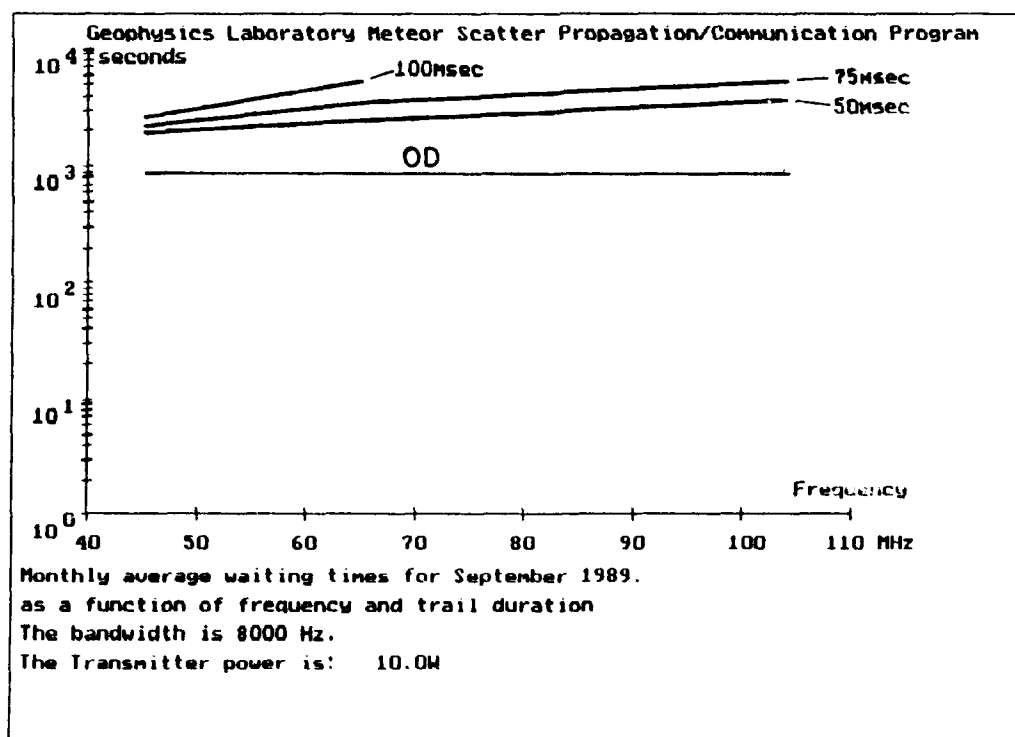


Figure F49. Same as Figure F46 but for September 1989



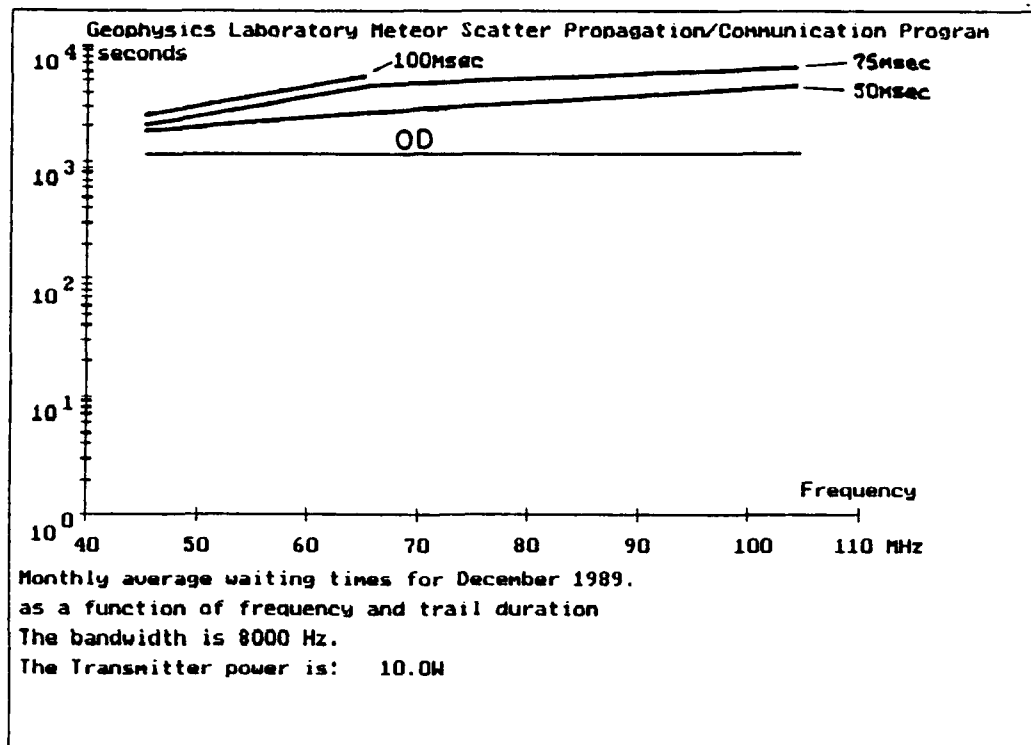


Figure F50. Same as Figure F46 but for December 1989

**END  
FILMED**

DATE:

**11-92**

**DTIC**